

**DEVELOPMENT OF
MUCOADHESIVE BIOPOLYMERS
FOR FOOD FORMULATION**

By

MOHD FAIZAL ALI

A thesis submitted to
The University of Birmingham
for the degree of
DOCTOR OF PHILOSOPHY

School of Chemical Engineering

University of Birmingham

2015

UNIVERSITY OF
BIRMINGHAM

University of Birmingham Research Archive

e-theses repository

This unpublished thesis/dissertation is copyright of the author and/or third parties. The intellectual property rights of the author or third parties in respect of this work are as defined by The Copyright Designs and Patents Act 1988 or as modified by any successor legislation.

Any use made of information contained in this thesis/dissertation must be in accordance with that legislation and must be properly acknowledged. Further distribution or reproduction in any format is prohibited without the permission of the copyright holder.

ABSTRACT

Development of mucoadhesive biopolymer has received great attention in the pharmaceutical application due to its ability to retain the drug dosage at the specific targeted area. This special property could be applied in food formulation for optimum delivery of the active ingredients in the mouth. This research was carried out to study, correlate and review several *in vitro* analytical methods that can be used in development process for characterisation of mucoadhesive polymer. Four well known mucoadhesive biopolymers namely, chitosan, pectin, sodium alginate and sodium carboxymethylcellulose (CMC) were used in this study. A modified rheological characterisation was used to study the interaction between the biopolymers with mucin and the assessment was based on the viscosity synergism. The detachment force characterisation was carried out via pull-off and tensile test using texture analyser and atomic force microscopy (AFM). Kinetic interaction study was done using quartz crystal microbalance with dissipation monitoring (QCMD) and interpretation of data from the modified rheological characterisation. Meanwhile, the removal of biopolymer emulsion after water flushing in a flow cell was observed under a microscope. It was found that mucoadhesion properties of tested biopolymers were affected by the concentration of biopolymer solutions, molecular weight, contact time, ionic strength and pH. Sodium alginate was characterised as the most mucoadhesive material by all the methods while QCMD shows CMC has the highest interaction with mucin layer compared to sodium alginate and pectin.

ACKNOWLEDGEMENTS

First and foremost, I would like to thank God the Almighty for His guidance and help in giving me the strengths to complete this thesis. I would like to acknowledge to Universiti Malaysia Pahang for the financial support throughout my study.

In particular, I would like to express my sincere appreciation to my supervisor, Prof. Serafim Bakalis and co-supervisor, Prof. Ian T Norton for the encouragement, knowledge, motivation, patience and time in helping me to complete my PhD study.

I would like also to acknowledge other contributors to the work, especially Dr. James Bowen for his help in AFM. For his help with QCMD, I would like to thank Dr. Roger Parker from Institute of Food Research, Norwich. Many thanks to Dr. James Covington (University of Warwick) for his help in fabrication process of flow cell. Big thanks also go out to Dr. Benjamin Le Révérend for his guidance during my early year of study.

A lot of thanks to my wife, Diana Ghazale and handsome son, Muhammad Faris for always being at my side and for the moral support during my hard time.

My big appreciation goes to my mother-in-law, Nor Hashimah Abdullah, for her ideas that helped me in editing process of this thesis. Finally, thank you to my beloved family and friends who always pray for my happiness and successfulness.

TABLE OF CONTENTS

Abstract	ii
Acknowledgement	iii
Table of Contents	iv
List of Figures	xi
List of Tables	xxiv
List of Symbols and Abbreviations	xxvii
1 INTRODUCTION	1
1.1 General Introduction	2
1.2 Literature Review	7
1.2.1 Mucoadhesion	7
1.2.1.1 Theory of Mucoadhesion	8
1.2.1.2 Mechanism of Mucoadhesion	12
1.2.1.3 Factors Affecting Adhesion	14
1.2.2 Mucoadhesive Polymer	19
1.2.3 Emulsion and Gel Particles	24
1.2.4 Mucous Layer and Mucin	27
1.2.5 Mucoadhesion Analysis	29
1.2.5.1 <i>In vitro</i> Measurement	30
1.2.5.2 <i>Ex vivo</i> and <i>In vivo</i> Study	35
1.3 Objectives of Study	37
1.4 Significances of Study	37

2	Methodology	38
2.1	Introduction	39
2.2	Methodology	39
2.2.1	Rheometer	39
2.2.1.1	Working Principles	39
2.2.1.2	Instrumental Setup	46
2.2.2	Texture Analyser	50
2.2.2.1	Working Principles	50
2.2.2.2	Instrumental Setup	52
2.2.3	Quartz Crystal Microbalance with Dissipation Monitoring (QCMD)	55
2.2.3.1	Working Principles	55
2.2.3.2	Instrumental Setup	58
2.2.4	Atomic Force Microscopy (AFM)	60
2.2.4.1	Working Principles	60
2.2.4.2	Instrumental Setup	63
2.2.5	Flow Cell with Microscope Imaging	64
2.2.5.1	Working Principles	64
2.2.5.2	Instrumental Setup	66
3	Rheological Characterisation	68
3.1	Introduction	69
3.2	Materials and Methods	71
3.2.1	Experimental Considerations	71

3.2.2	Sample Preparation	72
3.2.3	Instrumental Setup	72
3.3	Result and Discussion	77
3.3.1	Characterisation of Chitosan and Mucin Solution	77
3.3.2	Different Concentration and Concentration of Polymers	82
3.3.3	Effect of Different Degree of Esterification of Pectin on Adhesive Capability	93
3.3.4	Effect of Holding Time Before Shearing Process	94
3.3.5	Effect of the Amount of Mucin and Sodium Alginate at Same Concentration	96
3.3.6	Effect of Ionic Strength on Sodium Alginate and the Mixture with Mucin	101
3.3.7	Viscosity Synergism, Normalised Parameter and Force of Mucoadhesion	105
3.3.8	Oscillation Analysis of the Biopolymer-Mucin Mixtures	112
3.3.9	Control Experiment	115
3.4	Conclusion	117
4	Pull-Off and Tensile Test Using Texture Analyser	119
4.1	Introduction	120
4.2	Materials and Methods	122
4.2.1	Pull-Off Experiment	122

4.2.1.1	Materials and Instrumental Preparation	122
4.2.2	Tensile Test	124
4.2.2.1	Materials and Instrumental Preparation	124
4.3	Result and Discussion	126
4.3.1	Pull-Off Experiment	126
4.3.1.1	Effect of Different Polymers and Concentration of Polymers	128
4.3.1.2	Effect of Different Holding Time on Mass Absorbed	136
4.3.1.3	Mass Changed During Holding Time	137
4.3.2	Tensile Test	143
4.3.2.1	Peak Force and Total of Work of Different Concentration and Biopolymers	143
4.3.2.2	Normalised Parameter	148
4.4	Conclusion	149
5	Mucoadhesion Measurement Using Atomic Force Microscopy (AFM)	150
5.1	Introduction	151
5.2	Materials and Methods	153
5.2.1	Continuous Solution	153
5.2.2	Preparation of 'Piranha' Solution	154
5.2.3	Preparation of Biopolymer Absorption onto Au Substrate and Mucin Coated Cantilever	154

5.2.4	Force Measurement	155
5.3	Result and Discussion	157
5.3.1	Force Measurement in Air	157
5.3.2	Force Measurement in Distilled Water	162
5.3.3	Different Ionic Strength and pH Environment	167
5.4	Conclusion	172
6	Mucoadhesion Kinetic Studies	173
6.1	Introduction	174
6.2	Materials and Methods	175
6.2.1	Kinetic Absorption by Quartz Crystal Microbalance with Dissipation Monitoring (QCMD)	175
6.2.2	Kinetic Interaction Analysis by Rheological Characterisation	177
6.3	Result and Discussion	177
6.3.1	QCMD	177
6.3.2	Rheological Characterisation	184
6.4	Conclusion	190
7	Mucoadhesion Testing on Mucoadhesive Biopolymer Formulation	192
7.1	Introduction	193
7.2	Materials and Methods	194
7.2.1	Preparation of Mucoadhesive Biopolymer Emulsion	194
7.2.2	Flow Cell Analysis	195

7.2.3	Preparation of Agar Gel Particles	198
7.3	Result and Discussion	198
7.3.1	Oil in Water Emulsion (O/W) with Mucoadhesive Biopolymer	198
7.3.2	Viscometric Experiment of Mucoadhesive Biopolymer Emulsion with Mucin Layer	202
7.3.3	Flow Cell Observation on Interaction Between Mucoadhesive Biopolymer Emulsion with Mucin Layer	205
7.3.4	Agar Gel Particles	213
7.4	Conclusion	217
8	Conclusion and Future Work	219
8.1	Introduction	220
8.2	Conclusions	220
8.2.1	Rheological Characterisation	220
8.2.1.1	Recommendation for Rheological Characterisation	226
8.2.2	Pull-off and Tensile Test Using Texture Analyser	227
8.2.2.1	Recommendation for Pull-off and Tensile Test Using Texture Analyser	230
8.2.3	Mucoadhesion Measurement Using Atomic Force Microscopy (AFM)	230

8.2.3.1	Recommendation for Mucoadhesion	
	Measurement Using Atomic Force	
	Microscopy (AFM)	234
8.2.4	Mucoadhesion Kinetic Studies	235
8.2.4.1	Recommendation for Mucoadhesion	
	Kinetic Studies	237
8.2.5	Mucoadhesion Testing on Mucoadhesive	
	Biopolymer Formulation	238
8.2.5.1	Recommendation for Mucoadhesion Testing	
	on Mucoadhesive Biopolymer Formulation	240
8.3	Correlation of Mucoadhesion from Different Analytical	
	Methods	240
8.4	Review of Analytical Methods used in This Study	242
8.4.1	Conclusion of Review	248
8.5	Future Work	251
	References	253

LIST OF FIGURES

Figure 1.1	The interpenetration or diffusion theory illustration where there are three stages involved for the interaction between a mucoadhesive polymer and mucin glycoprotein.	9
Figure 1.2	An illustration of the influence of the contact angle on the strength of mucoadhesion.	11
Figure 1.3	Illustration of fracture mechanisms.	12
Figure 1.4	Contact stage and consolidation stage in the mucoadhesion phenomenon.	13
Figure 1.5	Some scenarios where mucoadhesion can occur.	13
Figure 1.6	Molecular diagram of different mucoadhesives (A) Pectin, (B) Sodium alginate, (C) Sodium carboxymethyl cellulose (CMC) and (D) Chitosan.	21
Figure 1.7	Schematic of Mechanism leading to coalescence of an O/W emulsion.	26
Figure 1.8	Hypothetical model of stabilizing the O/W emulsion droplets with pectin.	26
Figure 1.9	Structure of human salivary monomeric mucins (MG2)- the MUC7 gene product.	28
Figure 1.10	Structure of human salivary monomeric mucins (MG1)- the MUC5B gene product.	29

Figure 1.11	Modified Wilhelmy plate method apparatus for mucoadhesion study.	33
Figure 2.1	Laminar shear of fluid between two plates.	40
Figure 2.2	Three dimensional schematic diagram of basic term in the determination of shear viscosity.	41
Figure 2.3	Steady state flow curve of fluid.	42
Figure 2.4	Schematic stress response to the strain deformation for elastic solid, viscous fluid and viscoelastic material.	44
Figure 2.5	Schematic of the front of AR rheometer.	45
Figure 2.6	Selection of rheometer geometries.	46
Figure 2.7	Schematic diagram of sample volume for the rheological characterisation experiments.	49
Figure 2.8	Typical applications of texture analyser.	51
Figure 2.9	Schematic diagram of a texture analyser equipment.	51
Figure 2.10	Typical graph of force versus time or distance for adhesion measurement.	52
Figure 2.11	TA. XT. Plus texture analyser instrument.	53
Figure 2.12	Experiment setup using texture analyser. (A) Pull-off experiment and (B) Tensile test experiment.	54
Figure 2.13	(a) Butterworth van Dyke (BVD) model of a quartz resonator and (b) Schematic diagram of internal circuit of the QCMD.	56
Figure 2.14	QCMD instrument with QAFC 302 axial flow chamber with temperature controlled loop.	59
Figure 2.15	Piezoelectric gold chip.	59

Figure 2.16	Reflection of laser beam from the cantilever to photodetector.	61
Figure 2.17	Atomic force causes the cantilever to bend corresponded by the sample surface tomography at nano-scale level.	61
Figure 2.18	A typical force curve during the measurement done by AFM.	62
Figure 2.19	Schematic diagram of AFM system.	64
Figure 2.20	Flow cell	67
Figure 2.21	Schematic diagram of the flow cell apparatus. (A) Reicher-Jung; (B) Flow cell; (C) Peristaltic pump; (D), Beaker containing pure distilled water; (E) Beaker containing solution removed from flow cell.	67
Figure 3.1:	Schematic diagram of the viscometric experiment.	75
Figure 3.2:	Steady state flow curve of 5% (w/v) mucin solution.	80
Figure 3.3	Flowcurve (steady state) of 1% (w/v) Chitosan in 1% (v/v) acetic acid solution measured with step up (0.2 s^{-1} to 1000 s^{-1}) followed by step down (1000 s^{-1} to 0.2 s^{-1}).	81
Figure 3.4	Viscosity profile 1% (w/v) Chitosan in 1% (v/v) acetic acid measured on different day after stored in fridge ($T \sim 5^{\circ}\text{C}$).	81
Figure 3.5	Steady state flow curve of 1% (w/v) chitosan in 1% (v/v) acetic acid, 5% (w/v) mucin and chitosan-mucin mixture which was mixed with a spoon (not magnetic stirrer).	84
Figure 3.6	Agglomeration of chitosan-mucin when mixed with spoon.	84
Figure 3.7	Stress sweep of 1% (w/v) chitosan solution in 1% (v/v) acetic acid.	87

- Figure 3.8** Frequency sweep 1% (w/v) chitosan in 1% (v/v) acetic acid and its mixture with 5% (w/v) mucin. 87
- Figure 3.9** Viscosity profile of 1.5 ml 1% (w/v) and 2% (w/v) different polymer solutions, water, polymer-mucin and water-mucin at shear rate of 50 s^{-1} . 4 ml of 10% (w/v) mucin solution was dried on the peltier stage for the shearing process. Measurement was done for 20 minutes after applying 5 minutes equilibrium time (holding time). 88
- Figure 3.10** Viscosity profile of 1.5 ml of 1% (w/v) high DE pectin mixed with 4 ml 10% (w/v) mucin at different of shear rate and 5 minutes holding time before the shearing process (— 40 s^{-1} , — 50 s^{-1} , — 60 s^{-1}). 91
- Figure 3.11** Viscosity of the mixture of 1.5 ml 1% (w/v) high DE pectin with mucin at different shear rates. Initially, the high DE pectin-mucin mixture was mixed at 50 s^{-1} shear rate after 5 minutes holding time. 91
- Figure 3.12** (a) Frequency sweep test for the mixture of 1.5 ml 1% (w/v) high DE pectin – 4 ml 10% (w/v) mucin (mixed at different shear rate: $\blacklozenge G' 40 \text{ s}^{-1}$; $\blacksquare G'' 40 \text{ s}^{-1}$ $\blacktriangle G' 50 \text{ s}^{-1}$; $\blacktimes G'' 50 \text{ s}^{-1}$; $\blackstar G' 60 \text{ s}^{-1}$; $\bullet G'' 60 \text{ s}^{-1}$) at different angular frequencies. (b) Tan δ for the mixture of 1.5 ml 1% (w/v) high DE pectin – 4 ml 10% (w/v) mucin (mixed at different shear rate: $\blacklozenge 40 \text{ s}^{-1}$; $\blacksquare 50 \text{ s}^{-1}$; $\blacktriangle 60 \text{ s}^{-1}$) at different angular frequencies. 92

- Figure 3.13** Viscosity profile of two different types of pectin (35% and 60% degree of esterification) mixed with 4 ml of 10% (w/v) mucin (temperature is 37°C, shear rate is 50 s⁻¹ and equilibrium time is 0 s). 94
- Figure 3.14** Viscosity profile of the 1.5 ml of 1% (w/v) high DE pectin mixed with 4 ml 10% (w/v) mucin (dried condition) at different initial holding times and shear rate of 50 s⁻¹. 95
- Figure 3.15** Initial viscosity of mixture of 1.5 ml of 1% (w/v) high DE pectin mixed with 4 ml 10% (w/v) mucin (dried condition) at different holding times and shear rate of 50 s⁻¹. 96
- Figure 3.16** Effect of amount of mucin in the combination of 1.5 ml of 2% (w/v) sodium alginate and 10 % (w/v) mucin on the viscosity of the mixture. (Shear rate: 50 s⁻¹; holding time: 0 s). 98
- Figure 3.17** Specific viscosity of sodium alginate-mucin with different amount of mucin in the mixture. (Shear rate: 50 s⁻¹; holding time: 0 s). 99
- Figure 3.18** Viscosity profile of the different volume of 2% (w/v) sodium alginate mixed with 4 ml of 10% (w/v) mucin (dried condition). (Shear rate: 50 s⁻¹; holding time: 0 s). 99

Figure 3.19	Effect of amount of sodium alginate solution on the viscosity for mixture of 4 ml of 10% (w/v) mucin and 2% (w/v) sodium alginate solution. Viscosity of different concentration of mucin solution is measured by mixing 0.4 g of mucin (in dried film condition) with different amount of water. (Shear rate: 50 s ⁻¹ ; holding time: 0 s).	100
Figure 3.20	Specific viscosity of sodium alginate-mucin at different amount of sodium alginate solution in the mixture. (Shear rate: 50 s ⁻¹ ; holding time: 0 s).	100
Figure 3.21	Viscosity profile of the different volume of 2% (w/v) sodium alginate with different concentration of NaCl mixed with 4 ml 10% (w/v) mucin. (5 minutes initial holding time and shear rate of 50 s ⁻¹).	103
Figure 3.22	Viscosity profile of the different volume of 2% (w/v) sodium alginate with different concentration of KCl mixed with 4 ml 10% (w/v) mucin. (5 minutes initial holding time and shear rate of 50 s ⁻¹).	103
Figure 3.23	Viscosities for mixtures of the 2% (w/v) sodium alginate in different concentration of salt and its mixture with 4 ml of 10% (w/v) mucin (dried condition) after 20 minutes shearing at 50 s ⁻¹ and 5 minutes initial holding time.	104
Figure 3.24	Variation of zeta potential (ζ) of an apple juice with salt concentration.	104

Figure 3.25	Force of mucoadhesion for three types of polymers. The mixture (polymer-mucin) was mixed at 37°C and 50 s ⁻¹ shear rate with 5 minutes holding time.	111
Figure 3.26	Dynamic moduli of the high DE pectin-mucin mixture.	114
Figure 3.27	Tan δ of the 2% (w/v) different polymer-mucin mixtures.	114
Figure 3.28	Viscosity profile of control experiment. The mixing was done at 50 s ⁻¹ and with 5 minutes of equilibrium (holding time).	116
Figure 3.29	Viscosity profile of the mixture 1.5 ml 10% (w/v) sugar, 1.5 ml 30% (w/v) sugar and 1.5 ml water with mucin. (shear rate: 50 s ⁻¹ ; holding time: 5 minutes).	117
Figure 4.1	Modified of a tensiometer for measurement of detachment force between mucoadhesive material and mucous layer.	121
Figure 4.2	An advanced dual tensiometer apparatus for tensile force measurement.	122
Figure 4.3	Schematic diagram of the TA.XT.Plus Texture Analyser. (A) Texture Analyser with moveable arm; (B), Dell PC running the programme Texture Analysis; (C), Clean or mucin coated slide; (D), Glass beaker containing the polymer solution.	124
Figure 4.4	Schematic diagram of tensile test. The arrows indicated with capital letters represent relevant forces experienced in the test. Unspecific force polymer (A), unspecific force of mucin (B) and specific force between the polymer and mucin (C).	125
Figure 4.5	Schematic diagram of important sequences in pull-off experiment.	127

Figure 4.6	Force balance that experienced by slide. Total force is the measurement recorded by texture analyser.	127
Figure 4.7	Force of pull-off experiment recorded by texture analyser for different types of polymer with mucin coated slide. (Holding time is 300 s).	130
Figure 4.8	Force of pull-off experiment recorded by texture analyser for different types of polymer with clean slide. (Holding time is 300 s).	130
Figure 4.9	Illustration of cohesion force recorded during pulling step.	132
Figure 4.10	Mass changed $[(M_i - M_o)/(M_{\infty} - M_o)]$ during holding time (420 s) for different polymer solutions.	133
Figure 4.11	Force profile of pull-off experiment recorded by texture analyser with different holding time (— 30 s, — 180 s, — 300 s, — 420 s) for 2% (w/v) high DE pectin solution with mucin coated slide.	137
Figure 4.12	Force profile with different modes speed of 2% (w/v) sodium alginate. Holding time is 100 s.	138
Figure 4.13	Force profile of different type of polymers (2% w/v) with holding time of 420 s. (Fast dipping into polymer solution and pulled out at 1 mm/s).	139
Figure 4.14	Force recorded during holding time.	141
Figure 4.15	Weight change of mucin slide during holding time.	141
Figure 4.16	Relative weight change of mucin slide during holding time.	142

Figure 4.17	Force versus times for 10% (w/v) mucin and 2% (w/v) high DE pectin solution indicating the general mucoadhesion and unspecific mucoadhesion. The curves were obtained from tensile testing of mucin-pectin solution (MP) (blue line), water-pectin solution (WP) (red line) and mucin-water solution (MW) (green line).	144
Figure 4.18	Net force, ΔF_{\max} (specific interaction) and net total work, ΔAUC (specific total work) of different polymers (high DE pectin, CMC and sodium alginate) at different concentration.	147
Figure 4.19	Normalised parameter of different polymer at different concentration.	148
Figure 5.1	Peak force between the polymer substrate and mucin.	160
Figure 5.2	Peak force between the sodium alginate (different ionic strength NaCl) substrate and mucin coated cantilever at different contact time.	160
Figure 5.3	Work between the polymer substrates and mucin coated cantilever at different contact time.	161
Figure 5.4	Work between the sodium alginate with different ionic strength (NaCl) and mucin cantilever at different contact time.	161
Figure 5.5	Peak force for polymer substrate and mucin coated cantilever at different contact time.	164
Figure 5.6	Work for polymer substrate and mucin coated cantilever at different contact time.	165

Figure 5.7:	Peak force (detachment force) for sodium alginate (different ionic strength NaCl) and mucin coated cantilever at different contact time.	165
Figure 5.8	Work for sodium alginate with different ionic strength (NaCl) and mucin coated cantilever at different contact time.	166
Figure 5.9	Peak force (detachment force) between different polymers and mucin cantilever at in different ionic strength solution (NaCl).	168
Figure 5.10	Work between different polymers and mucin coated cantilever at in different ionic strength solution (NaCl) environment.	168
Figure 5.11	Peak force (detachment force) between different polymers and mucin coated cantilever in different pH solution.	171
Figure 5.12	Work between different polymers and mucin coated cantilever in different pH solution.	171
Figure 6.1	Sequences for kinetic absorption study of mucoadhesive polymer on mucin layer.	176
Figure 6.2	QMCD frequency and dissipation shifts during the injection of sodium alginate solution on the absorbed mucin layer. F= Frequency and D= Dissipation. Frequencies: F1 (5 MHz); F3 (15 MHz); F5 (25 MHz); F7 (35 MHz).	179
Figure 6.3	QMCD frequency and dissipation shifts during the injection of CMC solution on the absorbed mucin layer. F= Frequency and D= Dissipation. Frequencies: F1 (5 MHz); F3 (15 MHz); F5 (25 MHz); F7 (35 MHz).	180

Figure 6.4	QMCD frequency and dissipation shifts during the injection of high DE pectin solution on the absorbed mucin layer. F= Frequency and D= Dissipation. Frequencies: F1 (5 MHz); F3 (15 MHz); F5 (25 MHz); F7 (35 MHz).	180
Figure 6.5	Schematic diagram of the expected frequency profile and the process happened during the formation of polymer-mucin layer.	181
Figure 6.6	Schematic diagram of the phenomenon happened during the experiment.	181
Figure 6.7	Frequency change after injection of tested polymer solution before the buffer rinse.	183
Figure 6.8	Relative frequency change after injection of tested polymer solution before the buffer rinse.	184
Figure 6.9	Focusing area for kinetic interaction analysis by rheological characterisation.	185
Figure 6.10	Viscosity profile during shearing of mucin layer with water, high DE pectin and low DE pectin. The shearing was done for 20 minutes (1200 s) with shear rate of 50 s^{-1} and 0 s holding time.	185
Figure 6.11	Viscosity change during shearing of mucin layer with water, high DE pectin and low DE pectin. From $t= 0 \text{ s}$ to $t= 800 \text{ s}$.	186
Figure 6.12	Relative viscosity change during shearing of mucin layer with water, high DE pectin and low DE pectin from $t= 0 \text{ s}$ to $t= 800 \text{ s}$.	186

Figure 6.13	Viscosity profile during shearing process for 1% (w/v) pectin, water, 10% (w/v) sugar and 30% (w/v) sugar with mucin layer. Shear rate of 50 s^{-1} and holding time 0 s and 5 minutes.	189
Figure 6.14	Relative viscosity change during shearing process for 1% (w/v) pectin, water, 10% (w/v) sugar and 30% (w/v) sugar with mucin layer. Shear rate of 50 s^{-1} and holding time 0 s and 5 minutes.	190
Figure 7.1	Silverson L4RT high speed mixer.	195
Figure 7.2	Dimension of flow cell.	197
Figure 7.3	Setup for flow cell analysis with Reichert-Jung microscope using 25x magnification lense.	197
Figure 7.4	Images of emulsion droplets made with different mucoadhesive polymers and concentration. (a) No polymer; (b) 0.1% (w/v) high DE pectin; (c) 1% (w/v) high DE pectin; (d) 2% (w/v) high DE pectin; (e) 1% (w/v) sodium alginate; (f) 2% (w/v) sodium alginate.	201
Figure 7.5	Viscosity profile of the shearing process of (O/W) emulsion with dried mucin layer. Three emulsion formulation were used which are 1% (w/v) and 2% (w/v) of sodium alginate and without polymer. Shear rate at 50 s^{-1} and holding time was 5 minutes prior to shearing process. The measurement done at $T=37^{\circ}\text{C}$.	203
Figure 7.6	Emulsion without mucoadhesive polymer on the mucin coated slide.	208

Figure 7.7	Emulsion without mucoadhesive polymer on the clean slide.	209
Figure 7.8	1% (w/v) Sodium Alginate O/W emulsion on clean slide.	210
Figure 7.9	1% (w/v) Sodium Alginate O/W emulsion on mucin coated slide.	211
Figure 7.10	2% (w/v) Sodium Alginate O/W emulsion on mucin coated slide.	212
Figure 7.11	Temperature ramp of 3% (w/v) agar with different shear rate: (a) 40 s^{-1} and (b) 100 s^{-1} . Cooling rate is $1.5^{\circ}\text{C}/\text{min}$.	214
Figure 7.12	Images of fluid agar gel formed with different shear rate. (a) 40 s^{-1} and (b) 750 s^{-1} .	215
Figure 7.13	Frequency sweep of 3% (w/v) Agar gel particle at 0.5% strain. Shear rate: (a) 40 s^{-1} and (b) 100 s^{-1} .	216
Figure 7.14	Flowcurve of 3% (w/v) agar gel particle produced by applying different shear rate: (a) 40 s^{-1} and (b) 100 s^{-1} .	216

LIST OF TABLES

Table 1.1	Reason of the encapsulation technology.	3
Table 1.2	Microencapsulation processes.	5
Table 1.3	Microencapsulation process for different suspending media.	5
Table 1.4	The polymer factors that affecting the mucoadhesion strength.	15
Table 1.5	The environmental factors that affecting the mucoadhesion processes.	17
Table 1.6	Physiological effect on the mucoadhesion strength.	18
Table 1.7	Example of mucoadhesive polymers. More (+) symbols indicate stronger adhesion.	23
Table 2.1	Viscoelastic parameters.	43
Table 2.2	Experiment procedures were used in rheological characterisation experiment and production of agar gel particles.	48
Table 2.3	Texture analyser setting for the pull-off and tensile test experiments.	54
Table 3.1	Summary of the experiment parameters used in rheological characterisation. All the tests were performed at temperature of 37°C.	75
Table 3.2	Apparent viscosity and observed viscosity of the different polymers and their mixture with 10% (w/v) mucin (1.5 ml of polymer solution was used for the mixing process) at 50 s ⁻¹ and 5 minutes holding time.	107

Table 3.3	Apparent viscosity, observed viscosity, expected viscosity and enhanced viscosity of 1% (w/v) high DE pectin, 1% (w/v) low DE pectin, water and their mixture with 10% (w/v) mucin (1.5 ml of solution was used for the mixing process) at 50 s ⁻¹ and 0 minutes holding time.	109
Table 3.4	Normalised parameter and force of adhesion of different polymers in DI water at 37°C and shear rate of 50 s ⁻¹ (5 minutes initial holding time).	109
Table 3.5	Apparent viscosity, observed viscosity, normalised parameter and force of adhesion of 2% (w/v) sodium alginate with different ionic strength. (5 minutes initial holding time).	111
Table 3.6	Apparent viscosity, observed viscosity, expected viscosity and enhanced viscosity of 2% (w/v) Mucin and water. The mixing was done at 50 s ⁻¹ and with 5 minutes of equilibrium (holding time).	116
Table 4.1	Maximum pull-off force using the Texture Analyser TA.XT.Plus for different polymer solutions (holding time is 300 s).	135
Table 4.2	Peak forces and Normalised parameter of tensile test for different of concentrations and polymers.	145
Table 4.3	Total work or area under curve (AUC) of tensile test for different of concentrations and polymers.	146

Table 5.1	Summary of the experiment parameters used in AFM experiment. All the tests were performed in room of 18°C and a relative humidity of 40-50%.	156
Table 5.2	The intrinsic viscosity and electrostatic persistence length of 3% (wt) sodium alginate solution.	164
Table 6.1	Calculated mass change and percentage of change of absorbed mucin layer before and after injection of polymer solution (sodium alginate, CMC and high DE pectin). $n= 5$ MHz (first overtone).	182
Table 7.1	Emulsion characteristic.	200
Table 7.2	Apparent viscosity (η_p), observed viscosity (η_{obs}), expected viscosity (η_{exp}) and enhanced viscosity or synergism (η_{enh}) of emulsion with sodium alginate (1% w/v and 2% w/v concentration) and without the sodium alginate and their mixture with 4 ml of 10% (w/v) mucin in dried layer (1.5 ml of emulsion was used for the mixing process) at 50 s^{-1} and 5 minutes holding time.	205
Table 8.1	Ranking order of mucoadhesion for the tested mucoadhesive biopolymers by different analytical methods.	242

LIST OF SYMBOLS AND ABBREVIATIONS

c	Concentration
t	Time
g	gram
r	radius
k	Spring constant
g	Gravitational acceleration
n	Flow behaviour index
η	Shear viscosity
η_{enh}	Viscosity synergism
η_{rel}	Normalised parameter
$\dot{\gamma}$	Shear rate
τ	Shear stress
x	Cantilever deflection
ρ	Density
f	Resonant frequency
v_o	Shear velocity
z	Valence of ion
γ	Surface tension
A	Area
B	Buoyancy
M	Mol

C_d	Drag Coefficient
C_m	Capasitor
R_m	Resistor
L_m	Inductor
D_b	Diffusion coefficient
F	Force
F_d	Viscous drag force
P	Pressure
S	Spreading coefficient
Na^+	Sodium ion
K^+	Potassium ion
G'	Storage or elastic modulus
G''	Loss or viscous modulus
G^*	Complex modulus
K	Consistency index
V	Volume
Da	Dalton
DI	Distilled water
DE	Degree of esterification
Pa	Pascal
Hz	Hertz
GI	Gastrointestinal
$Tan \delta$	Loss tangent
AUC	Area under curve

<i>CMC</i>	Sodium carboxymethyl cellulose
<i>DEX</i>	Dextran
<i>HPC</i>	Hydroxypropyl cellulose
<i>LVR</i>	Linear viscoelastic region
<i>O/W</i>	Oil in water emulsion
<i>W/O</i>	Water in oil emulsion
<i>QCMD</i>	Quartz crystal microbalance with dissipation monitoring
<i>AFM</i>	Atomic force microscopy
<i>SPR</i>	Surface plasmon resonance
<i>STM</i>	Scanning tunneling microscopy
<i>SP</i>	Stylus profilometer
FTIR-ATR	Fourier transform infrared-attenuated total reflectance spectroscopy
PAA	Poly (acrylic acid)

Chapter 1:

Introduction and Literature Review

1.1 General Introduction

Throughout the pharmaceutical industry and more recently, with the introduction of ‘functional foods’ in the food industry there is a need to deliver active components to consumers especially people with ailments. This is possible by encapsulation technology. This is an advanced technology which is growing in the pharmaceutical, cosmetic, food and printing industry (Heinzen, 2002). Encapsulation can be defined as a technique to coat an active ingredient or a mixture of active materials in a system (Madene et al., 2006). The system or coating material is called shell, wall, material, carrier or encapsulant while the active ingredient that is coated is known as the active material or core material. In food industry, the materials that are normally used as the core material are flavours, colourants, aroma compounds, fats and oils, vitamins and minerals (Shahidi and Han 1993). Enhancement of the quality of food through encapsulation technology has gained increasing importance in the manufacture of health food or functional food. The use of encapsulation technology to achieve a target of flavour release and some other functions encourages researchers to study the mechanisms of flavour release and make enhancement on the existing encapsulation technology. Similar emphasis is given in the pharmaceutical industry where encapsulation of drugs has been explored extensively in order to improve the therapeutic performance of drugs. The reasons for applying encapsulation technology in the industries mentioned are summarised in Table 1.1.

Table 1.1: Reason of the encapsulation technology. (Adapted from Finch and Bodmeier, 2005).

Reason	Description
Controlled release	Controlling the release of the active material in a carrier material to have various release profiles. This reason is mainly applied to the food and pharmaceutical industry.
Protection of core material against the atmospheric condition	Some of active ingredients are sensitive to the atmospheric condition such as moisture, atmospheric oxygen and temperature. Encapsulation can prevent any active materials from direct contact to the atmospheric condition and thus increase its functionality.
Protection of hygroscopic core contents	Flowability and direct compressible nature of hygroscopic core materials such as hygroscopic B group vitamins can be improved with iron phosphate by microencapsulating this core material before compressing it into tablets.
Masking of taste and odour	Compounds with unpleasant taste and odour can be masked by microencapsulation in hard gelatine capsules or by incorporating the unpleasant compound in sugar or film-coated tablets.
Flavour and aroma release	Encapsulation can control the release profile of

control	flavour and aroma at the appropriate or required condition in the human mouth. Besides, aroma or odour is controlled in fragrance to achieve a target of release time.
Other reason	Microencapsulation can protect the core materials from physical and chemical damage during the production process.

There are various methods of encapsulation to produce microcapsules and the variations of method depends on the core and wall polymer properties, the required wall thickness, rate of release, permeability, size of capsules and other physical properties (Finch and Bodmeier, 2005). The process of choosing a suitable method is also influenced by the economical aspect especially in the operation and maintenance cost involved during manufacturing. In principle, suspending media is one of the factors that influence the method of microencapsulation. Table 1.2 shows the process of microencapsulation and the range of size that can be produced while Table 1.3 shows the methods that can be used for different suspending media. Presently, encapsulation system in pharmaceutical industry is designed with the incorporation of mucoadhesive materials in order to achieve the target of release at specific area in the body such as in the mouth, nose, gastrointestinal (GI) tract and eye. Some of the current products that use mucoadhesion are Orabase by Bristol-Myers-Squibb (a mucoadhesive mouth paste used for mouth ulcers treatment) and Buccastem by Reckitt Benckiser (management of nausea with a mucoadhesive tablet that can adhere to the top of the mouth).

Table 1.2: Microencapsulation processes. (Source: Finch and Bodmeier, 2005).

Microencapsulation Process	Core Material	Approximate Particle Size, μm
Phase Separation (coacervation)	Solids and liquids	2-1200
Interfacial Polymerization	Solids and liquids	2-2000
Spray Drying and Congealing	Solids and liquids	6-600
Solvent Evaporation	Solids and liquids	5-500
Centrifugal Extrusion	Solids and liquids	1-5000
Air Suspension	Solids	35-5000

Table 1.3: Microencapsulation process for different suspending media. (Adapted from Finch and Bodmeier, 2005).

Suspending Media	Process
Liquid	<ul style="list-style-type: none"> - Complex coacervation - Polymer-polymer incompatibility - Interfacial polymerisation - Desolvation - Solvent evaporation from emulsion - Gelation - Pressure extrusion - Supercritical Fluid Technology

Gas	<ul style="list-style-type: none">- Spray drying and congealing- Fluidized Bed Process (including Wurster process)- Coextrusion vacuum coating- Gelation- Electrostatic deposition
-----	--

Treatment of diseases is effective if drug can stay at the optimal site of absorption long enough to be absorbed into the systemic circulation. For orally administered drugs the major site of drug absorption is the small intestine (Bowman & Rand 1980). Drug delivery systems utilise adhesive properties of some biopolymers to increase residence time hence enhancing their bioavailability. In view of the potential advantages, mucoadhesive polymers and drug delivery systems are presently being explored extensively by many researches especially in the pharmaceutical industry. Focuses of study are mainly on the qualitative and quantitative evaluation of mucoadhesion of polymers and the methods of formulation of drug delivery systems. In recent years various methods to assess mucoadhesiveness of polymers have been developed and these can be categorised into two categories: the direct assay methods (e.g. tensile test, atomic force microscopy, quartz crystal with dissipation and flow through technique) and the indirect molecular mucin-based assay method (e.g. rheology). Evaluating and understanding the behaviour of mucoadhesive biopolymers is a crucial initial step in the development of formulations.

1.2 Literature Review

1.2.1 Mucoadhesion

Adhesion can be defined as the tendency of two or more materials to stick together by a specific driving force. Mucoadhesion is a specific case of adhesion of two materials in which one of the surfaces is the mucosal surface (e.g. mucosal membrane or mucous layer) caused by interfacial forces (Smart, 2005). The surfaces are held together by chemical bonds, interlocking action or both through a combination of mechanisms. Generally, there are five types of chemical bonds that create the interaction between mucoadhesive materials and mucous layer. These are the ionic bonds (electrostatic attraction between oppositely charged particles), covalent bonds (sharing of electrons between atoms in a molecule), hydrogen bonds (attraction between hydrogen atom bonded to oxygen, nitrogen or fluorine in one molecule and the electronegative atoms in another molecule), van der Waals forces (dipole-dipole attraction and dipole-induced dipole attraction in polar molecules and dispersion forces for non-polar molecules) and hydrophobic interactions (this type of interactions occur when non-polar groups are present in aqueous solution) (Smart, 2005). Fundamentally, the primary bonds (ionic and covalent bonds) are stronger than the secondary bonds (hydrogen bond, van der Waals forces and hydrophobic interaction).

1.2.1.1 Theory of Mucoadhesion

Basically, theories that explain the fundamental adhesion can be used to explain mucoadhesion process. There are six theories for adhesion that have been extensively described and discussed in the literature. These are electronic theory, the diffusion theory, the adsorption theory, the mechanical theory, the wetting theory and fracture theory (Peppas and Sahlin, 1996; Ahuja and Khar, 1997; and Smart, 2005,). Each of the theory has its limitations and in view of this, it has been proposed that some of the interactions between adhesive substances with mucous layer involved combination of these theories. According to the electronic theory, mucoadhesion occurs as a result of the transfer of electrons between mucous layer and the mucoadhesive platform resulting in the formation of a double layer electronic charge at the interface. In this theory, the electrostatic forces are critical in generating bond adhesion. This theory is in effect when the mucoadhesive substances are oppositely charged as opposed to the mucous layer (Singh et al., 2013). The diffusion theory is commonly employed to explain mucoadhesion when there is a concentration gradient acting as a driving force. This time dependent process involves the interpenetration and entanglement between the mucoadhesive polymer chains with the glycoprotein chain network of the mucous layer (Andrews et al., 2009). The strength of this effect depends on the diffusion coefficient and the contact time between the mucoadhesive polymer and the mucous layer. The bonding formed is described as a semi permanent bond (Smart, 2005) and the degree of cross linking is also an important factor to the bonding strength (Dodou et al., 2005). According to Mathiowitz et al (1999), strength of the adhesion for mucoadhesive polymer will be at the maximum when the penetration depth reached the equivalent polymer chain size. Figure 1.1 shows the

illustration of interpenetration (diffusion) theory when the mucoadhesive substances are in contact with the mucous layer. The interpenetration depth of polymer into mucin networks can be estimated by Equation 1.1. Where I is the depth of interpenetration of polymer, t is the contact time, and D_b is the diffusion coefficient of the mucoadhesive material in the mucous.

$$I = (tD_b)^{1/2} \quad (\text{Equation 1.1})$$

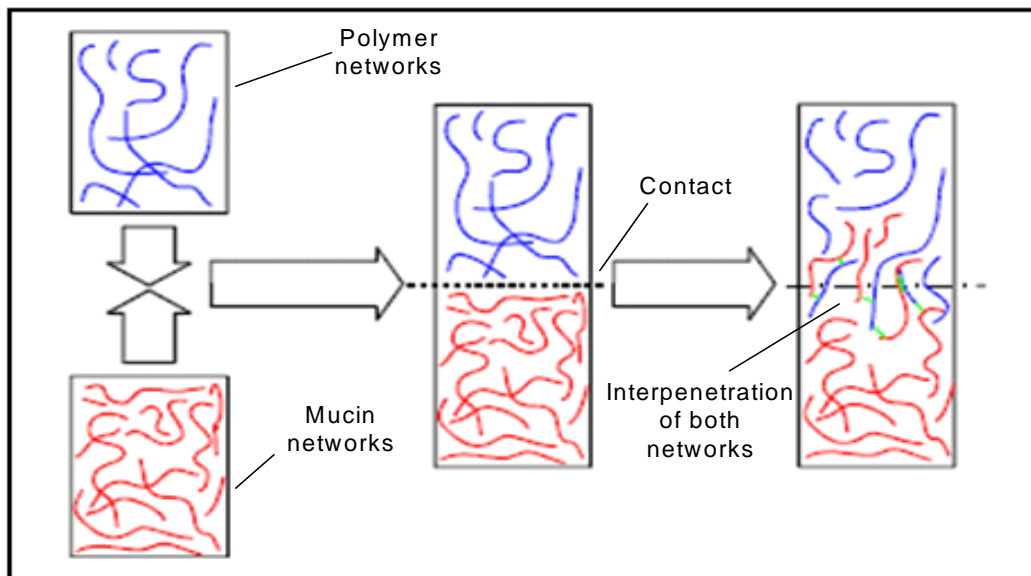


Figure 1.1: The interpenetration or diffusion theory illustration where there are three stages involved for the interaction between a mucoadhesive polymer and mucin glycoprotein. (Source: Smart, 2005).

Adsorption theory is believed to be the main contribution in adhesion phenomenon (Smart, 2005). This theory suggests that mucoadhesion is the result of various surface interactions through the formation of primary bonds (ionic and covalent bonds) and secondary bonds (hydrogen bonding and van der Waals forces,

hydrophobic interaction). Adhesion caused by the interlocking of liquid adhesive into irregularities on a rough surface is known as mechanical mechanism. Rough surface will provide wider or larger contact area between adhesive material and the surface of contact which results in increase of viscoelastic and dissipation of energy during joint failure (Derjaguin et al., 1977). Wetting properties of some adhesive materials is the basis of another theory which is the wetting theory. Wetting or spreading properties of the mucoadhesive polymers promote adhesion through wetting that occurs due to the ability of material to spread spontaneously onto the surface for the adhesion effect. The spreadability can be measured based on the spreading coefficient (S_{AB}) and this value can be calculated using Equation 1.2.

$$S_{AB} = \gamma_B - \gamma_A - \gamma_{AB} \quad (\text{Equation 1.2})$$

Where γ_A is the surface tension of the liquid A , γ_B is the surface tension of solid B and γ_{AB} is the interfacial energy between the solid and liquid. The value of S_{AB} should be positive for the liquid to spread spontaneously. Wettability or spreadability is also linked to the contact angle (θ) between the mucoadhesive polymer solutions and the mucous (mucin) layer. Figure 1.2 shows the influence of contact angle on the strength of mucoadhesion. Smaller contact angle would give better spreadability and wettability of the mucoadhesive polymer substance on the mucous layer thus increasing the adhesion strength and vice versa.

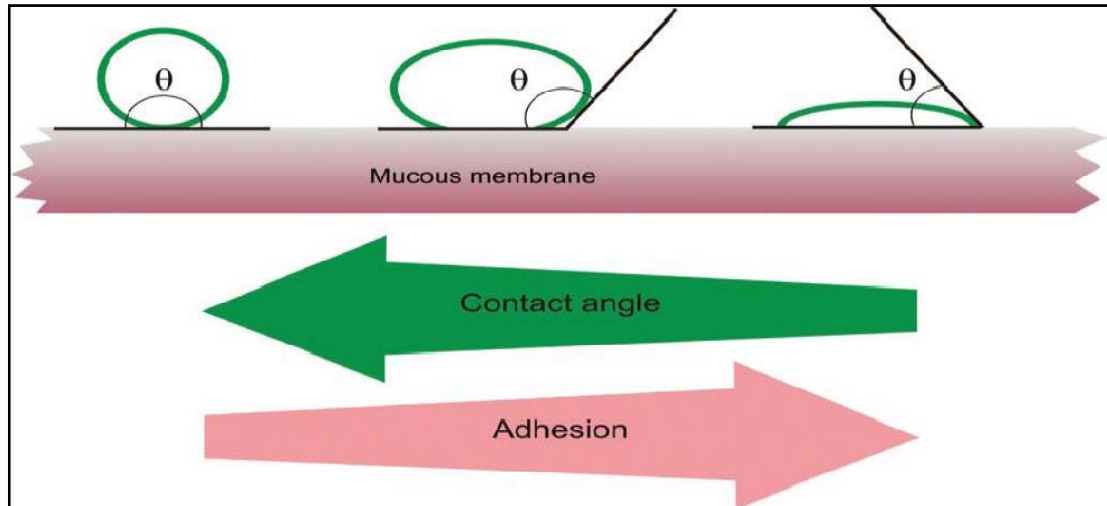


Figure 1.2: An illustration of the influence of the contact angle on the strength of mucoadhesion. (Source: Singh et al., 2013).

Another theory is the fracture theory where this adhesive bond occurred at the weakest point (Smart, 2005) and it depends on the cohesion of the mucous and the mucoadhesive polymer. Andrews et al. (2009) described that this adhesive bond is related to the force required to separate mucous and mucoadhesives polymer or in other word known as work of adhesion. The fracture theory is the most used theory to describe mucoadhesion. The detachment force is the maximum energy required for the separation or rupture of the two adhered substances (mucoadhesive polymer and mucous). The separation could happen at the interfacial of polymer-mucous, in the polymer structure or in the mucous network (Figure 1.3).

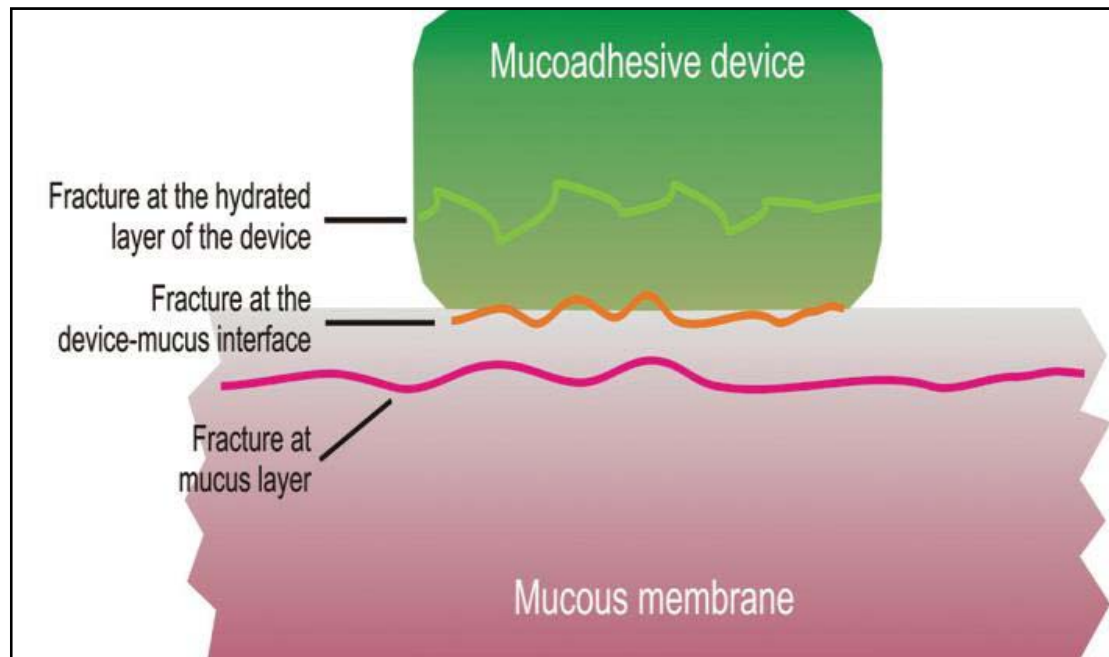


Figure 1.3: Illustration of fracture mechanisms. (Source: Singh et al., 2013)

1.2.1.2 Mechanism of Mucoadhesion

Mechanism of mucoadhesion involves two stages as proposed in the literature which are the contact stage and the consolidation stage (Wu, 1982). Contact stage can be defined as the intimate contact (wetting) between mucoadhesive materials with the mucous layer either from good wetting of the mucoadhesive surface or from the swelling of the mucoadhesive. Contact stage is facilitated physically or mechanically such as during delivery of food or any drug dosage in the oral cavity, eye and vagina (Smart, 2005). Contact materials will allow some interaction and deposition of particle that has adhesive effect to the targeted area (mucous layer). In the consolidation stage, the interpenetration of mucoadhesive polymer chains into mucous networks would be effective when a strong or prolonged adhesion is needed in the system and this stage occurred due to the various

physicochemical interactions. Figure 1.4 shows the stages of mucoadhesion while Figure 1.5 describes some scenarios where the mucoadhesion can occur.

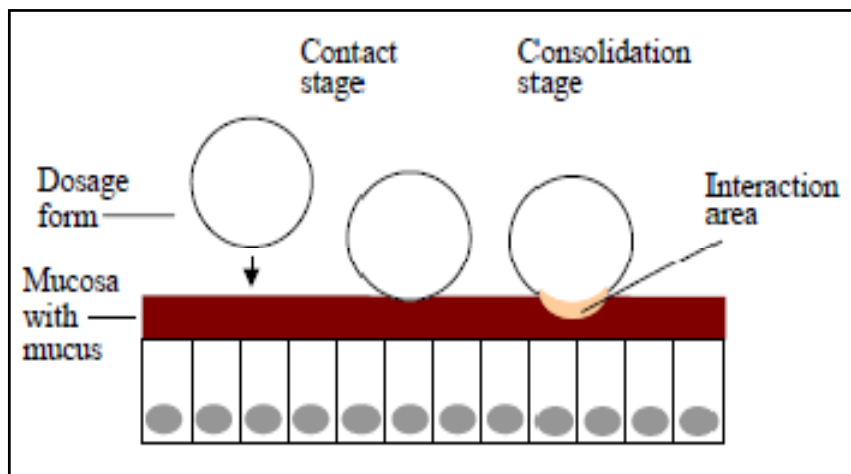


Figure 1.4: Contact stage and consolidation stage in the mucoadhesion phenomenon.

(Source: Smart, 2005).

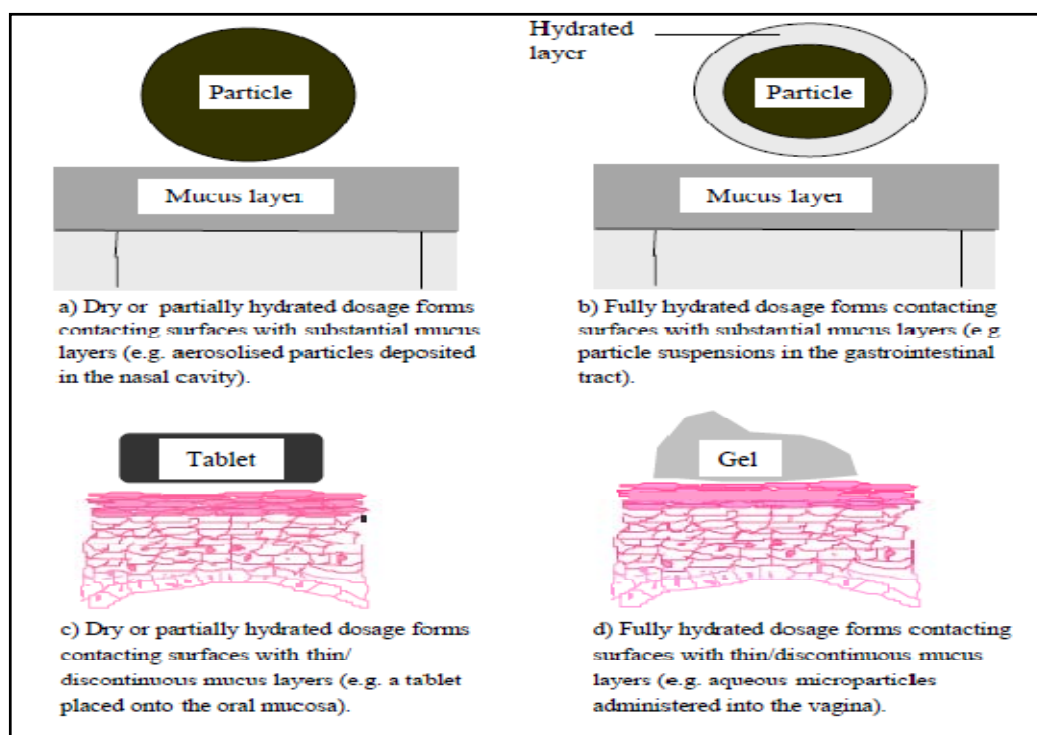


Figure 1.5: Some scenarios where mucoadhesion can occur. (Source: Smart, 2005)

The detachment of adhesion will normally occur at the weakest region of the binding and the strength and durability of the adhesive joint will depend on the cohesive nature of the weakest region (Smart, 2005). When the mucoadhesive material is overhydrated, it will be easily removed by forming slippery mucilage in between the mucoadhesive material and the mucin glycoprotein (Chen and Cyr, 1970). Therefore in order to prolong the adhesion, controlling the rate and extent of hydration between the mucoadhesive material and mucous layer are required. Other strategies such as cross-linking (Hägerström and Edsman, 2001) and introducing hydrophobic group (Inoue et al., 1998) have also been proposed to achieve prolong adhesion.

1.2.1.3 Factors Affecting Adhesion

Generally the factors affecting mucoadhesion can be divided into three categories. The first category is the factors contributed by mucoadhesive polymers or substances. This factor is affected by the chemical and physical properties of the mucoadhesive polymers such as its molecular weight, flexibility of the chains, concentration of mucoadhesive polymer in the system, degree of hydration (wettability and contact angle properties), molecular structure containing hydrogen bonding groups, molecular charge (anionic or cationic) and crosslinking capacity (Chen and Cyr, 1970; Park, 1983; Smart et al., 1984; Peppas and Buri, 1985). The description of these factors is summarised in Table 1.4. The second factor that affects mucoadhesion strength is the environmental aspect of the applied or targeted area. This factor includes pH of the substance and the surrounding, initial applied strength, contact or holding time, the moisture level, and existence of the different ionic

strength (Gu et al., 1988; Lenaerts and Gurny, 1990). Table 1.5 gives the description of each environmental factor. The physiological aspect of the human body or targeted area is also affecting the interaction between the mucoadhesive polymers with mucous layer. This factor is contributed by the reaction of mucous layer on the specific dosage or applied delivery systems, the condition (health) state, different region of mucous layer in body and the disease experienced by the patient and movement of the located tissue (Allen et al., 1979; Lehr et al., 1991; Lehr et al., 1992; Nikhil and Bhattacharya., 2009; Punitha and Girish., 2010). The description of physiological factors is summarised in Table 1.6.

Table 1.4: The polymer factors that affecting the mucoadhesion strength.

Factor	Description
Polymer molecular weight	There is an optimum molecular weight of polymer that can promote a good adhesion. The optimum value is in the range of 1×10^4 to 4×10^6 Da. Lower molecular weight would provide better flexibility of polymer chain and increase the interpenetration process whilst higher molecular weight will increase the entanglement polymer structure with mucin network.
Flexibility of polymer chains	It is important for the polymer to have a good flexibility chain to increase the degree of diffusion. Water soluble polymers that are crosslinked might have lower flexibility and thus will decrease the depth of interpenetration.
Degree of	Higher wettability is important during the first stage (contact)

hydration	with mucous layer. However the degree of hydration must be controlled to avoid formation of slippery mucilage that will reduce adhesion.
Polymer concentration	Polymer concentration represents the amount of available network for the interaction. Higher concentration will increase the adhesion strength but there is a limiting concentration for appropriate interaction.
Hydrogen bonding capacity	Hydrogen bonding is one of the attractive bonds formed in the mucoadhesion process. Higher capacity of hydrogen bonding site would increase the total adhesion with the mucin sialic acid group at carbohydrate side chain.
Molecular charge	Cationic nature of the polymer favours the interaction due to electrostatic attraction as mucin has negative charge. Electrostatic bonding is believed to be the strongest force attributed to mucoadhesion.
Crosslinking density	Higher crosslinking density in polymer network would decrease the adhesion due to insufficient polymer network mobility.

Table 1.5: The environmental factors that affecting the mucoadhesion processes.

Factors	Description
Surrounding pH	Many researchers have found that pH has a significant effect on the mucoadhesion because the charge of polymer and mucous layer will have different charge density due to deionisation process at different pH value. Maximum adhesion could be achieved at isoelectric point of a specific polymer.
Applied pressure or force	The amount of pressure or force applied to locate the delivery systems affects the depth of interpenetration during mucoadhesion. With suitable strength and contact time, a polymer will have mucoadhesive effect even though it has no mucoadhesion capability.
Contact time	Longer contact time would promote more interaction between the mucoadhesive polymers with mucous layer. The wetting and interpenetration will increase with increasing of contact time. However, there is a limiting time that could be applied during the contact.
Moisture level	The level of moisture is affecting the degree of swelling for the delivery systems especially in delivery of solid dry dosage. The moisture level is different at different parts of body.
Ionic strength	Ionic strength is affecting on both polymer structure and mucin network. The conformation of the structures is different at different ionic strength.

Table 1.6: Physiological effect on the mucoadhesion strength.

Factors	Description
Mucous layer reaction	Mucous turn over is dependent on the nature of the applied delivery systems and other factors such as the presence of food.
Health condition	The physiochemical properties of mucous layer are known to change during disease conditions such as common cold symptom, eye inflammation, fungal infection and others.
Different region of mucous layer	Different region in human or animal body is composed of different nature or condition of mucous layer. This is due to different ionic strength and pH value such as pH 6-7 in the mouth and acidic pH in the GI tract.
Movement of the located tissue	Movement occurs when there is an activity during the consumption of delivery systems such as speaking, drinking, peristalsis process of gut or esophagus and body movement.

1.2.2 Mucoadhesive Polymer

Mucoadhesive polymer is defined as a natural or synthetic polymer that is capable to interact with the mucous layer through several mechanisms (Yadav et al., 2010). The mucoadhesive polymers have recently gained a great deal of attention, in pharmaceuticals, in view of their potential in increasing residence time (Säkkinen et al., 2006, Cui et al., 2006; Andrews et al., 2009) and maintaining a high concentration gradient of drug across the epithelium (Govender et al., 2005). The usefulness and the ultimate bioavailability of a drug are, to an extent, determined by the length of time it is present at or in the desired site of action. Mucoadhesive can increase the residence time and hence potentially increase the bioavailability of a drug. Additionally, mucoadhesives have proven to increase the permeability of the epithelial wall (Lehr, 2000). This has been explained by their tendency to dehydrate the mucous layer causing the cells of the epithelium to ‘shrink’ and hence open up the tight junctions.

Most of the mucoadhesive materials are polymers which are composed of polar chemical functional groups such as hydroxyl (-OH), carboxyl (-COOH), amide (-NH) and sulphate (-SO₄H) groups that are able to interact with the mucin glycoprotein. Examples of mucoadhesives include the chitosan, carbopols, sodium alginate and others which have been extensively studied in the pharmaceutical application. Mucoadhesives have been formulated into several forms such as tablets, patches, and microparticles.

Generally, the mucoadhesive polymers can be divided into traditional and secondary advanced polymers. There are three types of traditional polymer used as a carrier in drug delivery systems. These are the anionic polymer (negatively charge), cationic polymer (positively charge) and non-ionic polymer. Anionic polymers are the most widely used in the formulation of drug delivery system. These polymers consist of carboxyl and hydroxyl group that can form strong hydrogen bonding with the sialic acid group in the mucin structure with the help of interpenetration and entanglement of the networks. Some examples of anionic polymers that have been investigated as potentials for mucoadhesives are pectin (Grabovac, 2005; Thirawong et al., 2008; Sriamornsak and Wattanakorn, 2008), sodium carboxymethylcellulose (CMC) (Andrews, 2009), sodium alginate and modified poly-acrylic acid (PAA) (Cleary et al., 2004; Wittaya-areekul et al., 2006; Sriamornsak et al., 2008; Senthil et al., 2011). Pectin is a polymer of α -D-galacturonic acid with 1-4 linkages (Aspinal, 1980). The acid groups along the chain are largely esterified with methoxy groups in the natural product. There can also be acetyl groups present on the free hydroxyl groups. Alginate is a polymer of alternating blocks of 1-4 linked α -L-guluronic and β -D-manuronic acids and sodium carboxymethylcellulose (CMC) is like other cellulose ethers which can be manufactured by replacing the hydroxyl groups of the cellulose molecule with other ether groups (Cerqueira et al., 2013). Figure 1.6 shows the molecular structure of some mucoadhesive polymers.

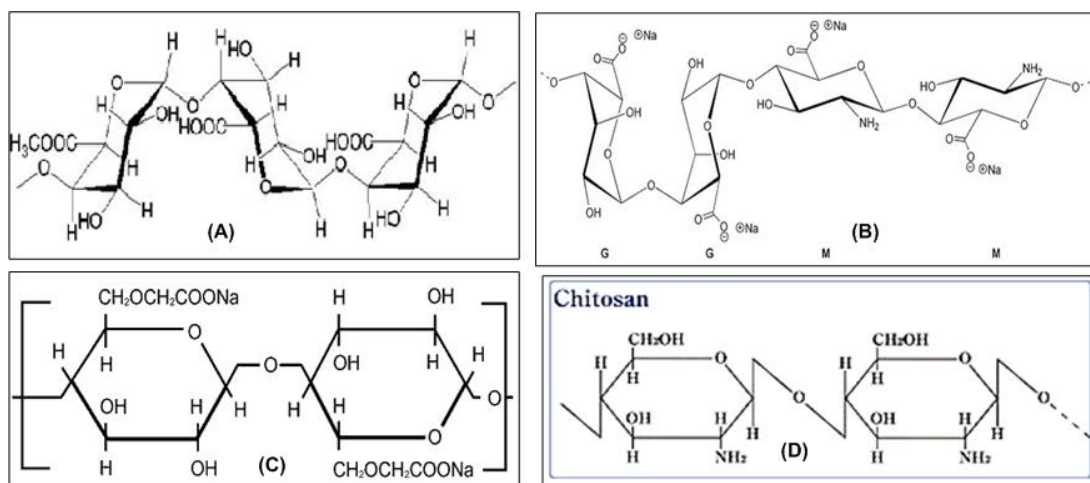


Figure 1.6: Molecular diagram of different mucoadhesives (A) Pectin, (B) Sodium alginate, (C) Sodium carboxymethylcellulose (CMC) and (D) Chitosan.

Cationic polymers have interaction with mucous layer mainly through electrostatic interaction due to the nature of negatively charged mucin network. The most popular cationic polymer used in the formulation is chitosan (Sogias et al., 2008) where the electrostatic interaction occurs between the amino groups with sialic acid group. Sogias et al. (2008) have reported that besides the electrostatic reaction, the mucoadhesiveness of chitosan is also due to presence of hydrogen bonding and hydrophobic effect. They have found that the turbidity analysis shows increasing of interaction up to ratio of 0.4 g/g (polymer/mucin) at pH 7 before the value started to drop due to excess of chitosan that caused the mucin network to disaggregate. Nonionic polymers such as hydroxypropylmethylcellulose, hydroxyethylcellulose and methylcellulose have a weaker mucoadhesion interaction as compared to anionic polymers (Mortazavi and Moghimi, 2003; Fröhlich and Roblegg, 2014). Table 1.7 shows some of mucoadhesive polymers with their mucoadhesion strength.

The disadvantage of traditional mucoadhesive polymer is the interaction could occur at any site of mucous layer rather than at targeted area which is known as non-specific interaction (Singh et al., 2013). This problem could be solved with invention of novel second generation mucoadhesive polymers that can work or interact at specific targeted area. The most common second generation polymers used in pharmaceutical is lectin (Lehr, 2000) and thiolated polymers (Dodou et al, 2005; Andrews et al, 2009). Different lectin molecules are capable to interact with different region of mucous layer in the body with the specific sugar activity. Meanwhile, the thiolated polymers consist of thiol groups that allow the formation of covalent bonds between cysteine-rich sub domains with mucous layer (Albrecht et al., 2006) and formation of disulphide bonds (Andreas et al., 2005).

Table 1.7: Example of mucoadhesive polymers. More (+) symbols indicate stronger adhesion. (Source: Singh et al., 2013)

Polymer	Bioadhesion Strength
Carbopol 934	+++
Carboxymethylcellulose	+++
Poly(acrylic acid /divinyl benzene)	+++
Tragacanth	+++
Sodium alginate	+++
Hydroxyethylcellulose	+++
Guar gum	++
Gelatin	++
Gum Karaya	++
Thermally modified starch	+
Pectin	+
Chitosan	+
Acacia	+
Polyethylene glycol	+
Psyllium amberlite	+
Hydroxypropylcellulose	+
Polyvinyl pyrrolidone	+

1.2.3 Emulsion and Gel Particles

Emulsion could be defined as the mixture of two or more liquids that are not mixable such as oil with water. Emulsion has been used widely in pharmaceutical and food industry as delivery systems. There are some examples of branded products which are delivering drugs using emulsion as carrier such as Amphotericin B, Diazemuls®, Vitalipid®, prostaglandin E and Diprivan® (Collins-Gold et al., 1990). Generally, there are two types of emulsion which are oil in water (O/W) where water is the continuous phase and water in oil (W/O) where oil acted as continuous phase. O/W emulsion is normally used in pharmaceutical for oral administration while for certain foods such as butter and salad dressings, W/O emulsions are used. Microemulsions have a size range of 0.1–5 µm with an average of 1–2 µm and nanoemulsions have a size range of 20–100 nm. Microemulsions are thermodynamically stable whilst nanoemulsions are kinetically stable (McClements, 2012). There is also a more complex structure of emulsion called the double layer or multiple emulsions (O/W/O and W/O/W). Double emulsion has a great potential usage in pharmaceuticals industry as controlled release delivery systems of drug (Garti, 1997). The stability of emulsions is a crucial factor for the emulsions to entrap the active ingredients and exist in stable form and withstand the environmental effect such as pH and temperature. This is important as for the ability of emulsions to control the release profile of active ingredients even when there is a change in the nature of the surrounding. Besides, the life span during storage is also affected by its stability.

Generally, the factors affecting the emulsions stability are the type and concentration of emulsifier, droplet size, environmental pH and ionic strength, viscosity, addition of stabilizer, heating and cooling process and container movements (Vaclavik and Christian, 2014). Partial breakdown of the emulsion structure happened during the storage which leads to separation between oil and water phase (coalescence process). This process is governed by four mechanisms which are creaming, sedimentation, flocculation and disproportionation as shown in Figure 1.7. In order to overcome the rapid rate of breakdown process of emulsion, emulsifiers and stabilizers were used in the formulation. Stabilizers and emulsifiers are able to reduce the interfacial tension between oil and water (Leroux et al., 2003). Some food grade mucoadhesive polymers have been used as emulsifier and stabilizer of emulsion in food and pharmaceutical industries such as pectin (Leroux et al., 2003), sodium alginate (Pongsawatmanit et al., 2006; Pallandre et al., 2007) and sodium carboxymethylcellulose (Diftis and Kiosseoglou, 2003). The application of food grade mucoadhesive polymers as emulsifier in emulsion formulation has an advantage to act as sustaining controlled release delivery system due its mucoadhesion properties. Figure 1.8 shows a model of stabilizing the emulsions using pectin proposed by Leroux et al. (2003).

The droplet size of emulsions is an important factor as a carrier because it determines the total available surface area for the mass transport. In complex emulsion system, there are several factors affecting the emulsion droplets size such as concentration, viscosity and interfacial properties of emulsifier and composition of oil phase (Weiss and Muschiolik, 2007). Higher concentration of emulsifier would

produce finer or smaller size of emulsion droplet (Nikovska, 2012). In the case of mucoadhesion properties, higher concentration of mucoadhesive polymer will increase the strength of adhesion.

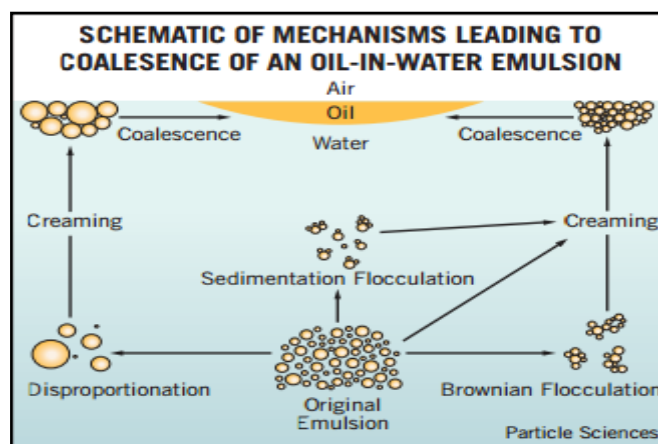


Figure 1.7: Schematic of Mechanism leading to coalescence of an O/W emulsion.

(Source: Particle Science, Drug Development Service article, 2011)

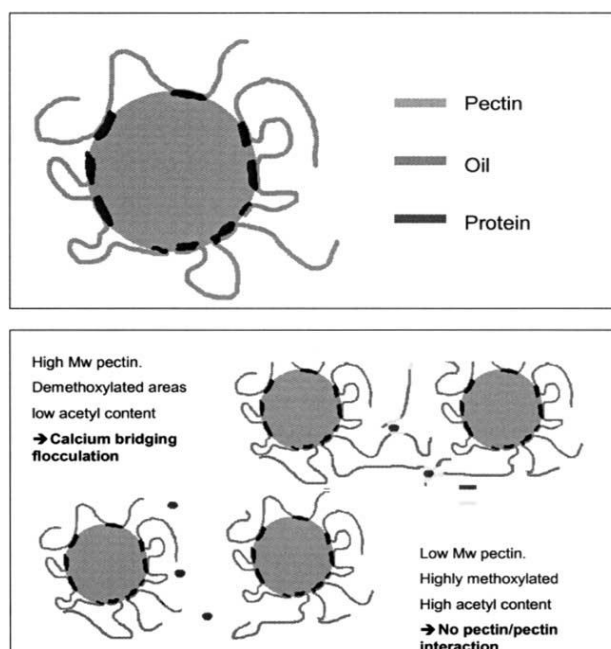


Figure 1.8: Hypothetical model of stabilizing the O/W emulsion droplets with pectin. (Source: Leroux et al., 2003).

Another medium that has been used widely as carrier in controlled delivery system is hydrocolloid gel particles. The interest of using hydrocolloids gel particles with the size of micrometer to nanometer is due to their biocompatibility, perception as natural materials and soft solid texture (Burey et al., 2008). There are several technique of producing hydrocolloids gel particles including ionic crosslinking gelation process of low methoxyl pectin (Fraeye et al., 2010), sodium alginate (Blandino et al., 1999) and chitosan (Ko et al., 2003), fluid agar gels by using shearing process (Norton et al., 1999), anionic and cationic polyelectrolyte gelation such as chitosan-pectin (Chang and Lin, 2000) and chitosan-alginate (Wittayaareekul et al., 2006) and others. The specific application of hydrocolloid gel particles as sustaining controlled release delivery system can be achieved by altering the particle size, mechanical strength, shape, microstructure and texture.

1.2.4 Mucous Layer and Mucin

Oral surface and gastrointestinal (GI) tract is generally covered by a mucous layer with a thickness of around 40 μm . The thickness can be determined by applying a filter paper strips on the mucous layer and the volume of saliva trapped in this paper will be used to calculate the thickness of the mucous layer on the human oral surface (Wolff and Kleinberg, 1998). Mucous layer contains 95% of water and mucins at 0.5-5% (van Aken et al., 2007). Mucins contain in the mucous layer have several roles in the human oral cavity such as tissue coating of oral hard and soft tissues, lubrication and modulation of oral flora (Tabak, 1990). Tabak (1990) explained that salivary mucins are high molecular weight glycoproteins sharing common features that include a peptide core (apomucin) and enriched with the

serine, threonine and proline residues and carbohydrate side chains (obligosaccarides). The obligosaccarides of mucins are link by the *O*-glycosidically to the theronine and serine. In the *O*-linked oligosaccharides of mucin may contain of galactose (Gal), fucose (Fuc), *N*-acetylgalactosamine (GalNAc), *N*-Acetylglucosamine (GlcNAc) and sialic acids (SA). There are two distinct structures of mucins which are MG2 (a low molecular weight species) and MG1 (multiple subunits covalently linked) and yield a suprastructure with an aggregate molecular weight in excess of 1 million. According to Zalewska et al. (2000), the MG2 is composed of three domains which are the N-terminal domain containing 144 amino acids, the central domain comprising of 145-283 amino acids in six tandem repeats of 12 amino acids each and the C-terminal domain contain 74 amino acids as shown in Figure 1.9 while Figure 1.10 shows the structure of MG1.

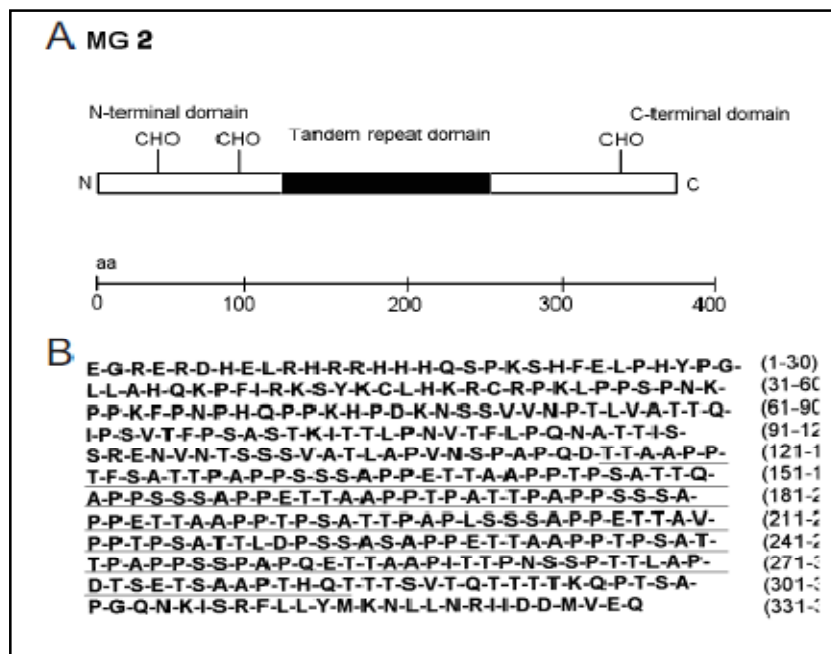


Figure 1.9: Structure of human salivary monomeric mucins (MG2)- the MUC7 gene product. (Source: Zalewska et al., 2000).

factors, mechanisms and kinetics of mucoadhesion. Besides, *in vitro* assessment is suitable to investigate the mucoadhesion properties of new formulation polymer. *Ex vivo* assessment is done using biological specimen from living organism (human and animal) such as GI tract, tongue and so on and measured using instrumental outside of the living organism meanwhile *in vivo* assessment is done by applying the formulation in live animal or human.

1.2.5.1 *In Vitro* Measurement

There are several *in vitro* measurement techniques that have been used to run the analysis on mucoadhesion such as morphological interaction by tensile test, physical interaction by rheological characterisation, kinetic absorptions by Quartz Crystal Microscopy with dissipation monitoring (QCMD) and surface interaction by Atomic Force Microscopy (AFM) and contact angle measurement (goniometer).

A) Rheological Characterisation

Physical interaction between mucoadhesive polymers with mucin can be characterised and measured by using rheology measurement. Intermolecular changes of polymer-mucin mixture could be contributed by chain interpenetration, entanglement or diffusion, chemical bonding and also electrostatic interaction will result in the different rheological properties (Pinhas and Peled, 2010). The rheological characterisation for assessment of mucoadhesion has been developed by Hassan and Gallo (1990). They have proposed an empirical equation to show the viscosity synergism which is showing the magnitude of viscosity change of polymer-mucin mixture compared to the total of polymer and mucin viscosity. The

experiment was done by mixing different ratio of polymer solution and mucin solution. The magnitude of viscosity change can be transformed as intermolecular frictional force per unit area. The same technique has been used by Thirawong et al. (2008) to study the mucoadhesion of different types of pectin with mucin in different media. They reported that high methoxy pectin has greater mucoadhesion strength compared to low methoxy pectin. Rossi et al. (2000) have characterised the interaction between chitosan hydrochloride with mucin by using viscometric measurement. The results obtained by them correlated with the turbidity experiments where a slightly acid-neutral pH favours the interaction between chitosan hydrochloride with mucin.

Besides the viscosity changes, rheological characterisation has successfully measured the changes of internal structure and viscoelastic properties of polymer and mucin solution alone with polymer-mucin mixture. The viscoelastic properties could be described through elastic moduli (G'), viscous moduli (G'') and loss tangent ($\tan \delta$). The assessment of the magnitude change in rheology parameters can be done with the same concept of viscosity synergism. Sriamornsak and Wattanakorn (2008) have studied the rheology synergism between pectin and mucin. They concluded that the mucoadhesion between pectin and mucin was due to molecular interpenetration thus reflects to the structural changes. The interactions between alginate and polyacrylate with mucin were studied by Fuongfuchat et al. (1996) using both parameters (viscometric and rheological synergism). They found that polyacrylate has stronger interaction with mucin as compared to sodium alginate. Polyacrylate-mucin mixture

shows gel like characteristic ($\tan \delta < 1$) and alginate-mucin mixture formed a viscous solution ($\tan \delta > 1$).

B) Tensile Test

The tensile test has been used to analyse the mucoadhesion between mucoadhesive polymers with mucin layer. The analysis could be done using texture analyser. The mucoadhesion could be evaluated through the measurement of maximum force (peak force) and total of work required to separate the mucoadhesive polymer with mucin substrate after certain time of contact (Thirawong et al., 2007). There are some parameters or variables that could be varied in order to study the influence of factors on mucoadhesion such as contact time, initial contact force and test environment (i.e. pH, ionic strength and temperature). Rossi et al. (1996) have made comparison between rheological and tensile test measurement on three different grades of sodium carboxymethylcellulose (CMC). They found that the mucoadhesion of CMC with mucin shown in tensile test was linked to information provided by rheological analysis where the work of adhesion was correlated with the value of rheological synergism. Hagesaether and Sande (2008) used tensile test in order to study the effect of plasticizer on the mucoadhesion of pectin film with mucin dispersion.

The tensile test is also done by using modified Wilhelmy plate method. This method was developed by Smart et al. (1984) using a glass plate and microforce balance. The experiment was done by measuring the force required to pull-off the dipped polymer coated plate from homogenised mucous in a container. The

maximum force to detach the plate from the mucous gel was recorded by microforce balance. The adhesion was expressed as a percentage of coated plate force to the clean plate. Through this experiment, they were able to measure mucoadhesion strength of several polymers and ranked accordingly based on the strength. Figure 1.11 shows the apparatus setting used by Smart et al. (1984) to measure mucoadhesion properties of several polymers.

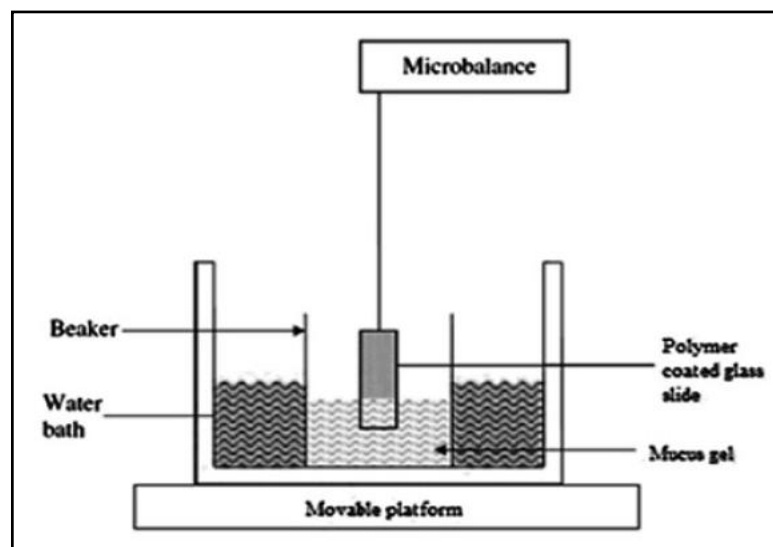


Figure 1.11: Modified Wilhelmy plate method apparatus for mucoadhesion study. (Source: Yu et al. 2014).

C) Atomic Force Microscopy (AFM)

Atomic Force Microscopy (AFM) is a powerful tool to be used to characterise the mucoadhesion at microscopic level through the surface morphology analysis and force (Drelich and Mittal, 2005). AFM has been utilized to study the mucoadhesion of some polymers. AFM is a sensitive technique for detecting and imaging bioadhesive polymers present on mucosal cell surfaces (Patel et al., 2000).

Patel et al. (2000) investigated the changes of the mucosal surfaces before and after the exposure with mucoadhesive polymer. The surface roughness of the cells was changed from smooth to higher degree of roughness due to absorption of mucoadhesive polymer into the mucosal cells. Deacon et al. (2000) investigated the characteristic of chitosan-mucin mixture in different ionic strength media through the molecular imaging analysis using AFM. They reported that the interaction between chitosan and mucin was driven by electrostatic and some hydrophobic effect. Sriamornsak et al. (2008) studied the mucoadhesion mechanisms of pectin with mucin with AFM imaging technique. They suggested that the mucoadhesion between pectin and mucin could be developed by adsorption mechanism or electrostatic repulsion.

Besides the imaging techniques, mucoadhesion force could also be measured using AFM. The colloidal probe measurement was developed by Ducker et al. (1991). This technique is done by using a colloidal-sized particle (most commonly a sphere) coated with material of interest to an AFM cantilever. The maximum force required to remove the colloidal probe after a certain time of contact with mucin layer was recorded by AFM. Cleary et al. (2004) have successfully investigated the detachment forces (adhesion) of polyether-modified poly(acrylic acid) (PAA) from mucin layer. They reported that hydrophobic interaction was the main contribution to the adhesion between PAA with mucin. Li et al. (2010) have proposed a new method to study the adhesion force with AFM by coating the AFM probe tip with chitosan-coated PLGA. Through this method, the measurement could be done at nano scale due to the smaller curvature radius of probe tip as compared to colloidal probe.

D) *Quartz Crystal Microscopy with Dissipation Monitoring (QCMD)*

The sensitiveness of QCMD in detecting the changes of mass absorbed on a layer has been utilized to study the kinetic adsorption of mucoadhesive polymer into mucin layer (Maheshwari and Dhathathreyan, 2006). The mass adsorbed on the mucin layer can be detected by the change of frequency and the nature of the layer after absorption can be interpreted by the change of energy dissipation value. The same concept is also applied in Surface Plasmon Resonance (SPR) in order to study the kinetic absorption. Chayed and Winnik (2007) investigated the mucoadhesive properties of polysaccharide based polymer to be used in oral drug delivery systems using QCM and SPR. They found a good correlation of data obtained from both instruments and conclude that the QCM is a sensitive equipment to investigate the mucoadhesive properties of biopolymers. They have observed different absorption rate of chitosan into mucin layer at different pH value due to different electrostatic interaction influenced by the ionisation process. Wang et al. (2007) have studied the effect of ionic strength on the absorption of pectin into the bovine serum albumin with QCMD. They reported that the frequency and dissipation value rapidly decreased with increasing of ionic strength above 0.02 M NaCl.

1.2.5.2 *Ex Vivo and In Vivo Study*

Ex vivo analysis involved a more complicated sample preparation from life stock and the life span of prepared sample is a critical issue. The properties and freshness of the prepared sample might be easily changed during storage. Dhawan et al. (2004) used small intestine from a rat to study the mucoadhesion of chitosan microspheres prepared with different methods. The rat was killed with an overdose

of barbiturate and the small intestine was removed and washed with physiological saline. The cleaned intestine was used immediately or within 2 days after storage at -15°C. The study was done by calculating the absorbed (retained) microspheres suspension by determining the amount of microsphere before and after the removal process using a Coulter counter. Thirawong et al. (2007) used GI tissue from different part of porcine GI tract. GI tract of slaughtered pig was removed and washed with deionised water and placed in a normal saline solution at 4°C. The sample was used within 6 hours from the time of preparation. For the *ex vivo* measurement, the tensile test was used to study the mucoadhesive properties of various pectins on the porcine gastrointestinal mucosa.

In vivo analysis for mucoadhesion characterisation was performed by monitoring the residence time of mucoadhesive polymer formulation in live human or animal. The *in vivo* analysis is able to give accurate information on the interaction. Besides, other pharmacokinetic data such as the release profile of formulated drug delivery system inside the targeted area can be obtained (Singh and Rana, 2012). Henriksen et al. (1996) studied the bioadhesion of chitosan coated liposomes on the eye of anaesthetised rat by observing the retention at different times. Säkkinen et al. (2006) used a technique called neuron activation-based gamma scintigraphy to evaluate the mucoadhesive effect of chitosan based microcrystalline formulation in human gastro-retentive system. They found that the interaction of the formulation was erratic and it is not reliable for gastro-retentive drug delivery systems.

1.3 Objectives of Study

The aim of this research include the following: (1) To assess, compare and correlate several *in vitro* methods for measuring mucoadhesive performance of a few mucoadhesive biopolymers with mucin. (2) To investigate the influence of several testing conditions on mucoadhesion using different *in vitro* instrumental techniques. (3) To modify *in vitro* analysis method to be used in mucoadhesion characterisation. (4) To design a simple experimental setup for qualification and quantification of mucoadhesive polymer formulation.

1.4 Significances of Study

The formulation of mucoadhesive delivery systems depend on the selection of suitable polymers with excellent mucosal adhesive properties and biocompatibility. The results of this study provide some insights into the choice of methods that can be used for the characterisation of mucoadhesive polymers towards the development of novel bioadhesive delivery system in the pharmaceutical and potentially in the food industry. The comprehensive description of the techniques discussed in this thesis could facilitate the selection of a characterisation method that meets the requirement of a specific study.

Chapter 2:

Methodology

2.1 Introduction

The techniques employed for mucoadhesion assessment in this study encompass various experimental methods. The description of the working principles and instrumental setup for each technique is discussed in details in this chapter.

2.2 Methodology

Mucoadhesion properties of pectin, sodium alginate, sodium carboxymethylcellulose (CMC) and chitosan were investigated using several instrumental techniques. Rheometer was used to study the flow change behaviour caused by the intermolecular interaction between mucoadhesive polymers with mucin. Mucoadhesion force measurement through modified Wilhelmy plate method and tensile test were carried out with Texture Analyser equipment. Atomic Force Microscopy (AFM) was used to measure the mucoadhesion forces (tack force and total of work) in different media or environments. Kinetic absorption study was carried out by using Quartz Crystal Microscopy with dissipation monitoring (QCMD) and rheometer. A flow cell was designed and fabricated for testing and investigating of mucoadhesion polymer formulation such as emulsion.

2.2.1 Rheometer

2.2.1.1 Working Principles

Rheometer is a device to measure the way in which a liquid, suspension, gel or slurry flows in response to applied forces. Rheometer has the advantage over normal viscometer as the device can measure the rheology parameters of fluid rather

than the single value of viscosity as measured by viscometer. Viscosity is the force required for fluid to resist the shear when there is friction between movement boundaries and fluid as shown in Figure 2.1. Sir Isaac Newton (ca. 1700) was the first to demonstrate with a mathematical description that fluid has resistance to deform and flow when a magnitude of stress is applied. The term used to describe this resistance to flow is viscosity and it refers to the internal friction of a moving fluid. Rheology can be defined as a science of deformation and flow of matter embracing elasticity and viscoelasticity under controlled testing condition. There are two types of rheometers: namely, the shear or rotational rheometers and the extensional rheometers. The shear rheometers measure the rheology parameters of fluid at controlled shear stress or shear strain while the extensional rheometers apply extensional stress or extensional strain.

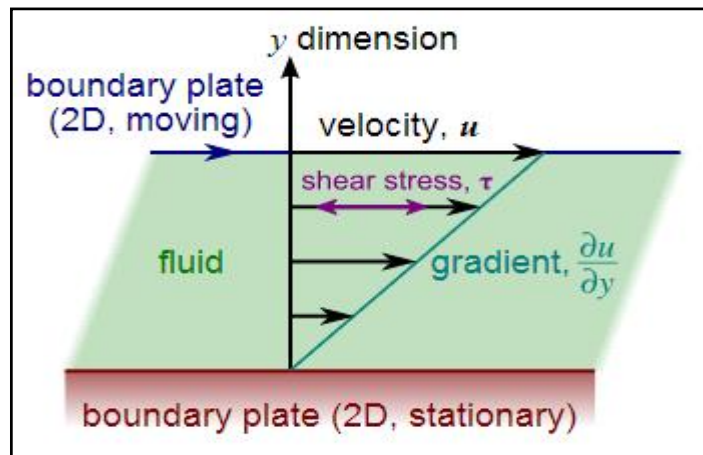


Figure 2.1: Laminar shear of fluid between two plates. (Source: Wikipedia website)

The rheometer measures the deformation in the non-destructive region of elastic or known as viscoelastic deformation. The actual behaviour of the sample can

be measured in a controlled stress situation. The three dimensional schematic diagram regarding the basic shear terms in the rheometry is shown in Figure 2.2. The term strain is defined as deformation in term of the displacement of particles composing a body and stress is the measurement of internal force acting within a body. Shear is defined as deformation of a body in one direction which is resulting from a force per unit area (shear stress) and having a perpendicular gradient (shear strain). The shear viscosity (η) can be calculated from Equation 2.1 which shows that this parameter is dependent on the temperature (T), pressure (p), time (t), shear rate ($\dot{\gamma}$) and physical-chemical structure of the sample.

$$\eta (T, p, t, \dot{\gamma}) = \frac{\tau}{\dot{\gamma}} \quad (\text{Equation 2.1})$$

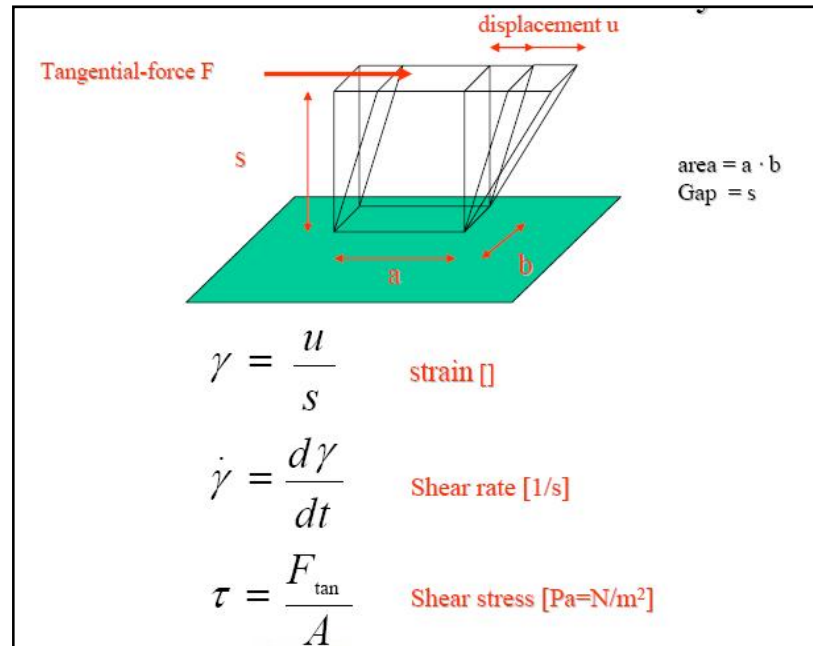


Figure 2.2: Three dimensional schematic diagram of basic term in the determination of shear viscosity. (Source: Malvern note, 2012)

Steady state flow curve is a technique to investigate the behaviour of fluid. Generally, fluid can be divided into two categories: Newtonian and non-Newtonian. The fluid is characterised as Newtonian fluid when its viscosity remains constant at different shear rate whilst for the non-Newtonian fluid, its viscosity changes with the shear rate. The description of the fluid behaviour and its example is shown in Figure 2.3.

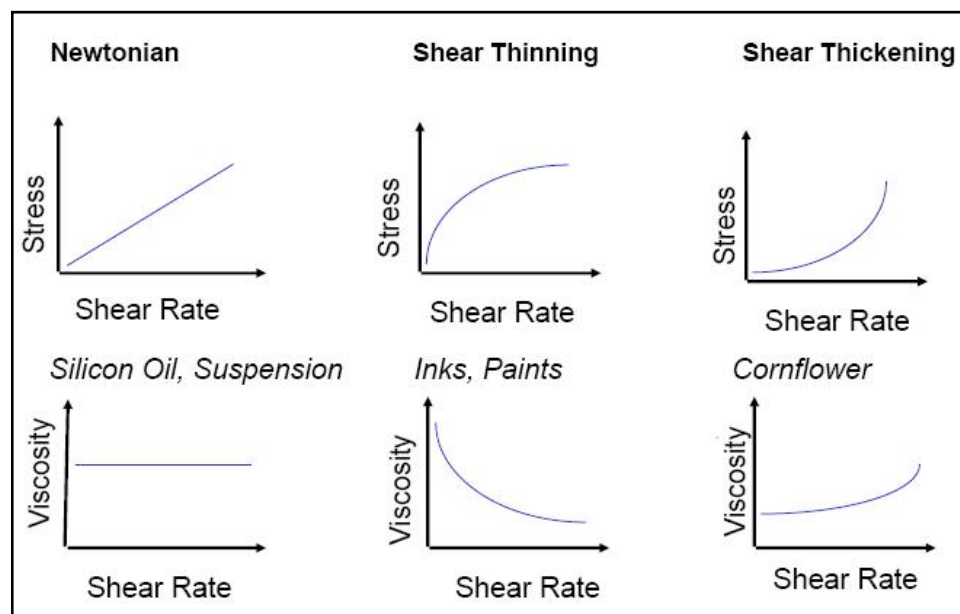


Figure 2.3: Steady state flow curve of fluid. (Source: Malvern note, 2012).

Besides viscosity, rheometer is capable to measure the viscoelasticity of fluids, semi fluids and solids. Viscoelasticity is the rheological property of material that exhibits both viscous and elastic properties when undergoing deformation. It can be measured using the standard experimental tool called the oscillatory rheology. The basic principle of oscillatory rheology is by applying a sinusoidal deformation (stress or strain) on the sample and measuring the response given by the sample

through the phase shifting or phase angle (δ) (Weitz et al., 2007). The viscoelastic parameter is described in Table 2.1 whilst Figure 2.4 shows the illustration of sample behaviour determined by the value of $\tan \delta$ (δ).

Table 2.1: Viscoelastic parameters.

Parameter	Description
$G^* = \text{Stress}^*/\text{Strain}$ $= G' + iG''$	Complex modulus (G^*) measures the overall resistance of the sample to deformation.
$G' =$ $(\text{Stress}^*/\text{Strain})\cos\theta$	Elastic or storage modulus (solid component) measures the elasticity of material. It refers to the capability of the sample to store energy.
$G'' =$ $(\text{Stress}^*/\text{Strain})\sin\theta$	Viscous or loss modulus (liquid component) is referring to the ability of sample in dissipating energy in the form of heat.
$\tan \delta = G''/G'$	Tan delta is measuring the material damping which is reflecting to the types of materials. The tan delta value indicates the strength of the internal network. When $\tan \delta > 1$, the sample is viscous and when $\tan \delta < 1$ the sample is elastic.

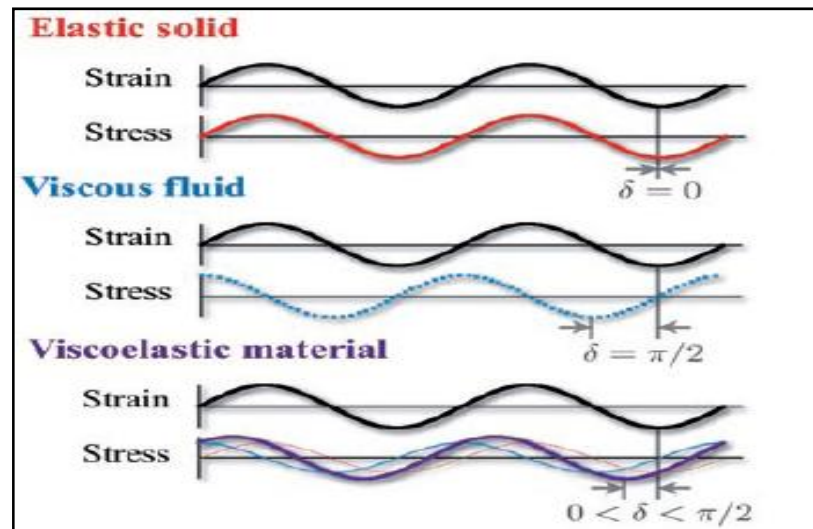


Figure 2.4: Schematic stress response to the strain deformation for elastic solid, viscous fluid and viscoelastic material. (Source: Weitz et al., 2007).

Figure 2.5 shows the schematic of the front of the AR rheometer. The behaviour of the sample is detected by the rheometer geometry and the signal is then transmitted to the optical encoder. The type of measuring geometry used is specific to the nature of the sample and the flow conditions generated. Figure 2.6 shows the basic selection of rheometer geometries depending on the viscosity of the sample. The concentric cylinder is used for very low viscosity material. The cone-plate geometry has the advantage of constant shear rate applied across the geometry and requires low volume of sample meanwhile the flat-plate geometry has flexible gap and is generally used for the low viscosity to soft solid samples such as pastes, gel and concentrated suspension. The geometries are made of metal or plastic. The stainless steel geometry is relatively heavy and has low thermal coefficient. It is suitable for amateur user as it is robust and suitable for most materials. The aluminium geometry is light with high thermal coefficient and its use is limited for

certain sample because of its chemical compatibility. The plastic (acrylic, polycarbonate and rigid PVC) is much lighter than metallic geometry. It has less inertial problem but again its use is limited to certain sample because of its chemical compatibility. Moreover, plastic geometry can only be used with temperature below 40°C.

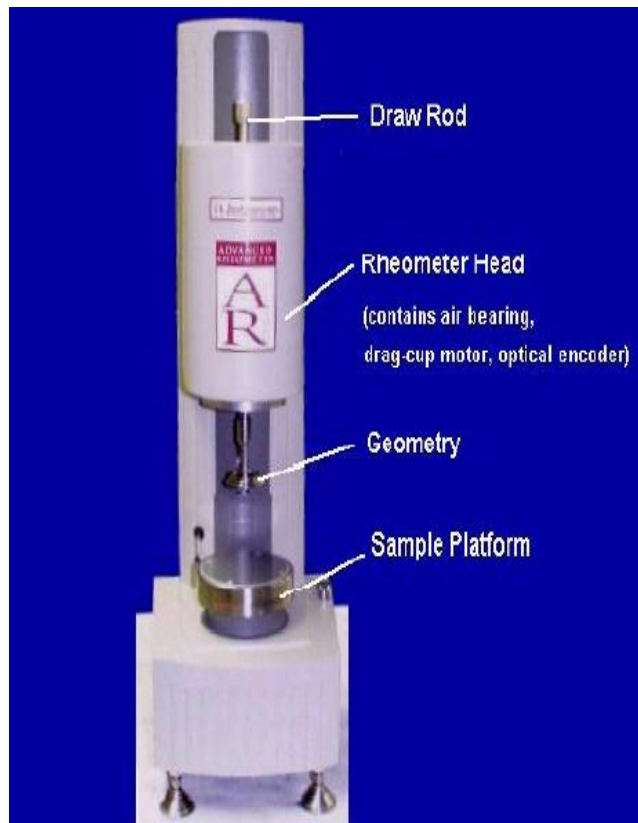


Figure 2.5: Schematic of the front of AR rheometer. (Source: AR 500/1000 rheometer hardware manual, 2000).

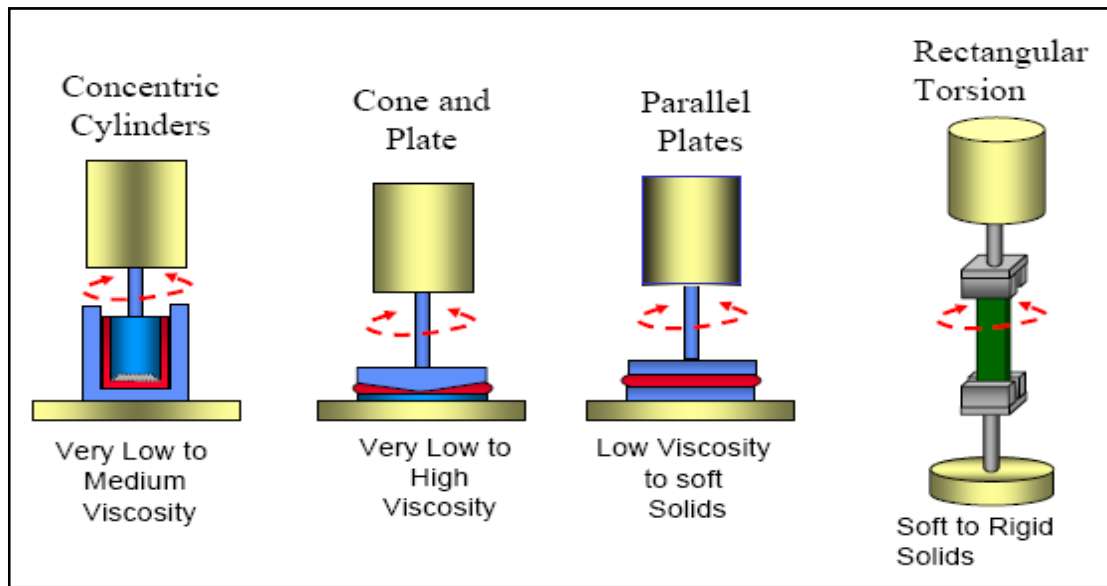


Figure 2.6: Selection of rheometer geometries. (Source: Somwangthanaroj, 2010).

2.2.1.2 Instrumental Setup

All rheological characterisation and kinetic interaction of mucoadhesive polymers with mucin experiments were carried out using an AR1000 Rheometer (TA Instruments, UK). The equipment was fitted with a water circulator (for temperature control) attached to the platform or peltier stage and connected to a compressed air supply ($P_{\max} = 2$ bar). The 60 mm acrylic flat-plate geometry was used for rheological characterisation and 40 mm aluminium steel flat-plate was used for production of agar gel particle experiment. All the data were recorded by TA Rheology Advantage software. The approximation volume of sample placed on the sample platform was calculated based on Equation 2.2 where V is the volume of sample, r is the radius of geometry and h is the gap between geometry with platform. The rotational mapping was done after each geometry replacement for the correction

of torque value by different geometries. After that, the auto zero gap step was performed for height calibration to determine the correct gap between geometry with platform. The solvent trap was used to minimise the evaporation effect on the sample through out the experiments. The procedures used in the experiments are described in Table 2.2. It is essential to ensure the appropriate volume of sample was used during the measurement as shown in Figure 2.7. The reproducibility of the data was determined by executing at least three replicates (with lowest standard deviation) of each measurement.

$$V = \pi r^2 h \quad \text{(Equation 2.2)}$$

Table 2.2: Experiment procedures were used in rheological characterisation experiment and production of agar gel particles.

Procedure	Description
Conditioning	Conditioning step is performed to allow the sample to reach equilibrium temperature set in the experiment. This step was performed each time before the next procedure.
Peak hold	Peak hold step is the measurement of viscosity of the sample at constant shear rate and temperature. This step was conducted for the investigation of the kinetic interaction during the mixing of mucoadhesive polymers with mucin layer.
Steady state flow curve	Steady state flow curve step is for the measurement of viscosity of the sample at different shear rate to investigate the rheological behaviour of the sample.
Stress Sweep	Stress sweep step is the measurement to determine the value of Linear Viscoelastic Region (LVR) of the sample. This step was performed in a range of oscillation stress with constant frequency.
Frequency Sweep	Frequency Sweep step is the measurement to determine the viscoelastic behaviour of the sample in LVR at different frequencies. This step was performed before the steady state flow curve step. It is to avoid the changes in internal structure caused by high shear rate applied in steady state flow curve step.

Temperature ramp	Temperature ramp step is the measurement of viscosity at constant shear rate and different temperature with fixed cooling or heating rate. This step was performed to investigate the formation of agar gel particles with different shear rate.
------------------	--

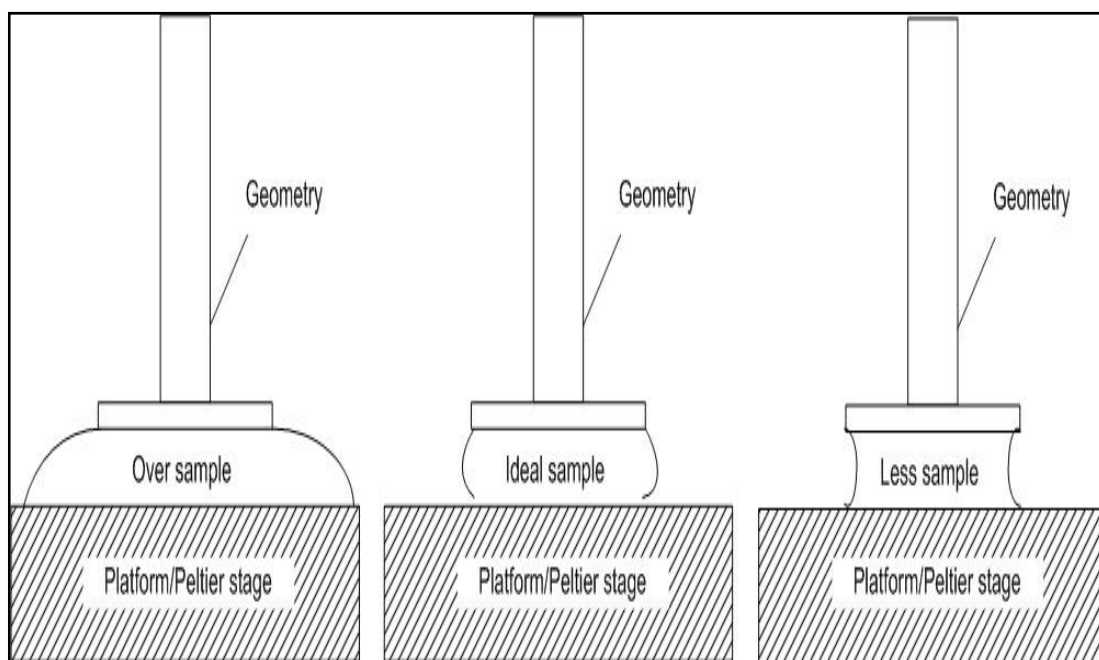


Figure 2.7: Schematic diagram of sample volume for the rheological characterisation experiments.

2.2.2 Texture Analyser

2.2.2.1 Working Principles

Texture analyser is a device to measure a complete texture profile of food or other samples with the application of controlled condition of stress and strain. It is used in various applications to quantify texture properties as summarised in Figure 2.8. Each object has different characteristic of physical structure depending on the size, shape and chemical compositions. The basic schematic of texture analyser instrument is shown in Figure 2.9. The texture analyser uses different probes or fixtures which are specially designed for a specific group of applications. The probe is attached to the texture analyser's moveable arm that can work in two ways depending on the mode of testing either compression or tension. Basically, the principle of a texture analyser is to deform the sample in a controlled manner and the response by the sample is detected by the load cell which is located inside the moveable arm and recorded by software provided by the manufacturer.

In adhesion study, the texture analyser is measuring the force required to overcome the attractive force between two surfaces. There are two important parameters obtained from the adhesion measurement namely, the tack force and the area under curve. The tack force is representing the maximum force to detach an adhered object from a surface while area under the curve is representing the total work or energy to fully separate the two adhered surfaces. Figure 2.10 shows a typical graph of force versus time or distance for adhesion measurement.



Figure 2.8: Typical applications of texture analyser. (Source: Stable Micro Systems website).

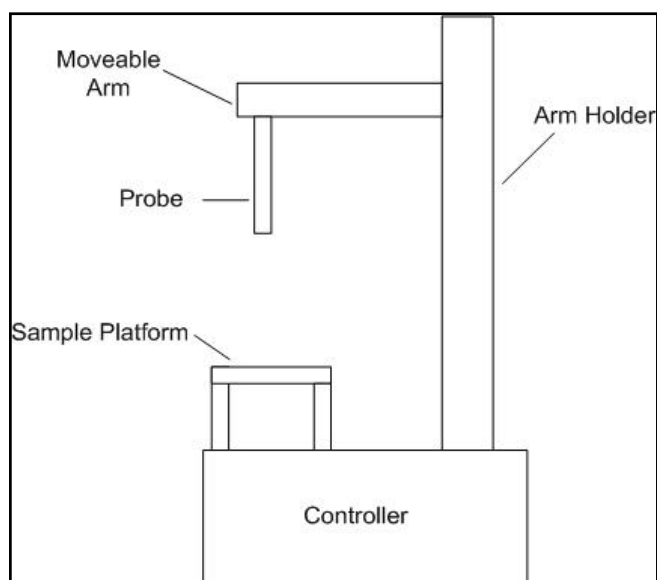


Figure 2.9: Schematic diagram of a texture analyser equipment.

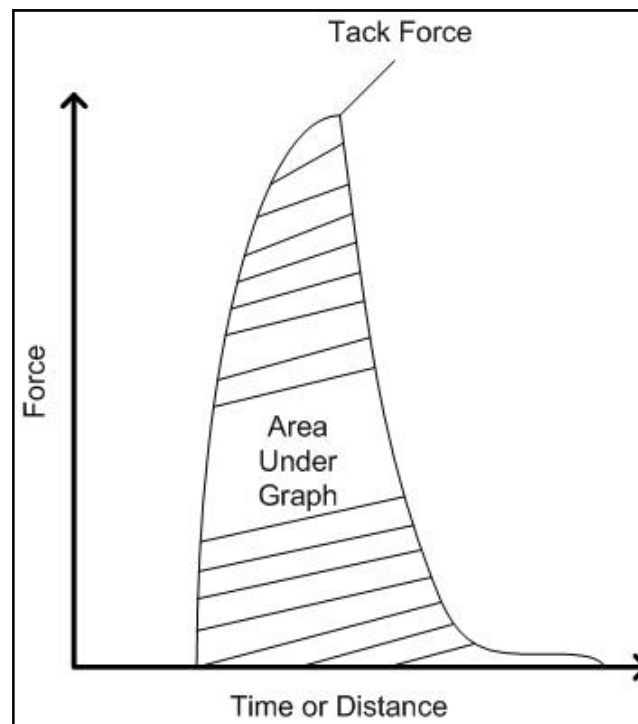


Figure 2.10: Typical graph of force versus time or distance for adhesion measurement.

2.2.2.2 Instrumental Setup

A TA.XT Plus Texture Analyser (Stable Micro Systems, UK) as shown in Figure 2.11 was used to perform pull-off and tensile test experiments. This device was fitted with a 5 kg load cell (force sensitivity is 0.1 g) and connected to a computer that run with Exponent 32-bit software for measurement recording and instrument controlling. The force and height calibration were performed each time before running the experiments to ensure the reliability and accuracy of the measurements. The weight calibration was done by running the weight calibration step from the Exponent 32-bit software using a calibration bar with the weight of 1 kg on the calibration platform. After the calibration step was done, the ‘check force’

was performed with the same step as calibration step. It was to ensure the calibration step was done correctly and the instrument measured the correct weight. The height calibration was done by using the ‘calibrate height’ step. The probe was moved close to the sample platform manually. Consequently, the moveable arm moved the probe automatically until it was in contact with sample platform. This position is referred to as the zero distance.



Figure 2.11: TA. XT. Plus texture analyser instrument. (Source: Mason Technology website).

The pull-off experiment setup is shown in Figure 2.12 (A). The mucin coated slide (labelled as sample in the figure) was set in place by using a self tightening roller grip. As for the tensile test experiment, the setup is shown in Figure 2.12 (B). The samples (polymer and mucin solution were spread evenly on Ø 20 mm

Benchkote paper with inert backing layer) were attached to the probe and sample platform by using double sided tape. The sequence used for both experiments was ‘Hold until Time’ with compression mode. The instrument setting for both experiments is shown in Table 2.3.

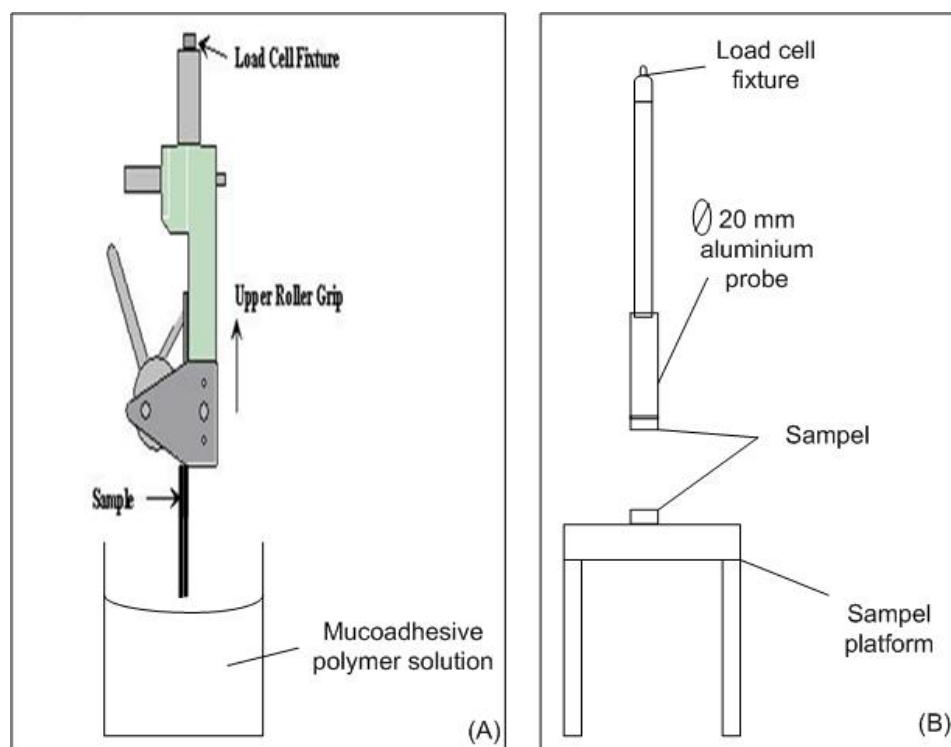


Figure 2.12: Experiment setup using texture analyser. (A) Pull-off experiment and (B) Tensile test experiment.

Table 2.3: Texture analyser setting for the pull-off and tensile test experiments.

Setting	Pull-off Experiment	Tensile Test Experiment
Test mode	Compression	Compression
Target mode	Distance	Force
Trigger type	Pre-travel distance	Auto (Force)

2.2.3 Quartz Crystal Microbalance with Dissipation Monitoring (QCMD)

2.2.3.1 Working Principles

The quartz crystal microbalance with dissipation monitoring is a highly sensitive and accurate measurement instrument that can be used to determine the kinetic absorption of mass and the viscoelastic properties of the absorbed layer. QCMD is cost effective, relatively easy to run with high resolution and possesses a wide detection range. The device can be used to detect the deposition of a monolayer or small molecules at a surface and also capable to detect larger amount or masses absorbed to the surface (Marx, 2003). The main working principle of QCMD is based on the piezoelectric effect which describes the relationship between mechanical stress and electrical voltage produced between surfaces of a solid dielectric (nonconducting substance). Historically, this phenomenon was first discovered by Curie brothers in 1880 (Curie and Curie, 1880). They reported that when quartz was under mechanical stress, electrical potential between deformed surfaces was produced and the voltage was proportional to the stress. Further research led to the development of first quartz crystal controlled oscillator using piezoelectric effect in an electric field in 1921. The phenomenon was further elucidated by Valasek (1921) who studied the effect of mechanical force and electric field on the piezoelectric response of Rochelle salt.

Quartz is the best known and the most widely used piezoelectric material due to its properties which includes high mechanical, durable, thermal stability and easy to be processed. Moreover, quartz of high quality and purity is readily available

at low cost. Figure 2.13a shows the Butterworth van Dyke (BVD) electrical model for a quartz crystal resonator. This model is often used to describe the electrical behaviour of a crystal resonator. The symbols in the circuit represent the component of the system where R_m (resistor) is corresponding to the dissipation of the oscillation energy from mounting structures and from the medium in contact with the crystal, C_m (capacitor) is corresponding to the store energy in the oscillation and it is related to the elasticity of the quartz and the surrounding and L_m (inductor) is corresponding to the inertial component of the oscillation which is related to the mass displaced during the vibration (Source: Stanford Research Systems). Figure 2.13b shows the schematic diagram of the internal circuit of the QCMD. The quartz crystals can produce a mechanical oscillation at its resonant frequency due to piezoelectric effect when an alternating electric (AC voltage) field is applied across the upper and lower metal electrodes of quartz surface.

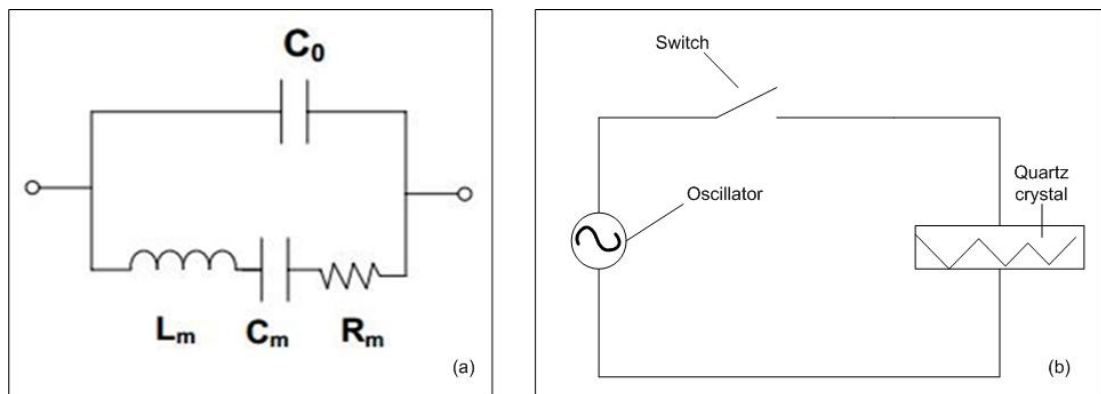


Figure 2.13: (a) Butterworth van Dyke (BVD) model of a quartz resonator and (b) Schematic diagram of internal circuit of the QCMD.

The frequency of oscillation decreases when there is an additional mass absorbed on the quartz crystal surface. The relationship between the frequencies with the mass was first discovered by Sauerbrey (1959). He reported that the mass absorbed on the quartz crystal surface was proportional to the change of frequency (negative value) and proposed a mathematical equation known as Sauerbrey equation (Equation 2.3) where Δm is the change of mass absorbed per unit area (ng cm^{-2}), ρ_o is the density of the quartz crystal (2650 kgm^{-3}), v_o is the shear velocity in quartz (3340 ms^{-1}), f_n is the resonant frequency (5 MHz) and Δf is the frequency change monitored by the instrument. The Sauerbrey equation is only valid to a rigid and elastic absorbed layer.

$$\Delta m = -\frac{\rho_o v_o}{2f_n^2} \Delta f \quad (\text{Equation 2.3})$$

The advantage of QCMD over conventional QCM is the ability of QCMD to provide information about the properties of the absorbed layer by monitoring the changes in dissipation value. The dissipation is the total energy loss in the system per oscillation cycle and can be defined mathematically as in Equation 2.4 where E_{lost} is the energy dissipated per oscillation and E_{stored} is the total energy stored in the system.

$$\Delta D = \frac{E_{\text{lost}}}{2\pi E_{\text{stored}}} \quad (\text{Equation 2.4})$$

Rodahl and Kasemo (1996) have developed an experimental setup that can measure the resonant frequency together with dissipation factor using a short-circuit quartz crystal microbalance. A relay was used to disconnect the signal intermittently. The decrease in frequency amplitude of oscillation during the process results in the sensor oscillation to decay exponentially where this phenomenon characterises the dissipation (energy lost). Through this method, frequency and dissipation changes can be measured at different overtone (3rd, 5th and 7th) of the resonant frequency of the crystal which is at 15 MHz, 25 MHz and 35 MHz respectively. When a soft (viscoelastic) layer is absorbed into the quartz crystal, the oscillation of the crystal will be dampened thus giving high dissipation value because of deformation that occur during the oscillation. As for a rigid and elastic layer, the dissipation value will be low.

2.2.3.2 Instrumental Setup

The study on the kinetic interaction of mucoadhesive polymer (sodium alginate, high DE pectin and sodium carboxymethylcellulose) with mucin was carried out using a QCMD model D300 (Q-Sense AB, Västra Frölunda, Sweden) with a QAFC 302 axial flow measurement chamber as shown in Figure 2.14. The chip used for the measurement in QCMD is a piezoelectric AT-cut quartz crystal with two gold electrodes supplied by Q-Sense (Figure 2.15). The experiments were done at a controlled temperature of 20°C. Approximately 30 minutes to one hour was allowed for the chamber to reach thermal equilibrium with temperature controller. The solutions of mucin and mucoadhesive polymers were injected into the measurement chamber using a burette through gravitational force. The mucin

solution was first injected into the system followed by the buffer rinse (four sequences). Mucin solution and biopolymers solutions were injected twice with 0.5 ml of each injection. The solutions were held in the loop for 15 minutes before a buffer rinse (four sequences with 0.5 ml each and three minutes holding time). The changes in frequency and dissipation value were recorded through a computer by using a software package that came with QCMD instrument.

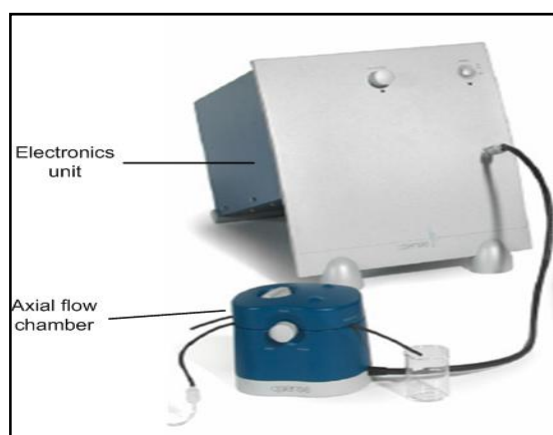


Figure 2.14: QCMD instrument with QAFC 302 axial flow chamber with temperature controlled loop.

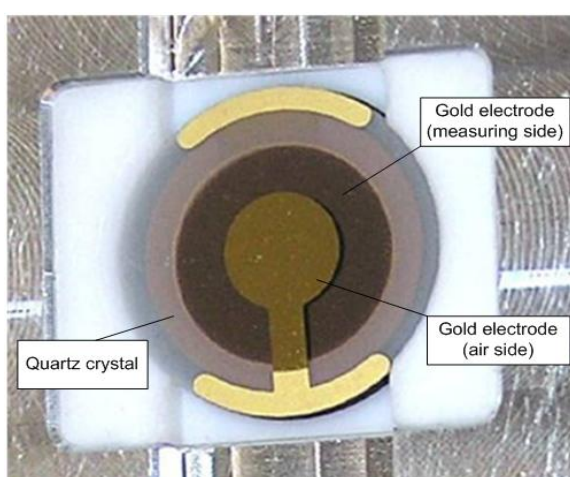


Figure 2.15: Piezoelectric gold chip.

2.2.4 Atomic Force Microscopy (AFM)

2.2.4.1 Working Principles

AFM is a powerful scanning probe microscope that can be used to produce imaging on the surface structure up to sub-nano meter scale and to measure surface forces. AFM was first developed by Binnig and Quate (1986) by integrating the principle of Scanning Tunneling Microscopy (STM) with the Stylus Profilometer (SP) by using an ultra small probe tip at the end of a cantilever. The basic principle of AFM is by detecting the cantilever spring bending when it touches the surface. The nano-scale (as small as 0.01 nm) reflection required an advanced technique for detection purpose. In this case, a laser beam is used to focus on the back of the cantilever. The beam of light from the laser is reflected to a position-sensitive photodetector and converted into electrical signal (Figure 2.16). This detection technique using laser beam was developed by Meyer and Amer (1988) and gained a patent (US RE37, 299). They explained that the displacement of the tip is caused by the interatomic forces when the tip has a contact with the sample surface (Figure 2.17). The electrical signal converted by photodetector will be sent to a computer unit to be transformed into images. The forces from the deflection of cantilever can be calculated by using Hooke's Law (Equation 2.5) where F is the force (μN - pN), k is the spring constant and (N/m) and x is the cantilever deflection. Figure 2.18 shows the typical graph of force curve of AFM.

$$F = -kx \quad (\text{Equation 2.5})$$

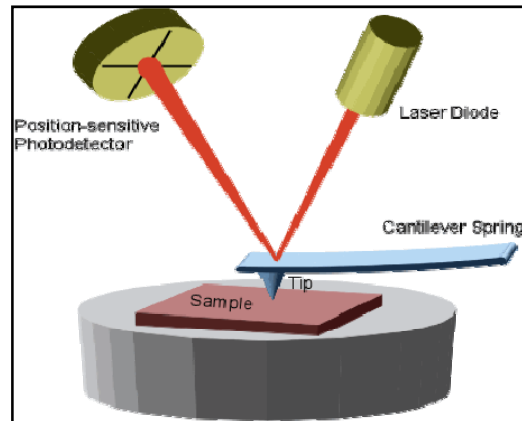


Figure 2.16: Reflection of laser beam from the cantilever to photodetector. (Source: Angewandte Physik website).

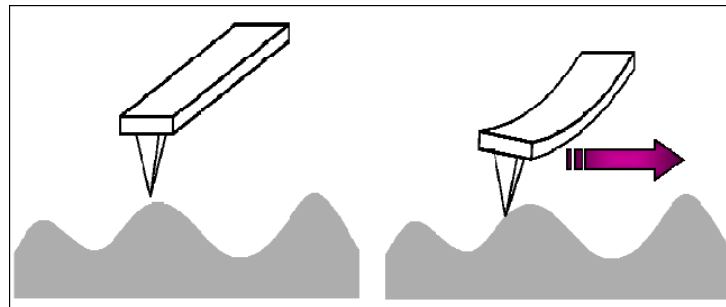


Figure 2.17: Atomic force causes the cantilever to bend corresponded by the sample surface tomography at nano-scale level.

The force curve (Figure 2.18) can be used to determine the properties of the sample such as adhesion, elasticity and hardness (Wilson and Bullen, 2007). Different probe or cantilever will have different spring constant. There are many types and sizes of probe used in AFM such as straight shape cantilever and V-shape cantilever. Some examples of the AFM tip at the end of cantilever are supertip, ultralever tip, diamond coated tip, FIB sharpened tip and gold coated Si_3N_4 tip. The

choice of the cantilever is important for the specific investigation to ensure the accuracy of measurement and production of images.

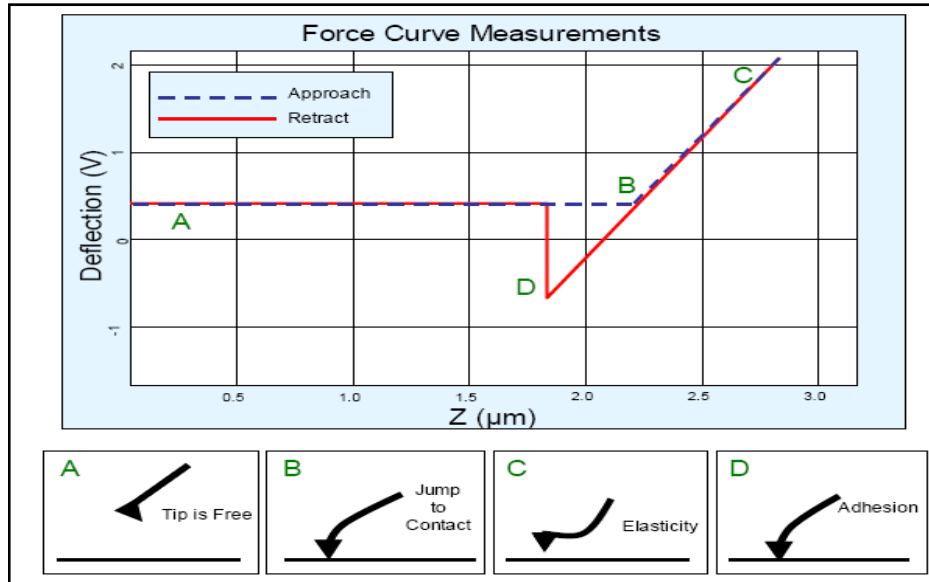


Figure 2.18: A typical force curve during the measurement done by AFM. (Source: Wilson and Bullen, 2007).

There are three modes of imaging by AFM which are contact mode, non-contact mode and tapping mode. Contact mode is where the tip of cantilever has a direct contact to the sample surface with constant deflection. The scanning using this mode needs little time (fast scanning) but it may damage the soft sample. However, scanning in liquid environment could overcome this problem. Second mode is non-contact mode where the cantilever tip does not have contact with the sample surface but oscillating above the fluid layer of sample with constant amplitude of oscillation frequency during the scanning. The third mode is tapping mode which is in between the contact and non-contact mode. Tapping mode is done by light tapping on the

sample surface and oscillating at resonant frequency. This technique can give a high resolution of measuring for sensitive surface such as biological sample.

2.2.4.2 Instrumental Setup

A Nano Wizard II atomic force microscope by JPK Instruments, UK, operating JPKSPM software was used to study the mucoadhesion properties of sodium alginate, high DE pectin and CMC at different condition including the ionic strength, pH and in different media (environment). The measurements were carried out at normal room temperature ($\sim 18^{\circ}\text{C}$) and a relative humidity of 40% - 50%. Figure 2.19 shows the schematic diagram of AFM system with the description of each component. Au-coated Si cantilevers modified with 5 μm colloidal SiO_2 at their apex were used; the SiO_2 was also Au-coated. Spring constant was measured according to the technique described by Bowen et al. (2010) and was calculated to 5.42 N/m. The substrate used in this experiment is Au coated on Si substrate (4 inches x 0.5 mm, $\langle 111 \rangle$ orientation and P-type) with the thickness of $50 \text{ nm} \pm 5 \text{ nm}$ (adhesion layer is chromium, Cr, with the thickness of 5 nm). The 4 inches Au substrate was broken up to the size of about 1 cm x 1 cm. The cantilever was coated with mucin and the Au substrates were coated with mucoadhesive polymer. The substrate was placed on the sample puck and mounted on the scanner tube using the internal magnet. The cantilever was placed in the probe holder using a pair of tweezers with the reflective coating side facing upward. The probe holder was then placed inside the AFM head. Then, the optical microscope was used to focus on the position of the cantilever and also for the laser beam alignment. The laser beam needs to be aligned to the end of the cantilever. Each measurement was done at

different places (15 points) on the substrates and an average value was calculated with standard error. The data was extracted from the software package provided by manufacturer and processed by using Microsoft Excel.

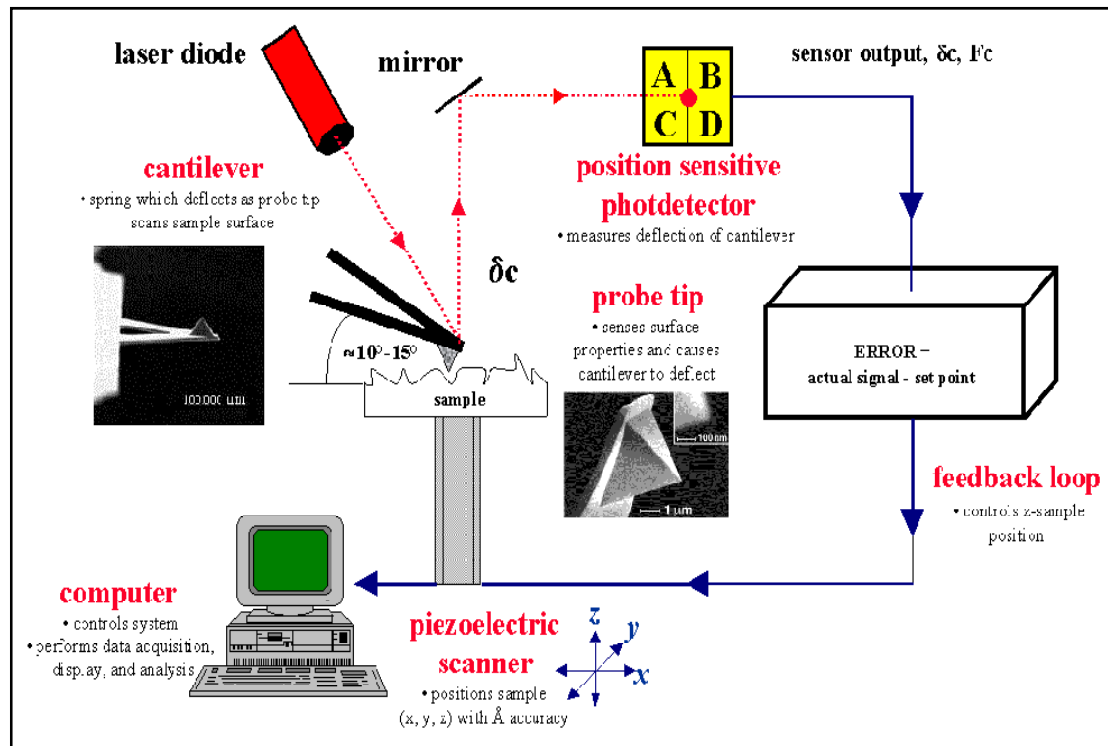


Figure 2.19: Schematic diagram of AFM system. (Source: Lecture note from College of Engineering, University of Utah).

2.2.5 Flow Cell with Microscope Imaging

2.2.5.1 Working Principles

Flow cell with microscopy assisted is a device or rig which is specially designed for monitoring and analysing bio-film attachment, growth and detachment. The flow cell allows direct visualisation the movement of particles up to microscopic

level by using a microscope. There are many uses of flow cell such as for cleaning study (Asteriadou *et al.*, 2009), initiation and growth of a biofilm (Palmer, 1999; Sternberg and Tolker-Nielsen, 2006) and others. As for mucoadhesion study, flow cell can be used as an *in vitro* model system representing some part of human or animal anatomy such as the mouth and the gastrointestinal (GI) track. The model system is prepared by covering the bottom of flow cell with a layer of mucin, depicting the presence of mucin on mucosal cell surfaces. The mucoadhesive material is then injected into the system. After a certain contact time, the system will be flushed with buffer (i.e. distilled water) with certain flow rate. During the flushing, the mucoadhesive particles or carrier system will be experiencing similar forces such as oral flow force (extensional flow, mixing and shearing) in the mouth and dislodging forces in the gastrointestinal tract (GI tract) (Hagesaether and Sande, 2008). The mucoadhesion characterisation is done by observation with a microscope located at the top of the flow cell to identify and analyse the movements of mucoadhesive particles. Flow cell offers some advantage including providing a defined and constant environment for better isolation and manipulation and can be prepared with ease for the experiment. However, flow cell cannot replicate the properties of the real biological sample accurately.

The basic principle of optical microscopy is magnification and observation. The microscope is capable to enlarge the image of the sample through a magnification lens. The degree of magnification is dependent on the magnitude of light waves bended by the lens. The light from the bottom of the microscope is contrasting the sample for the lens to capture the image. The contrast is important

during the observation because if all the light passed through the sample, there will be no details visible. A degree of light must be absorbed by the sample to create the visible images of the specimens. The quality or sharpness of the image is depending on the resolution. A good resolution will result in a sharp, define and clear images.

2.2.5.2 Instrumental Setup

A flow cell was designed and fabricated from Envisiontec R11 resin using Envisiontec Prototyping Machine from University of Warwick, UK (Figure 2.20). The schematic diagram of the experiment setup is shown in Figure 2.21. The flow cell was connected with two silicone tube with inner diameter of 2 mm. One tube was for flow in by using a peristaltic pump and another was for flow out into collecting beaker. Three layers of mucin were spread onto a microscope glass slide with 0.5 ml of mucin solution for each layer. Each layer was dried in the oven at 60°C for at least 20 minutes. The mucin layer dimension was the same as the flow cell dimension. The flow cell was placed and sealed on the glass slide with industrial silicone. Then, the system was placed under 25x magnification lens of Reichert-Jung microscope for imaging throughout the flushing process.

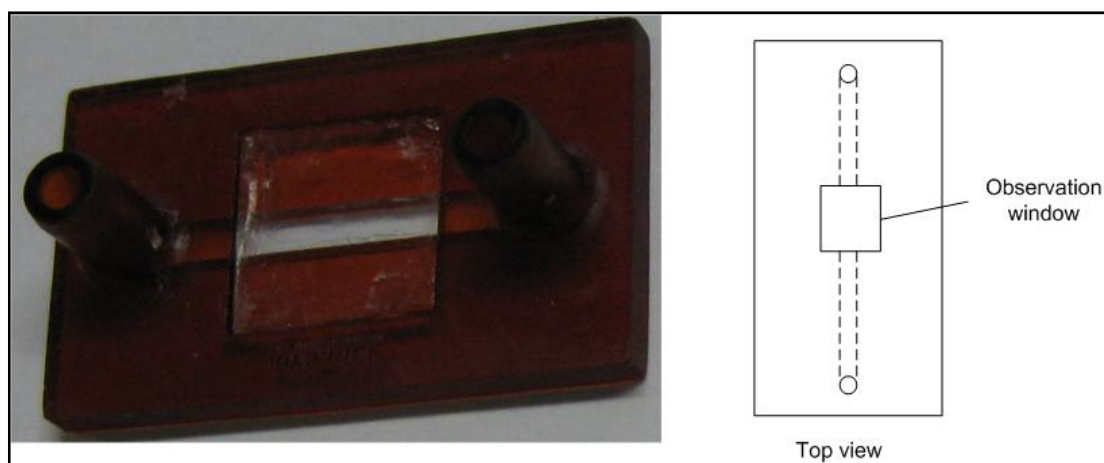


Figure 2.20: Flow cell

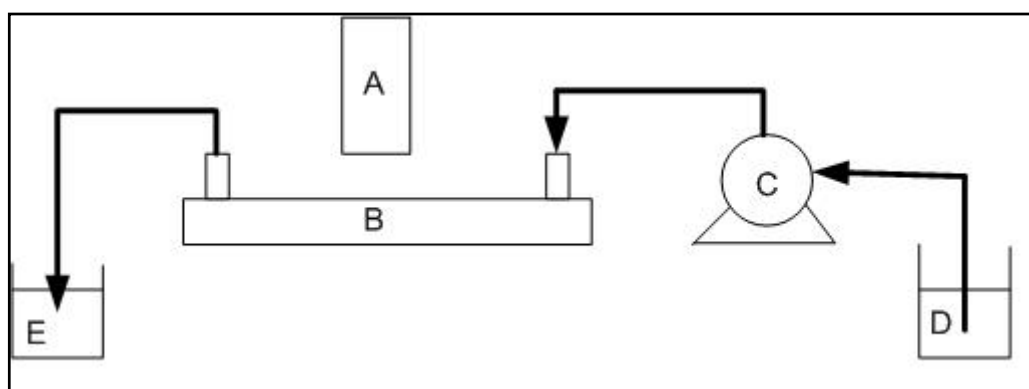


Figure 2.21: Schematic diagram of the flow cell apparatus. (A) Reicher-Jung; (B) Flow cell; (C) Peristaltic pump; (D), Beaker containing pure distilled water; (E) Beaker containing solution removed from flow cell.

Chapter 3:

Rheological

Characterisation

3.1 Introduction

Rheological technique that studies the flow and deformation of material due to applied stress and strain is useful in predicting the mucoadhesive properties of polymers or formulations. These techniques have been widely used by previous researchers to study the mucoadhesion properties and mechanisms of interaction of some biopolymers such as pectin, sodium alginate, chitosan and others (Hassan and Gallo, 1990; Mortazavi, 1995; Rossi et al., 2000; Thirawong et al., 2008; Sriamornsak and Wattanakorn, 2008). The interaction between the mucoadhesive polymers with mucin (or mucous) through chain interpenetration, structure conformation and chemical reaction will be reflected by the viscosity and rheology properties (Thirawong et al., 2008). Hence, the reflection of intermolecular friction as characterised by viscosity could be used to describe the mucoadhesion properties. The rheological characterisation for assessing the mucoadhesiveness of polymers *in vitro* was first discovered by Hassan and Gallo (1990). They have tested the interaction of several polymers (e.g. polyethylene glycol, dextran, chitosan, polyacrylic acid and others) with porcine gastric mucin. They introduced the term viscosity synergism and bioadhesion force in order to rank the adhesive strength of the polymers. The viscosity synergism is the increase in viscosity due to bioadhesion between polymers and mucin components in the mixture. The assessment has been considered successful when the results obtained by Hassan and Gallo (1990) were consistent with the results obtained by others.

Several different strategies can be used to study mucoadhesion when using rheology. One of them is the direct method of measuring the viscosity increment or

synergism at different shear rate using shear rheology. Besides the viscosity, the viscoelastic properties of the polymer-mucin mixture can be determined by oscillatory rheology. Rheological enhancement (synergism) is the term used to describe the magnitude of changes in viscoelastic properties of the sample due to mucoadhesion (Sriamornsak and Wattanakorn, 2008). In this technique, the sample is subjected to an oscillatory stress which is enough to excite the sample without breaking its molecular structure. Riley et al. (2001) have successfully investigated and characterised the polyacrylic acid (PAA) as mucoadhesive polymer and its interaction with homogenised pig gastric mucous using the rheological techniques. In their study, concentration and pH of the polymer and mucous were identified as some of the factors affecting the interaction. Another technique is the advanced frequency sweep analysis proposed by Mortazavi (2003). He used lower range frequency (0.0001 - 10 Hz) as compared to ordinary limited frequency sweep study (0.1 - 10 Hz) and reported that the technique could provide a more detailed and accurate data on change in intermolecular structure during the interaction of polymer with mucous layer.

Likewise, the purpose of this investigation is to study the mucoadhesion properties of five well known mucoadhesive biopolymers (chitosan, high DE pectin, low DE pectin, sodium alginate and sodium carboxymethylcellulose) and the factors that affect their interaction with mucin using similar rheological characterisation. However, there was a small modification in the technique used in this research. Instead of using mixtures of biopolymers and mucin as in previous studies, a thin

film of mucin was first prepared to mimic the mucous layer on to which the polymer would adhere as in the physiological system.

3.2 Materials and Methods

Highly viscous chitosan from crab shell, pectin from citrus peel (degree of esterification ~60%), acetic acid (ACS reagent, $\geq 99.7\%$), sodium alginate, sodium carboxymethylcellulose (average $M_w \sim 250000$), mucin type II with bound sialic acid of ~1%, sodium chloride, potassium chloride and starch were purchased from Sigma-Aldrich Company Limited, United Kingdom. Genu[®] low methoxy pectin (degree of esterification 35%) was kindly donated by CP Kelco, USA. All chemicals were analytical grade and used as received. Plain flour and table sugar were purchased from local Tesco store.

3.2.1 Experimental Considerations

The parameters chosen for the rheological characterisation were selected to match the conditions during oral processing. The shear rate mixing was selected to be between 40 s^{-1} and 60 s^{-1} . The values chosen were close to the shear rate observed during oral processing of low viscosity or fluid foods (Akhtar et al., 2006). The temperature was set at 37°C is also the normal temperature of human's mouth physiology. The use of mucin film as a model for mucous membrane was another consideration to create similar physiological conditions.

3.2.2 Sample Preparation

Chitosan solution with concentration of 1% w/v in 1% v/v of acetic acid was prepared by slowly adding chitosan (powder form, Fluka) into acetic acid while stirring with a propeller motor set at 400 rpm. Chitosan was added slowly into acetic acid (CH_3COOH) to avoid agglomeration of powder. The process of stirring was done until all of the chitosan has completely dissolved. In order to obtain a homogenous solution, around 12 hours (overnight stirring) was required.

Solution of 1% (w/v) and 2% (w/v) pectin, 1% (w/v) and 2% (w/v) sodium alginate, 1% (w/v) and 2% (w/v) sodium carboxymethylcellulose (CMC) and 5% (w/v) and 10% (w/v) mucin were prepared by slowly adding the powder into double distilled (DI) water and each of the mixture was stirred for at least three hours to ensure the material was fully dispersed in the solution. To study the effect of ionic strength on sodium alginate solution, 2.5% (w/v) of sodium alginate stock solution, 1 M NaCl and 1 M KCl were prepared. The necessary amount of each 1 M salt solution and DI water was added to 16 ml stock solution to make 20 ml of 2.0% (w/v) sodium alginate in 0.05 M, 0.10 M, 0.15 M and 0.20 M NaCl and KCl.

3.2.3 Instrumental Setup

Rheological analyses were performed using a rheometer (TA AR1000) equipped with a parallel plate geometry (60 mm diameter acrylic) and gap setting of 500 μm . Solvent trap was used to avoid evaporation of the sample during the measurement. Figure 3.1 shows the schematic diagram of the apparatus. All analyses were done at 37°C. First, a layer of mucin film was prepared by applying two

portions of 2 ml of 10% (w/v) on the peltier stage (diameter of film was 60 mm) with subsequent drying in between applications. Each film was thoroughly dried at 70°C for 20 minutes. Consequently, the film and polymer solutions were allowed to equilibrate at 37°C prior to analyses. Then 1.5 ml of polymer solution was poured onto the dried mucin layer. The effect of shear rates on viscosity was determined by measuring the viscosity during mixing process at shear rate of 40 s⁻¹, 50 s⁻¹ and 60 s⁻¹ for 20 minutes. After shearing for 20 minutes, the mixture was then subjected to a frequency sweep (oscillation) measurement at the linear viscoelastic region (LVR) where the oscillation stress was set at 0.1 Pa and the frequency (0.1 Hz to 20 Hz). LVR is the region where the stress or strain is enough to excite the sample but not enough to destroy the viscoelastic structure and was determined through stress sweep test. The mixture was then subjected to the flow curve measurement (steady state analysis) with the shear rate range of 20 s⁻¹ to 100 s⁻¹. As for the chitosan and chitosan-mucin mixture, the shear rate was set in the range of 0.2 s⁻¹ to 1000 s⁻¹. The above procedures were performed on all the four biopolymers (sodium alginate, CMC, high DE pectin and low DE pectin). However, only certain mucoadhesive biopolymers were chosen to study the influence of various factors on mucoadhesive properties. High DE pectin was used to study the effect of holding time prior to shearing process (0 minutes, 3 minutes, 5 minutes and 10 minutes) and different applied shear rate during shearing process (shear rate: 40 s⁻¹, 50 s⁻¹ and 60 s⁻¹). High DE pectin and low DE pectin were used to study the factor of molecular weight. Sodium alginate was used to see the effect of different amount of mucin in dried film (0.2 g, 0.3 g, 0.4 g, 0.5 g, 0.6 g and 0.7 g). Whereas the effect of different volume of sodium alginate solution on mucoadhesion was investigated using 1.5 ml (gap

setting: 500 μm), 2.25 ml (gap setting: 750 μm) and 3 ml (gap setting: 1000 μm). To study the mucoadhesion property of chitosan, 1% (w/v) chitosan with 1% (v/v) acetic acid solution was mixed with 5% (w/v) mucin solution in 1:1 ratio. The mixture was stirred with a spoon before a steady state flow curve (shear rate: 0.2-100 s^{-1}) measurement was done. The frequency sweep test was also performed on the sample with oscillation stress of 1 Pa and frequency range of 0.1-20 Hz.

Two blank experiments were performed in this study. In one control, the mucin layer was replaced with corn starch and then with plain flour. These two materials were chosen with initial hypothesis of no interaction between these materials with the biopolymers and would not show viscosity synergism. The concentration of corn starch and plain flour was 10% (w/v), similar to that of the mucin solution and the film was also prepared in the same way. As for the second control, the polymer solution was replaced with sugar (10% w/v and 30% w/v) and mucin solution (2% w/v). The purpose of the blank experiments was to ensure that the measurement taken from this study were the right parameters and was not due to errors in instrumentation measurements. Table 3.1 shows the summary of the parameters used in this experiment.

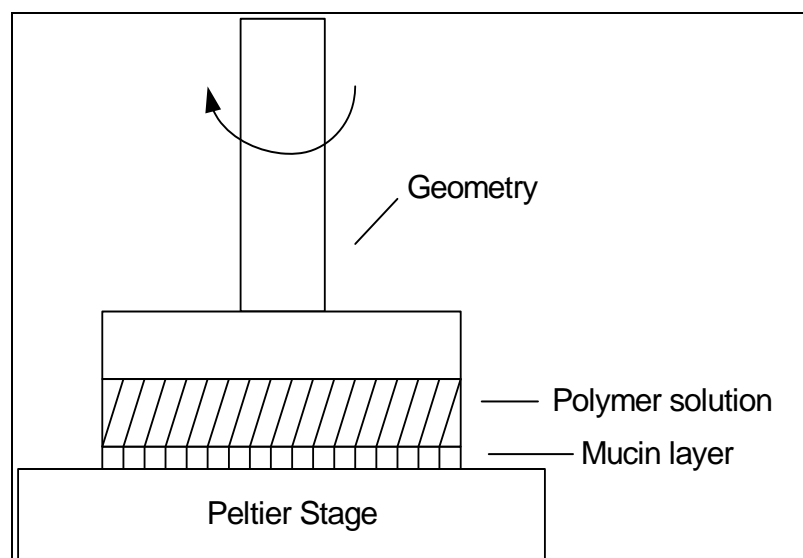


Figure 3.1: Schematic diagram of the viscometric experiment.

Table 3.1: Summary of the experiment parameters used in rheological characterisation. All the tests were performed at temperature of 37°C.

Experiment	Description	Tested biopolymers
Shearing using “peak hold” analysis	Shear rate: 50 s ⁻¹ Holding time: 5 minutes Shearing time: 20 minutes	Sodium alginate, CMC, high DE pectin and low DE pectin.
Frequency sweep test	Oscillation stress: 0.1 Pa Frequency: 0.1-20 Hz	The mixtures of biopolymer-mucin after shearing process.
Flow curve	Shear rate: 20-100 s ⁻¹	The mixtures of biopolymer-mucin after shearing process and frequency sweep test.

Different shear rate	The shearing process was done with shear rate of 40 s^{-1} , 50 s^{-1} and 60 s^{-1} .	High DE pectin
Different holding time before shearing	Shear rate: 50 s^{-1} Holding time: 0 minute, 3 minutes, 5 minutes and 10 minutes.	High DE pectin
Different molecular weight	Shear rate: 50 s^{-1} Holding time: 0 minute	High DE pectin and low DE pectin.
Different amount of mucin	Shear rate: 50 s^{-1} Holding time: 0 minutes Amount of mucin: 0.2 g, 0.3 g, 0.4 g, 0.5 g, 0.6 g and 0.7 g.	Sodium alginate
Different volume of sodium alginate solution	Shear rate: 50 s^{-1} Holding time: 0 minutes Volume of sodium alginate solution: 1.5 ml (gap: 500 μm), 2.25 ml (gap: 750 μm) and 3 ml (gap: 1000 μm).	Sodium alginate
Ionic strength	Salt: NaCl and KCl Shear rate: 50 s^{-1} Holding time: 5 minutes	Sodium alginate

Control experiment	Shear rate: 50 s^{-1} Holding time: 5 minutes	Corn starch, plain flour, sugar and mucin.
Mucoadhesion of chitosan	<u>Flow curve</u> Shear rate: $0.2\text{-}100 \text{ s}^{-1}$ <u>Frequency sweep</u> Oscillation stress: 1 Pa Frequency: $0.1\text{-}20 \text{ Hz}$	1% (w/v) chitosan in 1% (v/v) acetic acid was gently mixed with 5% (w/v) mucin solution using spoon.

3.3 Results and Discussion

3.3.1 Characterisation of Chitosan and Mucin Solution

The rheological behaviour of mucin and chitosan solutions was characterised by measuring the viscosity of each solution at different shear rates. Figure 3.2 and 3.3 shows that both solutions behave as a shear thinning solution (at certain point for chitosan) where the value of the viscosity decreased with increasing shear rates. Mucin solution behaves as a pure shear thinning solution (non-Newtonian fluid) whilst chitosan solution exhibits the behaviour of Newtonian and non-Newtonian fluid at different ranges of shear rates. Chitosan solution has a constant viscosity value (η_0) at very low shear rates (0.2 s^{-1} to 5 s^{-1}) which indicate that the solution behaves like Newtonian fluid within this range of shear rate. As explained by Graessley (1974), this behaviour is observed when the rate of the intermolecular disentanglements caused by the low shearing force is almost the same as the rate of formation of the new entanglements. However, at higher shear rates, the

rate of disentanglement due to shearing was higher than the rate of entanglement resulting in the lowering of viscosity as reflected by the shear thinning behaviour of non-Newtonian fluid. The high entanglement network present in the solution restricts the individual chains to move freely thus more time required for the formation of new entanglement network to replace the disrupted structure (Graessley, 1974). The shear thinning (pseudo-plastic) behaviour of the chitosan solution at high shear rate can be expressed by the power law or Ostward-De Waele equation as shown in Figure 3.3 where η_a is the apparent viscosity, $\dot{\gamma}$ is the shear rate, K is the consistency index, and n is the flow behaviour index (Nielsen, 1977). There are two distinctive slopes on the flow curve for chitosan as shown in Figure 3.3. The first slope indicates the transition process before the polymer turned to shear thinning solution. Hwang (1995) explained that the transition region shows an important rheological parameter that provides information on the mechanism during the early disentanglement stage which depends on the molecular structure and interaction properties of the polymer. Lowering of viscosity of chitosan solution could be observed at higher shear rates as shown by the second slope, suggesting that the chitosan networks undergo disruption at higher shear rates. The viscosity could not reach a steady value after application of stress because there was not enough time for rebuilding and stabilising the broken internal networks structure since the shearing rate was too high.

After measuring the viscosity from low shear rate to high shear rate (step up), the viscosity of chitosan and mucin solutions were then measured from high shear rate to low shear rate (step down) for the same shear range. This measurement (step up and step down) was performed in order to observe the thixotropic behaviour.

The thixotropic behaviour represents the “reversibility” or the degree of recovery of internal structure after experiencing the previous high shear rate (Vaz Jr. et al., 2011). Chitosan solution shows a hysteresis loop starting at lower shear rate ($\sim 100 \text{ s}^{-1}$) after recovering from high shearing rate. At high shear rate range ($1000\text{--}100 \text{ s}^{-1}$), the viscosity profile for step up and step down overlapped each other (shear thinning behaviour). However, when the shear rate was reduced to a minimum level ($100 - 0.2 \text{ s}^{-1}$) within the transition behaviour and Newtonian region, the viscosity profile for step down was lower than profile for step up. This implied that the new internal structure of chitosan networks formed at high shear rates failed to return completely to its initial state (quiescent structure) within the time duration of the experiment. As for the 5% (w/v) mucin solution, the viscosity profile for step up and step down almost overlaid each other throughout the shear rate range (shown by the two close lines within a small standard deviation). This indicates that 5% (w/v) mucin solution behaves as pure shear thinning liquid.

Figure 3.4 shows the steady state flow curve of the chitosan solution after being stored in the fridge ($T \sim 5^\circ\text{C}$) for one day, two days and nine days. The viscosities of chitosan solution decreased at lower shear rate when the measurements were done on different days after storage. At the shear rate of 0.2 s^{-1} , the viscosity of chitosan solution is $5.653 \pm 0.048 \text{ Pa.s}$ (day 1), $5.206 \pm 0.083 \text{ Pa.s}$ (day 2) and $4.032 \pm 0.044 \text{ Pa.s}$ (day 9) indicating roughly a decrease of 28% in the viscosity value over 9 days of storage. At higher shear rate, the viscosity remained almost constant. This viscosity decrease with increase in time of storage was the result of partial degradation of chitosan by the organic acid (Jun et al., 1994). No et al. (2006) have

also reported that the stability of the chitosan solution was influenced by the storage time and temperature. It was reported that the rate of change in viscosity of chitosan solution increased with increasing of storage temperature and time. Viscosity of 1% (w/v) chitosan solution in 1% acetic acid rapidly decreased from 2500 to 1500 cP (a decrease of 40%) within 24 hours when the solution was stored at room temperature (Sophaodora and Hutadilok, 1995). This was higher than the decrease of about 11% from the result obtained in this study. This was due to different storage temperature since the chitosan solution in this study was stored in the fridge ($T = \sim 5^{\circ}\text{C}$).

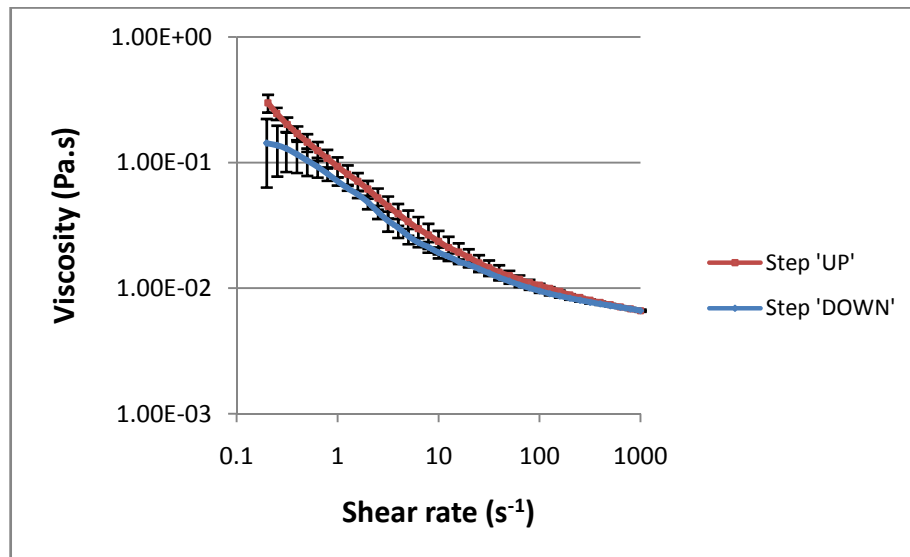


Figure 3.2: Steady state flow curve of 5% (w/v) mucin solution.

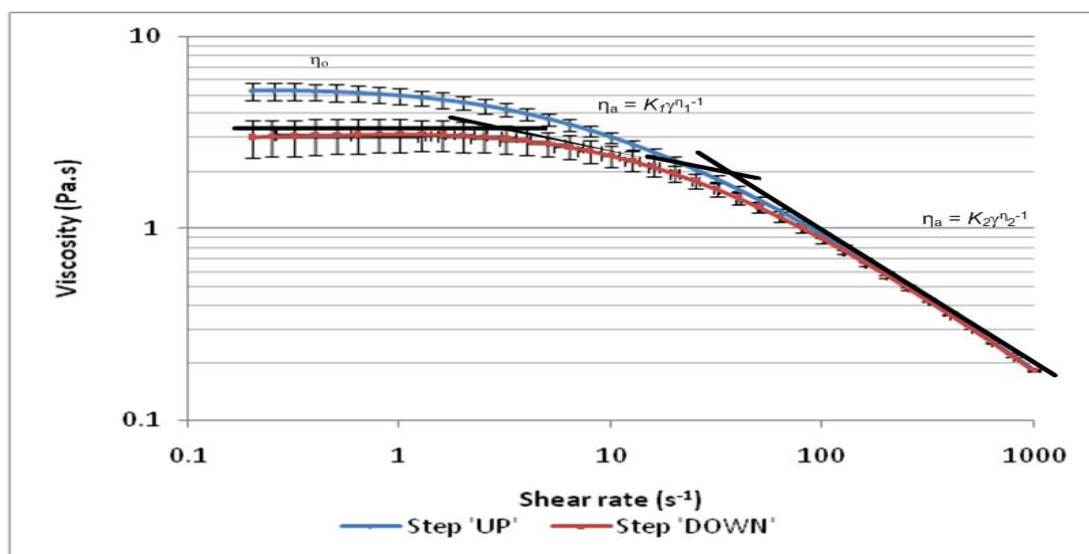


Figure 3.3: Flow curve (steady state) of 1% (w/v) chitosan in 1% (v/v) acetic acid solution measured with step up (0.2 s^{-1} to 1000 s^{-1}) followed by step down (1000 s^{-1} to 0.2 s^{-1}).

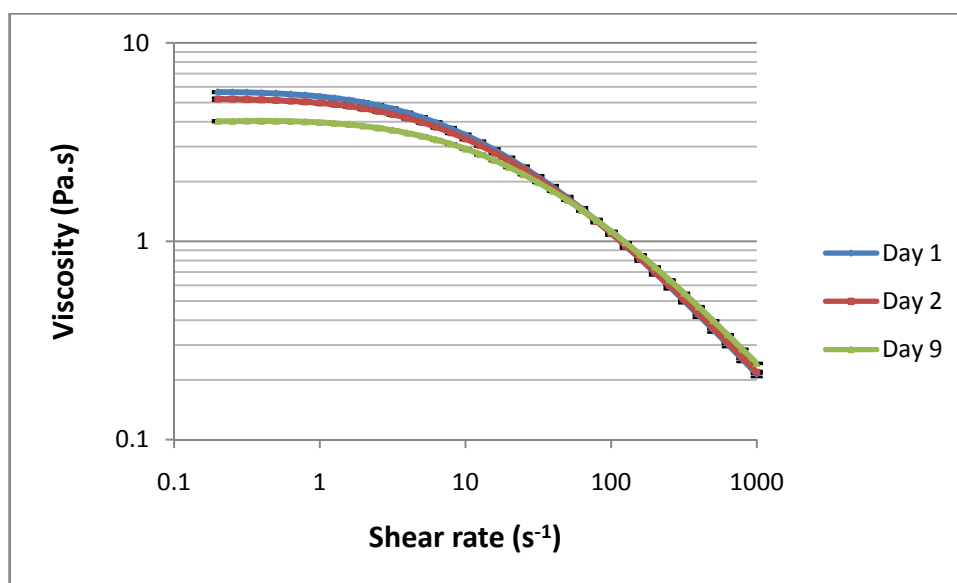


Figure 3.4: Viscosity profile 1% (w/v) chitosan in 1% (v/v) acetic acid measured on different day after stored in fridge ($T \sim 5^\circ\text{C}$).

3.3.2 Different Concentration and Different Polymers

Chitosan has been demonstrated to be a suitable mucoadhesive polymer by previous researchers (He et al., 1998 and Sudhakar et al., 2006). The main mechanism of the interaction is believed to be electrostatic and hydrophobic effect by the protonated amino group and hydroxyl groups in chitosan (Sogias et al., 2008). Hydrophobic effect exists due to the interaction among non polar groups in the polymer when dispersed in water (Garti and McClements, 2012). The hydrophobic groups exist through out biopolymers, for example the methylene groups in hydrophilic sugar residues. Chitosan consists of hydrophobic group ($-\text{CH}_3$) and hydrogen-bonding groups ($-\text{OH}$, $-\text{NH}$ and $-\text{C}=\text{O}$). Since chitosan is formed from deacetylation of chitin which is highly hydrophobic and insoluble in water (Dutta et al., 2004), the hydrophobic nature of chitosan is contributed mainly by the chitin component in the chitosan structure. In dispersion, water will favour the hydrogen bonding sites but not the hydrophobic groups thus the hydrophobic groups are available for the interaction with mucin components. The same mechanism was observed by Fefelova et al. (2007) on the mucoadhesion of amphiphilic cationic copolymers based on [2-(methacryloyloxy)ethyl] trimethylammonium chloride. They found that presence of hydrophobic component in the copolymer increased the absorption of macromolecules on the mucin surface.

Silletti et al. (2007) explained that the nature of chitosan which is positively charged promotes electrostatic interaction through bridging mechanism with mucin where the bonds are strong and irreversible (Silletti et al., 2007). However, there was an opposite effect when 1% (w/v) chitosan in 1% (v/v) acetic acid solution was

mixed with 5% (w/v) mucin solution. The result showed the viscosity of chitosan-mucin mixture was lower (instead of higher) as compared to chitosan solution and mucin solution alone as observed from the formation of less viscous mixture. This might be due to breakage of chitosan-mucin structure during stirring with a magnetic stirrer. To overcome this problem, the mixture was stirred using a spoon instead. Surprisingly, a very viscous fluid with gel like consistency was formed due to flocculation or aggregation of chitosan and mucin (Figure 3.6). A steady state viscosity measurement was carried out on the mixture at the shear rates ranging from 0.2 s^{-1} to 1000 s^{-1} . A rapid decline in viscosity profile shown in the Figure 3.5 indicated disruption and breakage of the agglomerate structure (chitosan-mucin) when higher shear rates were applied. After shearing, formation of white precipitate was observed in the dilute clear solution. The observed white precipitate could be polyelectrolyte complexes formed due to strong electrostatic interaction between positively charged chitosan components and the negatively charged mucin. The very strong electrostatic interaction between chitosan and mucin caused the chitosan-mucin complexes to be precipitated out of the solution in the form of white precipitate.

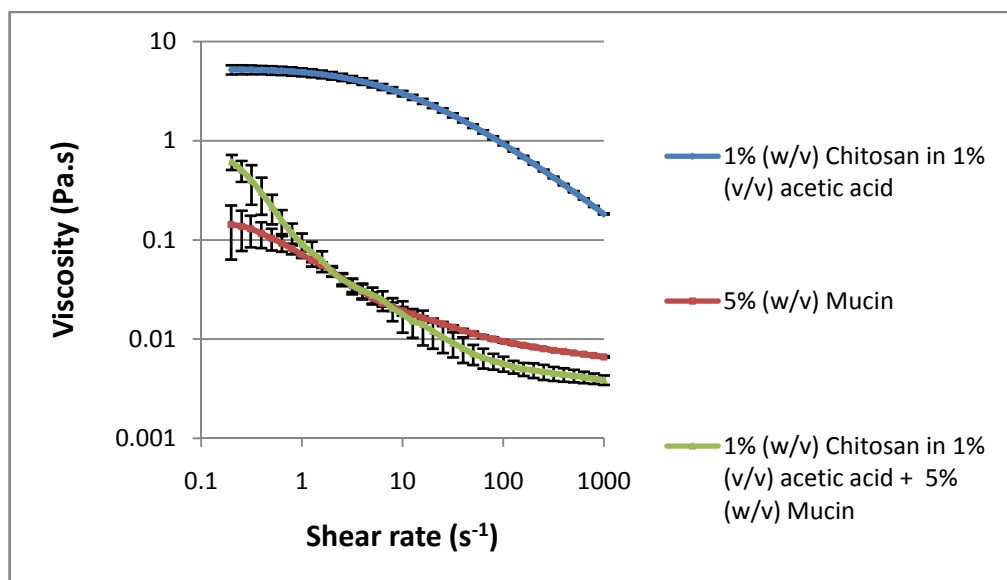


Figure 3.5: Steady state flow curve of 1% (w/v) chitosan in 1% (v/v) acetic acid, 5% (w/v) mucin and chitosan-mucin mixture which was mixed with a spoon (not magnetic stirrer).



Figure 3.6: Agglomeration of chitosan-mucin when mixed with spoon.

The same results were obtained by Rossi et al. (2001). They reported lower viscosity of chitosan-mucin mixture as compared to theoretical value ($\eta_{\text{chitosan}} + \eta_{\text{mucin}}$) obtained when they mixed chitosan solution with mucin solution in the ratio of 1:1 and 1:5 (chitosan:mucin). In order to eliminate the shearing effect that cause the breakage of the chitosan-mucin structure, an oscillation measurement (frequency sweep test) was done on the chitosan-mucin mixture with a low oscillation stress (1 Pa) which is within the Linear Viscoelastic Region (LVR) of 1% (w/v) chitosan in 1% (v/v) acetic acid solution. The value of LVR of the chitosan solution was obtained through the stress sweep test where LVR is indicated by the plateau line of the G' and G'' against oscillation stress plot. From Figure 3.7, the LVR value is in the range of 0.2 Pa to 10 Pa. The result obtained from the frequency sweep test for the chitosan-mucin mixture (Figure 3.8) showed lower value of G' (elastic modulus) and G'' (viscous modulus) for the mixture as compared to chitosan solution alone. The elastic modulus (G') of the chitosan-mucin mixture decreasing when the angular frequency was increased. This suggested that the structure of the network was breaking down during the measurement. It contradicted the value of G' chitosan solution which was increasing at higher angular frequency. However, the value of G'' of the chitosan-mucin mixture was increasing at higher angular frequency but lower than the value of chitosan mucin alone. The value of G'' is more dominant than G' indicating that the systems is viscous and has a weak internal network or structure which is easily disrupted or disturbed.

This finding is in agreement with Hagesaether et al. (2009) who reported that chitosan film had high swelling effect and disintegrated when immersed in water

during the swelling experiment. The disintegration indicates that chitosan has weak molecular structure and is easily fractured. Previous researchers had also tested the mucoadhesive properties of chitosan in other physical states such as in solid form; polyelectrolyte film (Hagesaether et al., 2009) and microsphere (He et al., 1998 and Dhawan et al., 2004). The results also indicated that chitosan is not suitable to be used as a sustaining control releases system due to weak internal micromolecular structure and low cohesiveness to prevent internal fracture (Dodou et al, 2005; Andrews et al, 2009). In order to enhance sustaining control release and mucoadhesive effect of chitosan, it is combined with other material to form stronger gel network. Examples of these are polyelectrolyte gel, which is the combination of chitosan with other negatively charge polymer (e.g. pectin) (Sriamornsak and Puttipipatkachorn, 2004; Marudova et al., 2005) and chitosan-TPP cross-link microparticles (Ko et al., 2002).

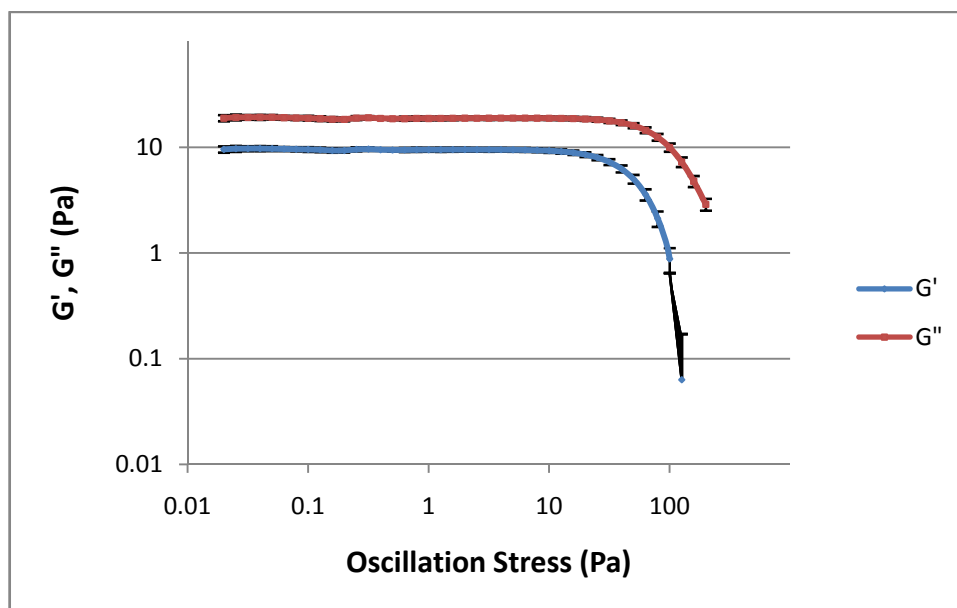


Figure 3.7: Stress sweep of 1% (w/v) chitosan solution in 1% (v/v) acetic acid.

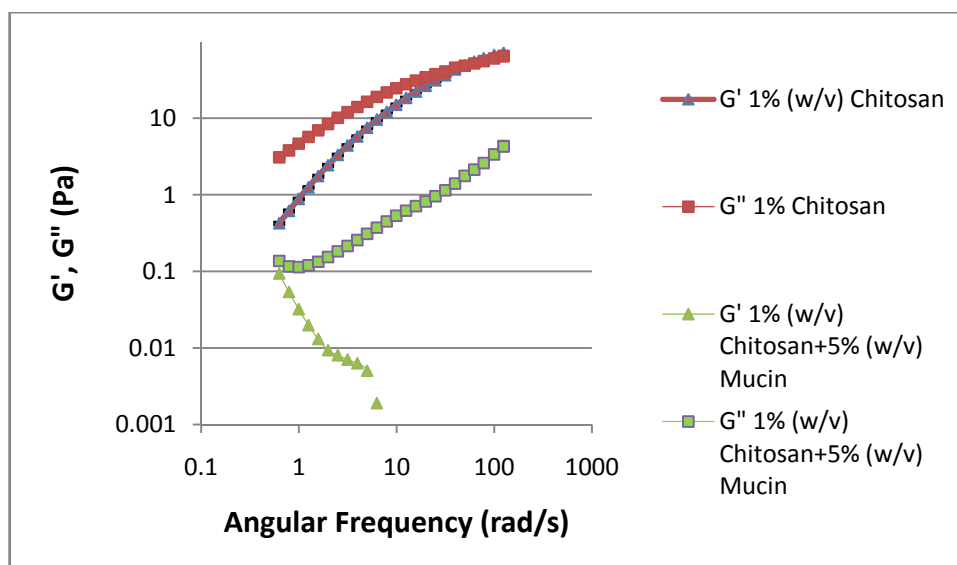


Figure 3.8: Frequency sweep 1% (w/v) chitosan in 1% (v/v) acetic acid and its mixture with 5% (w/v) mucin.

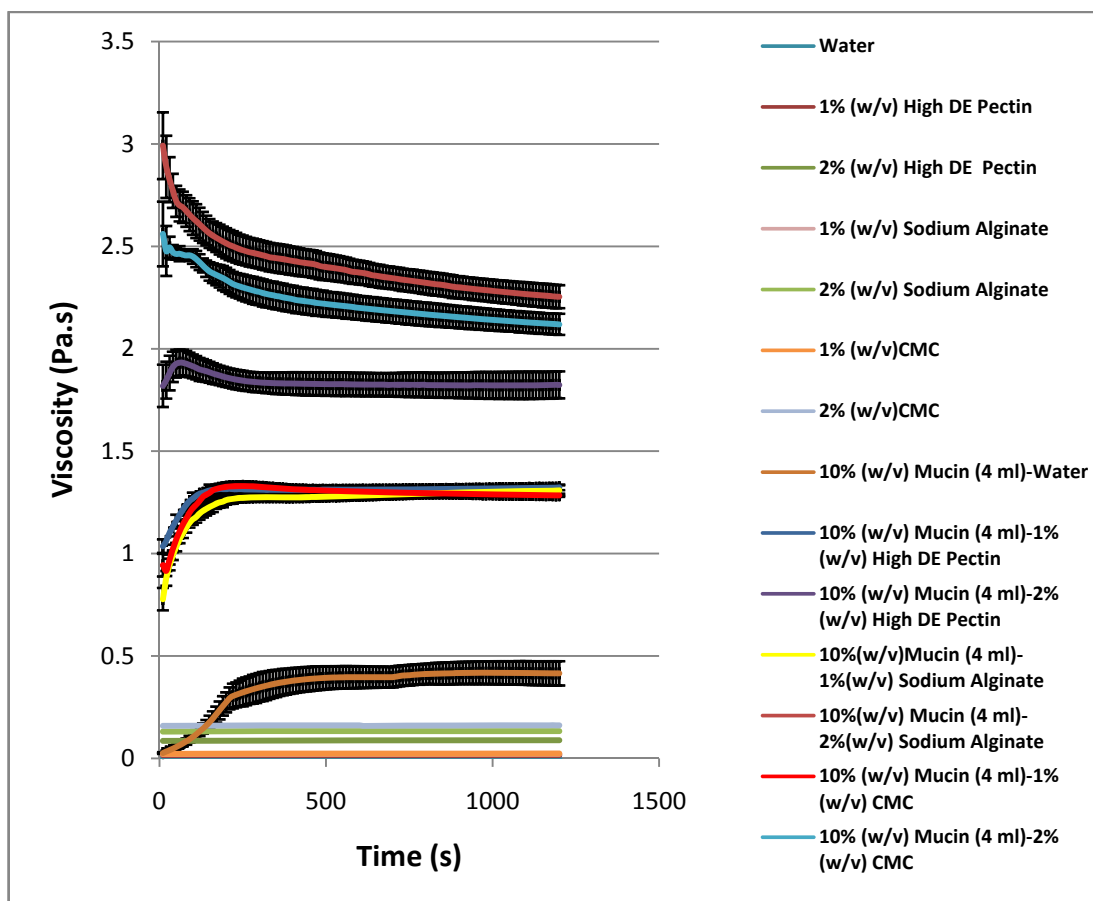


Figure 3.9: Viscosity profile of 1.5 ml 1% (w/v) and 2% (w/v) different polymer solutions, water, polymer-mucin and water-mucin at shear rate of 50 s^{-1} . 4 ml of 10% (w/v) mucin solution was dried on the peltier stage for the shearing process. Measurement was done for 20 minutes after applying 5 minutes equilibrium time (holding time).

Figure 3.9 shows the viscosity profile of 1.5 ml 1% (w/v) and 2% (w/v) of different polymer solutions, water, polymer-mucin and water-mucin at shear rate of 50 s^{-1} . Measurements were done for 20 minutes after 5 minutes of (holding time). After the holding time, the initial viscosity of the biopolymer-mucin system was significantly higher as compared to the viscosity of biopolymer alone. This resulted from the interaction between the biopolymer networks with mucin during holding

time. It is believed that during the holding, wetting mechanism prevails promoting the interaction between biopolymers with mucin through interpenetration of the networks and hydrogen bonding. Further shearing showed an increase in viscosity until the mixture became homogeneous and the viscosity came to a plateau. The viscosity of 2% (w/v) high DE pectin with mucin started with almost the same viscosity as the homogeneous mixture (Figure 3.9) due to strong interaction between polymer and mucin formed during holding time of 5 minutes but the viscosity decreased as a result of rearrangement or destroying effect of the bonding during shearing process. The viscosity finally levelled off indicating a homogenous mixture was formed after about 2 minutes. Similar results were obtained for other biopolymers which are sodium alginate and sodium carboxymethylcellulose (CMC). Interaction between these biopolymers with mucin are mainly due to hydrogen bonding between methoxyl, hydroxyl and carboxyl group and the amine group (glycoprotein component in mucin) (Hagesaether and Sande, 2007; Thirawong et al., 2008). Interlocking between polymer chains with the mucin glycoprotein network is also believed to be one of the mechanisms in the interaction. Higher concentration of polymer provides more binding sites with the mucin network, hence increasing the intermolecular interaction between higher concentration polymer and mucin network resulting in higher viscosity change.

The result in the Figure 3.10 shows the effect of different shear rates on the viscosity profile during the shearing or mixing process of the 1% (w/v) high DE pectin and mucin layer. The viscosity of the mixtures decreased with the increase in shear rates, indicating that the mixture has a shear thinning behaviour as shown in

Figure 3.11. However, the graph in Figure 3.11 showed a weak shear thinning effect as 1% (w/v) high DE pectin solution has Newtonian behaviour in the same range of shear rate. Thus, shear thinning behaviour of the high DE pectin-mucin mixture was contributed by the mucin solution and the interaction between the high DE pectin with mucin. Decrease in viscosity of the mixture was caused by the polymer chains disentanglement and breaking of the hydrogen bonds at higher shear rate (Aulton et al., 1997). Different shear rates resulted in different shear stress on the formation of the high DE pectin-mucin networks thus affecting the intermolecular structure arrangement. Higher shear rate results in smaller and weaker gel network thus resulting in lower viscosity of the mixture. However, the results from the frequency sweep measurement on the high DE pectin-mucin mixture (Figure 3.12a and 3.12b) show a very close profile of G' , G'' and $\tan \delta$ for those three shear rate mixtures. It means those three mixtures were not much different structurally. This indicates that the different of viscosity profiles during the shearing process with different shear rate could be contributed by the shear thinning behaviour of the mixture.

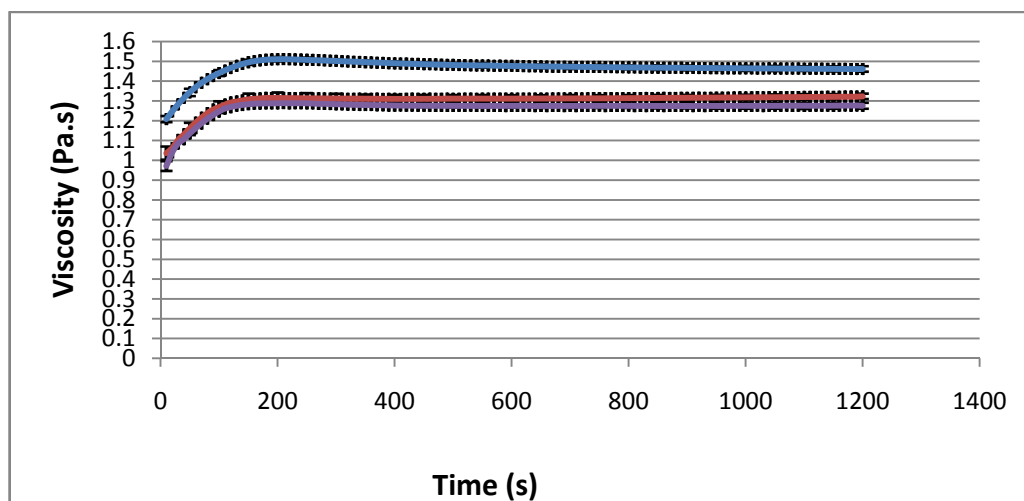


Figure 3.10: Viscosity profile of 1.5 ml of 1% (w/v) high DE pectin mixed with 4 ml 10% (w/v) mucin at different of shear rate and 5 minutes holding time before the shearing process (— 40 s⁻¹, — 50 s⁻¹, — 60 s⁻¹).

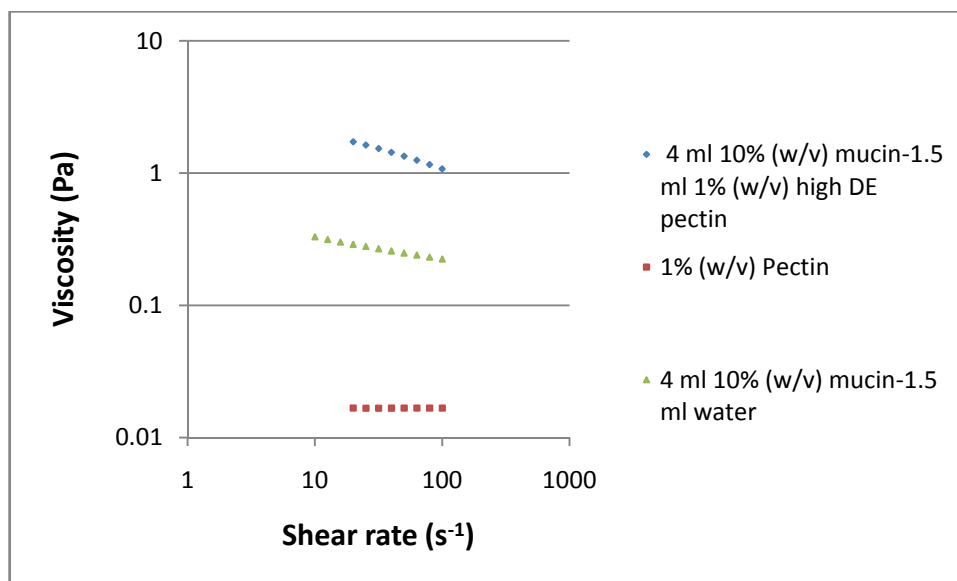


Figure 3.11: Viscosity of the mixture of 1.5 ml 1% (w/v) high DE pectin with mucin at different shear rates. Initially, the high DE pectin-mucin mixture was mixed at 50 s⁻¹ shear rate after 5 minutes holding time.

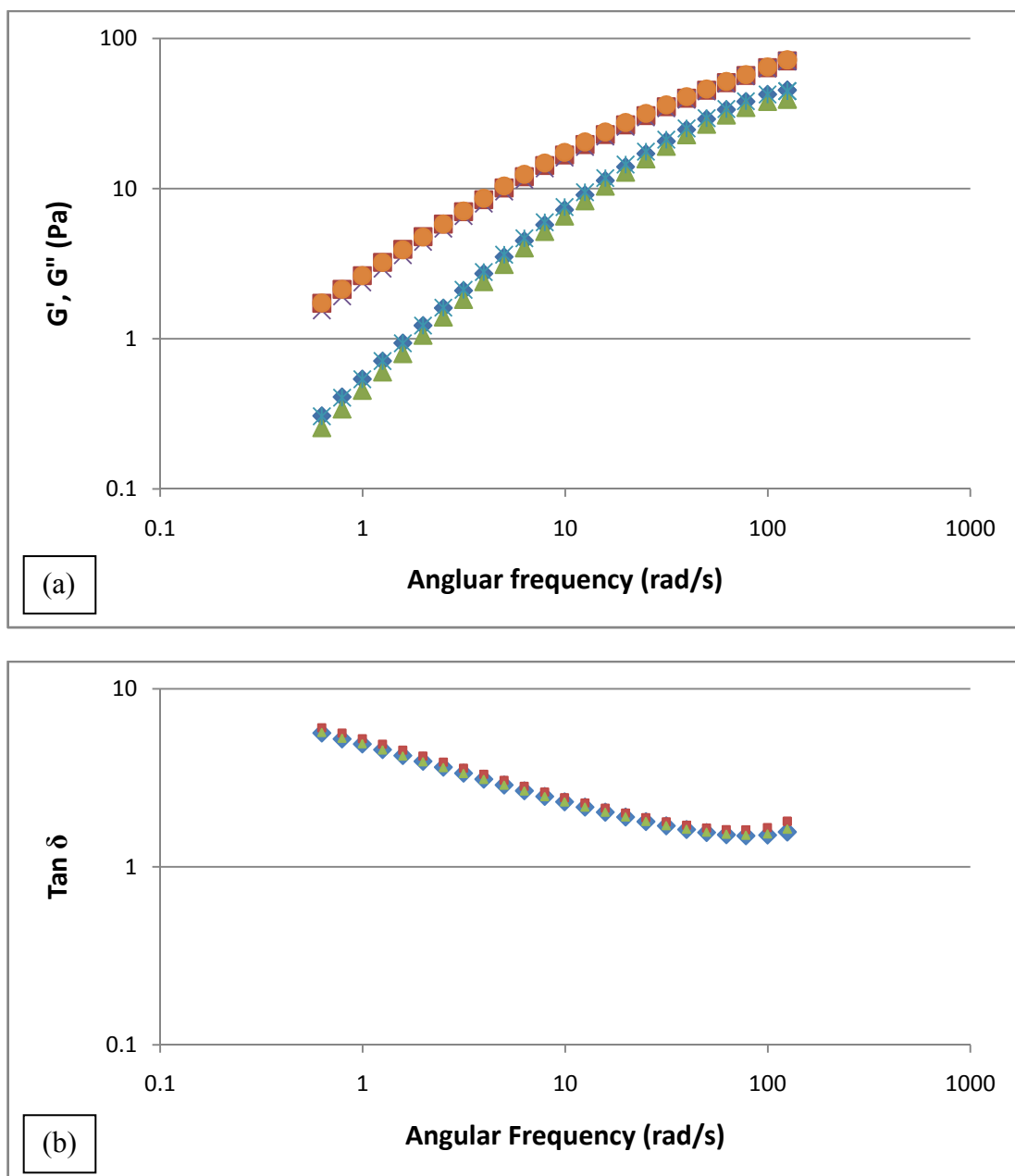


Figure 3.12: (a) Frequency sweep test for the mixture of 1.5 ml 1% (w/v) high DE pectin – 4 ml 10% (w/v) mucin (mixed at different shear rate: ◆ G' 40 s^{-1} ; ■ G'' 40 s^{-1} ▲ G' 50 s^{-1} ; ✕ G'' 50 s^{-1} ; ✕ G' 60 s^{-1} ; ● G'' 60 s^{-1}) at different angular frequencies. (b) $\tan \delta$ for the mixture of 1.5 ml 1% (w/v) high DE pectin – 4 ml 10% (w/v) mucin (mixed at different shear rate: ◆ 40 s^{-1} ; ■ 50 s^{-1} ; ▲ 60 s^{-1}) at different angular frequencies.

3.3.3 Effect of Different Degree of Esterification of Pectin on Adhesive

Capability

Two different types of pectin which are high DE pectin (Degree of esterification ~60%) and low DE pectin (Degree of esterification ~35%) were used to evaluate the effect of molecular weight and the initial viscosity of the solutions alone on mucoadhesive properties of polymers. The mixture was mixed with 0 s holding time. Figure 3.13 shows the viscosity profile of high DE pectin and low DE pectin at 1% (w/v) concentration mixed with 4 ml of 10% (w/v) mucin in dried condition at 37°C and shear rate of 50 s⁻¹. For the same concentration, the viscosity of low DE pectin is 0.003 Pa.s while for high DE pectin is 0.017 Pa.s. Through the Mark-Houwink equation, the intrinsic viscosity indicates the molecular weight of the specific polymer as it can be related to the volume that the individual polymer chain occupies in the solution (Christensen, 1954). It means low DE pectin has lower molecular weight than high DE pectin and this is reasonable as low DE pectin is manufactured by hydrolysis process of the pectin backbone. Difference in viscosity between these two types of pectin was 0.014 Pa.s but there was a big difference in viscosity of the mixture with mucin as shown in Figure 3.13. This indicates that high DE pectin has stronger interaction and binding with the mucin network compared to low DE pectin which probably resulted from the higher molecular weight. Moreover, the viscosity seemed to be related to the number of methoxyl and carboxyl groups in its molecule (Thirawong et al., 2008). In DI water (pH= ~7), the carboxyl group and sialic acid are negatively charged and the electrostatic interaction between them is generally repulsive. However this is overcome by hydrogen bonding and other physical interaction. Higher DE pectin most likely to have lower charge density

which increases the chain entanglement, inter-chain and intra-chain between the methyl groups (Thirawong et al., 2008). It is also believed that mucoadhesive binding sites on high DE pectin chain is denser than low DE pectin thus resulting in stronger interaction with the mucin network.

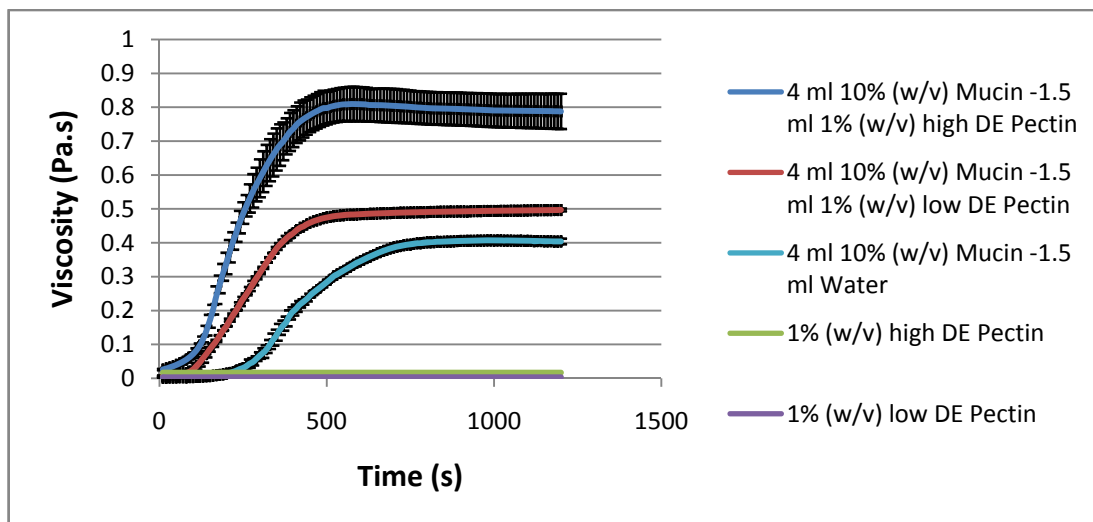


Figure 3.13: Viscosity profile of two different types of pectin (35% and 60% degree of esterification) mixed with 4 ml of 10% (w/v) mucin (temperature is 37°C, shear rate is 50 s⁻¹ and equilibrium time is 0 s).

3.3.4 Effect of Holding Time Before Shearing Process

Contact time between polymer and mucin is an important factor affecting the mucoadhesion force as hydration of mucin will increase upon increasing of contact time as shown in Figure 3.14. There is a big difference in recorded initial viscosity of the homogeneous mixture for zero holding time (0 s) and other holding time. This is because at 0 s holding time, the pectin network did not have enough time to form the interaction with the mucin network and the shearing prevented them from forming larger and stronger gel network. After 10 minutes holding time,

recorded initial viscosity shows the highest value which was 1.535 Pa.s before the value decreased. This indicated that shearing process destroyed the gel network formed during holding time. Figure 3.15 shows a linear relationship between the initial recorded viscosities of the mixture with holding time. This result correlates well with Shojaei et al. (2000) who reported that increasing contact time between copolymer (acrylic acid and 2-ethylhexyl acrylate) film and buccal tissue yielded a linear increase in mucoadhesive forces. Hydration or wetting mechanism is the first stage of mucoadhesion when a polymer has contact with mucous layer before the second stage of consolidation. Longer contact time provides enough time for the formation of secondary bonds promoting diffusional and depth interpenetration between polymer molecules with mucin glycoprotein network (Thirawong et al., 2007). Consequently, more mucoadhesive materials are bonded to mucin network, thus strengthening the mucoadhesion.

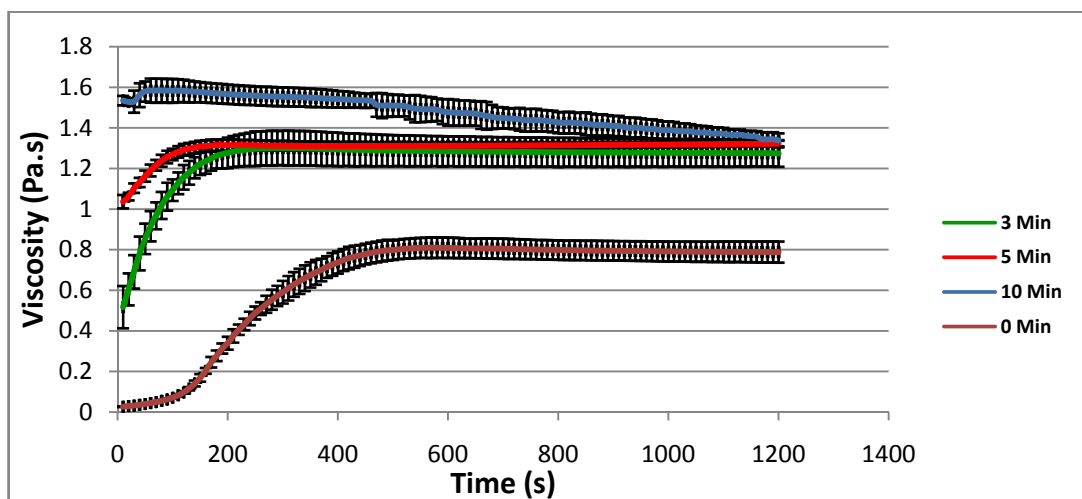


Figure 3.14: Viscosity profile of the 1.5 ml of 1% (w/v) high DE pectin mixed with 4 ml 10% (w/v) mucin (dried condition) at different initial holding times and shear rate of 50 s^{-1} .

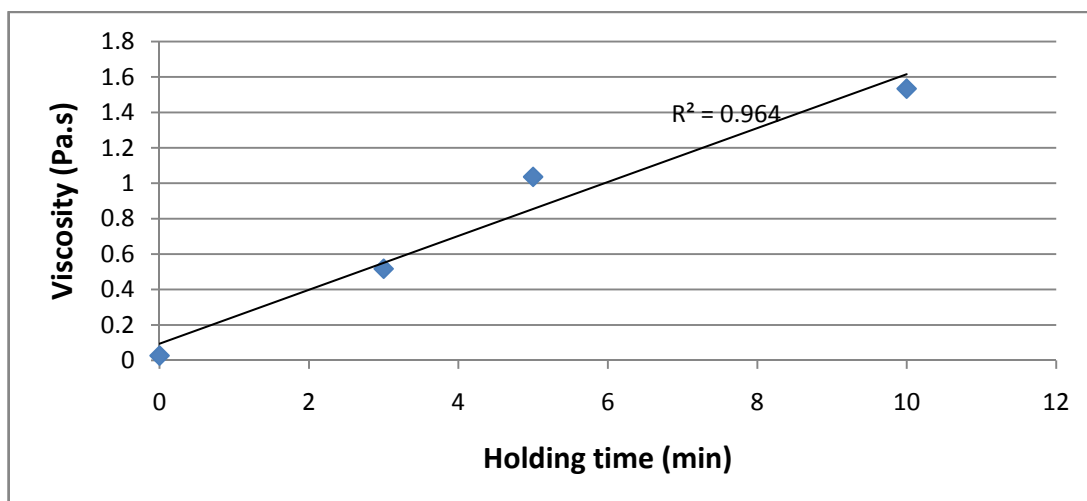


Figure 3.15: Initial viscosity of mixture of 1.5 ml of 1% (w/v) high DE pectin mixed with 4 ml 10% (w/v) mucin (dried condition) at different holding times and shear rate of 50 s^{-1} .

3.3.5 Effect of the Amount of Mucin and Sodium Alginate at Same Concentration

Besides the concentration of polymer, effects of the amount of mucin and volume of sodium alginate solution (same concentration) were also investigated. An increase in the amount of mucin used resulted in a gradual linear increase in the viscosity of the sodium alginate-mucin mixture for a range of 0 g - 0.4 g of mucin and a significant increase for a range of 0.4 g-0.7 g of mucin as shown in Figure 3.16. due to increase in the sialic acid groups which contributed to the formation of more hydrogen bonding and other interactions between sodium alginate and mucin. This result was similar to the relative viscosity that was reported earlier (Thirawong et al., 2008) where the interaction between mucoadhesive polymer and mucin not only depended on the polymer concentration but also on amount of the mucin in the system. With a small amount of mucin, it is possible that mucoadhesive binding sites

(on sodium alginate) are in excess. However, there is a limiting amount of mucin that has interaction with polymer network (Figure 3.17) beyond which the high viscosity of sodium alginate-mucin mixtures was not due to interaction of sodium alginate and mucin but due to the compact entanglement of the mucin molecules or chains. To validate this, the viscosity of mucin-water mixture with different amount of mucin was determined (Figure 3.16). From the graph, it can be observed that the viscosity of mucin-water mixture increased exponentially suggesting that at very high concentration, mucin molecules are highly entangled (Svensson, 2008). By calculating the difference between the apparent viscosity of sodium alginate-mucin and viscosity of mucin-water, the theoretical specific viscosity of sodium alginate-mucin was obtained. The specific viscosity of sodium alginate-mucin refers to the specific interaction between sodium alginate molecules with mucin. Figure 3.17 shows that the specific viscosity of sodium alginate-mucin is maximum at 0.5 g. It is suggesting that 0.5 g of mucin could be the limiting amount for maximum interaction of 0.03 g of sodium alginate (2% w/v of 1.5 ml solution) since viscosity was the parameter that used to quantify the strength of interaction. At higher amount, the mucin chains are believed to be highly entangled and this inhibits the effectiveness of interpenetration of sodium alginate structure into mucin networks due to the inflexibility of the mucin structure.

The relationship between the viscosity of the sodium alginate-mucin mixture for different volume of 2% (w/v) sodium alginate solution used was also investigated and the viscosity profiles are shown in Figure 3.18, Figure 3.19 and Figure 3.20. The results show the viscosity of the sodium alginate-mucin mixture and

specific viscosity of sodium alginate-mucin are inversely proportional to the amount of sodium alginate because of the dilution effect from the water. An increase in the amount of polymer solution used in the system provided more mucoadhesive binding sites, however this could not overcome the dilution effect from the excessive water in the system thus resulting in weak gel formation.

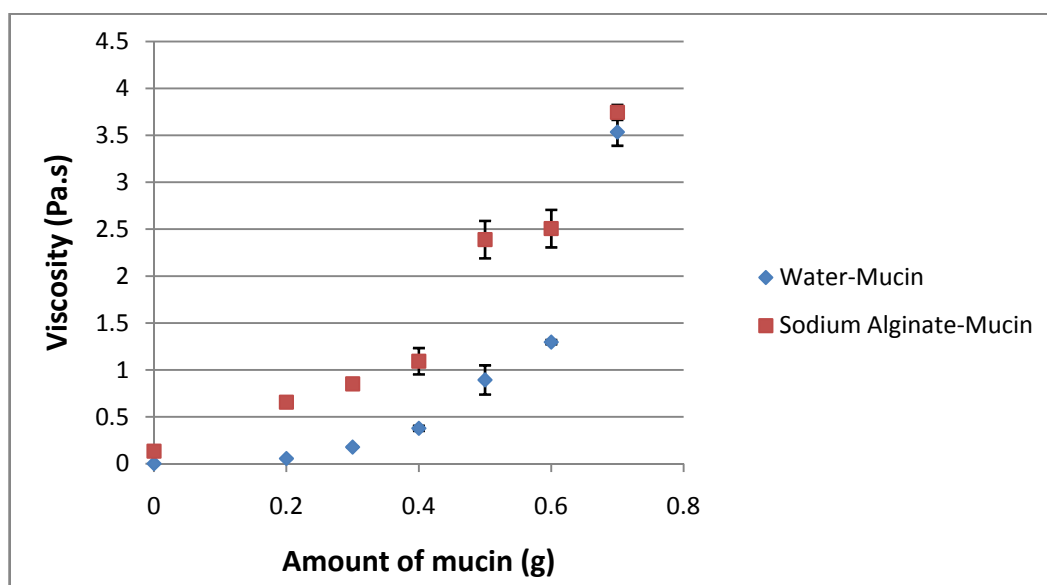


Figure 3.16: Effect of amount of mucin in the combination of 1.5 ml of 2% (w/v) sodium alginate and 10 % (w/v) mucin on the viscosity of the mixture. (Shear rate: 50 s^{-1} ; holding time: 0 s).

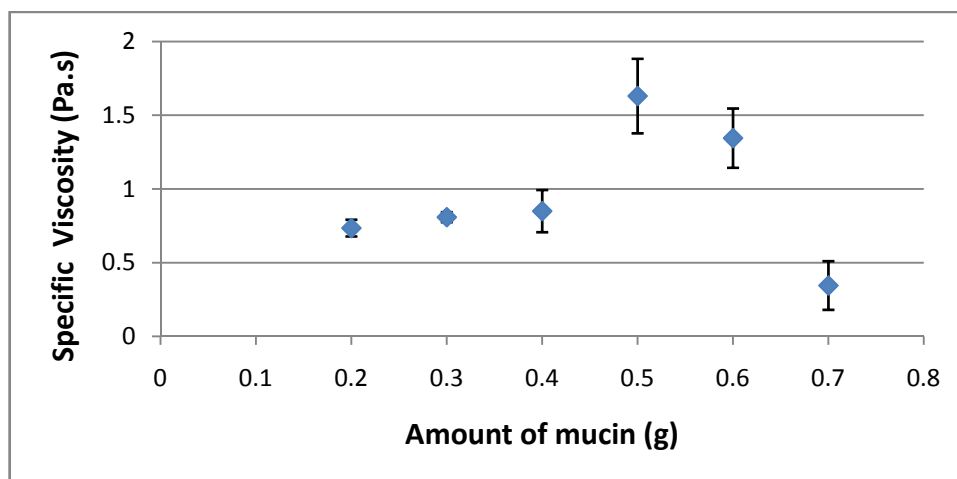


Figure 3.17: Specific viscosity of sodium alginate-mucin with different amount of mucin in the mixture. (Shear rate: 50 s^{-1} ; holding time: 0 s).

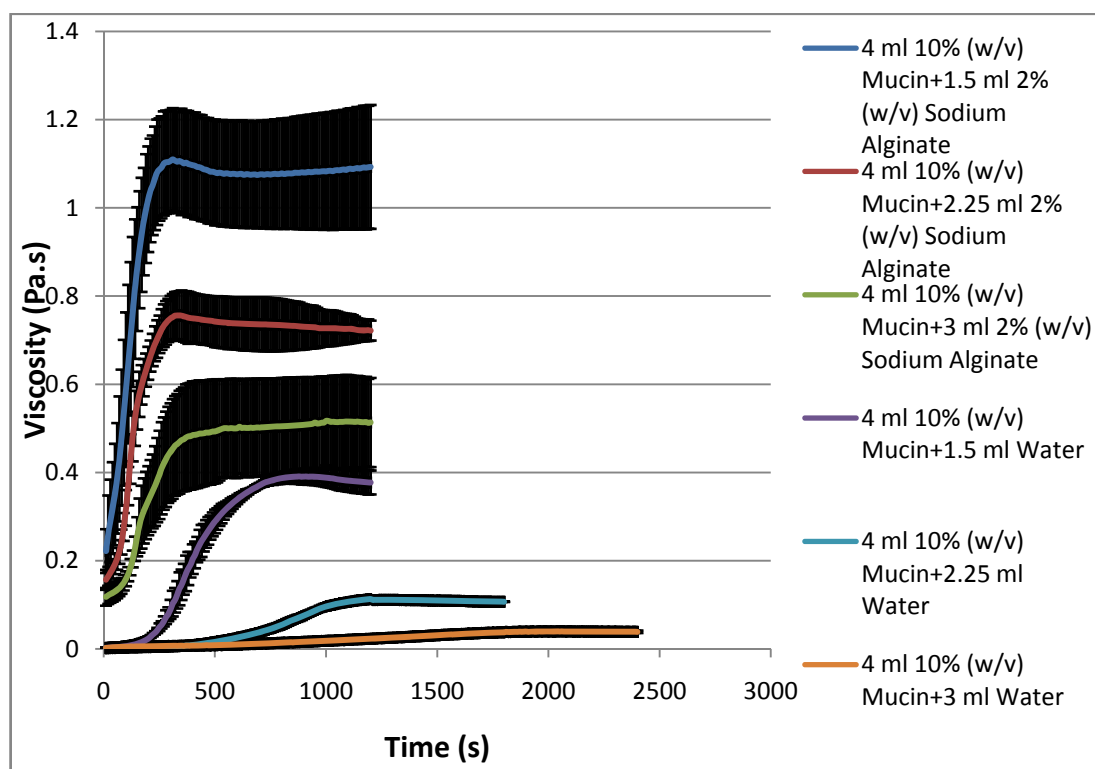


Figure 3.18: Viscosity profile of the different volume of 2% (w/v) sodium alginate mixed with 4 ml of 10% (w/v) mucin (dried condition). (Shear rate: 50 s^{-1} ; holding time: 0 s).

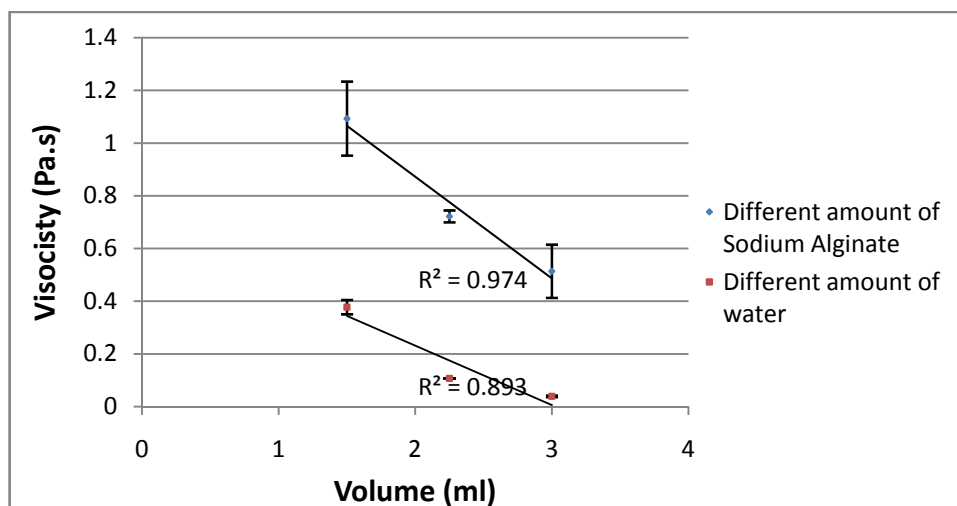


Figure 3.19: Effect of amount of sodium alginate solution on the viscosity for mixture of 4 ml of 10% (w/v) mucin and 2% (w/v) sodium alginate solution. Viscosity of different concentration of mucin solution is measured by mixing 0.4 g of mucin (in dried film condition) with different amount of water. (Shear rate: 50 s^{-1} ; holding time: 0 s).

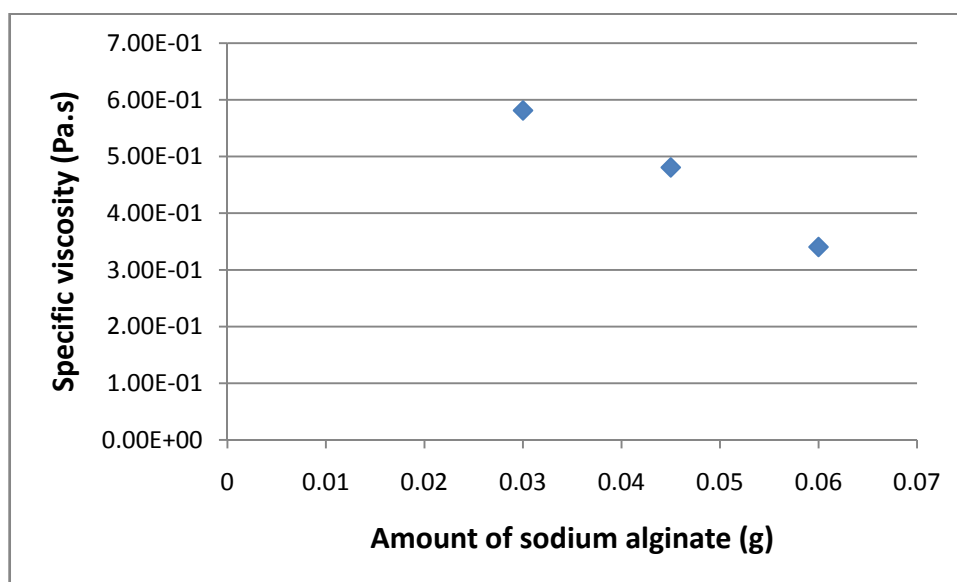


Figure 3.20: Specific viscosity of sodium alginate-mucin at different amount of sodium alginate solution in the mixture. (Shear rate: 50 s^{-1} ; holding time: 0 s).

3.3.6 Effect of Ionic Strength on Sodium Alginate and the Mixture with Mucin

Ionic strength (a measure of the salt concentration) in the media affects the strength and process of the mucoadhesion between polymers and mucin (Peppas and Sahlin, 1996; Amit et al., 2011). In this study, the effect of ionic strength on bioadhesive capability of sodium alginate was investigated using two different salts namely, sodium chloride (NaCl) and potassium chloride (KCl). These salts were selected as both Na^+ and K^+ have the same charge of +1 but different electrochemical potential. The viscosity of the 2% (w/v) sodium alginate solution with different salt concentration and the mixture with 4 ml of 10% (w/v) mucin (dried condition) was measured at shear rate of 50 s^{-1} and the viscosity profiles are shown in Figure 3.21 and Figure 3.22. In Figure 3.23, the result clearly shows how the viscosity of sodium alginate-mucin mixture was affected by the increase in concentration of both Na^+ and K^+ in the system. The viscosity of the mixtures were sharply decreased at concentration of 0.5 M for both types of ion (Na^+ and K^+) but further increase in the ionic strength did not affect the viscosity of the mixture.

Small increase in ionic strength in sodium alginate solution leads to the infolding of the macromolecules resulting in a decrease in viscosity of solution. Evidently, the electric double layer of sodium alginate gets thinner owing to the compression of the diffusion layer (Oberyukhtina et al., 2001). At low ionic strength in the solution, the macromolecules are infolded to the greatest extent resulting in a decreasing in the viscosity of sodium alginate solution. The thickness of the double layer structure which is affected by the presence of ionic strength could be explained

by the Debye Screening Length (K , nm⁻¹) (Hunter, 1986) as shown in Equation 3.1 where c is the concentration of ion and z is the valence of ion i respectively.

$$K = 3.288 \sqrt{\frac{1}{2} \sum c_i z_i^2} \quad (\text{Equation 3.1})$$

The K parameter will increase with increasing of ionic strength (concentration) in the solution due to the shrinking effect of the diffuse double layer closer to charged particles (Benitez and Lozano, 2006). This phenomenon is referred as compression of the double layer. The compression of the double layer also decreases the zeta potential value and the internal electro-repulsion thus decreasing the viscosity of sodium alginate solution. The compact structure of sodium alginate contributes to the weaker interaction between sodium alginate networks and mucin due to decrease in interpenetration and interlocking capability. The presence of Na⁺ and K⁺ in the sodium alginate could also affect the mucin structure during the shearing process. The difference in electrochemical properties of these ions were resulting in different of sodium alginate zeta potential value because the potential falls off more rapidly with the structure distance (length) as explained by Benitez and Lozano (2006). They reported (Figure 3.24) that Na⁺ resulting lower zeta potential value on an apple juice as compared to K⁺ in which means that the structure double layer is more compact because the zeta potential value was solely attributed by the contraction of double layer around the charged structure. The less negative of the zeta potential value was resulted from the more compact of the sodium alginate structure and consequently the less interaction between the two materials as reflected by the low viscosity (Figure 2.3).

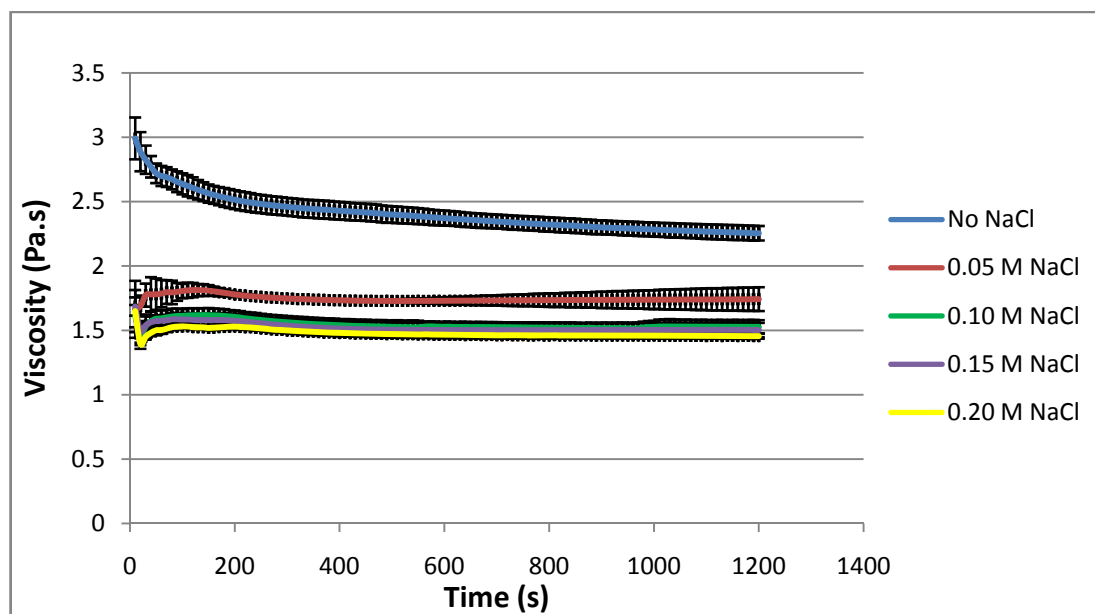


Figure 3.21: Viscosity profile of the different volume of 2% (w/v) sodium alginate with different concentration of NaCl mixed with 4 ml 10% (w/v) mucin. (5 minutes initial holding time and shear rate of 50 s^{-1}).

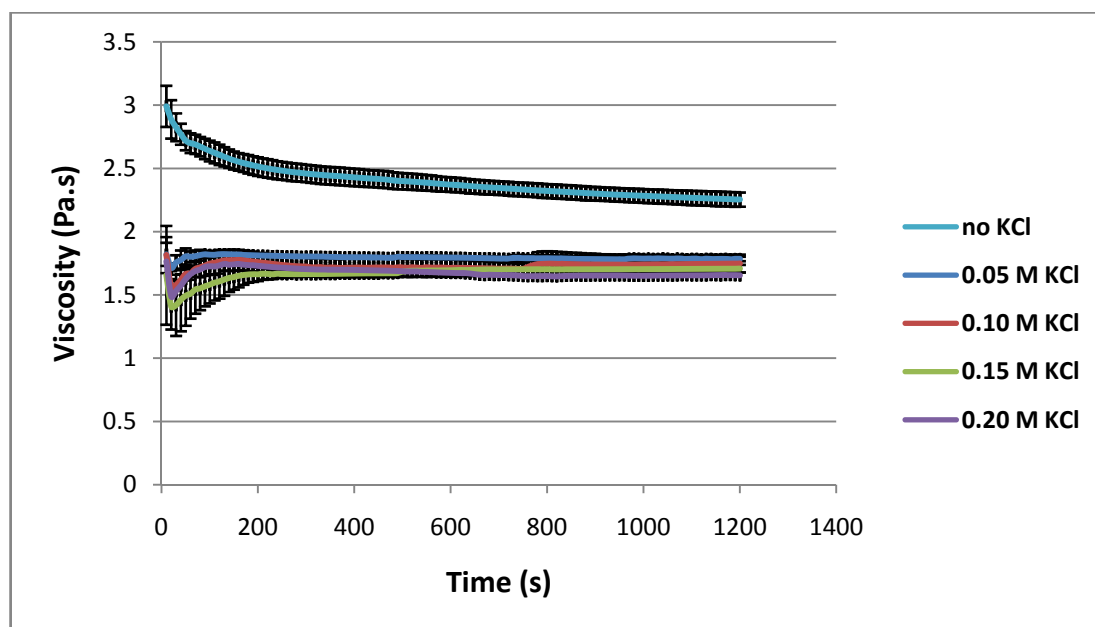


Figure 3.22: Viscosity profile of the different volume of 2% (w/v) sodium alginate with different concentration of KCl mixed with 4 ml 10% (w/v) mucin. (5 minutes initial holding time and shear rate of 50 s^{-1}).

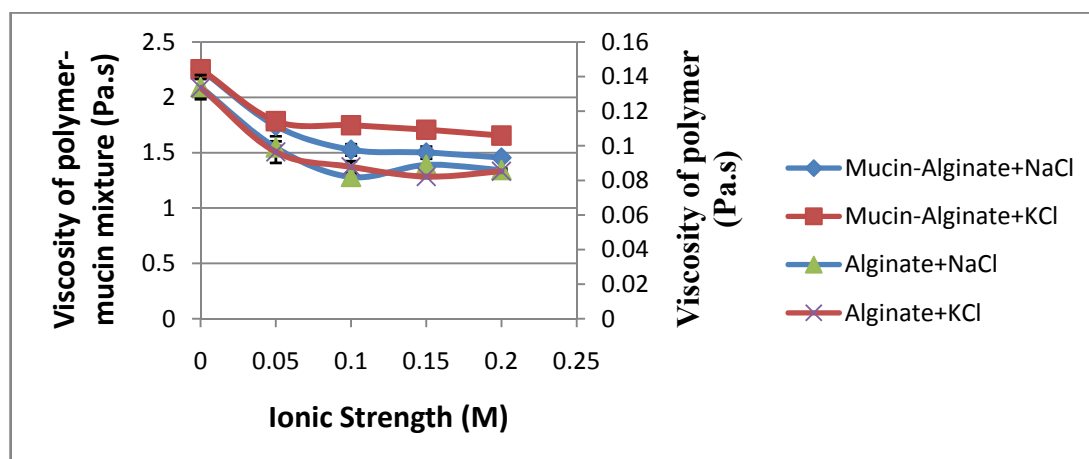


Figure 3.23: Viscosities for mixtures of the 2% (w/v) sodium alginate in different concentration of salt and its mixture with 4 ml of 10% (w/v) mucin (dried condition) after 20 minutes shearing at 50 s^{-1} and 5 minutes initial holding time.

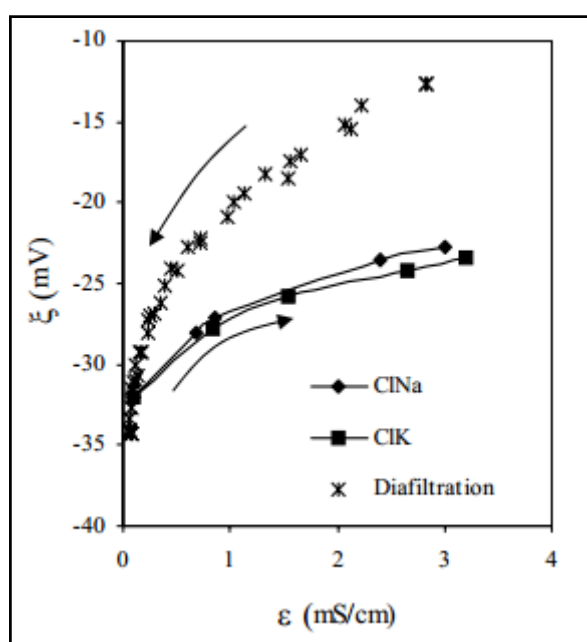


Figure 3.24: Variation of zeta potential (ζ) of an apple juice with salt concentration. (Source: Benitez and Lozano, 2006).

3.3.7 Viscosity Synergism, Normalised Parameter and Force of Mucoadhesion

In this study, the mucoadhesive properties of sodium alginate, CMC, high DE pectin and low DE pectin were studied and characterised by viscosity of biopolymer-mucin mixture. Apparently the observed viscosity of mixture is greater than the algebraic sum of its components and is termed as ‘viscosity synergism’. This parameter was first proposed by Hassan and Gallo (1990) based on viscometric measurement on mixtures of some mucoadhesive polymers with mucin solution. The viscosity synergism (enhancement) of the mixture is calculated based on equation proposed by Hassan and Gallo (1990) as shown in Equation 3.2. Where η_{obs} is the observed viscosity (measured by rheometer) of the system (polymer-mucin mixture), η_m is the viscosity of water-mucin mixture and also represents the viscosity of mucin in system (1.5 ml solution), η_p is polymer viscosity, η_{exp} is the expected viscosity ($\eta_m + \eta_p$) and η_{enh} is the viscosity enhancement component due to bioadhesion. The value of viscosity enhancement (η_{enh}) can be obtained by rearranging Equation 3.2 to Equation 3.3. This equation is only valid to be applied for systems with the same concentration, temperature, and shear rate (Hassan and Gallo, 1990).

$$\eta_{obs} = \eta_m + \eta_p + \eta_{enh} \quad (\text{Equation 3.2})$$

$$\eta_{enh} = \eta_{obs} - (\eta_m + \eta_p) \quad (\text{Equation 3.3})$$

Viscosity synergism value (η_{enh}) supports the view that the interaction between biopolymers with mucin is due to physical and chemical interaction. Higher value of viscosity synergism indicates stronger interaction. The presence of

functional groups such as the carboxyl (-COOH) and hydroxyl (-OH) in the biopolymer structure promotes hydrogen bonding. Apart from the formation of hydrogen bonding, the interaction is strengthened by the physical interlocking between the biopolymer structures with mucin chains. These interactions are capable of overcoming the electrostatic repulsion exists in the system caused by the same charge (negative) from biopolymers and mucin. The result in Table 3.2 shows that biopolymers under this study have good mucoadhesive properties (high viscosity synergism) for concentration of 2% (w/v) as compared to 1% (w/v) biopolymer solution. This corresponds well with the results obtained from the previous study by Madsen et al. (1998) which shows that the interaction between polymer with mucin was concentration dependent. At higher concentration of polymer, more functional groups are present in the mixtures and thus promoting a stronger bond formation between the polymers and mucin. But at lower concentration of biopolymer solution, there is inadequate functional group to form strong interaction with mucin resulting in poor mucoadhesive properties. Based on the value of η_{enh} for 2% (w/v) solutions, the rank order for mucoadhesive performance is sodium alginate > CMC > high DE pectin. Polymer molecular weight also plays an important role in mucoadhesion. Result in Table 3.2 shows that sodium alginate which has higher molecular weight than pectin exhibits higher mucoadhesion. However, polymers with a very high molecular weight could lead to higher degree of entanglement within the polymer network thus inhibits interaction with mucin (Hagesaether and Sande, 2007). This reason could explain on the lower η_{enh} of CMC (molecular weight ~250000 Da) as compared to sodium alginate (12000-180000 Da). High DE pectin has higher value in all aspects (viscosity of its solution and the mixture with mucin) compared to low

methoxy pectin as shown in Table 3.3. The big difference between these two types of pectin is due to different strength of bonding take place during the shearing process as mentioned in section 3.3.3.

Table 3.2: Apparent viscosity and observed viscosity of the different polymers and their mixture with 10% (w/v) mucin (1.5 ml of polymer solution was used for the mixing process) at 50 s^{-1} and 5 minutes holding time.

Polymer	Polymer Concentration (%, w/v)	η_p (Pa.s)	η_{obs} (Pa.s)	η_{exp} (Pa.s)	η_{enh} (Pa.s)
High DE Pectin	1	0.017 ± 0.007	1.323 ± 0.013	0.432 ± 0.011	0.891 ± 0.017
	2	0.089 ± 0.005	1.824 ± 0.066	0.504 ± 0.009	1.321 ± 0.067
Sodium Alginate	1	0.023 ± 0.008	1.309 ± 0.025	0.438 ± 0.011	0.871 ± 0.027
	2	0.134 ± 0.007	2.254 ± 0.056	0.549 ± 0.011	1.705 ± 0.057
CMC	1	0.024 ± 0.001	1.285 ± 0.007	0.439 ± 0.009	0.846 ± 0.011
	2	0.160 ± 0.001	2.119 ± 0.052	0.575 ± 0.009	1.544 ± 0.053
Mucin	0	0.0008 ± 0.0001	0.415 ± 0.008	0.415 ± 0.008	0

Another parameter that can be used to quantify the mucoadhesion is the relative viscosity enhancement (η_{rel}) or normalised parameter which is expressed as a proportion of the observed viscosity to the expected viscosity as shown in Equation 3.4. The normalized parameters can be used to compare samples of different cohesive properties and viscosity and the value indicates the relative increase (Ferrari et al., 1997). Value of 1 for η_{rel} indicates no synergism in the viscosity while higher value shows the potential for mucoadhesive associations between biopolymers with the mucin. Table 3.4 shows the calculated η_{rel} and it is found that sodium alginate has the highest η_{rel} followed by CMC and high DE pectin.

$$\eta_{rel} = \eta_{obs} / \eta_{exp} \quad (\text{Equation 3.4})$$

Interaction and binding between biopolymer-mucin systems can be transformed into mechanical work or energy and this work contributes to the changes in shape or molecular arrangement and thus changing the viscosity. A bioadhesive force is needed between the carrier product with the mucous layer in order to successfully retain the product on the surface as the product will be subjected to the oral flow force (extensional flow, mixing and shearing) in the mouth and dislodging forces in the gastrointestinal tract.

Force of mucoadhesion (F) represents the additional intermolecular frictional force per unit area and can be expressed by Equation 3.5 (Thirawong et al., 2008) where $\dot{\gamma}$ is the shear rate (s^{-1}). Calculated value of adhesion forces are shown in Table 3.4 for tested biopolymers at shear rate of 50 s^{-1} (5 minutes holding time) and Figure 3.25 shows the plots of mucoadhesion force of each polymer. Sodium alginate showed strongest mucoadhesion force with the value of $85.29 \pm 2.85 \text{ Pa}$ for 2% (w/v) concentration followed by CMC ($77.24 \pm 2.63 \text{ Pa}$) and high DE pectin ($66.04 \pm 3.33 \text{ Pa}$).

$$F = \eta_{enh} \dot{\gamma} \quad (\text{Equation 3.5})$$

Table 3.3: Apparent viscosity, observed viscosity, expected viscosity and enhanced viscosity of 1% (w/v) high DE pectin, 1% (w/v) low DE pectin, water and their mixture with 10% (w/v) mucin (1.5 ml of solution was used for the mixing process) at 50 s^{-1} and 0 minutes holding time.

Type of Pectin	η_p (Pa.s)	η_{obs} (Pa.s)	η_{exp} (Pa.s)	η_{enh} (Pa.s)	η_{rel}	F (Pa)
High DE (~60%)	0.017 \pm 0.007	0.788 \pm 0.052	0.420 \pm 0.012	0.368 \pm 0.053	1.9	18.4 \pm 2.65
Low DE (~35%)	0.0032 \pm 0.0001	0.497 \pm 0.004	0.406 \pm 0.098	0.091 \pm 0.008	1.2	4.55 \pm 0.4
Water	0.0008 \pm 0.0001	0.404 \pm 0.098	0.404 \pm 0.098	0	1.0	0

Table 3.4: Normalised parameter and force of adhesion of different polymers in DI water at 37°C and shear rate of 50 s^{-1} (5 minutes initial holding time).

Polymer	Polymer Concentration (%, w/v)	η_{rel}	F (Pa)
High DE Pectin	1	3.07	44.59 \pm 0.84
	2	3.62	66.04 \pm 3.33
Sodium Alginate	1	2.99	43.59 \pm 1.37
	2	4.11	85.29 \pm 2.85
CMC	1	2.93	42.34 \pm 0.53
	2	3.69	77.24 \pm 2.63
Water	0	1	0

Apart from the factors mentioned earlier, various environmental factors also play an important role in mucoadhesion. Since the biopolymers used in this study are negatively charged, presence of positive ions such as Na^+ and K^+ would reduce the anionic nature of biopolymer and consequently its ability to interact with mucin is reduced as discussed in section 3.3.6. Table 3.5 shows the calculated parameters for the effect of ionic strength on the interaction between sodium alginate and mucin. It

is clearly observed that additional of 0.05 M of NaCl and KCl into the sodium alginate solution markedly reduces mucoadhesion. However, additional concentrations of more than 0.05 M of salts result in less effect on mucoadhesion. Between the two salts, the effect of KCl on mucoadhesion is less than NaCl as indicated by the η_{rel} value, where the η_{rel} of sodium alginate in 0.20 M KCl is 3.32 whilst sodium alginate in 0.20 M NaCl is 2.91. This can be explained by the fact that K^+ is more electropositive (higher tendency to be in the ionic form) than Na^+ hence would bind less to the negative sites in the sodium alginate molecules. There are more free binding sites available for sodium alginate in KCl solution resulting in stronger mucoadhesion as compared to in the NaCl solution. Moreover, the conformational structure of sodium alginate in KCl is less compact than in NaCl due to less contraction of double layer.

Table 3.5: Apparent viscosity, observed viscosity, normalised parameter and force of adhesion of 2% (w/v) sodium alginate with different ionic strength. (5 minutes initial holding time).

Ionic Strength (M)	Ion	η_p (Pa.s)	η_{obs} (Pa.s)	η_{exp} (Pa.s)	η_{enh} (Pa.s)	η_{rel}	F (Pa)
0	NaCl	0.134±0.007	2.254±0.056	0.548±0.013	1.706±0.057	4.11	85.29±2.87
	KCl	0.134±0.007	2.254±0.056	0.548±0.013	1.706±0.067	4.11	85.29±2.87
0.05	NaCl	0.099±0.001	1.743±0.093	0.513±0.011	1.230±0.09	3.40	61.49±4.68
	KCl	0.096±0.011	1.786±0.018	0.510±0.016	1.276±0.023	3.50	63.79±1.19
0.1	NaCl	0.082±0.001	1.527±0.052	0.496±0.011	1.031±0.053	3.08	51.54±2.66
	KCl	0.088±0.001	1.749±0.071	0.502±0.011	1.247±0.072	3.48	62.34±3.59
0.15	NaCl	0.089±0	1.502±0.055	0.503±0.011	0.999±0.056	2.98	49.94±2.80
	KCl	0.082±0.001	1.708±.030	0.496±0.011	1.212±0.032	3.44	60.59±1.60
0.2	NaCl	0.086±0.001	1.455±0.021	0.500±0.011	0.955±0.023	2.91	47.74±1.19
	KCl	0.085±0.001	1.656±0.013	0.499±0.011	1.157±0.017	3.32	57.84±0.85

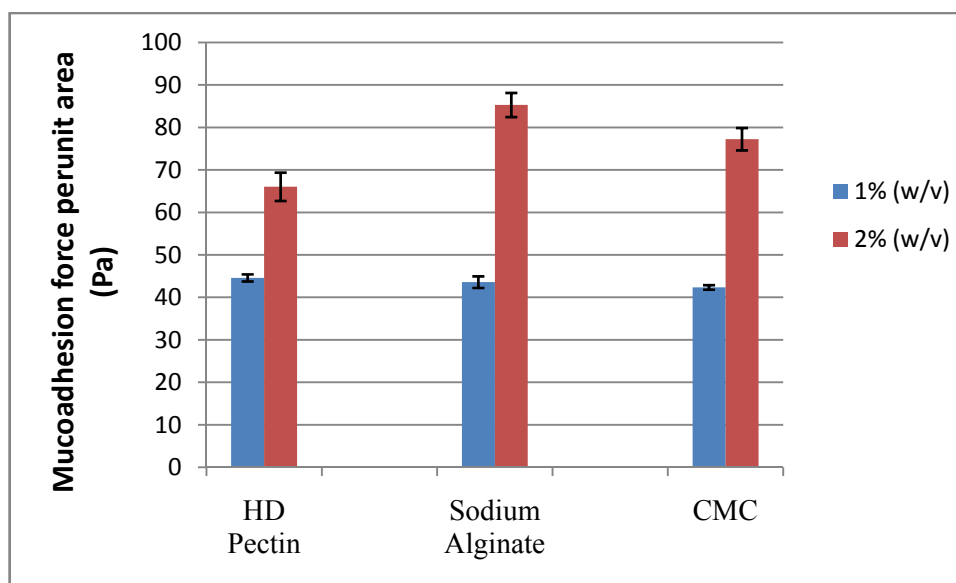


Figure 3.25: Force per unit area of mucoadhesion for three types of polymers. The mixture (polymer-mucin) was mixed at 37°C and 50 s⁻¹ shear rate with 5 minutes holding time.

3.3.8 Oscillation Analysis of the Biopolymer-Mucin Mixtures

Oscillation test was performed to analyse the viscoelastic properties of the biopolymer-mucin mixture after the shearing process by measuring the dynamic moduli (G' and G'') for a range of oscillation frequency. G' is the energy stored modulus or elastic modulus and it is reflecting as the solid (gel) like component of a viscoelastic material whilst G'' is the energy lost modulus and it is reflecting the liquid like component (Ferry, 1980). Beside the dynamic moduli, tangent delta were used to describe the overall viscoelasticity of the sample where $\tan \delta < 1$ indicates a solid or gel-like component or elastic behaviour and $\tan \delta > 1$ indicates a liquid or viscous like component (Sriamornsak and Wattanakorn, 2008). Each of the biopolymer-mucin mixtures after shearing was subjected to an initial stress sweep in order to find the linear viscoelastic region (LVR) at which the values of the moduli are independent of the applied deformation (stress and strain). Within this stress or strain range, the sample was continuously excited but it never exceeded to the point large enough to destroy the structure of the mixture. After establishing the stress sweep test, the frequency sweep test was performed for the biopolymer-mucin mixtures at temperature of 37°C with the frequency range of 0.1-20 Hz at a fixed oscillation stress of 0.1 Pa.

Figure 3.26 shows the dynamic moduli (G' and G'') for the 1% (w/v) and 2% (w/v) pectin mixed with 4 ml of 10% (w/v) mucin (dried condition). From the graph, it can be observed that both mixtures formed a weak strength of physical entangled network (more liquid like) as the value of G'' is bigger than G' . Madsen et al. (1998) described that the profiles of G' and G'' is related directly to the nature or

strength of sample. Cross-linked gel has G' larger than G'' and they are not influenced by the oscillation frequency and experimental time but physical entangled network would have G'' greater than G' at some points in the frequency range with a substantial decline in G' at low frequency. Physically entangled network needs time to untangle at low frequency while at high frequency there is not enough time for any network rearrangement resulting in an elastic deformation. From this description, all the tested polymer-mucin mixtures (pectin, sodium alginate and CMC) behaved like physical entangled network which was weaker in gel strength than cross-linked gel.

CMC-mucin mixture has the highest elastic property at lower frequency where it has the lowest value of $\tan \delta$ as shown in Figure 3.27. The value of $\tan \delta$ (δ) was decreasing (towards to 1) when higher frequency was applied on the sample. At the highest frequency (124 rad/s), sodium alginate-mucin and CMC-mucin mixture reached the value of $\tan \delta$ close to 1. Different effect was observed on high DE pectin-mucin mixture, where the value of $\tan \delta$ increased a little at the highest angular frequency. This might be caused by the rearrangement of network at higher frequency resulting in the different behaviour of the mixture.

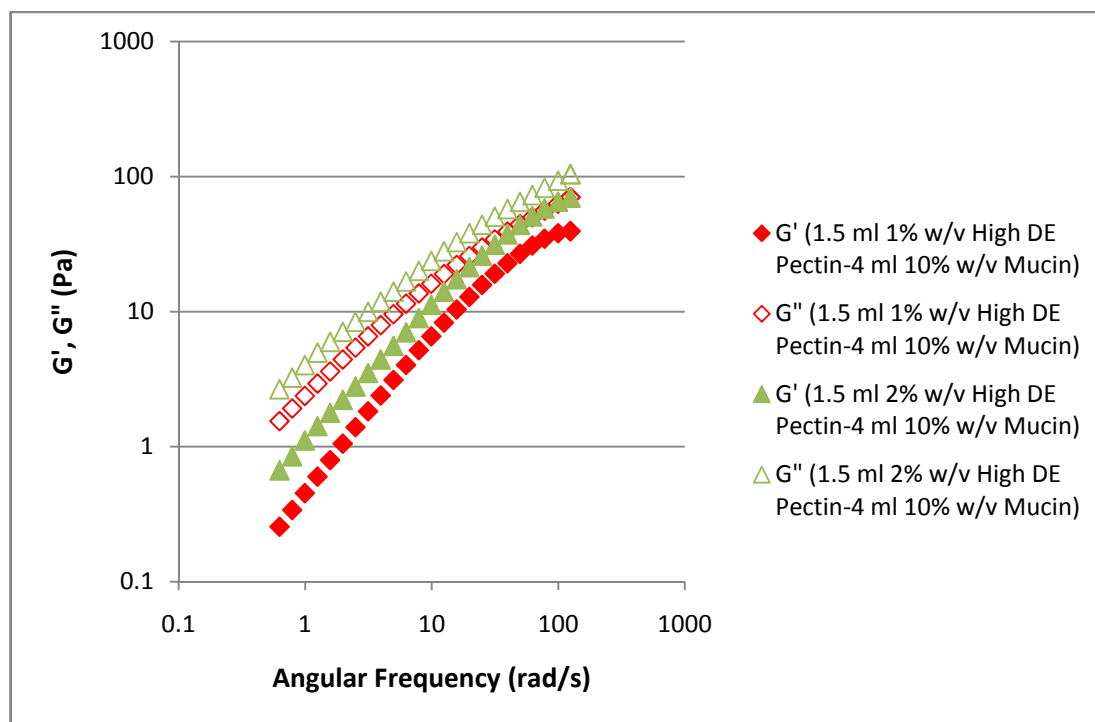


Figure 3.26: Dynamic moduli of the high DE pectin-mucin mixture.

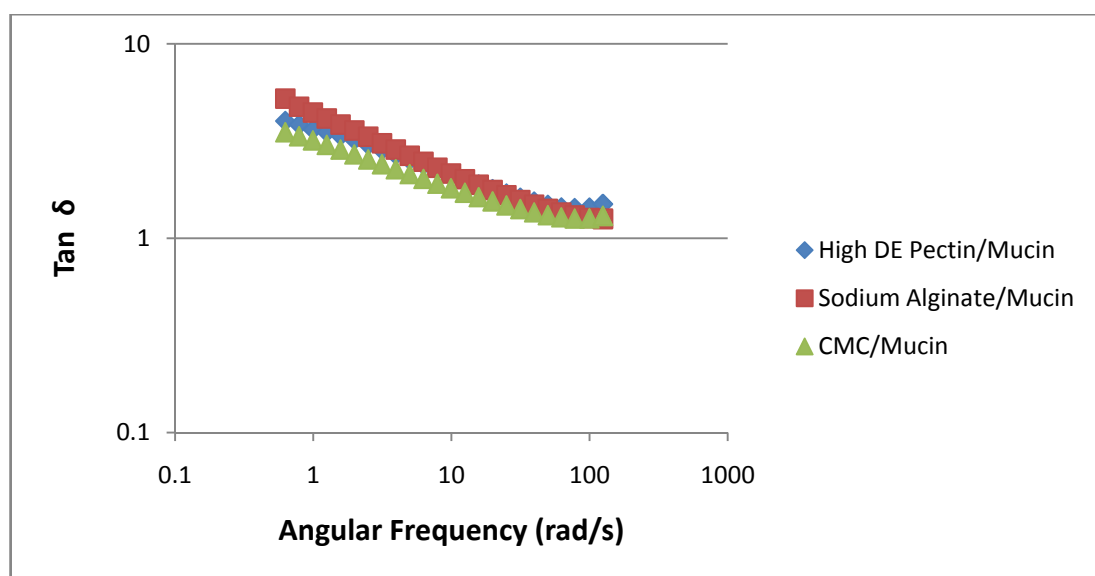


Figure 3.27: $\tan \delta$ of the 2% (w/v) different polymer-mucin mixtures.

3.3.9 Control Experiment

The viscosity profile of control experiment is shown in Figure 3.28. Control experiment with starch and plain flour were not successful due to the inability of those substrates to mix with sodium alginate solution. Two separate layers were produced and thus measured viscosity did not come to a plateau over 20 minutes shearing but was continuously increasing. Whereas, control experiment using mucin to replace sodium alginate solution (mucoadhesive polymer) was successful and the result is shown in Figure 3.28. Viscosity of 2% (w/v) mucin at 50 s^{-1} is $0.0021\pm0.0001\text{ Pa.s}$ and distilled water is $0.0008\pm0.0001\text{ Pa.s}$ at room temperature. Viscosity of water-mucin mixture was $0.415\pm0.008\text{ Pa.s}$ and thus the expected viscosity (η_{exp}) of mucin-mucin mixture would be $0.416\pm0.008\text{ Pa.s}$. However, observed viscosity (η_{obs}) was $0.437\pm0.014\text{ Pa.s}$ which means it shows an increment or synergism. With the different of $0.028\pm0.016\text{ Pa.s}$ (η_{enh}) or 6.73% (from expected viscosity), it could be contributed by error in experiment.

The value of normalised parameter, 1.07 for mucin-mucin mixture, as shown in Table 3.6 was much lower than the normalised parameter of other polymers (Table 3.4) of the same concentration indicating no significant viscosity synergism or increment in mucin-mucin mixture. The control experiment of mucin-mucin system successful showed that all the tested polymers have mucoadhesive properties due to several mechanisms and bonding but was not contributed by instrumental error. Viscosity profile of the control experiment using sugar as replacement for mucoadhesive polymer can be seen in Figure 3.29. From the graph, there is an increase for 10% (w/v) Mucin and 30% (w/v) sugar which might be contributed by

the sugar molecular structure that consist of glucose and fructose which has hydroxyl (–OH). This hydroxyl groups are believed to have ability to form interaction with the mucin structure through dipole interaction or hydrogen bonding resulting in viscosity synergism.

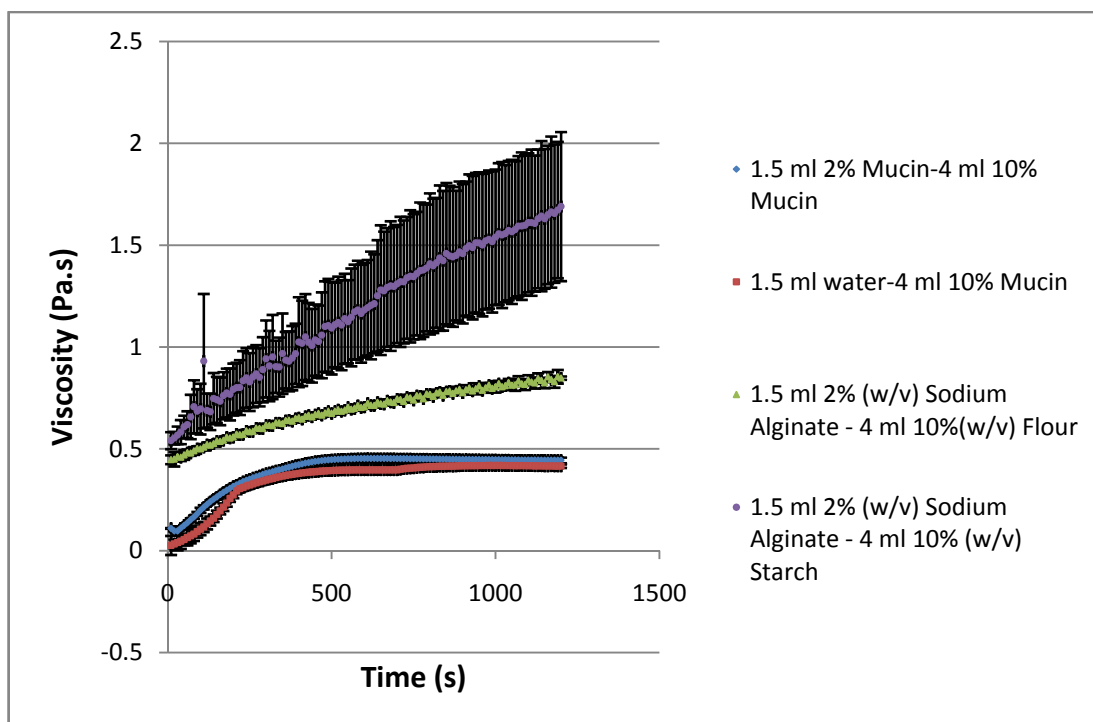


Figure 3.28: Viscosity profile of control experiment. The mixing was done at 50 s^{-1} and with 5 minutes of equilibrium (holding time).

Table 3.6: Apparent viscosity, observed viscosity, expected viscosity and enhanced viscosity of 2% (w/v) mucin and water. The mixing was done at 50 s^{-1} and with 5 minutes of equilibrium (holding time).

Mixtures	η_p (Pa.s)	η_{obs} (Pa.s)	η_{exp} (Pa.s)	η_{enh} (Pa.s)	η_{rel}
2% (w/v) Mucin	0.0021 ± 0.0001	0.437 ± 0.014	0.416 ± 0.008	0.028 ± 0.016	1.07
Water	0.0008 ± 0.0001	0.415 ± 0.008	0.415 ± 0.008	0	1

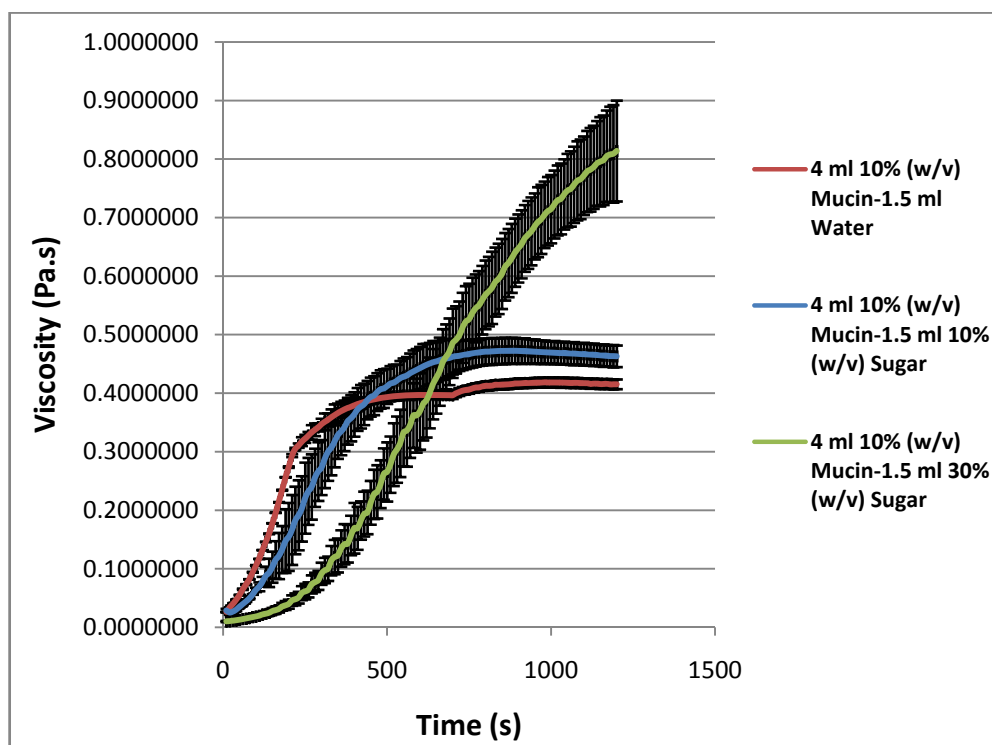


Figure 3.29: Viscosity profile of the mixture 1.5 ml 10% (w/v) sugar, 1.5 ml 30% (w/v) sugar and 1.5 ml water with mucin. (Shear rate: 50 s^{-1} ; holding time: 5 minutes).

3.4 Conclusion

The evaluation of mucoadhesiveness of chitosan, pectin and sodium alginate has been carried out using rheology instrument. Based on the value of viscosity synergism and normalised parameter, the rank order of mucoadhesion for the three biopolymers tested was found to be sodium alginate > CMC > high DE pectin and mucoadhesion of high DE pectin was higher than low DE pectin at 1% (w/v) concentration. The study also confirmed that the mucoadhesive properties were influenced by several factors which are concentration and types of polymer, contact time and ionic strength. Rheological characterisation can be considered as a

reasonably good method to characterise the mucoadhesive properties of polymer for preliminary study in order to rank them according to their mucoadhesiveness and to study the factors that affect the ability of polymer to interact with mucin. Oscillation rheology can be used to study the viscoelasticity of the biopolymer-mucin mixtures which is also reflecting to the strength of interaction between biopolymer and mucin. It is interesting to note that the mucoadhesion is affected by introducing a very low ionic strength, thus emphasizing the need of suitable formulation during designing process of carrier system so as to optimise mucoadhesion properties of a mucoadhesive material in enhancing the performance of certain types of active ingredients.

Synergism parameter is a simple way to describe the strength of adhesive or interaction hence this information is useful in order to evaluate the characteristic of the interaction. The control experiment conducted was used as reference to distinguish between mucoadhesive interaction and non-mucoadhesive interaction and as a check for the reliability and the accuracy of the method used in the research.

Chapter 4:
Pull-off and Tensile Test
Using Texture Analyser

4.1 Introduction

In this chapter, mucoadhesion characterisation of sodium alginate, sodium carboxymethylcellulose (CMC) and high degree of esterification (DE ~60%) pectin were studied using a texture analyser. Two methods were used namely, the pull-off and the tensile tests. The pull-off experiment was first designed by Smart et al. (1984) using a microforce balance with moveable base instead of Texture Analyser. This technique is based on Wilhelmy plate method which is used for measuring the surface tension of liquid. In their research, several polymers have been tested and ranked according to the strength of mucoadhesion. The procedure involved dipping clean slides and polymer coated slides (dried in an oven at 60°C) into mucous gel. The mucoadhesion of the tested polymers were then expressed as a percentage to the clean plate. Some of the factors that affect mucoadhesion such as molecular weight, contact time and pH were also investigated in their research. They found that the optimum adhesive force was exhibited by polymers with molecular weight more than 78600Da and longer contact time increased the mucoadhesive interaction. It was also observed that adhesion force of 1% gelatine gel decreased with increasing of pH but reached the optimum adhesion at the isoelectric point of the gelatin molecule. Sam et al. (1992) employed two different methods to coat the slides with the polymer. Firstly, the slide was coated with the same method as Smart et al. (1984) and the second method was using sticky agent which is Eudragit RS100 as the primer base to hold the dry polymer powder. The Wilhelmy plate method is a simple and efficient method to assess mucoadhesion of polymer and is suitable for preliminary study. However, this technique has limitation due to the dissolution of the dried layer (slide

coating) producing a slippery mucilage after long exposure in the mucous gel as found by Smart et al. (1984)

Tensile test is another method designed by previous researchers by modifying the Wilhelmy plate method. Tensile test is used to measure the detachment force between mucin (mucous layer) with the polymer substrate and also the total work required in detachment process. Figure 4.1 and 4.2 shows an example of tensile test by using modified tensiometer. The advanced dual tensiometer apparatus was able to measure two adhesive components which are tensile and shear. Thus, in this experiment the tested sample could be subjected to similar forces that act on sample in the mouth or GI tract of human. The tensile test method was used by Hagesaether and Sande (2007) to investigate the mucoadhesive of various types of pectin and the factors affecting the adhesion.

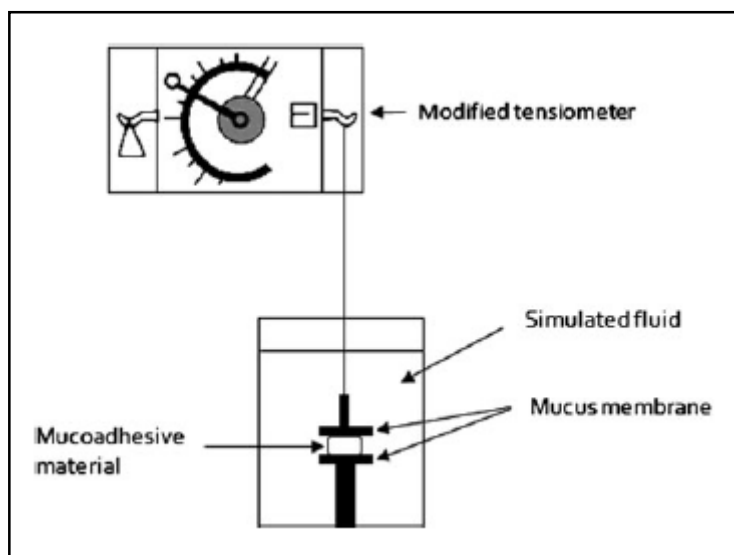


Figure 4.1: Modified of a tensiometer for measurement of detachment force between mucoadhesive material and mucous layer. (Source: Yu et al., 2014)

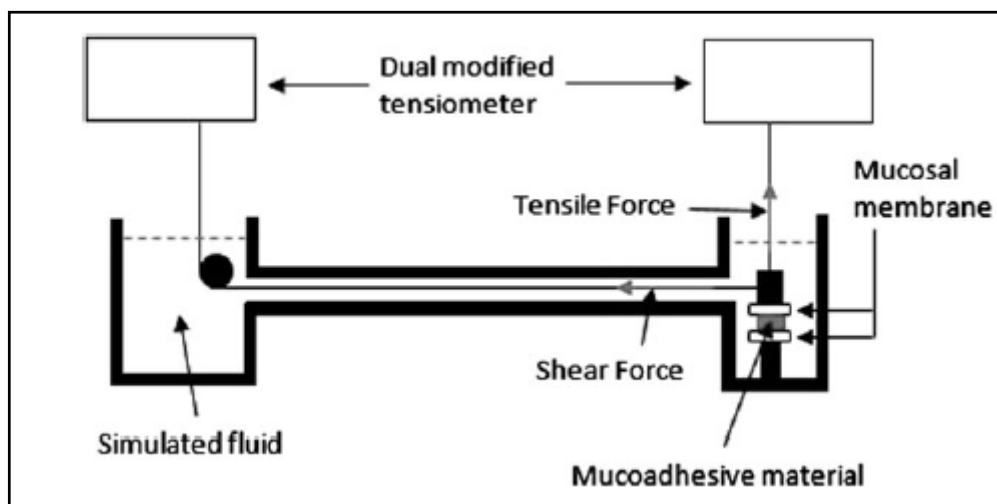


Figure 4.2: An advanced dual tensiometer apparatus for tensile force measurement. (Source: Yu et al., 2014).

4.2 Materials and Methods

Highly viscous chitosan from crab shell, pectin from citrus peel (degree of esterification ~60%), acetic acid (ACS reagent, $\geq 99.7\%$), sodium alginate, sodium carboxymethylcellulose (CMC) (average $M_w \sim 250000$) and mucin type II with bound sialic acid of ~1% were purchased from Sigma-Aldrich Company Limited, United Kingdom. All chemicals were analytical grade and used as received.

4.2.1 Pull-Off Experiment

4.2.1.1 Materials and Instrumental Preparation

Solution of 1% (w/v), 2% (w/v) and 3% (w/v) high DE pectin (Degree of esterification ~60%), 1% (w/v) and 2% (w/v) sodium alginate, 10% (w/v) mucin and 1% (w/v) sodium carboxymethylcellulose (CMC) were prepared by slowly adding

the powder into double distilled water and stirring for at least three hours to ensure the material was fully dispersed. 1% (w/v) chitosan solution was prepared by adding slowly the high viscosity chitosan powder into 1% (v/v) acetic acid and stirred using a motorised rotor with impeller for at least 12 hours. Chitosan is not soluble at neutral pH (pH 7) and only soluble in acidic condition where the amine group in chitosan will be protonated.

A microscope slide (0.2 cm x 2.1 cm x 7.6 cm) was coated with 0.5 ml of 10% (w/v) mucin dispersion by applying two layers of 0.25 ml for each side (total of mucin on each side is 0.5 ml). The dimension of slide covered with mucin layer was 2.1 cm x 3.0 cm. Each layer was dried in an oven at 70°C for 30 minutes to ensure all water had evaporated and this stage was repeated so each side of microscope slide had 2 coatings. A TA.XT.Plus Texture Analyser supplied by Stable Micro Systems Limited, United Kingdom consisting of a fixed platform and a moveable arm was setup so that the arm lowers at a rate of 1 mm/s, holds for 5 minutes and then raises up at a rate of 1 mm/s. The experiment was done by using “Hold until Time” sequence with compression mode. The slide was attached to the upper arm with self tightening roller grips probe and a 5 kg load cell. The arm was lowered until the slide had penetrated into 30 ml of polymer solution by using “Distance target mode) (in a 60 ml beaker) with 30 mm travel distance (9 mm at air space and 21 mm in polymer solution) In order to study the effect of different holding time, the setup was changed to 30 seconds, 3 minutes and 7 minutes. The maximum force was recorded when the slide detached from the polymer surface. Figure 4.3 shows the schematic diagram of this experiment.

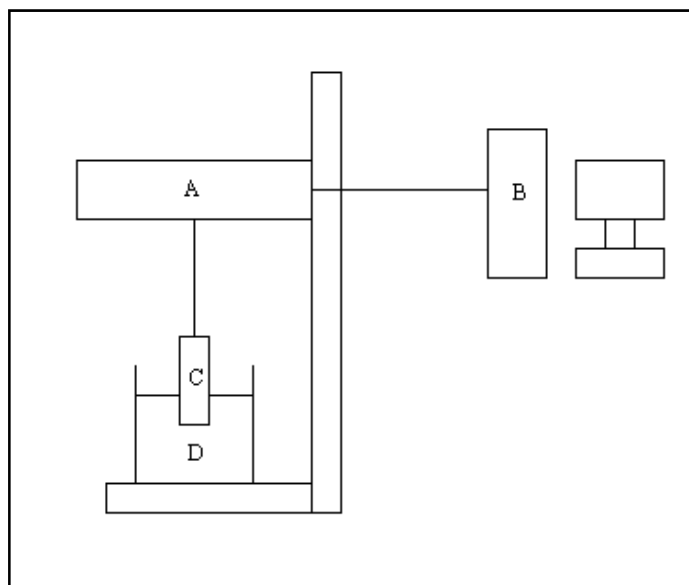


Figure 4.3: Schematic diagram of the TA.XT.Plus Texture Analyser. (A) Texture Analyser with moveable arm; (B), Dell PC running the programme Texture Analysis; (C), Clean or mucin coated slide; (D), Glass beaker containing the polymer solution. (Adapted from Smart et al., 1984).

4.2.2 Tensile Test

4.2.2.1 Materials and Instrumental Preparation

A TA.XT.Plus Texture Analyser (Stable Micro Systems Limited, United Kingdom) was used with a 20 mm diameter aluminium probe and 5 kg load cell. The experiment was done by using “Hold until Time” sequence with compression and force target mode. 125 μl of polymer solution (pectin, sodium alginate and CMC with 1% (w/v) and 2% (w/v) concentration) and 10% (w/v) mucin dispersion were evenly spread on a filter paper (20 mm diameter) with an inert backing layer (Benchkote paper). The samples were allowed to rest for 20 minutes to ensure proper interaction between the polymer and the filter paper. The polymer sample was

attached to the probe (moveable arm) and mucin sample was attached with double sided adhesive tape to the platform as shown in Figure 4.4. The probe was then lowered until it reached contact with the mucin sample and a preload of 200 gram force was applied for 100 s. After that, the probe was raised with a speed of 0.01 mm/s. In order to measure the unspecific interaction, polymer samples and mucin sample were also tested with distilled water (solvent).

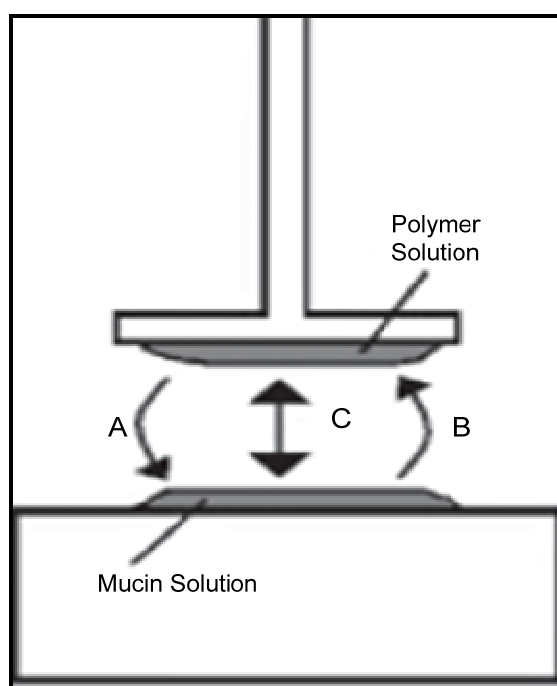


Figure 4.4: Schematic diagram of tensile test. The arrows indicated with capital letters represent relevant forces experienced in the test. Unspecific force polymer (A), unspecific force of mucin (B) and specific force between the polymer and mucin (C). (Source: Hagesaether and Sande, 2007).

4.3 Results and Discussion

4.3.1 Pull-Off Experiment

Figure 4.5 shows the sequence of pull off experiment and displayed graph by Texture Analyser when the probe experienced the forces. Between point (a) and (b) the slide is above the solution. At this position, the force measured by the Texture Analyser is set to zero when the slide moves in ambient air. Point (b) is the point at which the slide touches the surface of the solution, and due to the surface tension a meniscus is formed between the slide and the solution. Between (b) and (c) the probe is experiencing positive force as the solution resists the movement of the slide into it. This is possibly an indication of the viscous force and bouncy force as shown in Figure 4.6. Besides, there is also mucoadhesion force involved during first contact of polymer with mucin (initial wetting bonding). More force is required to push the slide through a more viscous solution as both forces is dependent on depth of slide immersed in polymer solution and viscosity of solution. At point (c) the slide is held for different holding time so that the mucin is re-hydrated and interactions between mucin and polymer can occur. After holding time, the slide is raised up and the Texture Analyser displays a negative force. At point (d) the slide is just touching the top of the solution and the maximum force pull-off force is recorded, between points (d) and (e) a capillary bridge or ‘string’ can be seen. The capillary bridge is broken at point (e) and the slide travels in air medium to the starting point. Point (f) is the end point of the experiment whereby the non-zero force is due to some solution that remains ‘adhered’ to the slide.

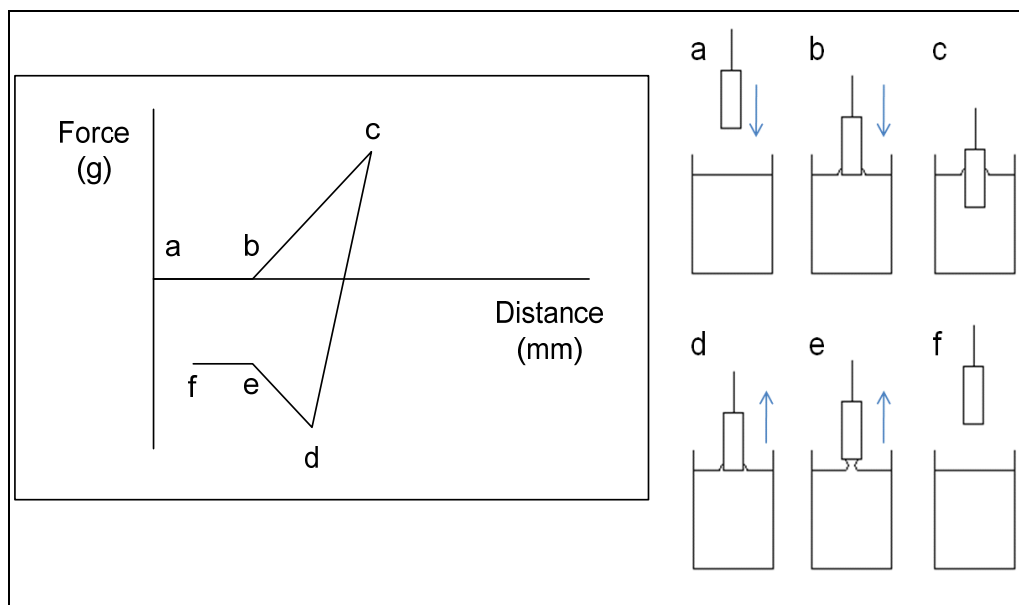


Figure 4.5: Schematic diagram of important sequences in pull-off experiment.

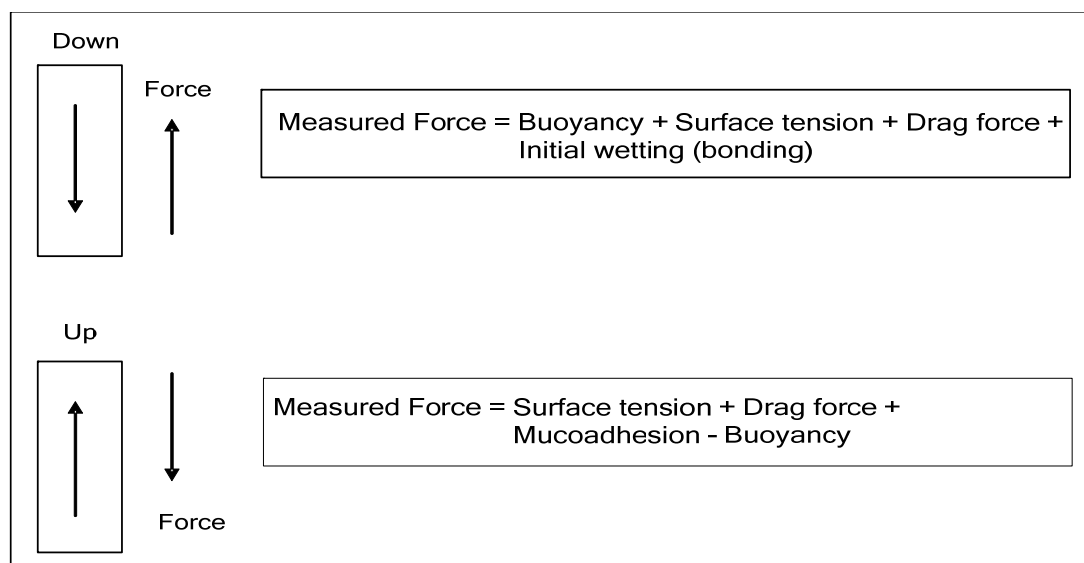


Figure 4.6: Force balance that experienced by slide. Total force is the measurement recorded by texture analyser.

4.3.1.1 Effect of Different Polymers and Concentration of Polymers

Different concentration of polymers and types of polymers show different effect on mucoadhesion as reflected by the force profile measured during pull-off experiment as shown in Figure 4.7. During dipping process into the polymer solution, the slide experienced several forces as described in Figure 4.6. Higher concentration of polymer solution recorded higher force as shown in Figure 4.7, and 3% (w/v) pectin solution gives the highest value. The same profile can be observed from Figure 4.8. From both Figures (4.7 and 4.8), the ascending order of force can be sorted by water, 1% (w/v) high DE pectin, 2% (w/v) high DE pectin, 2% (w/v) sodium alginate and 3% (w/v) high DE pectin for dipping step (step B-C). At this step, the viscous drag force plays the main role on the force measurement. According to Stokes' Law (Equation 4.1), the viscous drag force is proportional to solution viscosity and velocity of particles with the assumption that the surface is smooth. Equation 4.1 shows the viscous drag force of a sphere particle where F_d is the viscous drag force, μ is the viscosity of fluid, R is the radius of the spherical particle and v is the velocity of the particle. The viscosity of 2% (w/v) sodium alginate solution is 0.134 Pa.s while 2% (w/v) high DE pectin is 0.089 Pa.s (measured with rheometer). The difference in viscosity of these polymers (sodium alginate and high DE pectin with same concentration) results in different force measurement during the dipping process. In this study, the experiment were done in a different way compared to Smart et al (1984) and Sam et al. (1992) where the slides were coated with mucin instead of the polymer as used by the earlier researchers.

$$F_d = 6\pi\mu Rv \quad \text{(Equation 4.1)}$$

There was an increase in value of forces between mucin coated slide and clean slide. There are two factors contributing to the different measurement which are the surface roughness of the slide and mucoadhesion interaction between polymers with the mucin layer on the slide. Dried mucin layer on the slide caused the surface of the slide to be slightly rough thus increasing the viscous drag force. Drag force equation is proportional to drag coefficient (referring to the roughness of the surface) as shown by Equation 4.2 where F_d is the viscous drag force, ρ is the density of fluid, C_d is the drag coefficient, A is the reference area and v is the velocity of the particle.

$$F_d = \frac{1}{2} \rho v^2 C_d A \quad (\text{Equation 4.2})$$

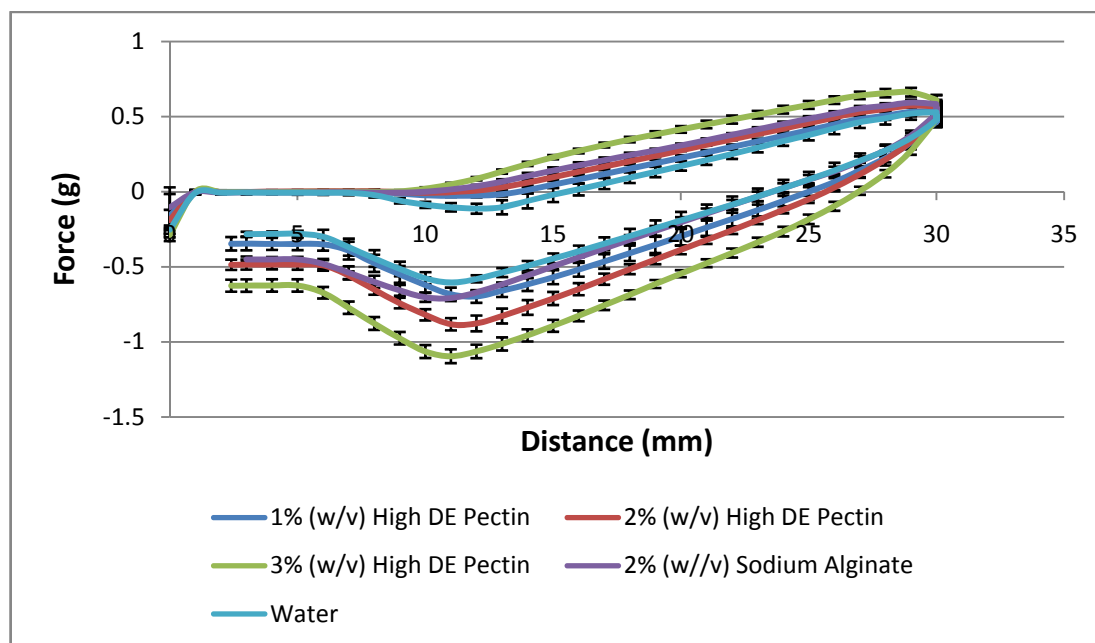


Figure 4.7: Force of pull-off experiment recorded by texture analyser for different types of polymer with mucin coated slide. (Holding time is 300 s).

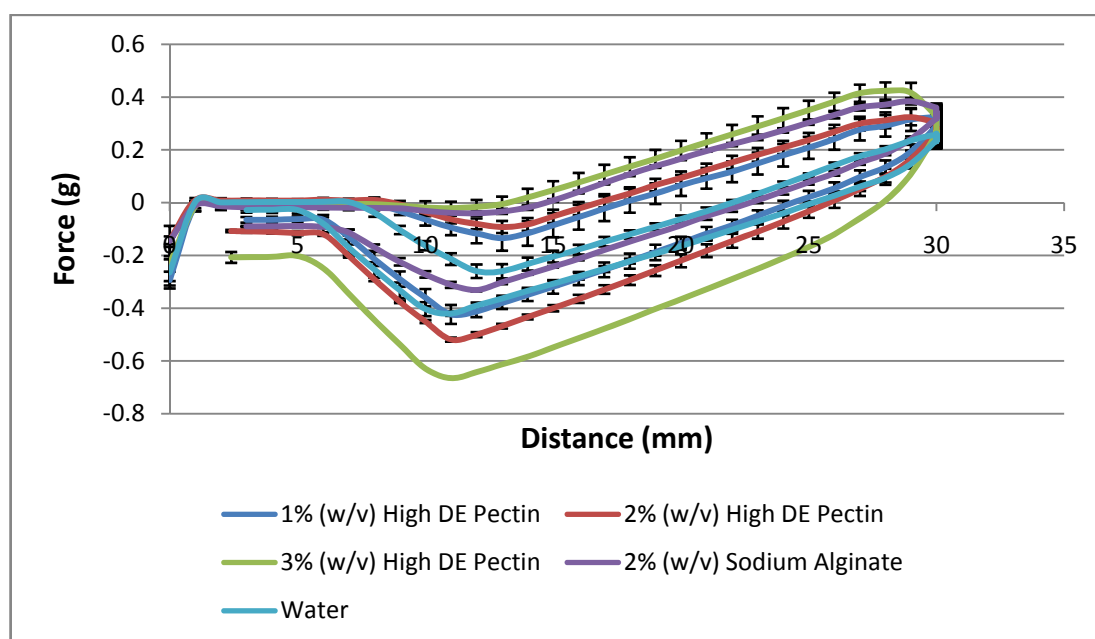


Figure 4.8: Force of pull-off experiment recorded by texture analyser for different types of polymer with clean slide. (Holding time is 300 s).

Pulling step (C-D) shows different rank of force measurement between sodium alginate solution and high DE pectin solution. Sodium alginate shows lower force measurement during pulling step as compared to high DE pectin solution. At point C (holding time), the polymers have mucoadhesion interaction with mucin layer due to hydrogen bonding and interpenetration of polymer structure with mucin network. Therefore, the force measured during the pulling step is the cohesion of the solution. This finding is based on the fact that some of the polymer solution remained on the slide after pulling step (E-F). The force balance can be illustrated as shown in Figure 4.9. The cohesion of the polymer solutions is lower than the mucoadhesion of polymers with mucin layer hence the force measurement is mainly on the cohesiveness of the polymer solutions. This argument is in agreement with Sam et al. (1992) where the force measured in their experiment was mainly based on the cohesiveness of mucous gel. Polymers solution remained on the slide (mucin coated) because mucoadhesion interaction polymer-mucin is greater than cohesion of the solution itself. It means that the cohesiveness of sodium alginate solution is lower than high DE pectin solution of the same concentration. This result is contradicting with the nature of sodium alginate which is believed to have stronger cohesiveness than pectin. Seixas et al. (2013) explained that pectin film has higher swelling properties and is totally soluble in water as compared to alginate film. This is because alginate has higher rigidity and lower deformability. This conflicting result may also be caused by different types of materials used in the experiment.

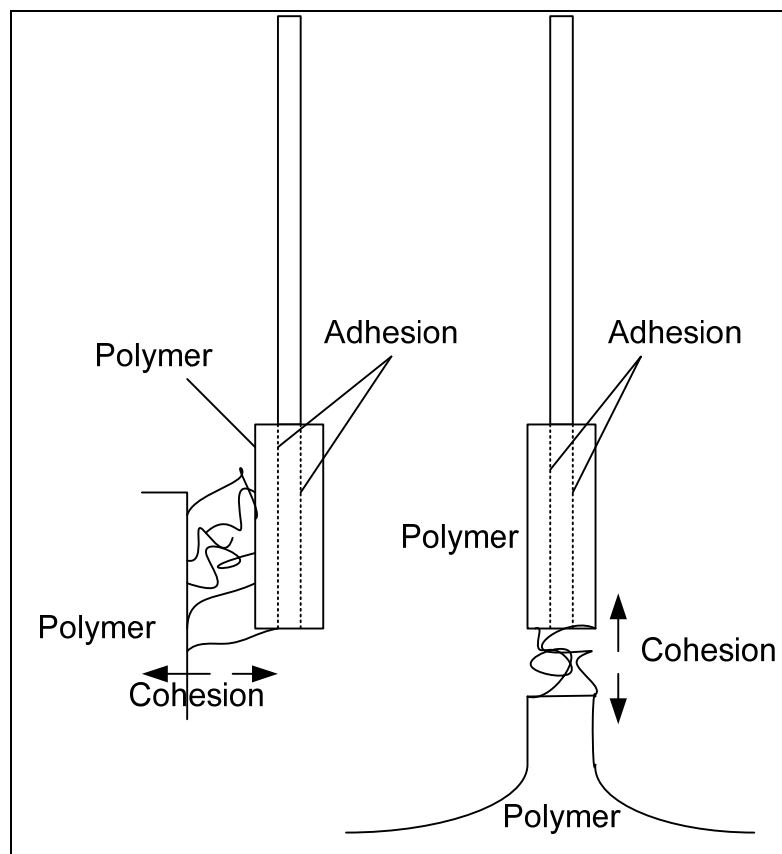


Figure 4.9: Illustration of cohesion force recorded during pulling step.

The cohesiveness of the solution is increased with increasing of concentration due to stronger polymer structure network, which is formed with higher availability of polymers. This can be seen in both Figure 4.7 and 4.8 where 3% (w/v) high DE pectin solution has greater force measurement as compared to 1% (w/v) and 2% (w/v). The same effect can be seen at point D (peak force or detachment force). However, the amount of sodium alginate solution remained on the slide is almost the same with pectin solution. This result shows that sodium alginate has better mucoadhesion effect than pectin which is the same result obtained in the rheological characterisation chapter. The amount of sodium alginate attached on the mucin layer is more than pectin but the bulk solution attached to the slide is the

reverse. This result can be explained by interpreting the mass changed at holding time as shown in Figure 4.10. It can be seen that sodium alginate has higher rate of mass changed as compared to pectin solution at the same concentration (2% w/v) despite the rate being very marginally different. It is clear that wetting is one of the main mechanisms during the mucoadhesion process. The rate of mass change of water is higher than 2% (w/v) sodium alginate and high DE pectin (1% and 2% w/v) and close to 3% (w/v) high DE solution. Smart (2005) explained that the first step of adhesion is an intimate contact (contact stage) where wetting process occurs between the mucoadhesive polymer and mucous layer followed by consolidation step where various physicochemical interactions take place.

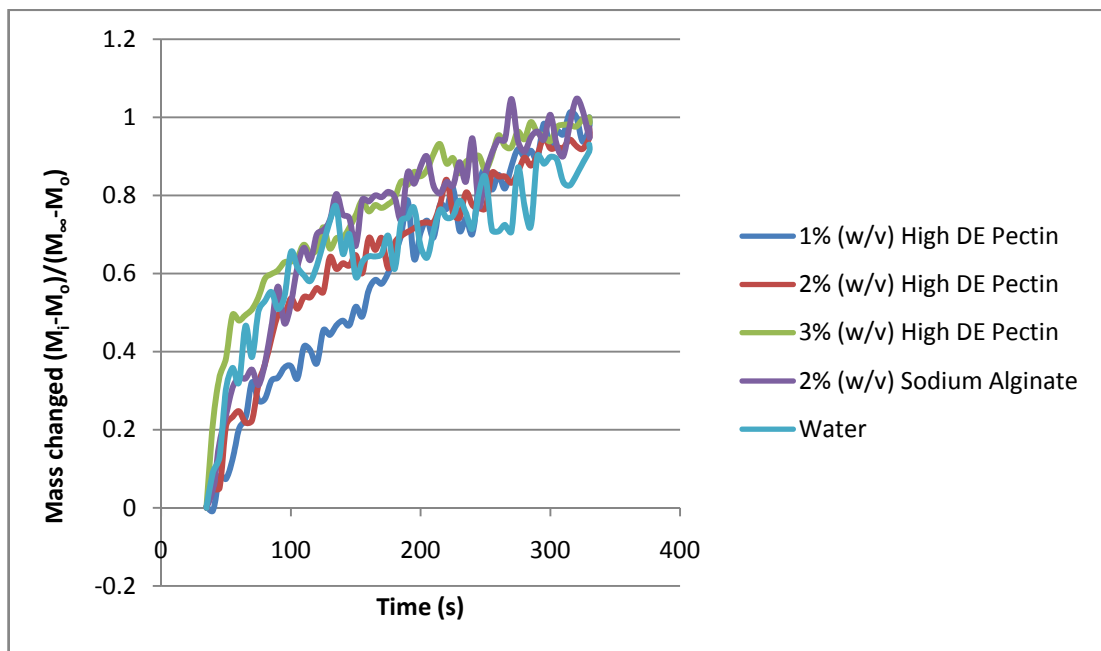


Figure 4.10: Mass changed $[(M_i - M_0)/(M_\infty - M_0)]$ during holding time (420 s) for different polymer solutions.

Table 4.1 shows the value of the maximum pull off force (peak force). 3% (w/v) high DE pectin solutions show the highest values as compared to other solutions with the maximum force of 1.098 ± 0.045 g. The interesting point is 2% (w/v) sodium alginate solution shows lower peak force as compared to 2% (w/v) pectin solution for the both clean slide and mucin coated slide but the value of mucoadhesion is slightly higher. This value is emphasizing the fact that sodium alginate has better mucoadhesion properties than pectin. Similar result was reported by Hagesaether and Sande (2007) where sodium alginate has better mucoadhesiveness as compared to pectin with DE of 70% (high DE). Smart et al. (1984) also reported that sodium alginate has higher mucoadhesion than pectin. The observation as illustrated in Figure 4.8 shows that there was some polymer solution sticking on the clean slide due to hydrophilicity of the slide surface which promotes interactions with the polymer solutions.

However, the difference of mucoadhesion interaction between sodium alginate and pectin (2% w/v concentration) appeared to be small. Sam et al (1992) explained that this result was obtained because of the maximum force measured in the experiment was related to the cohesion force between the samples instead of the correct tack force required to separate the mucoadhesive polymer from mucin. Basically, measurement of mucoadhesion interaction was based on the amount of polymers interacting with the mucin coated slide which also reflecting the maximum pull-off force. For example, the mass of the mucin coated slide and clean slide with 2% (w/v) sodium alginate were 0.451 ± 0.019 g and 0.089 ± 0.003 g respectively which gives the difference of 0.362 ± 0.020 g. Whereas, for 2% (w/v) pectin solution was

0.486±0.107 g and 0.107±0.005 g which gives a difference of 0.379±0.107 g. 1% (w/v) chitosan solution in 1% (v/v) acetic acid was also tested using this technique. The result is not published in this thesis due to failure to show adhesive effect as observed in the rheological characterisation.

Table 4.1: Maximum pull-off force using the Texture Analyser TA.XT.Plus for different polymer solutions (holding time is 300 s).

Polymer	Maximum Pull Off Force (g) and Percentage of Different		
	Clean Slide	Mucin Coated	Mucoadhesive Interaction
1% (w/v) high DE Pectin	0.444±0.022	0.711±0.041	0.267±0.047 (160%)
2% (w/v) high DE Pectin	0.522±0.008	0.894±0.046	0.372±0.047 (171%)
3% (w/v) high DE Pectin	0.667±0.014	1.098±0.045	0.431±0.047 (164%)
2% (w/v) Sodium Alginate	0.336±0.009	0.721±0.018	0.385±0.002 (215%)
Water	0.434±0.010	0.620±0.014	0.186±0.002 (142%)

*Maximum force has been positively valued of negative peak in the graph.

*Percentage value is the relative percentage of mucin coated over clean slide.

4.3.1.2 Effect of Different Holding Time on Mass Absorbed

The effect of different holding time at point (C) can be seen in Figure 4.11. The force recorded and experienced by the slides increased with longer holding time. From previous literature review, the interaction between mucoadhesive polymers with mucin is a function of time. Longer contact time will allow the entanglement and interpenetration of polymer network into mucin structure to form stronger bonding and to allow more interaction to occur. Moreover, the hydrogen bonding between the carboxyl and hydroxyl group in sodium alginate and pectin with amine group of mucin increased with increasing contact time. One of the theories in the mucoadhesion is diffusion theories (Smart, 2005). The diffusion of the polymer chain into the mucin network is dependent on the diffusion coefficient and the contact time. The influence of these variables in diffusion theory can be elaborated from Fick's second law (Equation 4.3) where c is the concentration in dimensions of (amount of substance/length³. e.g. molm⁻³), t is time, D is diffusion coefficient in dimensions of (length² per time. e.g. m²s⁻¹) and x is the position (e.g. m).

$$\frac{\partial c}{\partial t} = D \cdot \left(\frac{\partial^2 c}{\partial x^2} \right) \quad (\text{Equation 4.3})$$

However, there is a time limit for the polymer to be in contact with mucin because when the contact time is too long, the interaction between polymer and mucin will decrease due to the formation of slippery mucilage (Smart, 2005). In this experimental context, too long holding time hydrates the mucin causing the layer to detach from the slide. The detachment can also be explained based on the diffusion theory of adhesion which emphasizes that diffusion at the interface between polymer

and mucin is a two-way process where polymer diffuses into mucin and the reverse (mucin diffuses into polymer) also occurs. Therefore, diffusion of mucin into polymer weakens its attachment to the slide causing the mucin to detach from the slide. The diffusion theory is supported by Fick's second law which states that diffusion at the interface (area between two surfaces) happens in two directions.

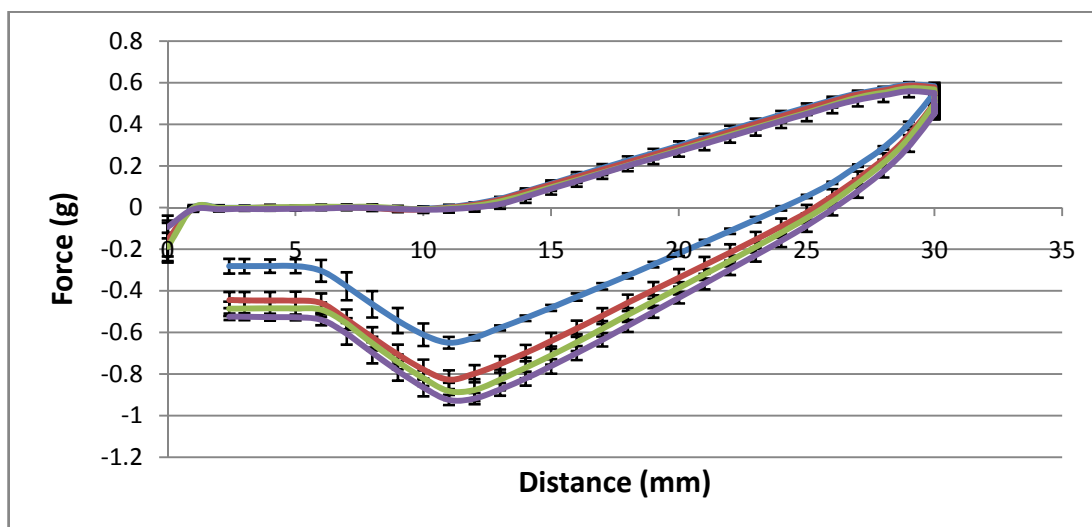


Figure 4.11: Force profile of pull-off experiment recorded by texture analyser with different holding time (— 30 s, — 180 s, — 300 s, — 420 s) for 2% (w/v) high DE pectin solution with mucin coated slide.

4.3.1.3 Mass Changed During Holding time

The results obtained from the normal pull off experiment sequence (dipping and pulling at same rate) do not give accurate or complete information about the mucoadhesion interaction between the tested polymers and mucin layer. In order to get more information on the mucoadhesion such as the rate of interaction between tested polymers and mucin layer, holding step (point C) would be the point of interest for the study. A study on the effect of the dipping step (B-C) on the overall

mucoadhesion interaction was carried out with fixed holding. This study was done in order to get general information whether current dipping speed and process has any influence on the overall mass absorbed. The test was done with different speed of dipping and pulling but with the same total time of cycle (dip and pull). 2% (w/v) sodium alginate solution was used for this experiment with three modes as described below:

A= Dipping into polymer solution, B= Pulling out from solution

Mode 1= A: 0.5 mm/s, B: 1.5 mm/s

Mode 2= A: 1.0 mm/s, B: 1.0 mm/s

Mode 3= A: 1.5 mm/s, B: 0.5 mm/s

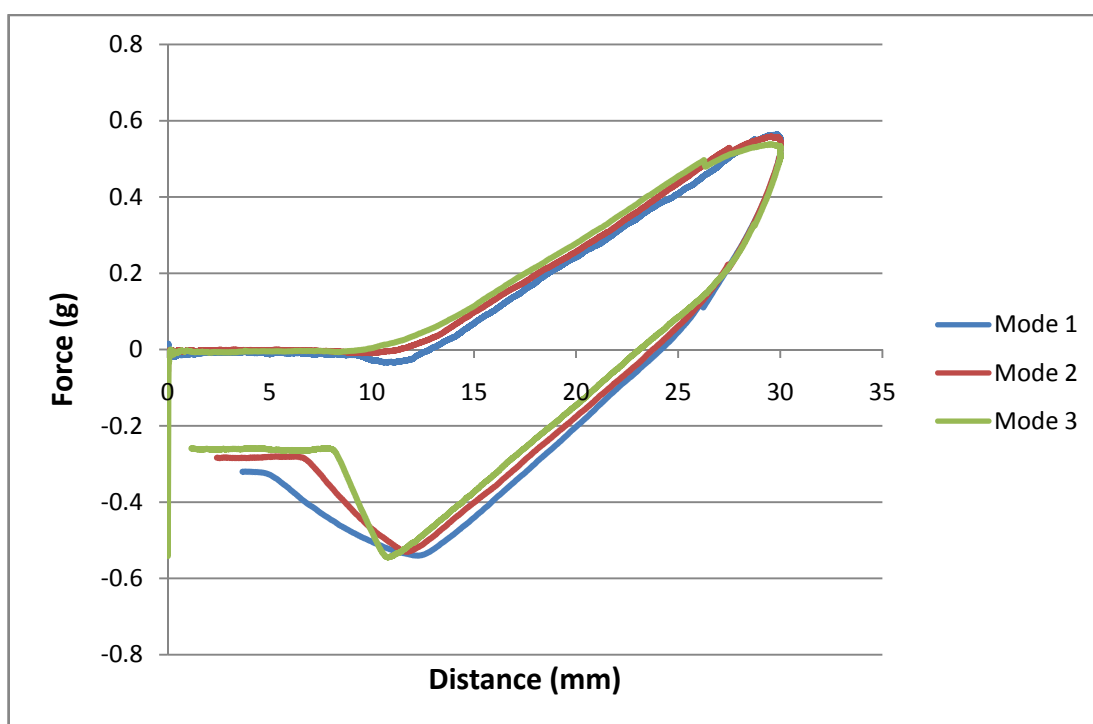


Figure 4.12: Force profile with different modes speed of 2% (w/v) sodium alginate.

Holding time is 100 s.

Figure 4.12 shows the force profile of the different modes of dipping and pulling. It is clear that dipping step has influenced on the total mass of sodium alginate attached to mucin slide. Mode 1 has the most weight of sodium alginate whilst Mode 3 has the least. Slower dipping process of Mode 1 allows more time for sodium alginate and water component (in the solution) to form interaction with mucin layer as compared to faster speed in Mode 3. However, Mode 3 shows the highest force measurement because the speed (velocity) of slide is a factor in drag force. Therefore, the effect of dipping process has been eliminated through the very fast dipping speed. The dipping speed was set at 30 mm/s and the pulling speed was maintained at 1 mm/s.

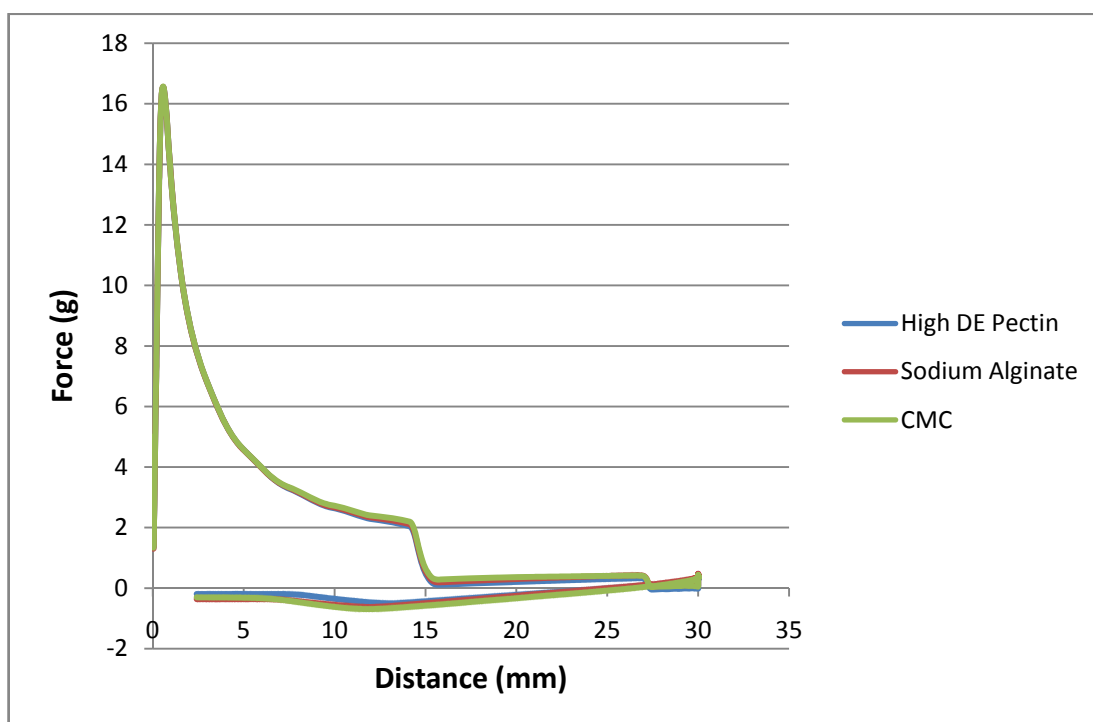


Figure 4.13: Force profile of different type of polymers (2% w/v) with holding time of 420 s. (Fast dipping into polymer solution and pulled out at 1 mm/s).

Figure 4.13 shows the force profile experienced by the mucin slides during fast dipping step for three polymer solutions which are high DE pectin, sodium alginate and CMC, each with a concentration of 2% (w/v). The force recorded at holding time is shown in Figure 4.14. At this point, the forces involved were buoyancy (up) and mass absorbed on the mucin layer (down). At starting point of the holding time, the buoyancy was at the maximum and the negative slope indicated that buoyancy was countered by polymer mass absorbed on the mucin slide. The buoyancy (Equation 4.4) is a function of the solutions' density, thus the buoyancy effect experienced by the slide should be the same for all polymer solution due to same concentration (B is buoyancy, ρ is liquid density, V is the volume of the displaced body of liquid and g is the gravitational acceleration). The different values of force measured at starting point might be caused by the different values in surface tension. Surface tension acted as a capillary effect at the edge of the slide and solution surface. The surface tension counters the force of the buoyancy. The surface tension value of 2% (w/v) sodium alginate is 56.0 mN/m and 2% (w/v) CMC is 78.2 mN/m measured using Du Nuoy Ring method (Lee et al., 2012). This is the reason why CMC shows lower force measurement profile at starting point during holding time.

$$B = \rho V g \quad \text{(Equation 4.4)}$$

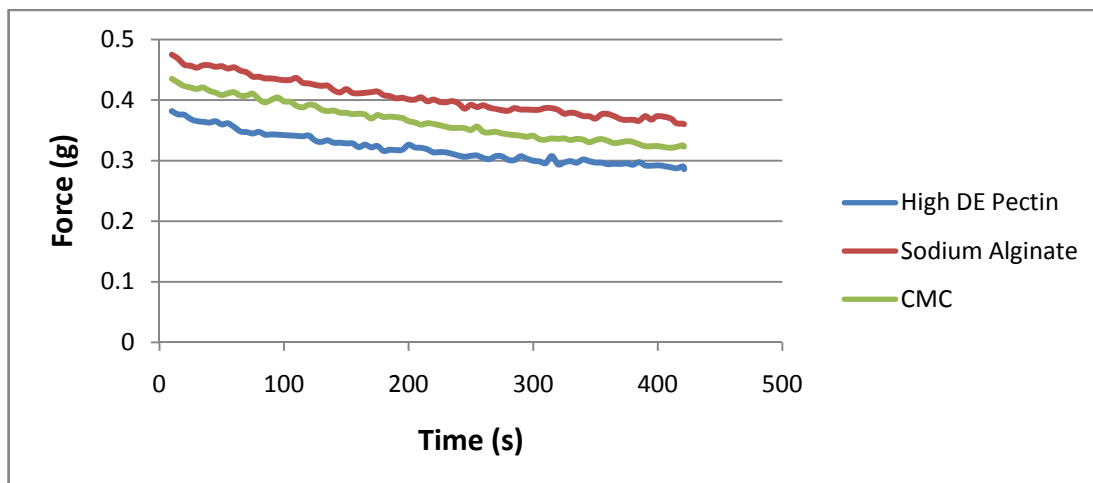


Figure 4.14: Force recorded during holding time.

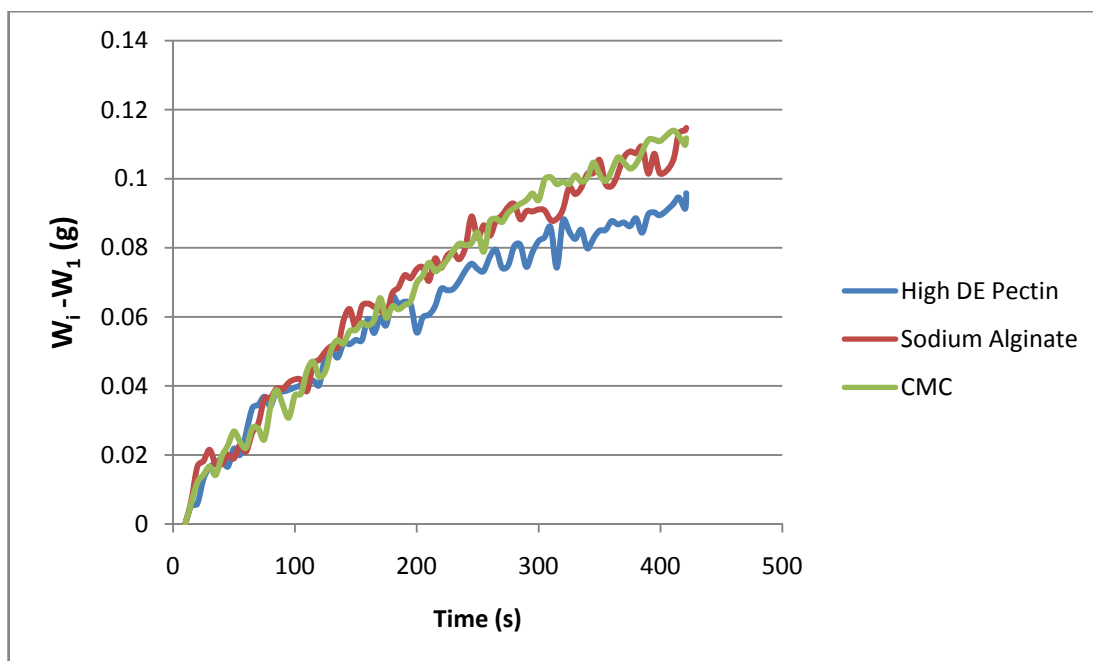


Figure 4.15: Weight change of mucin slide during holding time.

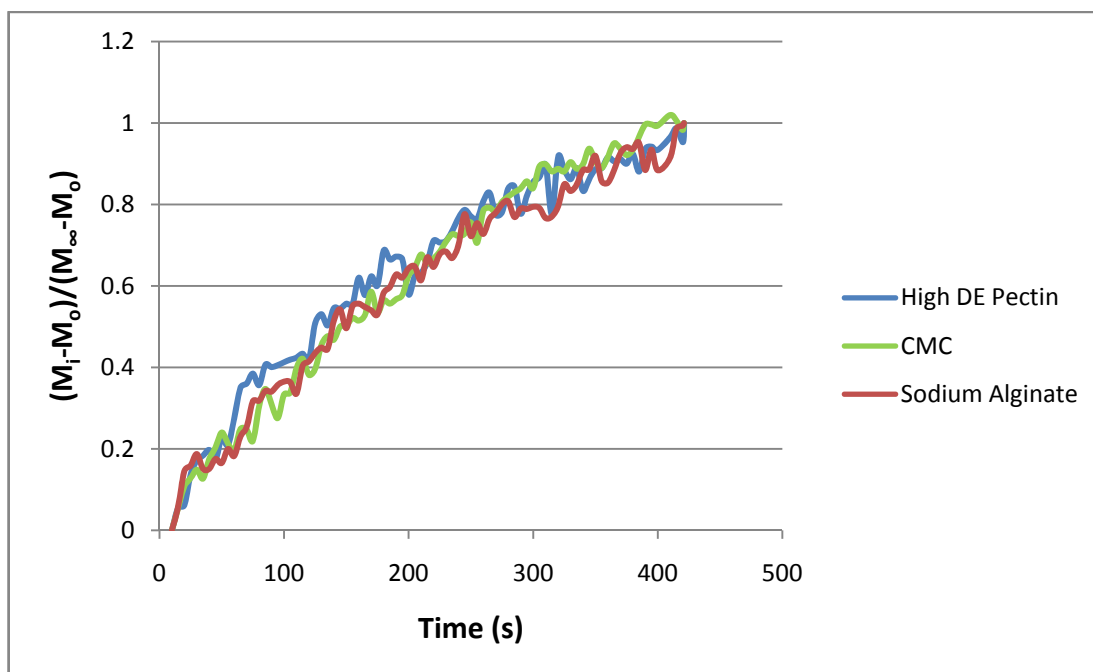


Figure 4.16: Relative weight change of mucin slide during holding time.

Figure 4.15 and 4.16 shows the weight change and the relative weight change of the mucin slide during holding time. All three polymers show almost the same rate of weight change during the holding time but pectin solution has lower rate after about 200 s. The holding time applied in this experiment was not long enough to get a plateau (zero rate). Longer holding time should be applied to get an ideal saturated interaction between tested polymers with the mucin layer. However, longer holding time will result in detachment of mucin layer from the slide and dissolve in the polymer solution. This experiment can be considered successful in studying the absorption rate (represent the total interaction) of mucoadhesive polymer solution into the mucin layer. Thus, it is possible to study the dynamic interaction between mucoadhesive polymer and mucin layer using this experiment.

4.3.2 Tensile Test

4.3.2.1 Peak Force and Total of Work of Different Concentration and Biopolymers

Tensile test is another useful measurement technique to qualify and quantify the mucoadhesive for polymers. Figure 4.17 shows an example of force profile when filter paper with pectin spread was detached from mucin spread filter paper after 100 s holding time and constant pre-force of 200 g. Peak of force is often referred to as the adhesive strength or tack force and it is related to the force needed to start separating the mucoadhesive material from the mucin layer. This force will reflect the overall strength between them. Figure 4.17 shows the peak force mucin-high DE pectin, water-high DE pectin and mucin-water. Pectin-mucin peak gives the total of adhesion force. In order to assess the specific interaction, net force was estimated using Equation 4.5 where MP is mucin-polymer force, WP is water-polymer force and MW is mucin-water force. WP and MW are also known as unspecific interaction.

$$Net\ Force = MP - (WP + MW) \quad \text{(Equation 4.5)}$$

Area under curve (AUC) represents the total of work required for the detachment of the mucoadhesive material from the mucin layer. This leads to a conclusion that total of work is a better measurement of adhesive capability than peak force because the product will be subjected to the oral flow forces (extensional flow, mixing and shearing etc) in the mouth and dislodging forces in the gastrointestinal tract (GI tract)

(Hagesaether and Sande, 2008). However, this is only true if total of work correlates well with the peak force. This correlation is clearly shown by bar graphs in Figure 4.18. The numerical results for the tensile test are shown in Table 4.2 and 4.3.

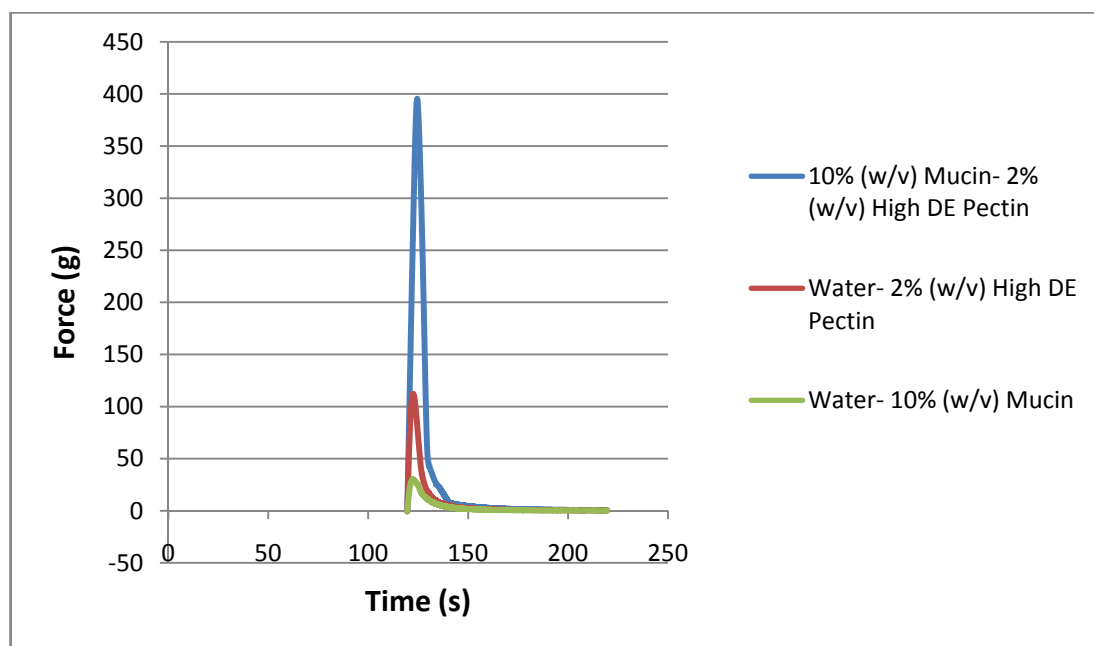


Figure 4.17: Force versus times for 10% (w/v) mucin and 2% (w/v) high DE pectin solution indicating the general mucoadhesion and unspecific mucoadhesion. The curves were obtained from tensile testing of mucin-pectin solution (MP) (blue line), water-pectin solution (WP) (red line) and mucin-water solution (MW) (green line).

Table 4.2: Peak forces and Normalised parameter of tensile test for different of concentrations and polymers.

Polymer	MP (g)	WP (g)	MW (g)	Net (g)	Normalised Parameter
1% (w/v) Pectin	238.97±18.02	1.47±0.64	26.75±2.20	210.75±18.17	7.47
2% (w/v) Pectin	479.37±29.16	139.83±4.29	26.75±2.20	312.78±29.56	1.88
1% (w/v) CMC	265.20±34.70	7.35±1.61	26.75±2.20	231.10±34.81	6.78
2% (w/v) CMC	492.25±71.77	68.3±4.69	26.75±2.20	397.20±71.95	4.18
1% (w/v) Sodium Alginate	329.67±166.16	46.87±24.00	26.75±2.20	256.05±167.90	3.48
2% (w/v) Sodium Alginate	616.50±26.91	98.30±4.83	26.75±2.20	491.45±27.43	3.93

Table 4.3: Total work or area under curve (AUC) of tensile test for different of concentrations and polymers.

Polymer	MP (g.s)	WP (g.s)	MW (g.s)	Net (g.s)	Normalised Parameter
1% (w/v) Pectin	1041.33±117.12	7.25±2.60	421.38±67.19	612.71±135.05	1.43
2% (w/v) Pectin	2449.84±380.83	730.77±141.19	421.38±67.19	1297.69±411.68	1.13
1% (w/v) CMC	1281.14±120.03	33.74±4.92	421.38±67.19	826.02±137.64	1.81
2% (w/v) CMC	2896.67±168.22	643.02±25.26	421.38±67.19	1832.26±182.89	1.72
1% (w/v) Sodium Alginate	2156.64±59.05	243.15±87.23	421.38±67.19	1492.11±124.92	2.25
2% (w/v) Sodium Alginate	3337.39±241.08	410.78±28.93	421.38±67.19	2505.23±251.93	3.01

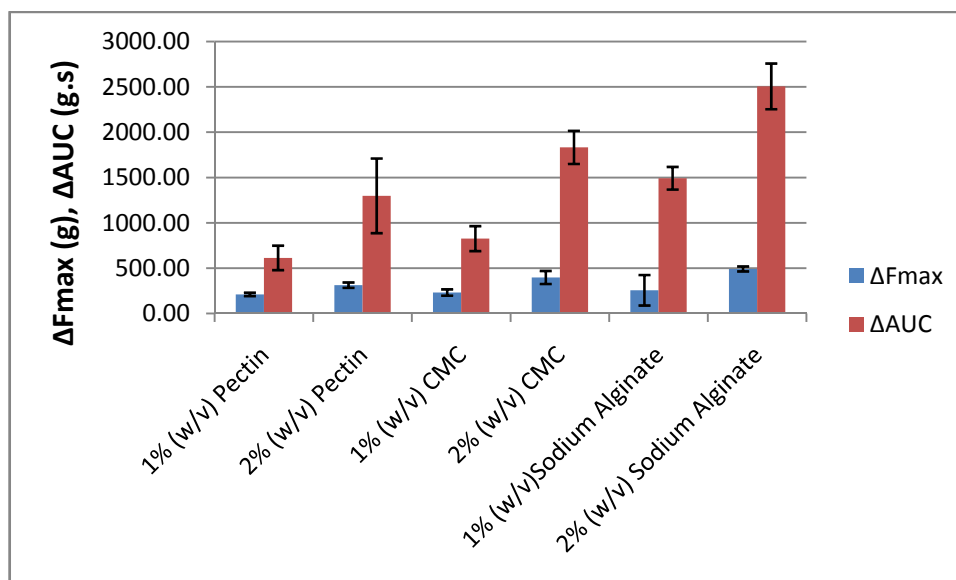


Figure 4.18: Net force, ΔF_{max} (specific interaction) and net total work, ΔAUC (specific total work) of different polymers (high DE pectin, CMC and sodium alginate) at different concentration.

Pre-loaded force was introduced to increase the contact of pectin with mucin to mimic the process in the mouth where force is applied on food (between palate and tongue) during mastication. 2% (w/v) pectin solution shows bigger specific interaction force as compared to 1% (w/v) pectin with a difference of 116.67 g for peak force and 649.67 g.s for AUC. This result also correlates well with results from rheology experiment and pull-off experiment where an increase in polymer concentration increases the availability of mucoadhesive material to form binding and interaction with mucin. Sodium alginate shows the strongest interaction with mucin as compared to high DE pectin and CMC. The same result is obtained from rheology and pull-off experiment.

4.3.2.2 Normalised Parameter

The normalised parameters were calculated based on Equation 4.6. Ferrari et al. (1997) described that normalised parameters can be used to compare the mucoadhesiveness of samples that have different cohesiveness and viscosity value. It shows the relative increment in mucoadhesive by the specific interaction to total unspecific interaction. However the normalised value does not show the exact strength of the mucoadhesion for a specific polymer. Calculated values of normalised parameter for tested polymers are shown in Figure 4.19. The normalised parameters are not correlated to the peak force and area under curve (AUC). 1% (w/v) pectin solution shows the highest increase in net force from the unspecific reaction with highest value of normalised parameter (7.47) meanwhile the 2% (w/v) pectin shows the lowest value of 1.18.

$$\text{Normalised parameter} = \frac{\text{Net force}}{\text{total unspecific interaction}} \quad (\text{Equation 4.6})$$

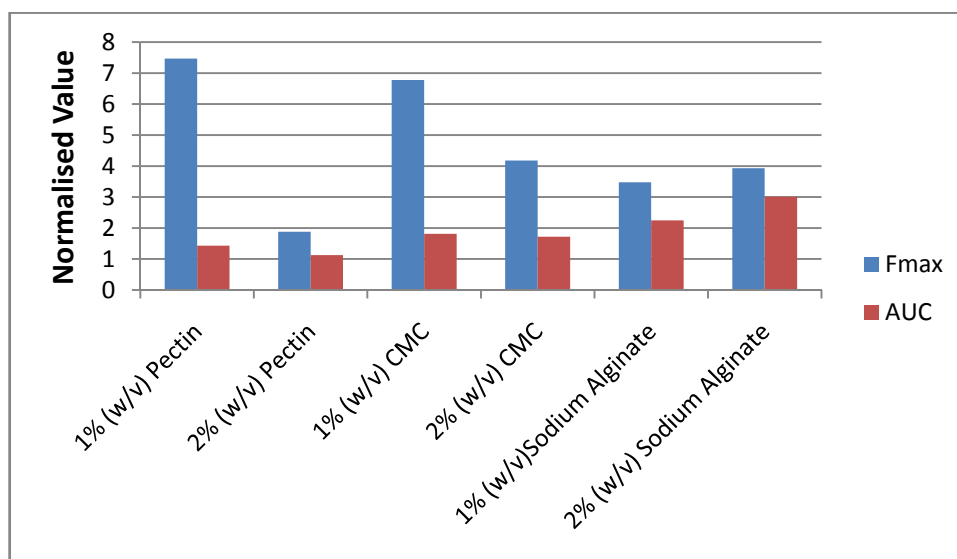


Figure 4.19: Normalised parameter of different polymer at different concentration.

4.4 Conclusion

A good assessment on the mucoadhesive polymers with mucin layer was obtained from the pull-off experiment even though the peak force and total mass attached to the mucin slide were not accurate. Pull-off experiment offers as a tool to study the dynamic absorption of mucoadhesive polymer into the mucin layer during holding time. The interactions between mucoadhesive polymer with mucin occurs in the second time frame which shows that the interaction is a very progressive process. The effect of different surface tension caused by different polymers can be eliminated by conducting the experiment done by Sam et al (1992). They used mucin or mucous homogenised gel as continuous sample instead of different polymer solution. However this methodology would require more mucin sample which is known to be expensive and limited in its availability as compared to mucoadhesive polymer. Tensile test offers a better method of assessment on the strength of mucoadhesion as shown by the tested mucoadhesive polymer with mucin layer. Higher peak force shows the higher interaction capability of mucoadhesive polymer. Total of work or area under curve shows the ability of the mucoadhesive polymer to withstand the continuous forces in the physiological conditions of human body.

Chapter 5:
Mucoadhesion
Measurement Using
Atomic Force Microscopy
(AFM)

5.1 Introduction

Atomic Force Microscopy (AFM) is a powerful tool which can be used as *in-vitro* method to study the adhesion between two materials and for the surface morphological characterisation of solid materials at the micro- and nano- scale. The AFM ability to measure the detachment force at microscopic level has been proven as a useful tool to study the mucoadhesion between mucoadhesive polymer with mucin (Deacon et al., 2000; Cleary et al., 2004; Catron et al., 2006; Sriamornsak et al., 2010; Joergensen et al., 2011). The colloidal probe technique developed by Ducker et al. (1991) has been widely used to study the characterised and synthesised mucoadhesive bio-polymer with mucin or mucous layer. In this technique, a colloidal particle coated with the interested polymer which is normally spherical such as silica is attached to AFM cantilever free end. The probe is then brought to contact with the mucin or mucous layer for a finite time, typically 0.01 s and greater, followed by pull off from the surface to measure the detachment force of these two materials. The same technique was used by Cleary et al. (2004) to investigate the adhesiveness of Polyether-Modified poly(acrylic acid) to mucin. They reported that the adhesion force of Pluronic-PAA was affected by the pH and ionic strength. The ionisation state of mucin and Pluronic-PAA is different at different pH. This will result in different hydrogen bonding strength and interpenetration effectiveness. Increasing ionic strength reduced the electronic repulsion in intramolecular of Pluronic-PAA. This led to contraction of the Pluronic-PAA structures which reduced the entanglement ability between the mucin chains and Pluronic-PAA structures (Ron and Bromberg, 1998).

Besides the force, the characterisation of mucoadhesive biopolymer with mucin was done by investigating through the imaging technique by using tapping mode and contact mode. Sriamornsak et al. (2010) investigated the possible mechanisms contributed to the mucoadhesion between different types of pectin with mucin using AFM topographic imaging and mucin-particle method. They reported that the adsorption was one of the mechanisms of the interaction between the pectin and mucin. Deacon et al. (2000) observed the aggregation formed (topographic images) when chitosan was mixed with gastric mucin at different ionic strength. The topographic imaging was done using TappingMode™. The images showed average diameter of the aggregation at 0.1 M was found to be 0.7 μm but at 0.2 M and 0.3 M the average diameter was 150 nm. This led to the conclusion that ionic strength has an influence on the size of the aggregation. Since size of aggregation is used to characterise mucoadhesive interaction, the result implies that the interaction between chitosan and mucin is greatly reduced at higher ionic strength. At higher ionic strength, charge suppression reduces the electrostatic interaction between chitosan and mucin.

In this chapter, the mucoadhesion characterisation of sodium alginate, sodium carboxymethylcellulose (CMC) and high degree of esterification (DE ~60%) pectin were studied using AFM with respect to the effect of contact time, ionic strength and pH on the peak force and work.

5.2 Materials and Methods

Pectin from citrus peel (degree of esterification ~60%), sodium alginate, sodium carboxymethylcellulose (average M_w ~250000), mucin type II with bound sialic acid of ~1%, sodium chloride, buffer solution HPCE (pH 2, pH 3, pH 4, pH 5, pH 6 and pH 8), and hydrogen peroxide 30 wt. % (ACS reagent) were purchased from Sigma-Aldrich Company Limited, United Kingdom. Sulphuric acid 95% was purchased from Fisher Chemical Scientific, Loughborough, UK. All chemicals were analytical grade and used as received. A modified AFM cantilever with 5 μ m SiO₂ Glass Particle - Gold Coated was purchased from Novascan Technologies Inc, Ames, USA.

5.2.1 Continuous Solution

Solution of 2% (w/v) of high degree of esterification (DE ~60%) pectin, sodium alginate, sodium carboxymethylcellulose (CMC) and 10% (w/v) mucin was prepared by slowly adding the powder into double distilled (DI) water and stirring for at least 3 hours to ensure all the material was fully dispersed. To study the effect of ionic strength on sodium alginate solution, 2.5% (w/v) of sodium alginate stock solution and 1 M NaCl were prepared. The appropriate volume of 1 M salt solution and DI water was added to 16 ml stock solution to make 20 ml of 2.0% (w/v) sodium alginate in 0.05 M, 0.10 M, 0.15 M and 0.20 M NaCl.

Solutions with different ionic strengths (0.05 M, 0.10 M, 0.15 M and 0.20 M NaCl) were prepared by diluting 1 M NaCl stock solution with DI water to study the effect of different ionic strength environment on mucoadhesion. Buffer solutions of

different pH (pH 2-8) were used as received from supplier (Sigma-Aldrich) to study the different pH environment.

5.2.2 Preparation of ‘Piranha’ Solution

“Piranha” solution is a mixture of concentrated sulphuric acid and 30% (w/v) hydrogen peroxide in the ratio of 70:30 respectively. 140 ml of concentrated sulphuric acid was poured into a beaker submerged in 2 cm depth of ice in an ice bath and allowed to cool for 30 minutes. Then, 60 ml of 30% (w/v) hydrogen peroxide was added and the mixture was allowed to cool for a further 30 minutes. This “piranha” solution is a very strong oxidising agent and should be used with caution.

5.2.3 Preparation of Biopolymer Absorption onto Au Substrate and Mucin Coated Cantilever

The mucin has been coated (absorbed) onto the cantilever Au surface and the mucoadhesive polymer has been absorbed onto Au substrates. Au substrate was placed in the “Piranha” solution, Au side up, and left for 10 minutes. The Au substrate was then washed with HPLC grade water and then immersed (without allowing the substrates to dry) in 2% (w/v) high DE pectin for at least 2 hours. The substrate was then removed from the solution and dried using an inert gas (Ar or N₂). The whole procedure was repeated with these other solutions, 2% (w/v) alginate solution with ionic strength of 0 M, 0.05 M, 0.10 M, 0.15 M and 0.20 M NaCl and 2% (w/v) CMC respectively. The same procedures were used for the preparation of mucin coated cantilever. However, only a small amount of “Piranha” solution and

10% (w/v) mucin solution was dropped on the cantilever. Handling of substrates and cantilever was done using chemically resistant Dumostar tweezers (Agar Scientific, UK).

5.2.4 Force Measurement

Force measurements were carried out using a Nano Wizard II AFM (JPK Instruments, UK), operating JPKSPM software for data acquisition. All measurements were performed in contact mode. Measurements were performed in air at room temperature of 18°C and a relative humidity of 40-50%. In order to study the different liquid environment, the substrates were immersed in the solution for at least 60 s to equilibrate. The measurements were done with contact time of 60 s. Different substrates (absorbed with the mucoadhesive biopolymers) were used for each adjustment parameters to ensure the freshness of the sample for each experiment. The force measurements were taken at fifteen different points and the average measurement was calculated. Table 5.1 shows the summary of the parameters studied in this experiment.

Table 5.1: Summary of the experiment parameters used in AFM experiment. All the tests were performed in room of 18°C and a relative humidity of 40-50%.

Environment	Tested substrates	Contact time between cantilever and substrate
Air	Sodium alginate, high DE pectin, CMC and sodium alginate with ionic strength of 0 M, 0.05 M, 0.10 M, 0.15 M and 0.20 M NaCl.	0 s and 60 s.
Distilled water	Sodium alginate, high DE pectin, CMC and sodium alginate with ionic strength of 0 M, 0.05 M, 0.10 M, 0.15 M and 0.20 M NaCl.	0 s, 60 s and 300 s.
Different ionic strength solutions. Ionic strength of 0.05 M, 0.10 M, 0.15 M and 0.20 M NaCl.	Sodium alginate, high DE pectin and CMC.	60 s
Different pH solutions. pH 2,3,4,5,6,7 and 8.	Sodium alginate, high DE pectin and CMC.	60 s

5.3 Results and Discussion

The force measurement for the substrate with sodium alginate, high DE pectin and CMC was done in ambient air and distilled water environment. The discussion will focus on the results obtained for each environment as well as the comparison of the two.

5.3.1 Force Measurement in Air

Figure 5.1 shows the peak force when the mucin coated cantilever was detached from the Au substrate coated with sodium alginate, high DE pectin and CMC after contact time at 0 s and 60 s. Sodium alginate shows the highest peak force at both 0 s and 60 s with the value of 1574 ± 1 nN (0 s) and 1552 ± 3 nN (60 s) respectively. Whereas, the peak force for high DE pectin was 1566 ± 3 nN (0 s), 1546 ± 4 nN (60 s) and for CMC was 1555 ± 2 nN (0 s), 1542 ± 2 nN (60 s). Based on the results, the rank order of mucoadhesiveness of the assayed polymers is sodium alginate > high DE pectin > CMC. The result obtained from AFM measurements is conflicting with rheological characterisation and tensile test where CMC has lower value of peak force than high DE pectin. The peak force for all the samples is lower for 60 s contact time compared to 0 s contact time (Figure 5.1). This phenomenon might be caused by the over wetting effect from the environment humidity thus resulting in the slippery effect at the tip of cantilever which gave lower peak force reading. The 40-50% relative humidity could be considered as low which might not give much effect to the formation of slippery mucilage. However, longer contact time might increase the water content (accumulation) at the contact point of cantilever and substrates. Xiao and Qian (2000) did the study to investigate the

effect of air humidity on the capillary force. They reported the capillary force was greatly affected by the humidity content in air where the capillary force increased at first (up to 70% relative humidity) and then decreased at the higher relative humidity (more than 70% relative humidity). The capillary force became weaker at too high humidity content in air. There was not much change of peak force for the sodium alginate substrate with different ionic strength with 0 s and 60 s contact time. The peak force with 60 s contact time decreased at very minimal rate as compared to 0 s contact time as shown in Figure 5.2. Additional of ion in the sample would cause the hydrophobic effect between cantilever and substrate. Zangi et al. (2007) have observed an increase in hydrophobic interaction when the charge density of ions (Na^+ , Cl^-) increases between two hydrophobic plates. Probably, this hydrophobic effect could overcome the capillary force (effect) when the measurement was done in air. Capillary force is one of the components when measuring the micro-adhesion using AFM in air besides the adhesion force and electrostatic force (Ouyang et al., 2001).

However, a different effect can be seen from the work as shown in Figure 5.3. The work increased with increasing contact time for all the polymer substrates and sodium alginate with different ionic strength (Figure 5.3 and Figure 5.4). CMC shows highest work followed by sodium alginate and high DE pectin. Work (area under the force-displacement plot) is another important parameter in the world of adhesion where this parameter can be expressed as the total energy needed to detach the adhered sample from the adherent surface. Difference of work could be contributed by the different degree of chain entanglement between polymer

molecular networks with mucin structure. Longer contact time allows more interaction through the hydrogen bonding, diffusion and interlocking to occur. Thus more work is required to detach the mucin coated cantilever from the substrates. Peak force represents the highest force to start separating between two adhered surfaces at highest point whilst the area of work represents the total energy required to fully detach the two interacting materials or break the strong and weak bonding (Hagesaether and Sande, 2008). Generally, work will be correlated with peak force but for some cases this is not observed depending on the nature of polymers and the experiments.

The work for sodium alginate substrate (contact time 0 s) decreased with increasing ionic strength as shown in Figure 5.4. However, the result is different for 60 s of contact time where the highest work of adhesion is at ionic strength of 0.05 M and lowest at 0.20 M (same as for 0 s contact time). Generally, the adhesion force decreases with increasing ionic strength in sodium alginate due to stronger intramolecular repulsion between negatively charged groups in the molecular structures. Oberyukhtina et al. (2001) explained that the repulsion of negatively charged molecules in sodium alginate will increase the free energy for compact and unfolded conformations. The unfolded structure of sodium alginate formed decreases the degree of entanglement and interpenetration between the intermolecular structures of sodium alginate with mucin network. The same result was obtained by Zhang et al. (2001) where an increase in ionic strength reduced the viscosity of sodium alginate due to the screening effect on the electrostatic interaction (repulsion) between intramolecular structures.

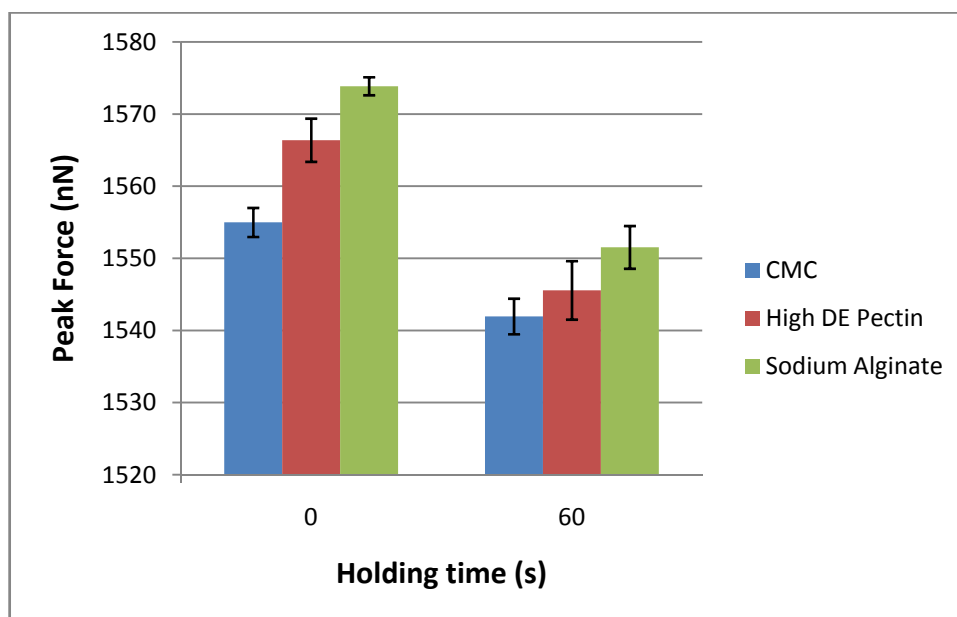


Figure 5.1: Peak force between the polymer substrate and mucin.

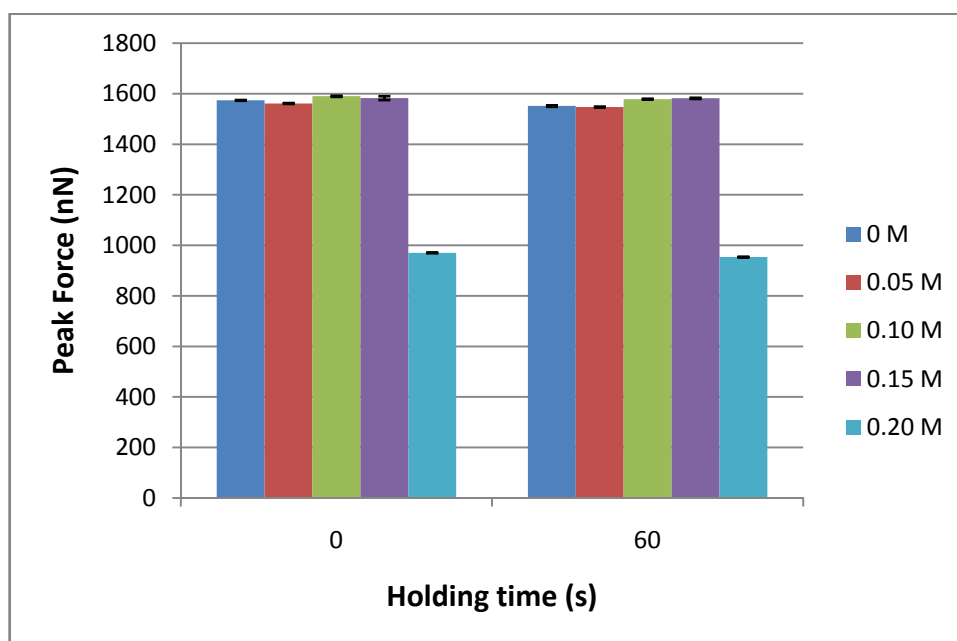


Figure 5.2: Peak force between the sodium alginate (different ionic strength NaCl) substrate and mucin coated cantilever at different contact time.

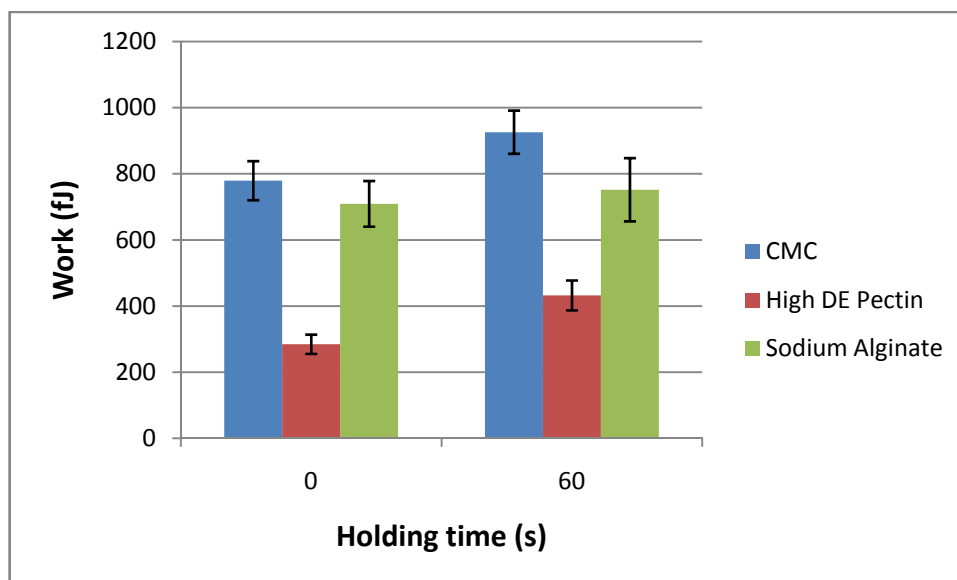


Figure 5.3: Work between the polymer substrates and mucin coated cantilever at different contact time.

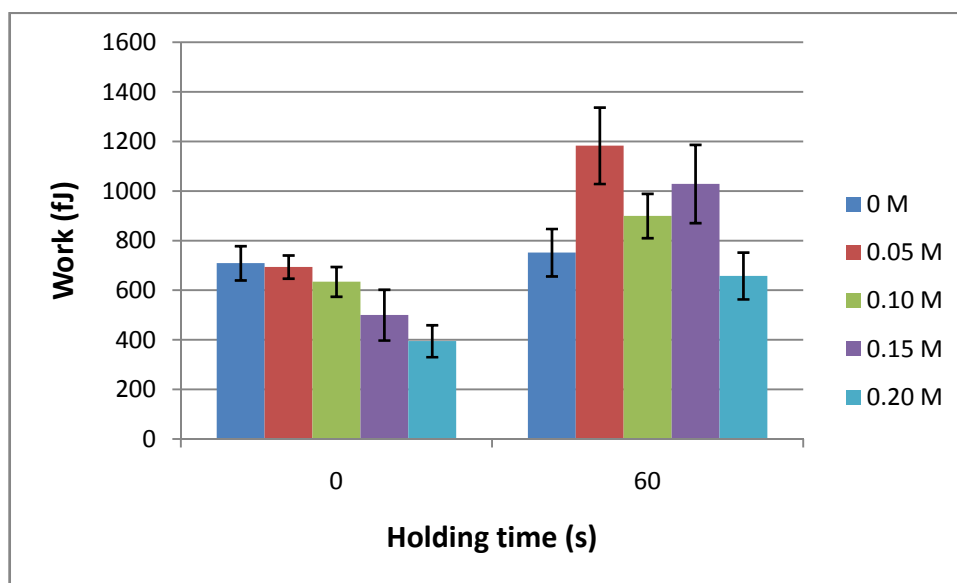


Figure 5.4: Work between the sodium alginate with different ionic strength (NaCl) and mucin cantilever at different contact time.

5.3.2 Force Measurement in Distilled Water

In order to eliminate the capillary and electrostatic effect during the measurement in air, the mucoadhesion force between mucoadhesive polymer substrates with mucin coated cantilever was done in distilled water. There were three different contact times applied during the contact of cantilever and substrates which are 0 s, 60 s and 300 s. Figure 5.5 and 5.6 show the peak force (detachment force) and work for sodium alginate, CMC and high DE pectin with different contact time measured in distilled water environment. There was an increase in the value of peak force and work for all samples when the contact time was increased from 0 s to 60 s. Sodium alginate shows the highest peak force with the value of 86.8 ± 9.5 nN while CMC exhibits the lowest with a value of 19.2 ± 2.1 nN respectively. The same sequence was obtained from the measurement in air where sodium alginate shows the highest peak force and CMC the lowest.

However, peak force and work of adhesion (Figure 5.5 and Figure 5.6) were decreased when the contact time between mucin coated cantilever was extended to 300 s for sodium alginate and high DE pectin. CMC shows increasing peak force and area of work after 300 s of contact time but the force was still lower than recorded by high DE pectin and sodium alginate. It shows that there is a limiting contact time allowed to form a strong bonding or interaction. Longer contact time in water environment will cause over wetting effect at the interface of mucin-polymer thus decreasing the adhesion force. There is insufficient interaction between polymer with mucin if too short of time applied during the contact while too long contact time will form slippery mucilage at the interface (Peppas and Huang, 2004). The same effect

was observed in Figure 5.7 (peak force) and Figure 5.8 (work) for sodium alginate with different ionic strength substrates. Sodium alginate without ionic and with 0.05 M NaCl shows decreasing of peak force and area of work for the contact time of 300 s as compared to 60 s whilst there was an increase in the two parameters for sodium alginate with ionic strength of 0.10 M, 0.15 M and 0.20 M. As previously explained (Oberyukhtina et al., 2001), the ionic strength altered the sodium alginate structure to be more compact conformations and thus resisting the effect of over wetting at the interface.

The effect of ionic strength on the adhesion force between sodium alginate with mucin was greatly affected as shown in the Figure 5.7. There is a large decrease of peak force between sodium alginate without ionic salt and with 0.05 M NaCl. However, further increase of ionic strength in sodium alginate does not give much effect on the overall mucoadhesion capability. This can be seen for both peak force and area of work with 0 s and 60 s contact time. The same results were reported by Oberyukhtina et al. (2001), where with 0.02 M NaCl, the viscosity of the sodium alginate decreased sharply but further increase of ionic salt concentration in the solution had no effect on the viscosity. They explained that the zeta potential (ζ) of the solution with 0.02 M NaCl tends to decrease to zero which results in reduced of viscosity. Zhang et al. (2001) also reported the electrostatic persistence lengths of sodium alginate solution was rapidly reduced at low ionic salt concentration (0.01 M - 0.05 M) but further increase of ionic strength, the change was only marginal as shown in Table 5.2.

Table 5.2: The intrinsic viscosity and electrostatic persistence length of 3% (wt) sodium alginate solution. (Source: Zhang et al., 2001).

Ionic concentration (mol/l)	Electrostatic persistence length (Å)	Intrinsic viscosity (ml/g)
0.5	125.7	107.1
0.2	126.2	111.2
0.1	128.2	116.6
0.05	131.5	123.1
0.02	141.2	143.2
0.01	157.4	166.7

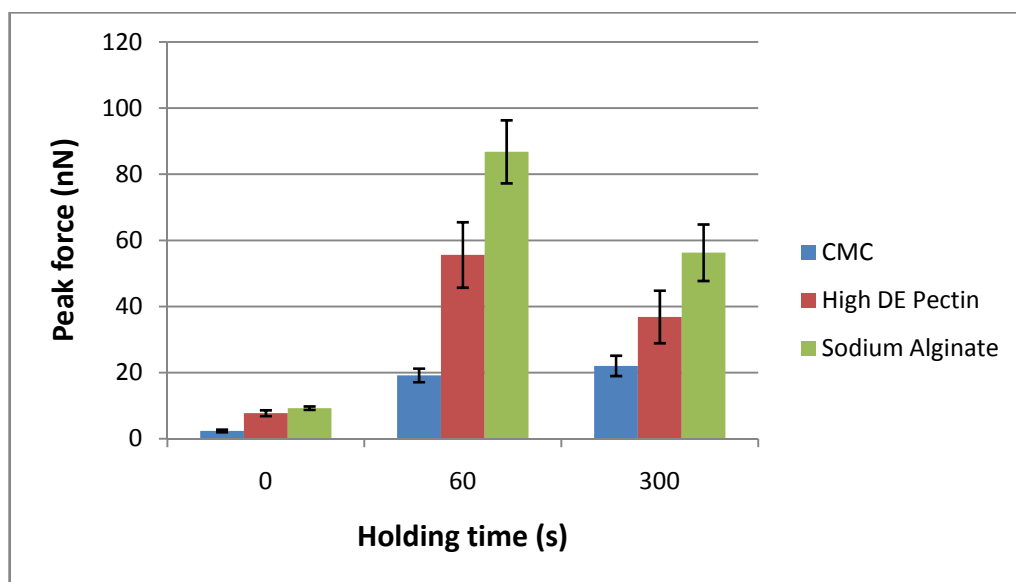


Figure 5.5: Peak force for polymer substrate and mucin coated cantilever at different contact time.

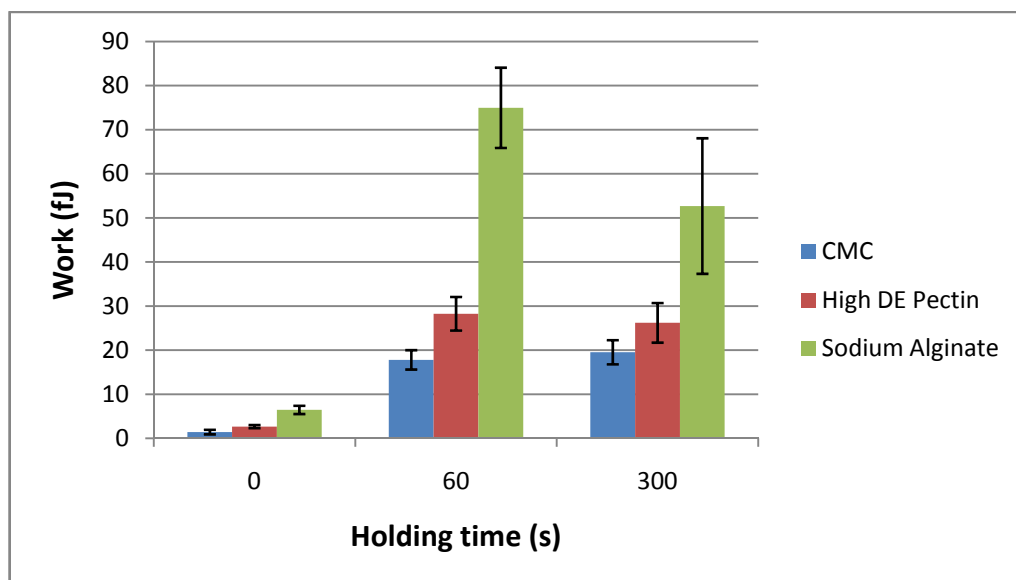


Figure 5.6: Work for polymer substrate and mucin coated cantilever at different contact time.

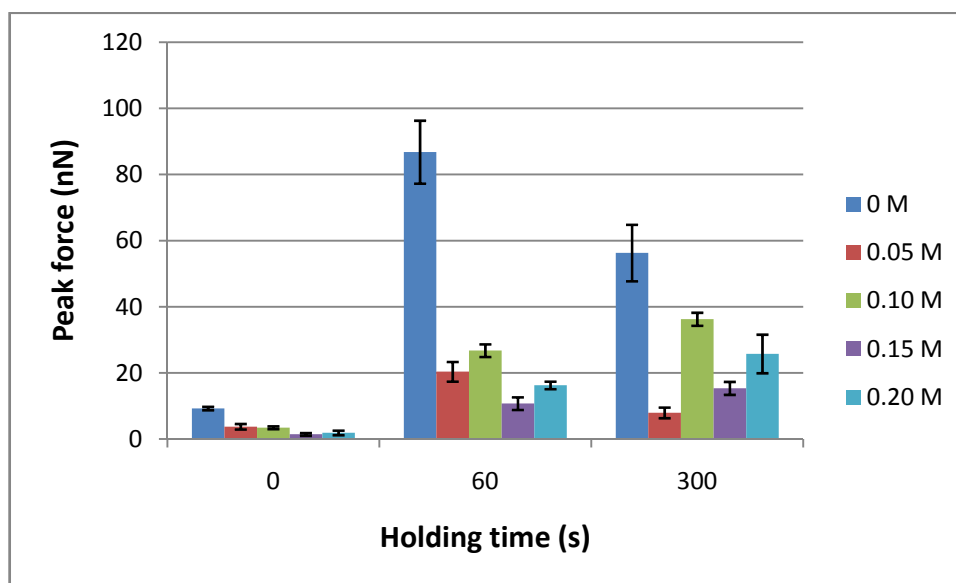


Figure 5.7: Peak force (detachment force) for sodium alginate (different ionic strength NaCl) and mucin coated cantilever at different contact time.

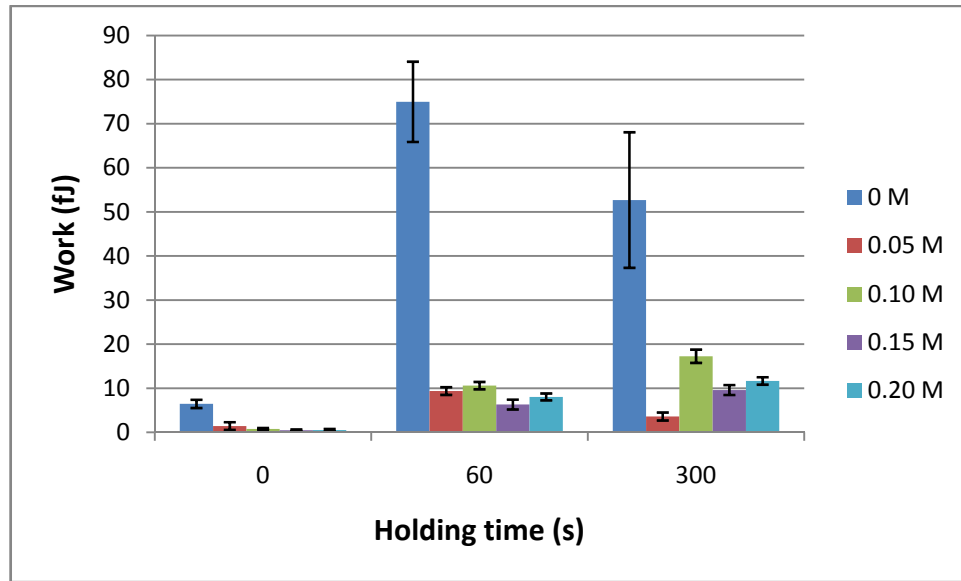


Figure 5.8: Work for sodium alginate with different ionic strength (NaCl) and mucin coated cantilever at different contact time.

The measurement of both peak force and work were significantly lower when the measurement was done in water as compared to in air environment. As for example, peak force (60 s contact time) of sodium alginate-mucin in water environment was 86.8 ± 9.5 nN whereas the measurement in air was 1552 ± 3 nN. As described by Ouyang et al. (2001), the adhesion force measured by AFM in air environment is contributed by three components of force which are the capillary force, adhesion force and electrostatic force between two plates. Meanwhile, the effect of capillary force and electrostatic force can be eliminated when the measurement is done in water. The force measured in water is only contributed by adhesive force due to chemical bonding such as hydrogen bond and van der Waals interaction. Besides, the movement of the cantilever was affected by the greater resistance in the water as compared to in the air thus the speed of the cantilever to move during pull off from the substrate is much slower (Ouyang et al., 2001).

5.3.3 Different Ionic Strength and pH Environment

The effect of ionic strength of the environment on the mucoadhesion property of sodium alginate, CMC and high DE pectin was also investigated by measuring the peak force and work for each polymer in salt solution environment with different ionic strength. Figure 5.9 and 5.10 show the peak force and work for each polymer in distilled water, 0.05 M, 0.10 M, 0.15 M and 0.2 M NaCl. The measurements were done after 60 s of contact time (highest measured force). For sodium alginate, the change in peak force was similar to the change in distilled water environment at 0 M, 0.05 M and 0.10 M NaCl, but there was a four-fold increase in peak force at 0.15 M NaCl. This is in contrast with the result for sodium alginate substrate with 0.15 M NaCl measured in water environment which showed a decrease in peak force at this ionic strength. CMC exhibits an increase in peak force with increase in ionic strength (Figure 5.9) in contrast to the viscosity measurement done by Yang and Zhu (2007) who reported that the viscosity of CMC decreased with increasing ionic strength due to electrostatic shielding of Na^+ ions on the ionized carboxyl group in the CMC chain forming a more compact structure. Consequently, the interaction between CMC and mucin is reduced due to low degree of interpenetration and diffusion of the networks. The irregular trend was also observed with works for sodium alginate and CMC. On the contrary, mucoadhesion of high DE pectin decreased with increasing ionic strength with regards to the work (figure 5.10). The work of high DE pectin decreased from 28.3 ± 3.8 fJ (0 M NaCl) to 25.4 ± 0.6 fJ (0.05 M NaCl). Further increase in ionic strength did not affect the work for high DE pectin.

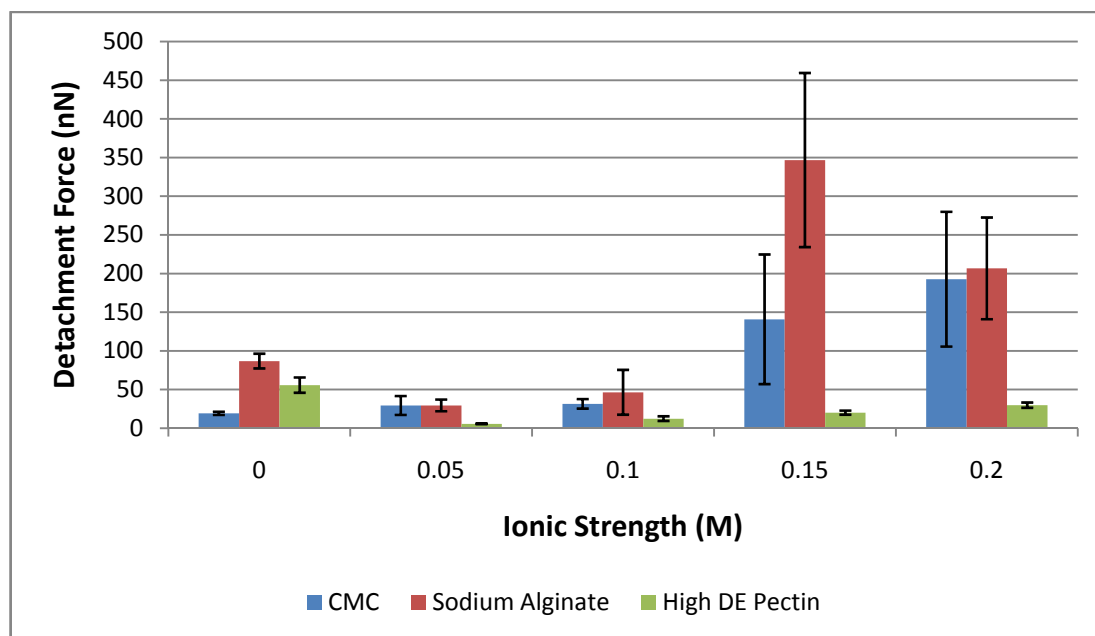


Figure 5.9: Peak force (detachment force) between different polymers and mucin cantilever at in different ionic strength solution (NaCl).

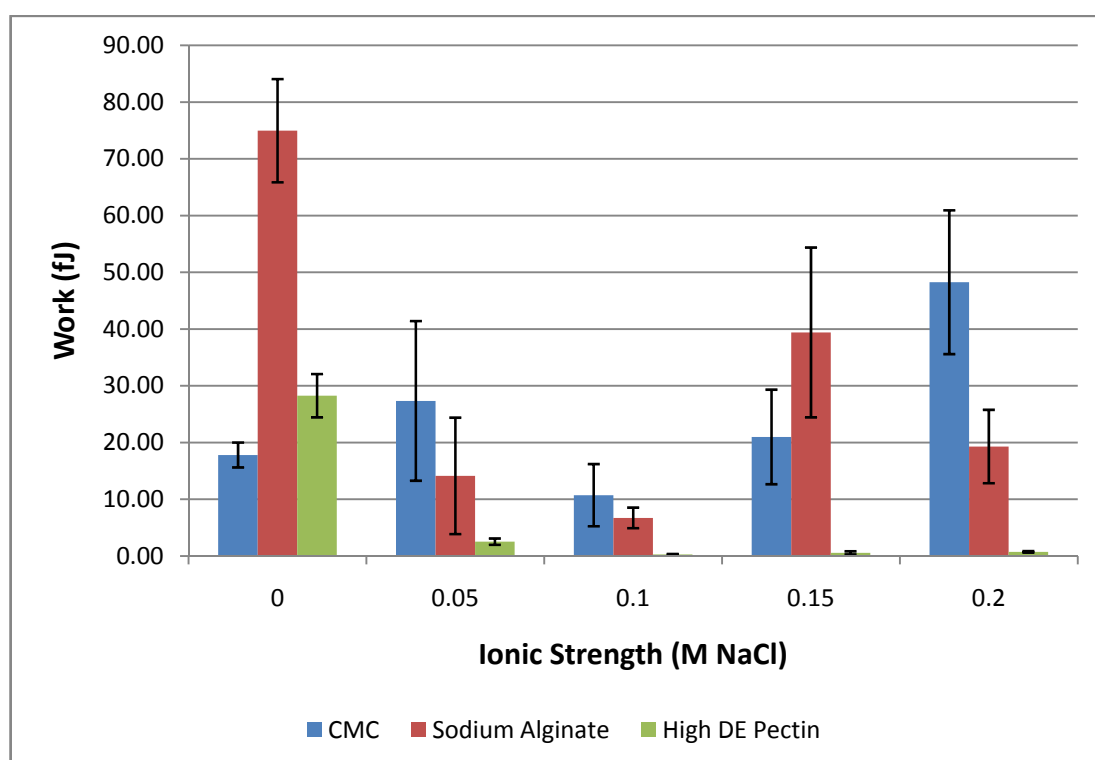


Figure 5.10: Work between different polymers and mucin coated cantilever at in different ionic strength solution (NaCl) environment.

Figure 5.11 and 5.12 show the effect of the different pH environment on the mucoadhesion of sodium alginate, CMC and high DE pectin. At pH 2 and pH 3, CMC shows higher peak force than sodium alginate by 11.5% and 15.2% respectively. However, the peak force of sodium alginate significantly increased in pH 4 (210 ± 93 nN) and pH 5 (205 ± 88 nN) solutions. All polymers show the highest peak force in the pH range of 4 to 5 close to the pK_a value of each polymers: pK_a value of pectin is 3.5-4.5 (measured as pK_a galacturonic acid) (Ralet et. al., 2002), pK_a sodium alginate is 5.4 (Paradies et al., 2010) and pK_a CMC is 4.30 (Source: drugfuture website). At low pH, the carboxyl groups of mucin and polymers are mainly in the protonated form thus favouring hydrogen bonding which is the main component in mucoadhesion resulting in labile intermolecular cross-links (Riley et al., 2001). Disruption of carboxylic groups in sodium alginate structure will reduce when pH is lowered, diminishing the hydrophilic properties of sodium alginate to some level. This will increase the hydrophobic properties in the alginate structure (Yang et al., 2009).

At pH close to pK_a of polymers, the amount of ionised and the unionised forms are balanced hence the repulsion between ionised polymers is minimised and at the same time there is sufficient unionised form to interact with mucin through hydrogen bonding. When pH is increased, mucous sialic acid groups and the carboxyl groups in polymers become ionised. At this stage, the interaction is expected to decrease due to electrostatic repulsion but increase in ionization will lead to a greater degree of extension in polymer chains and mucous network which leads to better entanglement and interpenetration between the two (Cleary et al., 2004).

This optimum degree of ionisation will ensure the sufficient network expansion and promote the interlocking between the polymer-mucin structures without the over hydrating effect. This result can be observed through the highest peak force and work achieved at pH 4 to pH 5.

However, further increase in pH resulted in lower adhesion force due to overpowering of electrostatic repulsion. Also, high water content in the polymers (due to absorption of water at higher pH) caused the formation of loosely packed polymer structure. This extensive uncoiling of the polymer chain led to a reduction in the degree of mechanical entanglement and penetration, and coupled with stronger repulsion between the ionized carboxylic groups resulted in insignificant adhesion to the mucin (Tur and Ch'ng, 1998). At higher pH (pH 7.5), Tur and Ch'ng (1998) reported that the polymers (which contains carboxylic group) have higher negative zeta potential and swelling properties of poly(acrylic) acid due to greater ionisation of carboxylic group. The ionisation process results in the increase in electrostatic repulsion between adjacent carboxylic groups and the subsequent formation of an expanded polymer network.

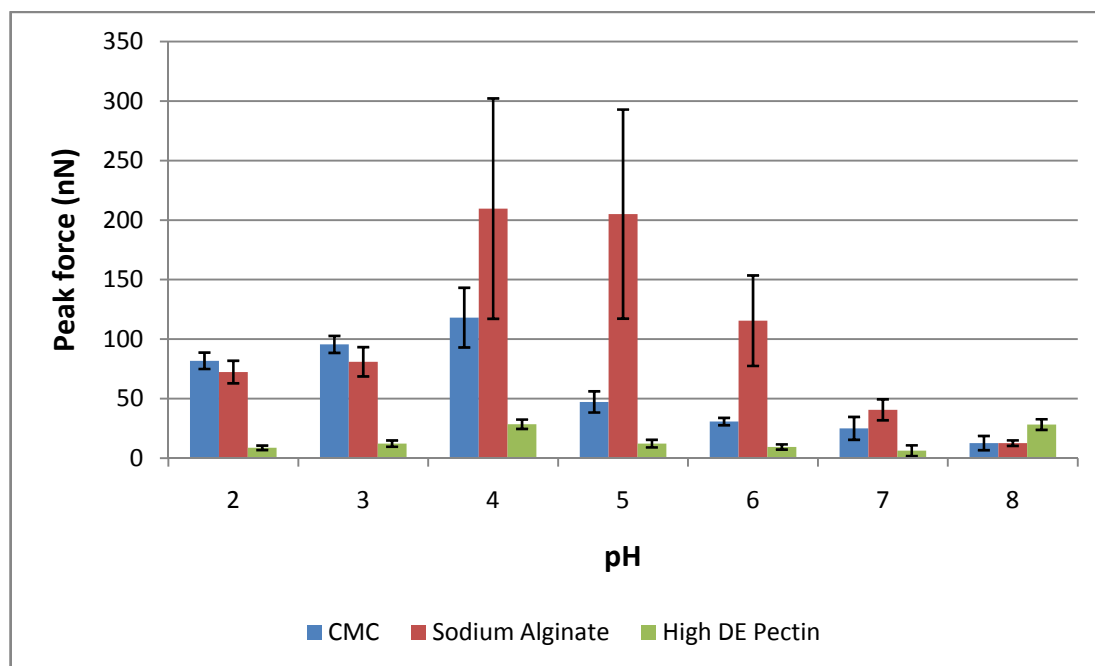


Figure 5.11: Peak force (detachment force) between different polymers and mucin coated cantilever in different pH solution.

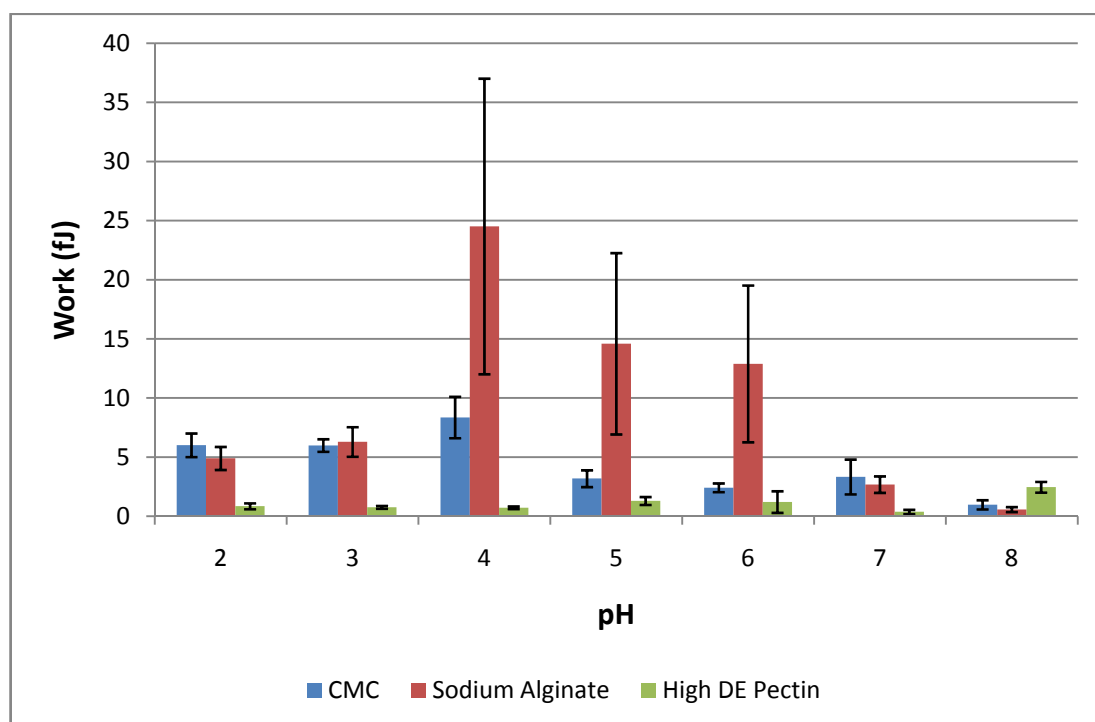


Figure 5.12: Work between different polymers and mucin coated cantilever in different pH solution.

5.4 Conclusion

The technique applied in this study using Atomic Force Microscopy (AFM) was successfully carried out to measure the exact mucoadhesion force (peak force and work). Cohesiveness effect of the polymer can be eliminated using AFM as the materials are in dried form, absorbed into the Au substrate and cantilever as compared to other technique (Wilhelmy plate method and Tensile Test) which uses polymer in solution. Measurement in air is not the accurate measure of the mucoadhesion force between polymer substrate and mucin coated cantilever since the measured value is also attributed by two other forces: the capillary and the electrostatic force. However, the measurement of peak force and work acquired can still be used to compare mucoadhesive polymers. Based on the results, sodium alginate shows the highest capability to form strong adhesion with mucin as compared to CMC and high DE pectin. This result corresponds with the findings from rheological characterisation, pull-off experiment and tensile test.

It is clear that the mucoadhesion between tested polymers and mucin are affected by ionic strength and pH of the environment. These factors are affecting both the structure of polymer and mucin thus resulting in different measured mucoadhesion force. This study emphasizes the importance of designing delivery system or food formulation that is suitable for the environment of the targeted area since different part of the human physiology has different pH value. Thus, understanding the conditions in which mucoadhesive materials demonstrate optimum mucoadhesion performance is important in developing effective drug delivery systems and food formulation.

Chapter 6:

Mucoadhesion Kinetic

Studies

6.1 Introduction

Kinetic can be defined as movement or motion in terms of energy or mass involved in a length of time. Absorption kinetics is a way to define the rate for certain amount of particle or substrate to be absorbed into a surface. Besides the adhesion force, mucoadhesion could also be investigated through the assessment of absorption kinetics. There are various measurement techniques that have been used to evaluate the absorption kinetic between mucoadhesive polymer and mucin such as Fourier transform infrared-attenuated total reflectance (FTIR-ATR) spectroscopy (Durrer et al., 1994), Surface Plasmon Resonance (SPR) spectroscopy (Chayed and Winnik 2007) and Quartz Crystal Microscopy with Dissipation Monitoring (QCMD) (Feldötö et al., 2008). Chayed and Winnik (2007) successfully studied the mucoadhesive properties of polysaccharide based polymer such as hydrophobically modified (HM) derivatives of dextran (DEX) and hydroxypropylcellulose (HPC) with different molecular weight. They found that the absorption kinetics of the polymers involved two steps: a rapid rate followed by a slower process until equilibrium state is attained. Feldötö et al., 2008 studied the absorption kinetics by injecting mucin solution onto modified gold surface (QCMD chips) with different groups and charges thiols. Wang et al. (2007) reported that the absorption of pectin onto bovine serum albumin decreased with increasing of ionic strength. The viscoelastic of the absorbed layer increased at low ionic strength (0.02 M NaCl) but mass absorbed and dissipation value decreased at higher ionic strength.

In this chapter, absorption kinetic of sodium alginate, sodium carboxymethylcellulose (CMC) and high DE (degree of esterification ~ 60%) pectin

were studied using QCMD by measuring the absorption of polymer-mucin at the interface with dissipation monitoring for the purpose of comparison in mucoadhesion properties. The absorption kinetic for the tested mucoadhesives was also evaluated using the viscometry measurements obtained from the modified rheological characterisation method (Chapter 3).

6.2 Materials and Methods

Pectin from citrus peel (degree of esterification ~60%), sodium alginate, sodium carboxymethylcellulose (average M_w ~250000), mucin type II with bound sialic acid of ~1% and 2% (v/v) and Hellmanex II solution were purchased from Sigma-Aldrich Company Limited, United Kingdom. All chemicals were analytical grade and used as received.

6.2.1 Kinetic Absorption by Quartz Crystal Microbalance with Dissipation Monitoring (QCMD)

The concentration of polymer solutions (sodium alginate, CMC and high DE pectin) and mucin used in this experiment was at 0.6% (w/v). The solutions were prepared by slowly adding the polymer powder into distilled water and stirring the mixture for at least three hours to ensure the material was fully dispersed. The absorption processes were performed on gold-coated QCMD chips as supplied by Q-sense at controlled temperature of 20°C. All solutions were incubated at this temperature in water bath for at least one hour prior to the experiment for temperature equilibrium. The initial mucin base layer was prepared by injecting 0.5 ml of mucin solution into temperature controlled loop (chamber) and allowed to stay

there for 3 minutes for absorption process. A further 0.5 ml mucin solution was injected into the cell and held there for 15 minutes. After that, four sequences of 0.5 ml buffer rinse (distilled water) were carried out in the same way with 3 minutes holding time for each injection. The absorption study of mucoadhesive biopolymer solutions on the mucin layer were done with the same sequences as build up of mucin layer followed by three sequences of buffer rinse. The sequences of the whole process are shown in Figure 6.1. The chips were cleaned for each of the experiment by injecting 1.0 ml of 2% Hellmanex II solution into the loop and held for 3 minutes followed by three sequences of buffer rinse. The chips were then rinsed again with distilled water and dried with N₂ (nitrogen gas).

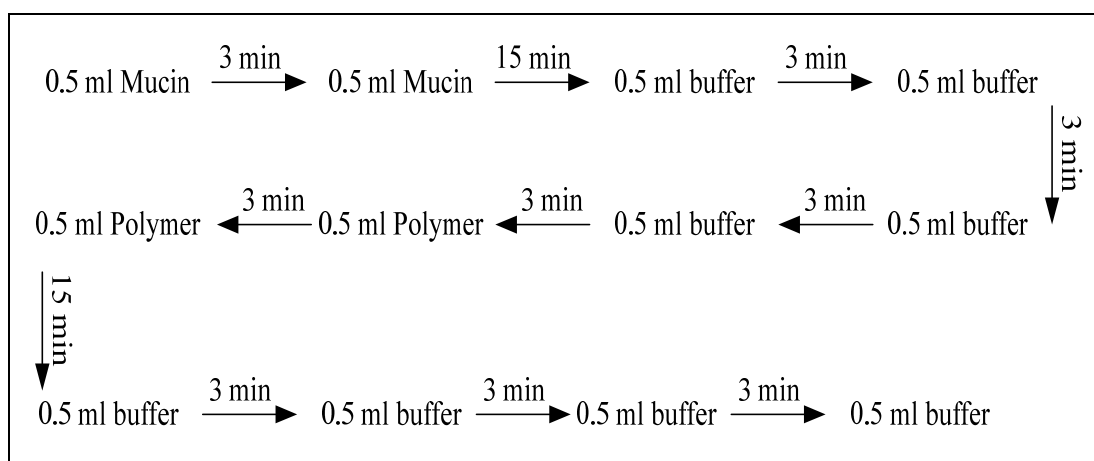


Figure 6.1: Sequences for kinetic absorption study of mucoadhesive polymer on mucin layer.

6.2.2 Kinetic Interaction Analysis by Rheological Characterisation

The study on kinetic interaction of mucoadhesive polymer with mucin was carried out by applying 0 s holding time before the shearing process started. The procedure used for this experiment has been described in section 3.2.3. The analysis of the kinetic interaction is done based on the viscosity profile during the mixing or shearing process at the area before the polymer solution and mucin formed a homogenous mixture. A homogenous mixture is formed when the viscosity profile reaches a plateau.

6.3 Results and Discussion

6.3.1 QCMD

A QCMD was used to study the kinetic interaction or absorption of mucoadhesive polymer (sodium alginate, CMC and high DE pectin). The frequency changes observed in the graph are proportional to the total mass of polymer and mucin deposited which also includes associated buffer or solvent. The frequency ($-\Delta f/n$) and dissipation ($\Delta D/n$) changes with different overtone for each mucoadhesive polymer are shown in Figure 6.2 (sodium alginate), 6.3 (CMC) and 6.4 (high DE pectin) respectively. All three polymers showed the same profile of $-\Delta f/n$ and $\Delta D/n$. There was a big change in $-\Delta f/n$ for the first 3 minutes (first 0.5 ml injection of mucin layer) followed by a small increase in $\Delta D/n$. This change is due to the deposition of mucin on the gold chips. A small increase in dissipation indicates that the mucin layer formed on the gold coated chips is rigid and elastic. A further increase in frequency was observed when second 0.5 ml mucin solution was injected

and held for 15 minutes in the loop accompanied with a very small change in the dissipation. Before the deposition of mucoadhesive polymer on the mucin layer, there was a sequence of buffer rinse. After the buffer rinse sequences were done, there was a small drop in frequency and dissipation observed from all the graphs. Four sequences of buffer rinse were done to remove all the mucin particles that were not absorbed into the gold chips. Besides, this process was done to observe the reversible possibility of the absorbed mucin layer because the increases in the frequency shown in the graph might be caused by the bulk effect in the loop. However, it can be observed that mucin layer formed on the gold chip was rigid and had good absorption ability when a plateau line was obtained during all four sequences of buffer rinse. The decrease in frequency implies a loss in mass which could be removal of unabsorbed mucin particles in the bulk phase.

After buffer rinse sequences, there was a plateau line obtained which shows the exact amount of mucin absorbed into the gold coated chip. Figure 6.5 shows the schematic diagram of the expected result of frequency change during the formation of polymer-mucin layers. However, there were unexpected results obtained for all the tested mucoadhesive polymers after two injections of polymer solutions as shown in Figure 6.2, 6.3 and 6.4. The frequency ($-\Delta f/n$) was expected to increase due to additional hydrated mass of polymer absorbed into the mucin layer through mucoadhesive interaction between tested polymer and mucin. But the opposite profile (decreasing in frequency, $-\Delta f/n$) indicates that the reverse process occurred where the hydrated mucin layer was removed from the gold chip. The rapid decrease in frequency ($-\Delta f/n$) however was countered by the big increase of dissipation value.

This change suggests that the structure formed between polymer-mucin was viscoelastic rather than elastic. This phenomenon could be illustrated with a schematic diagram as shown in Figure 6.6. After rinsing with buffer, the agglomeration of polymer-mucin formed was flushed away from the system and the frequency ($-\Delta f/n$) and dissipation value dropped drastically with some mucin layer still remained on the gold coated chips (frequency value did not return to zero). The results obtained in this experiment suggested that the absorption of mucin layer on the gold coated chip was not strong enough to counter the interaction force with the mucoadhesive polymer thus resulting in the removal of mucin from the gold coated chip.

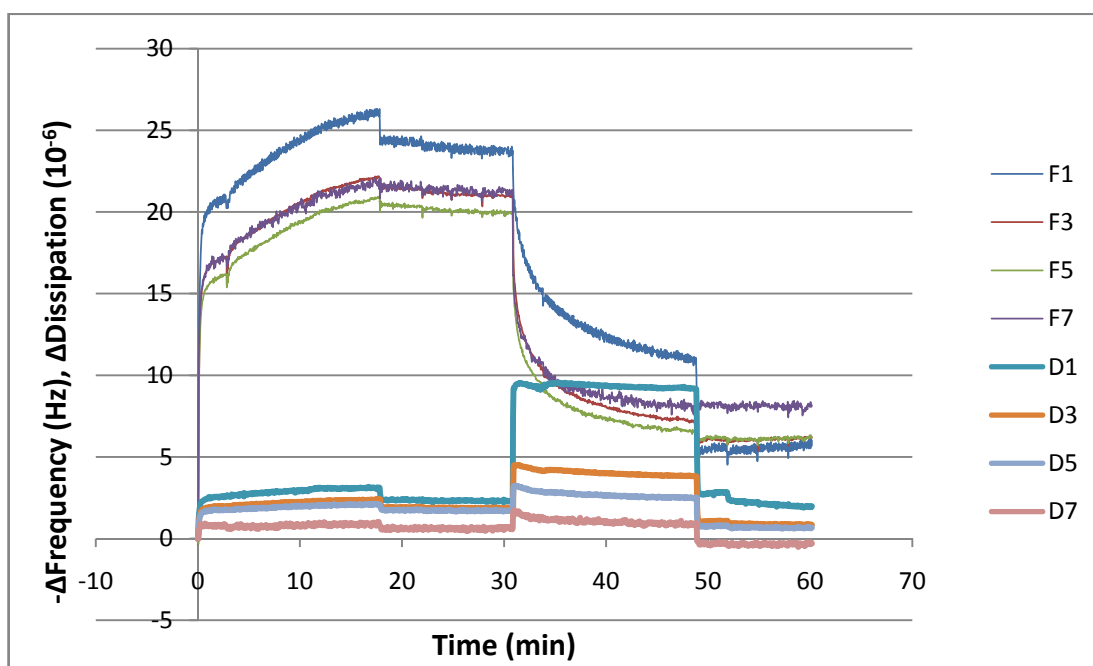


Figure 6.2: QMCD frequency and dissipation shifts during the injection of sodium alginate solution on the absorbed mucin layer. F= Frequency and D= Dissipation. Frequencies: F1 (5 MHz); F3 (15 MHz); F5 (25 MHz); F7 (35 MHz).

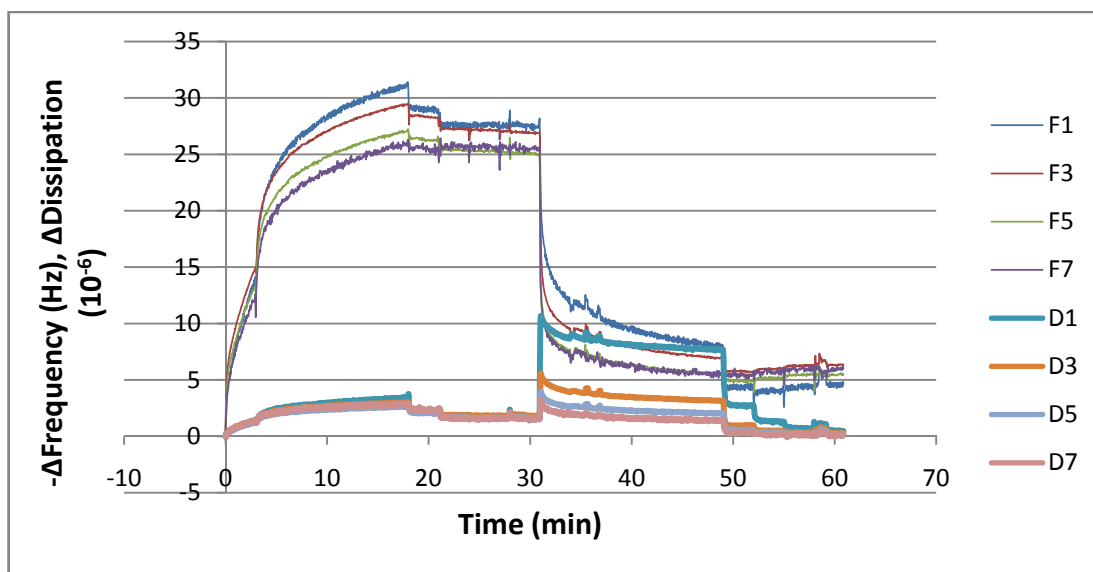


Figure 6.3: QMCD frequency and dissipation shifts during the injection of CMC solution on the absorbed mucin layer. F= Frequency and D= Dissipation. Frequencies: F1 (5 MHz); F3 (15 MHz); F5 (25 MHz); F7 (35 MHz).

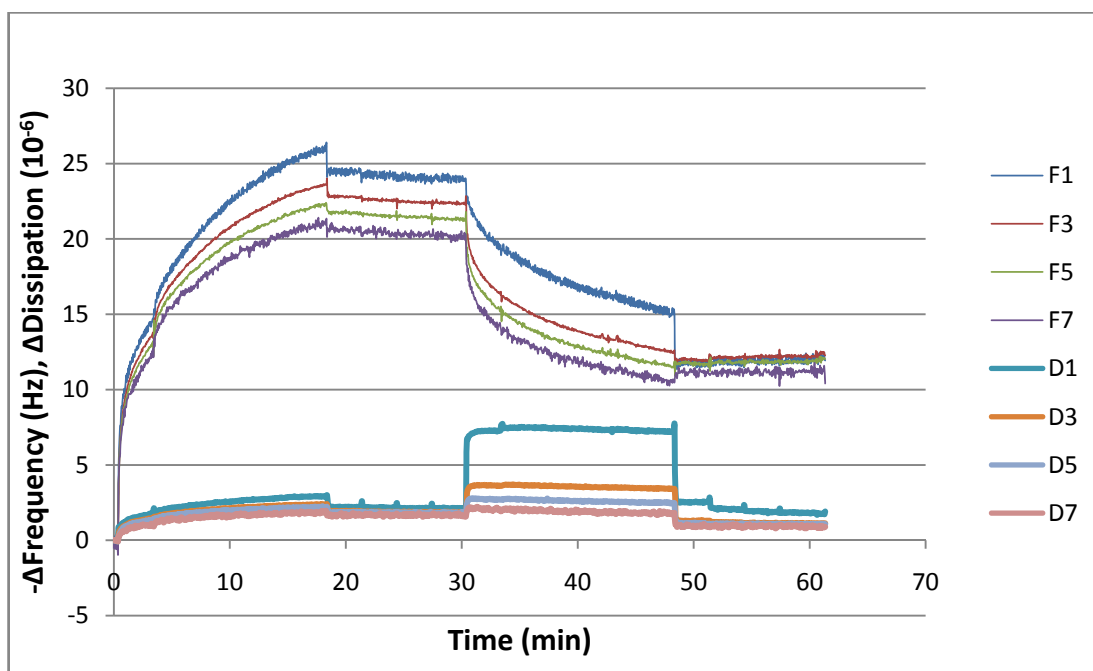


Figure 6.4: QMCD frequency and dissipation shifts during the injection of high DE pectin solution on the absorbed mucin layer. F= Frequency and D= Dissipation. Frequencies: F1 (5 MHz); F3 (15 MHz); F5 (25 MHz); F7 (35 MHz).

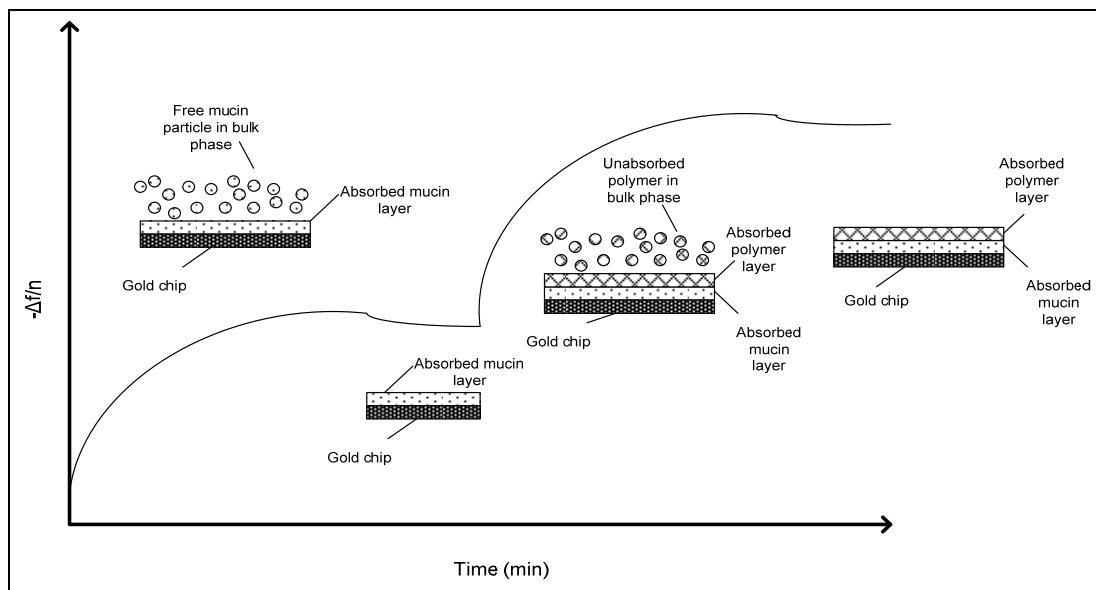


Figure 6.5: Schematic diagram of the expected frequency profile and the process happened during the formation of polymer-mucin layer.

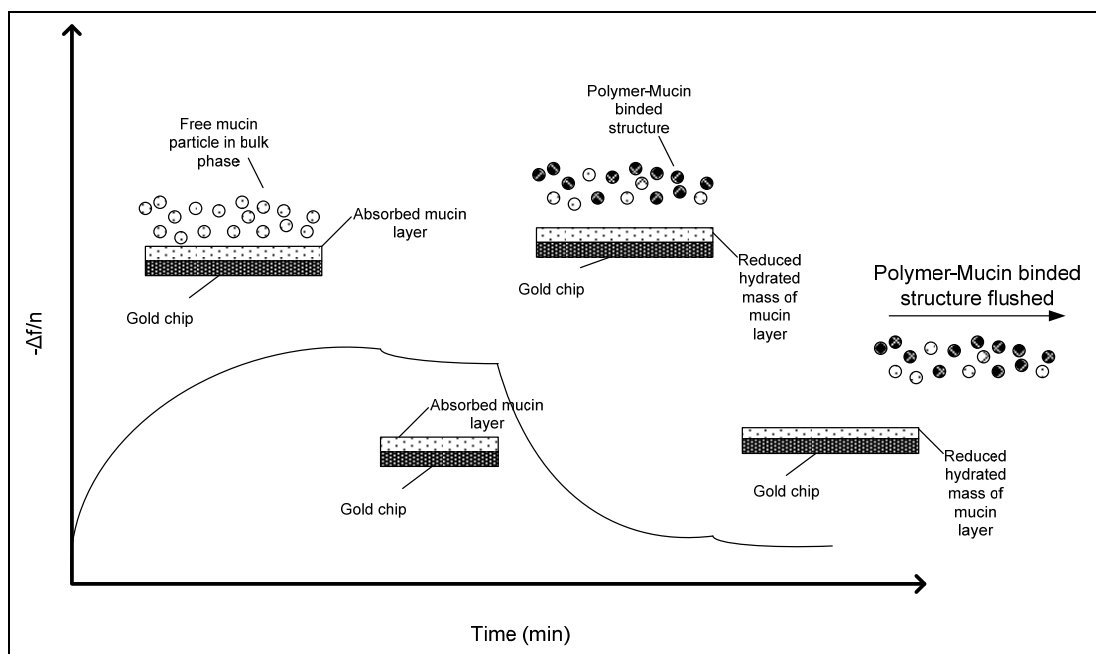


Figure 6.6: Schematic diagram of the phenomenon happened during the experiment.

A further analysis was made on the result obtained from this experiment. The mass of absorbed mucin layer before and after polymer injection was calculated in order to quantify the interaction between each tested polymer with mucin. This analysis was done because of failure to determine the mass of the polymer absorbed onto mucin layer. The calculation of absorbed mass was performed by using the Sauerbrey equation. The model or equation developed by Sauerbrey (1959) can be used in this experiment since the nature of the mucin layer absorbed into gold coated chip was rigid and elastic. The Sauerbrey equation is not suitable to be used to model the absorbed mass if the structure was viscoelastic. As for viscoelastic, the Voigt model which was developed by Voinova et al. (1999) could be used as the appropriate model.

Table 6.1: Calculated mass change and percentage of change of absorbed mucin layer before and after injection of polymer solution (sodium alginate, CMC and high DE pectin). $n=5$ MHz (first overtone).

Polymer	Before ($-\Delta f/n$ Hz)	After ($-\Delta f/n$ Hz)	Mass change (ng/cm^2)	Percentage change (%)
Sodium Alginate	23.478	5.533	3176.62	76.43
CMC	27.634	4.721	4056.06	82.92
high DE pectin	24.108	11.794	2179.82	51.08

Table 6.1 shows the mass change per area and percentage of change of absorbed mucin layer before and after injection of tested polymer solution. The value of frequency change was taken at the point after buffer rinse as this value shows the exact mass of absorbed layer. The mass change per area indicates the total removal

mass of mucin layer from the gold coated chip into the polymer solution bulk due to interaction between the components. CMC shows the highest removal mass with 82.92% followed by sodium alginate, 76.43% and high DE pectin, 51.08%. This result suggested that mucin was more strongly attracted to CMC than to other tested polymers. Also the result indicated that the rate of interaction between mucin and CMC is the highest as shown in Figure 6.7 and 6.8. The interaction rate is one of the important parameters in studying mucoadhesion properties of mucoadhesive polymer besides the overall mucoadhesion force. The sensitiveness of QCMD could distinguish the rate of absorption between sodium alginate, CMC and high DE pectin. Whereas, the results from kinetic absorption analysis using texture analyser showed almost the same rate of interaction for all three polymers.

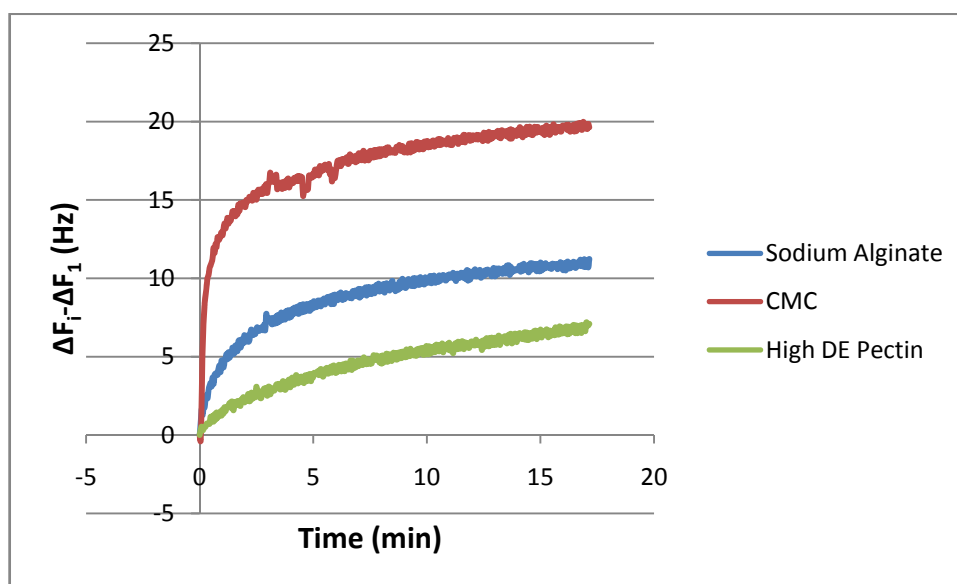


Figure 6.7: Frequency change after injection of tested polymer solution before the buffer rinse.

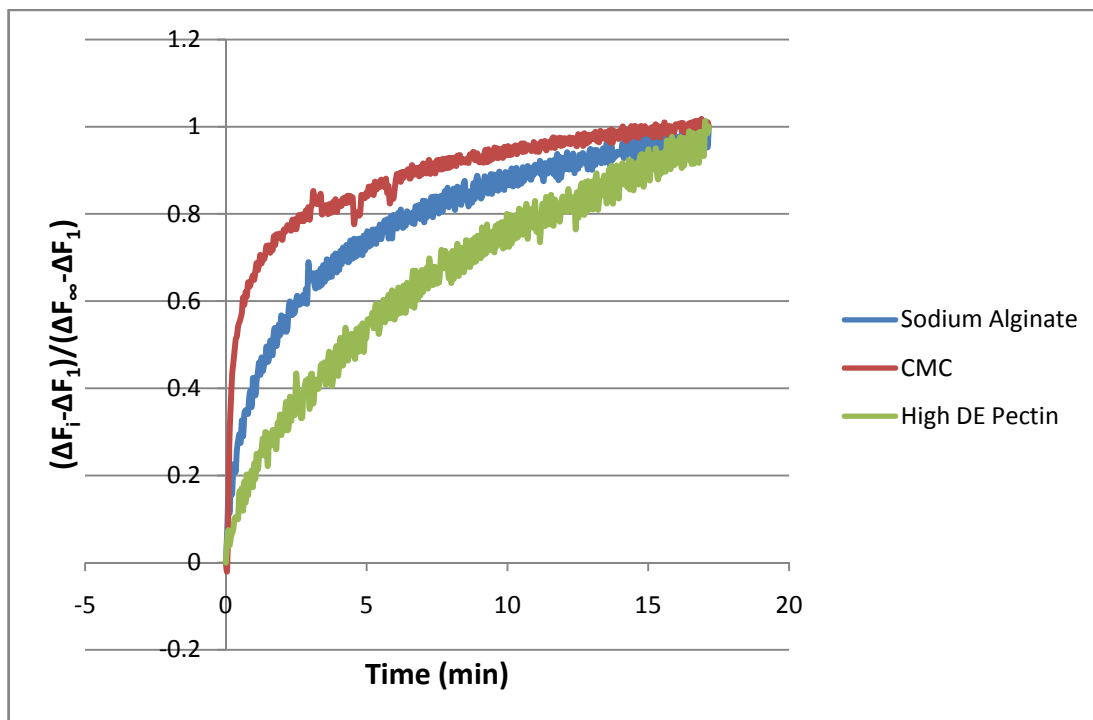


Figure 6.8: Relative frequency change after injection of tested polymer solution before the buffer rinse.

6.3.2 Rheological Characterisation

The experimental results from the modified rheological characterisation method can be used to analyse the kinetic interaction on the mucoadhesive polymer with mucin. This analysis was done by referring to the viscosity profile during the shearing process from the beginning until a homogeneous mixture was formed (plateau line) as shown in Figure 6.9. There are two components of interaction during the shearing process before the formation of the homogeneous mixture which are the dissolution of mucin (mucin dissolves in water) and the interaction between mucoadhesive polymer with mucin. In this section, two examples are used for the kinetic interaction study from the rheological characterisation experiments. The first analysis is the comparison of kinetic interaction between high DE pectin and low DE

pectin. Figure 6.10 shows the viscosity profile during the shearing for mucin layer with water, high DE pectin and low DE pectin. It can be observed that high DE pectin reached the plateau (homogeneous mixture) earlier than low DE pectin and water.

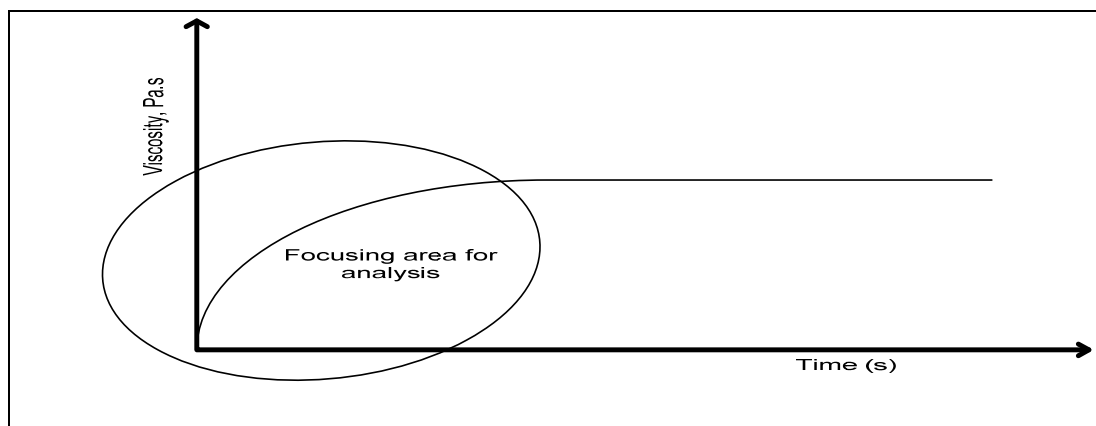


Figure 6.9: Focusing area for kinetic interaction analysis by rheological characterisation.

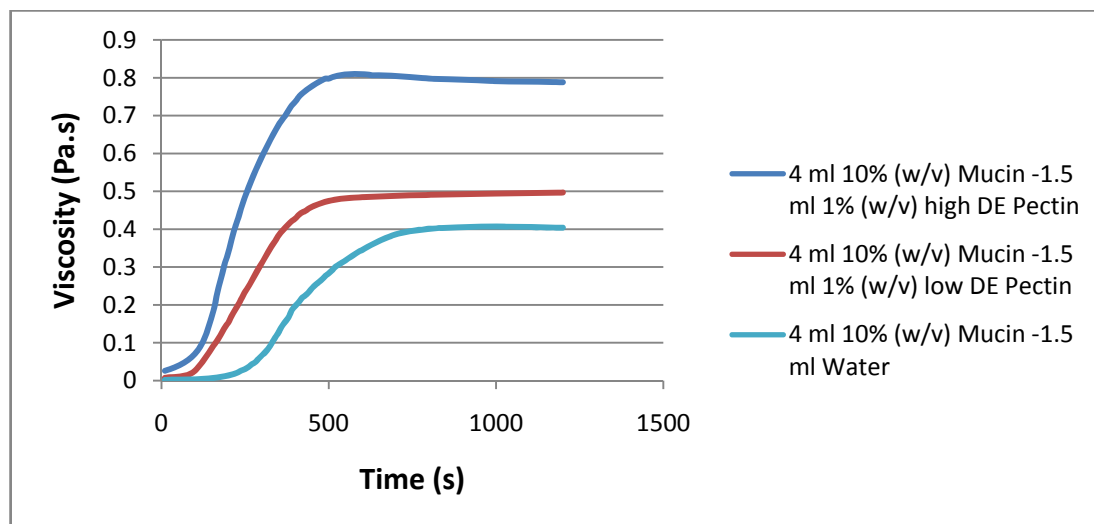


Figure 6.10: Viscosity profile during shearing of mucin layer with water, high DE pectin and low DE pectin. The shearing was done for 20 minutes (1200 s) with shear rate of 50 s^{-1} and 0 s holding time.

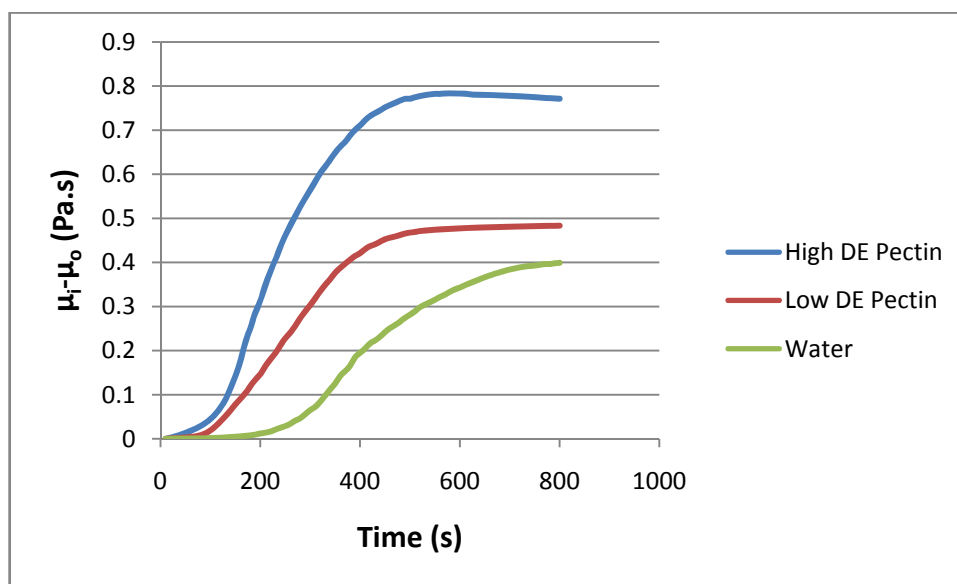


Figure 6.11: Viscosity change during shearing of mucin layer with water, high DE pectin and low DE pectin. From $t = 0$ s to $t = 800$ s.

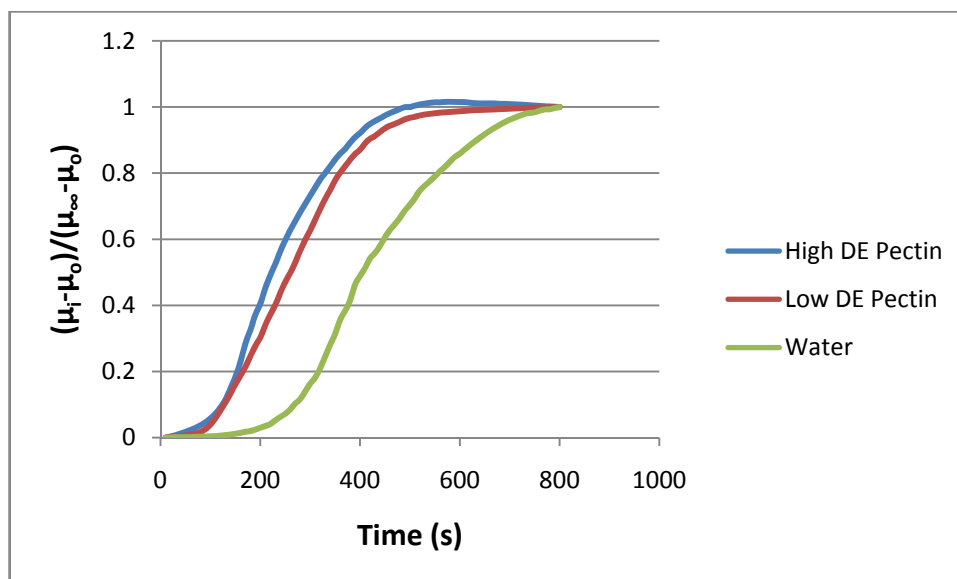


Figure 6.12: Relative viscosity change during shearing of mucin layer with water, high DE pectin and low DE pectin from $t = 0$ s to $t = 800$ s.

The analysis of kinetic interaction is done from $t = 0$ s until $t = 800$ s. The specific rate of interaction between tested polymers with mucin can be interpreted by the relationship shown in Equation 6.1. Interaction rate of water indicates the dissolution of mucin layer into water component of polymer solution. Thus by deducting the value of interaction rate of polymer with water would give the specific interaction rate between polymer components with mucin. Figure 6.11 shows the viscosity changes during the shearing process. It can be observed that high DE pectin shows the highest change in viscosity as compared to low DE pectin. As described earlier, high DE pectin has higher molecular weight than low DE pectin. Therefore, high DE pectin is more favourable for mucoadhesion process. Sriamornsak and Wattanakorn (2008) reported that high DE pectin has greater interaction as compared to low DE pectin by comparing the value of viscosity synergism. However the different in relative viscosity change between high DE pectin and low DE pectin as shown in Figure 6.12 was quite small but still the high DE pectin shows higher rate of increment in interaction.

$$\text{Specific Interaction} = \text{Rate of Polymer} - \text{Rate of water} \quad \text{Equation 6.1}$$

Another aspect discussed in this section is the comparison between mucoadhesive polymer (high DE pectin) with a control experiment (table sugar). Table sugar is composed of sucrose (disaccharide) which is the combination of glucose and fructose. The chemical structure of table sugar which consists of hydroxyl group might give some interaction with mucin through hydrogen bonding. Figure 6.13 shows the viscosity profile during the shearing process for 1% (w/v) high

DE pectin, water, 10% (w/v) sugar and 30% (w/v) sugar with mucin layer at the shear rate of 50 s^{-1} . In order to compare the rate of interaction with different holding time, 0 s and 5 minutes holding time were applied to the 1% (w/v) high DE pectin before shearing. It can be observed in Figure 6.14 that 5 minutes holding time increased the rate of interaction between 1% (w/v) high DE pectin solution with mucin layer rapidly. It is shown by the sharp increase of relative viscosity change as compared to 0 s holding time. Furthermore, higher initial dissolution rate of mucin layer with water after 5 minutes holding time can be observed within the first 200 s. This result shows the importance of contact time which allows the wetting mechanism to manifest. However, the presence of sugar slows the dissolution of mucin into water. This can be observed by lower relative viscosity change shown by the 10% (w/v) sugar solution. Further increase of sugar concentration with 30% (w/v) in water results even slower rate of dissolution of mucin. The measured viscosity at the first point after 5 minutes holding time of 10% (w/v) sugar solution-mucin was almost the same with water-mucin and 1% (w/v) high DE pectin with 0 s holding time. The viscosity were $0.0288 \pm 0.0022 \text{ Pa.s}$ (10% w/v sugar-mucin), $0.0263 \pm 0.0005 \text{ Pa.s}$ (water-mucin) and $0.0263 \pm 0.0039 \text{ Pa.s}$ (1% w/v high DE pectin-mucin) respectively. Measured viscosity at first point for 30% (w/v) sugar-mucin was even lower with the value of $0.0101 \pm 0.0010 \text{ Pa.s}$. The formation of hydrogen bonding between water molecules with sugar component reduced the binding sites of water molecule for the formation of hydrogen bonding with mucin structure during the dissolution process. Besides, this result suggests that sugar presumably reduced the flexibility of mucin structure thus preventing interpenetration and interlocking between the networks during the holding time. Sharad et al. (2011) explained that

diffusion theory is dependent on the flexibility of the polymer structure that allows interpenetration and entanglement between both polymer and mucin. Higher flexibility with the porous polymer structure would favour the diffusion of mucin strand to form interlocking between the networks. This process is a two way diffusion process where the rate of diffusion is dependent on the diffusion coefficient of both components (Ravi et al., 2010).

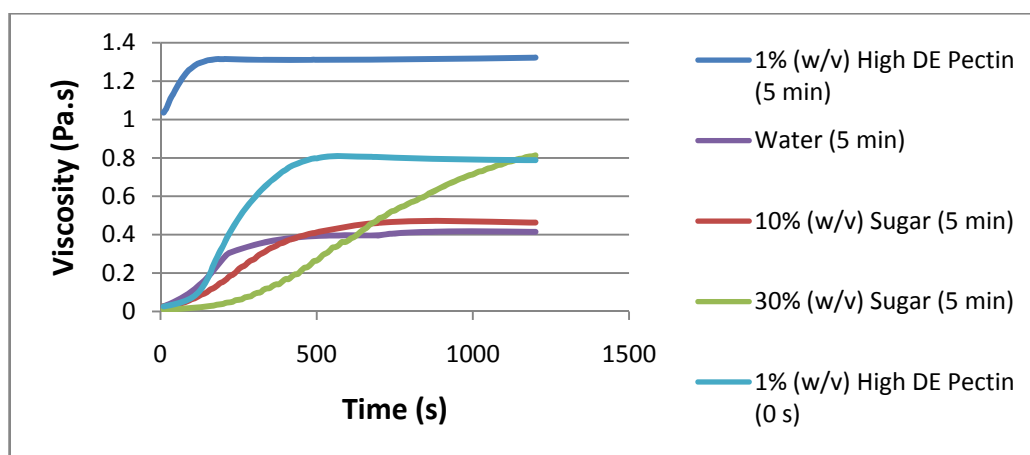


Figure 6.13: Viscosity profile during shearing process for 1% (w/v) high DE pectin, water, 10% (w/v) sugar and 30% (w/v) sugar with mucin layer. Shear rate of 50 s^{-1} and holding time 0 s and 5 minutes.

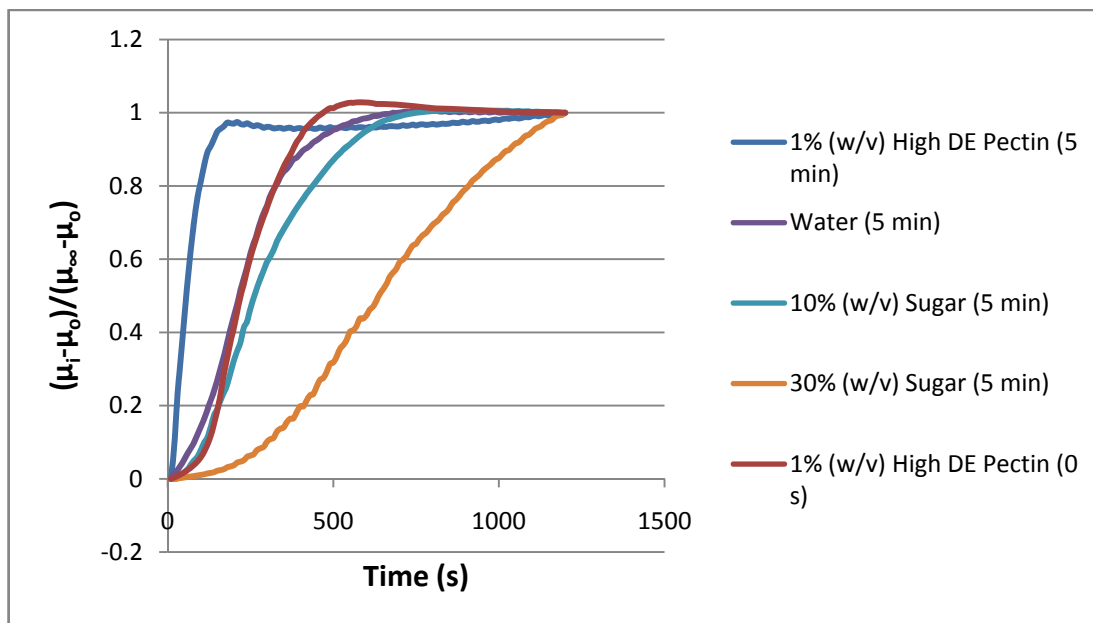


Figure 6.14: Relative viscosity change during shearing process for 1% (w/v) high DE pectin, water, 10% (w/v) sugar and 30% (w/v) sugar with mucin layer. Shear rate of 50 s^{-1} and holding time 0 s and 5 minutes.

6.4 Conclusion

Kinetic absorption study using QCMD shows opposite result from the expected may be due to the removals of absorbed mucin mass from the gold coated chip into tested polymer solution. However, there is some important and useful information that could be elaborated from the frequency and dissipation changes. The sensitiveness of QCMD is proven by its ability to detect the small difference in kinetic interaction of sodium alginate, CMC and high DE pectin with mucin. The analysis of kinetic interaction by QCMD shows that CMC has higher interaction rate as compared to sodium alginate and high DE pectin.

The data from the modified rheological characterisation (in chapter 3) could also be used to study the kinetic interaction between mucoadhesive polymers with mucin as described in section 6.3. High DE pectin shows higher specific interaction rate with mucin as compared to low DE pectin. The comparison between the known mucoadhesive polymer (high DE pectin) with sugar revealed the important factor of diffusivity in mucoadhesion.

Chapter 7:
Mucoadhesion Testing on
Mucoadhesive Biopolymer
Formulation

7.1 Introduction

In recent years, several formulations and types of control release system have been formulated with the incorporation of mucoadhesive polymers. Such formulations include the microspheres (Allamneni et al., 2012; Singh et al., 2013), emulsion suspensions (Sailaja and Amareshwar, 2011), buccal patches (Deshmane et al., 2009; Mishra et al., 2011) and tablets (Shaheen et al., 2006; Patil et al., 2011; Mitra et al., 2012). These formulations offer potential advantages in drug delivery system to improve therapeutic performance of drug by sustaining the drug release. In view of this, the mucoadhesion properties of designed formulations have been evaluated by *in vitro*, *ex vivo* and *in vivo* methods. The *in vivo* method offers accurate and reliable information on the study but this method requires a live specimen for the test and is time consuming. While, *ex vivo* uses part of the organ from human or animals as specimen and this requires special consideration in handling as to maintain its physiological properties. In contrast, the *in vitro* method is a simpler way of investigation and yet capable of providing valuable information in the preliminary study on the mucoadhesion properties of tested mucoadhesive polymer and control release system. Moreover, *in vitro* methods allow for more rapid evaluations under well controlled experimental conditions.

For this investigation, sodium alginate was used in a simple emulsion formulation. The mucoadhesion properties of the sodium alginate emulsion system were evaluated via flow cell equipment and the modified rheological characterisation. Two emulsions incorporated with sodium alginate and high DE pectin were formulated to investigate the effect of different mucoadhesive

biopolymers on size of emulsion droplets. The effect of different concentration of mucoadhesive polymers in the emulsion system on the size of droplets was also determined by observing the emulsion droplets under a microscope. A flow cell was designed to analyse the mucoadhesion effect of sodium alginate emulsion by observing the detachment of the emulsion droplets from the mucin layer during flushing process. The observation process was done under a microscope. The rheological characterisation on the interaction of emulsion with mucin was conducted using the method as discussed in chapter 3. The results of these *in vitro* assessment methods are discussed based on the outcome achieved.

7.2 Materials and Methods

Pectin from citrus peel (degree of esterification ~60%), sodium alginate, mucin type II with bound sialic acid of ~1% and agar powder were purchased from Sigma-Aldrich Company Limited, United Kingdom. All chemicals were analytical grade and used as received. Vegetable oil was purchased from local Tesco store.

7.2.1 Preparation of Mucoadhesive Biopolymer Emulsion

The O/W emulsion (oil in water emulsion) was prepared with 80% (w/v) aqueous or water and 20% (w/v) oil phase and also 98% (w/v) aqueous and 2% (w/v) oil phase. The oil solution was slowly added to the aqueous phase (high DE pectin (0.1% (w/v), 1% (w/v) and 2% (w/v) concentration) and sodium alginate solution (1% (w/v) and 2% (w/v) concentration). The emulsion without mucoadhesive polymer was also prepared for the control emulsion experiment. The emulsion was

prepared using a Silverson L4RT high shear mixer (Figure 7.1) by mixing the oil and aqueous phase (mucoadhesive biopolymer solution) at a speed of 8500 rpm.



Figure 7.1: Silverson L4RT high speed mixer. (Source: Firstenberg Machinery website).

7.2.2 Flow Cell Analysis

0.5 ml of 10% (w/v) mucin suspension was spread onto a microscope glass slide forming a layer with dimension of 17 mm x 46 mm (flow cell dimension). The slide was dried in an oven for at least 20 minutes at a temperature of 60°C. This process was repeated twice in order to get good mucin layer. The microscopic images of the mucin layer and emulsions were observed by using Reichert-Jung

microscope with 25x magnification lens. Firstly, the emulsions and mucin layer were observed before the removal studies using the flow cell were done. The flow cell used in this study was fabricated from Envisiontec R11 resin by using Envisiontec Prototyping Machine from University of Warwick. The flow cell was sealed onto the mucin coated slide using industrial silicone. The flow cell then was placed under the microscope with the lens directly focused on the mucin layer through the glass window. Figure 7.2 and 7.3 show the dimension of flow cell and the setup of the experiment respectively. Using a disposable pipette, the emulsion was injected into the flow cell to fill the internal passage of the flow cell. The emulsion was held inside the flow cell for 3 minutes. After holding time, the channel was washed with double distilled water at a flow rate of 0.24 ml/s using a peristaltic pump (minimum speed of flow rate). The pump was stopped at certain intervals and the photographs of the microscopic images taken for removal studies. The whole procedure was repeated for 1% (w/v) and 2% (w/v) sodium alginate emulsion.

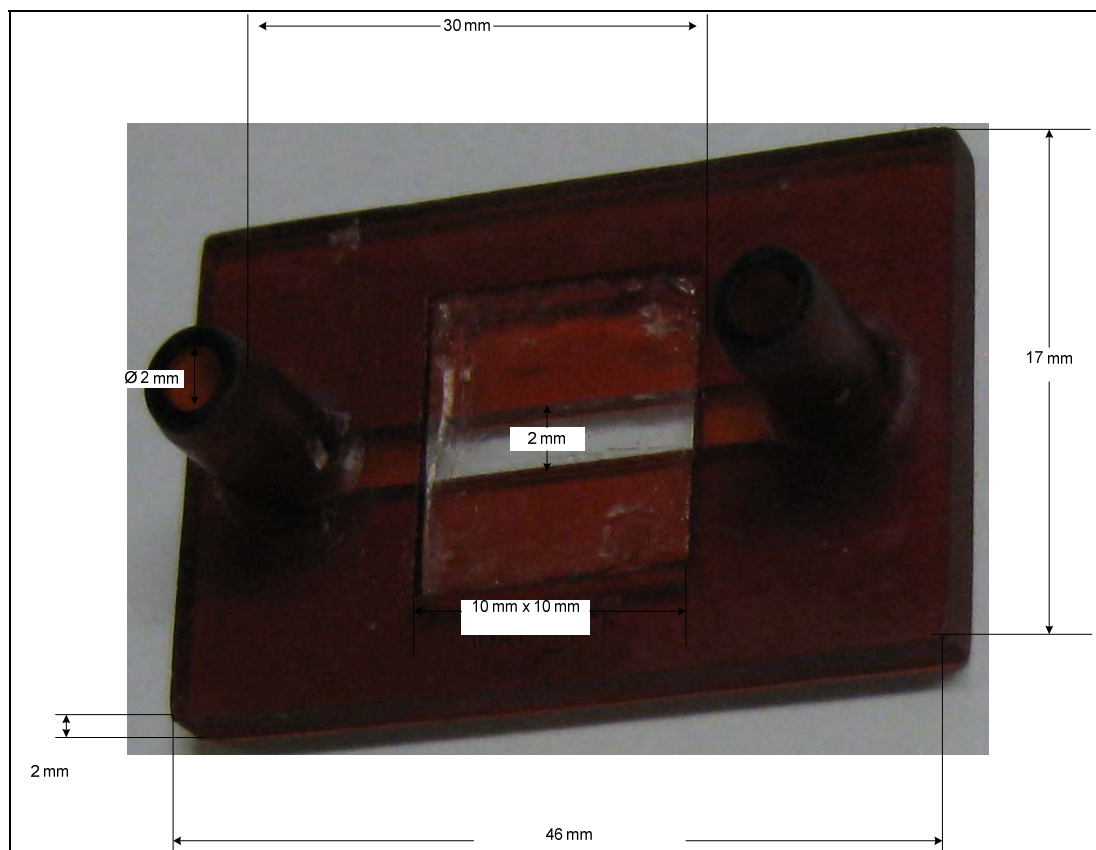


Figure 7.2: Dimension of flow cell.



Figure 7.3: Setup for flow cell analysis with Reichert-Jung microscope using 25x magnification lens.

7.2.3 Preparation of Agar Gel Particles

The method for preparing of agar gel particles used in this study was adapted from Norton et al. (1999). 3% (w/v) of agar solution was prepared by slowly adding the agar powder into preheated double distilled water ($T = 85^{\circ}\text{C}$). The mixture was stirred for at least 3 hours to ensure the agar powder was fully dissolved. The process of making agar gel particles and rheological characterisation was done using AR1000 rheometer with 40 mm flat aluminium steel plate geometry. The 1.5 ml agar solution at a temperature of 85°C was placed on the peltier stage. The initial equilibrium time was set for 2 minutes before the shearing process was done. The agar solution was then cooled to 10°C (cooling rate $1.5^{\circ}\text{C}/\text{min}$) and simultaneously sheared at shearing rate of 40 s^{-1} and 100 s^{-1} (Temperature ramp step). The gap between geometry with peltier stage was set at $500\text{ }\mu\text{m}$ and solvent trap was used to minimise the evaporation effect on the sample. After the temperature ramp step, the gel temperature was raised to 25°C with 2 minutes equilibrium time. Then, the gel particles were subjected to a frequency sweep test at 0.5% strain over a frequency range of 0.1-20 Hz. The flow curve of gel particles was measured at 25°C with the shear rate ranging from $1\text{--}1000\text{ s}^{-1}$.

7.3 Result and Discussion

7.3.1 Oil in Water (O/W) Emulsion with Mucoadhesive Biopolymer

Mucoadhesive polymers are known to act as surface active ingredients (surfactants) that lower the surface tension of oil. The mucoadhesive polymer molecules would assemble on the surface of the oil droplets and hence cause the oil

droplets to adhere to the mucous layer. Emulsion of high DE pectin and sodium alginate (80% aqueous phase and 20% oil phase) was observed under a microscope (Reichert-Jung microscope with 25x magnification lens) and the microscopic images are shown in Figure 7.4. The size (diameter) of oil droplets in the emulsion without mucoadhesive biopolymer was in the range of 20-30 μm . Addition of 0.1% (w/v) high DE pectin reduced the size of droplets to 10-15 μm in diameter. A further increase in polymer concentration produced even smaller emulsion droplets. The summary of size of droplets in the emulsion is shown in Table 7.1. Higher polymer concentration would mean the presence of more stabilizing polymer around the oil droplets, leading to the complementary of two factors: 1) Reduction of oil droplet size was due to a reduction in the interfacial tension between oil and aqueous phases; 2) Reduction of droplet size as polymer concentration increases was due to the increase of the interaction between the polymer molecules (hydrophobic effect). The size range of emulsion droplets shown in the Figure 7.4 is suitable to be used for the flow cell observation experiment.

Table 7.1: Emulsion characteristic.

Aqueous phase (80% w/v)	No polymer	0.1% (w/v) high DE pectin	1% (w/v) high DE pectin	2% (w/v) high DE pectin	1% (w/v) sodium alginate	2% (w/v) sodium alginate
Observation	Loose	Loose	Aggregation	Compact aggregation	Aggregation	Compact aggregation
Diameter (µm) of droplets	20-30	10-15	5-10	2-7	5-10	1-5

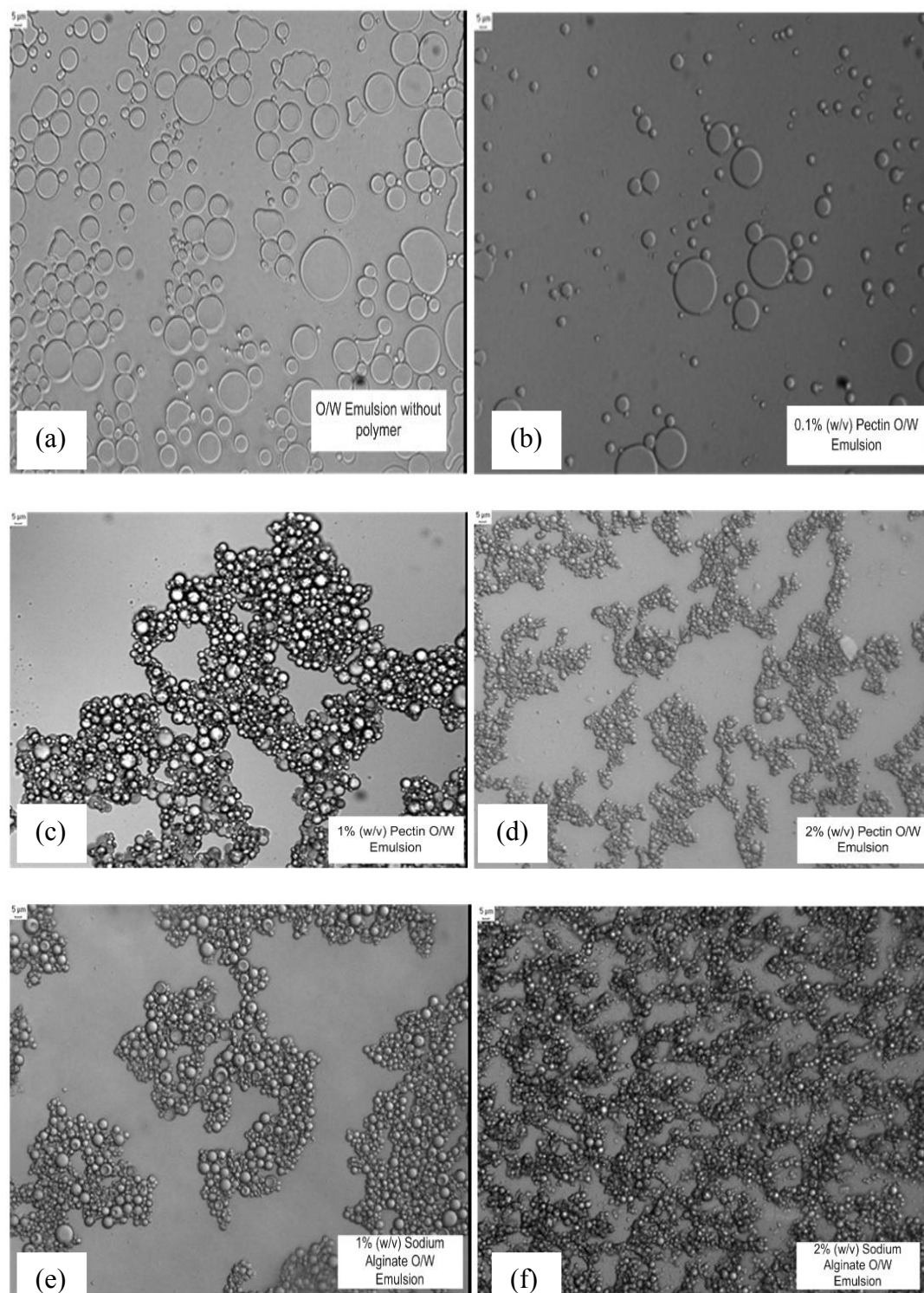


Figure 7.4: Images of emulsion droplets made with different mucoadhesive polymers and concentration. (a) No polymer; (b) 0.1% (w/v) high DE pectin; (c) 1% (w/v) high DE pectin; (d) 2% (w/v) high DE pectin; (e) 1% (w/v) sodium alginate; (f) 2% (w/v) sodium alginate.

7.3.2 Viscometric Experiment of Mucoadhesive Biopolymer Emulsion with Mucin Layer

The mucoadhesion properties of mucoadhesive polymer in emulsion system have been tested using rheological characterisation. The method used in this experiment was the same as described in section 3.2.3. Figure 7.5 shows the viscosity profile during the mixing or shearing of sodium alginate emulsion with mucin layer after 5 minutes holding time. Different profiles were observed during the shearing process for the emulsion with polymer and emulsion without polymer. The viscosity of emulsion without polymer increased gradually until a near plateau line was achieved. Meanwhile, the viscosities of emulsion with sodium alginate (both concentrations) increased sharply for a short time before the value slowly dropped until an approximate plateau was achieved. The same profile was observed during shearing of 2% (w/v) sodium alginate with mucin layer. As mentioned in chapter 3, there were dissolution and mucoadhesion interaction of sodium alginate solution with dried mucin layer. Erratic lines produced (for 1% (w/v) and 2% (w/v) emulsion) indicated the instability of the emulsion under shearing process. The emulsion droplets might experience breakage or disruption caused by the applied shear. Thus this complex phenomenon (mucoadhesion interaction and instability of emulsion) affected the smoothness of the viscosity profile.

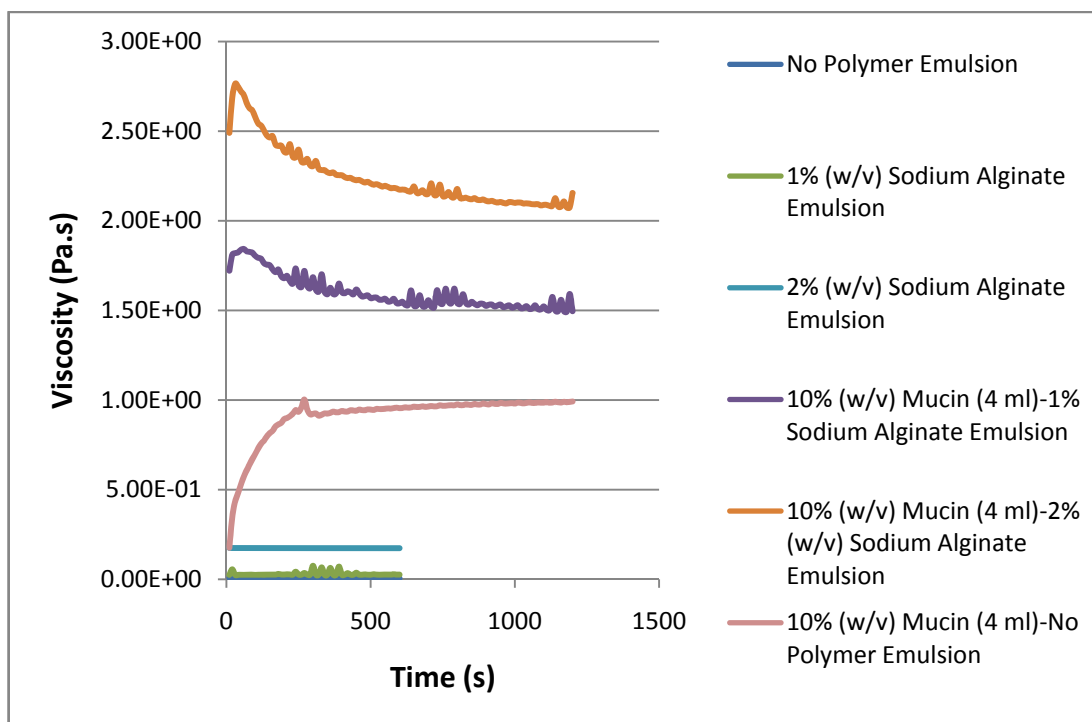


Figure 7.5: Viscosity profile of the shearing process of (O/W) emulsion with dried mucin layer. Three emulsion formulation were used which are 1% (w/v) and 2% (w/v) of sodium alginate and without polymer. Shear rate at 50 s^{-1} and holding time was 5 minutes prior to shearing process. The measurement done at $T = 37^\circ\text{C}$.

Calculated synergism, normalised value and intermolecular frictional force for emulsion with sodium alginate system are shown in Table 7.2. Emulsion with higher concentration of sodium alginate shows higher synergism with the value of $0.990 \pm 0.230 \text{ Pa.s}$ as compared to emulsion with 1% (w/v) sodium alginate ($0.473 \pm 0.163 \text{ Pa.s}$). The normalised parameter (η_{rel}) could also be used to compare the polymer solution and the emulsion system. Polymer solution has higher normalised parameter as compared to emulsion system with the polymer solution of the same concentration. For example, 2% (w/v) sodium alginate has the normalised parameter of 4.11 (Table 3.3) and emulsion with 2% (w/v) sodium alginate has the

value of 1.85 respectively. The mucoadhesion properties of sodium alginate emulsion were reduced by the presence of oil in the emulsion system due to the nature of oil that has hydrophobic effect. Shearing caused the breakage of the emulsion particles, releasing the oil into the system and this will hinder the process of interaction between the mucin and sodium alginate despite the amount of sodium alginate in the emulsion system being only 20%, less than in the sodium alginate solution. In most cases, the stability of emulsion is affected by the homogeneity and fineness of the brine-dispersed droplets (Al-Homadhi, 2000). The stability of emulsion was weakened by the mucoadhesion between the sodium alginate (wall) with mucin. This creates a competition of emulsion to maintain the integral structure of sodium alginate wall. The creaming of the emulsion used in this experiment was observed as early as 10 minutes after the preparation where there was a separation of two phases (emulsion and aqueous phase). Thus the mucoadhesion ability of mucoadhesive polymer emulsion is not suitable to be evaluated by using a shearing based measurement technique as shearing caused the emulsion to separate into different phases and this would result in erroneous viscosity measurements.

Table 7.2: Apparent viscosity (η_p), observed viscosity (η_{obs}), expected viscosity (η_{exp}) and enhanced viscosity or synergism (η_{enh}) of emulsion with sodium alginate (1% w/v and 2% w/v concentration) and without the sodium alginate and their mixture with 4 ml of 10% (w/v) mucin in dried layer (1.5 ml of emulsion was used for the mixing process) at 50 s^{-1} and 5 minutes holding time.

Sodium Alginate Concentration (% w/v)	η_p (Pa.s)	η_{obs} (Pa.s)	η_{exp} (Pa.s)	η_{enh} (Pa.s)	η_{rel}	F (Pa)
0	0.006±0.001	0.992±0.103	0.992±0.103	0	1	
1	0.030±0.007	1.495±0.126	1.022±0.103	0.473±0.163	1.46	23.65
2	0.174±0.005	2.156±0.206	1.166±0.103	0.990±0.230	1.85	49.50

7.3.3 Flow Cell Observation on Interaction Between Mucoadhesive Biopolymer Emulsion with Mucin Layer

A specially designed flow cell was fabricated and used to study the mucoadhesion ability of mucoadhesive biopolymer emulsion onto mucin layer. The investigation was done by observing the amount of emulsion droplets being removed when the flow cell with mucin coated slide and clean slide were flushed with distilled water. However, the quantitative comparison based on droplet counts was not possible because of difficulty in counting the droplets due to migration effect of the droplets across the field of view of the microscope. However based on visual observation, it was still possible to compare the amount of different emulsion droplets sticking on the mucin coated slide and on the clean slide.

Figure 7.6 shows a sequence of images during the flushing process of emulsion droplets without mucoadhesive biopolymer on the mucin coated slide. It shows that some emulsion droplets were moved out from the focused area after 70 s of flushing was done. Further flushing with distilled water removed more droplets as seen at 230 s and 310 s. Meanwhile, flushing of the emulsion droplets on the clean slide shows total removal of the droplets at as early as 81 s (Figure 7.7). The same pattern could be observed for the 1% (w/v) sodium alginate emulsion where massive amount of the droplets were removed after 92 s of flushing time as shown in Figure 7.8. Ability of emulsion droplets to stick and be retained on the mucin coated slide was increased with the addition of mucoadhesive biopolymer into the formulation. This could be observed from Figure 7.9 and 7.10. A longer time was needed to remove some sodium alginate emulsion droplets compared to emulsion without biopolymer.

Longer retaining time of droplets on the mucin coated layer resulted from the mucoadhesion interaction between the mucoadhesive biopolymer enveloping the emulsion droplets with the mucin layer. Thus more force and longer time were required to remove the droplets from the mucin coated slide. Longer exposure of the system to water was believed to weaken the adhesion between sodium alginate emulsion droplets with the mucin network through over hydration that formed a slippery mucilage effect at the interface. However, the observation of emulsion droplets in the flow cell channel was difficult because there were multilayers of droplets as the thickness of internal passage could accommodate a few layers of emulsion droplets. In contrast, observation of droplets on a slide covered with thin

slide cover was clearer because there was only one layer of droplets between the microscope slide and the slide cover.

Another aspect to be considered is that the loss of droplets might not be totally due to detachment from the mucin layer but might be due to breakage of droplets caused by the flow force during flushing. There was high possibility for this to occur as the emulsion was proved to be unstable when ‘creaming’ was observed just 10 minutes after it was prepared. Despite the uncertainty in the accuracy of the result (amount of droplets observed) obtained from flow cell observation, the analysis on the microscopic images gives a reasonably clear picture on the mucoadhesion ability of tested emulsion system. Thus the flow cell can be used to investigate the properties of mucoadhesive formulation system. For better result, a more stable micro or nano form of mucoadhesive formulation such as sodium alginate cross-linked with cation ion bead, polyelectrolyte micro capsule (combination of anionic and cationic polymer), multilayer coating emulsion or micro-gel particles could be used in this experiment. Another way of analysis using this *in vitro* method is by determining the amount of the formulation microspheres before and after passing through the internal passage of the flow cell. This could give a quantitative evaluation on the amount of the microspheres adhered on the mucin layer. This technique has been used by He et al. (1998) where they used a gut loop (similar to the flow cell internal passage) of a rat to evaluate the mucoadhesion properties of chitosan microspheres by calculating the amount of microspheres before and after passing the microspheres through the gut. The microscopic images obtained from the flow cell can be improved further by using a microscope with

higher magnification. A more detailed and clearer image can provide more valuable information on mucoadhesion.

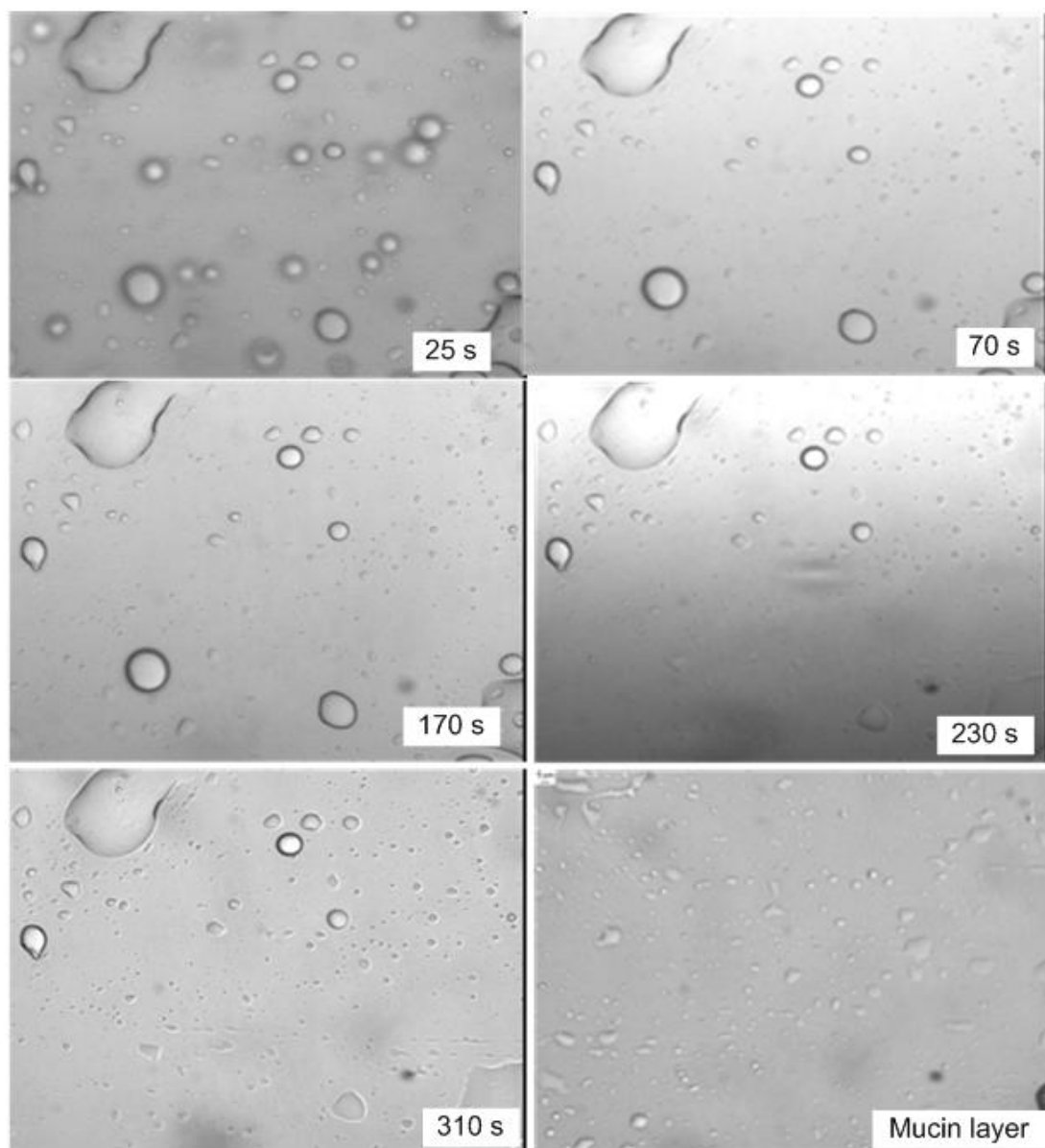


Figure 7.6: Emulsion without mucoadhesive polymer on the mucin coated slide.

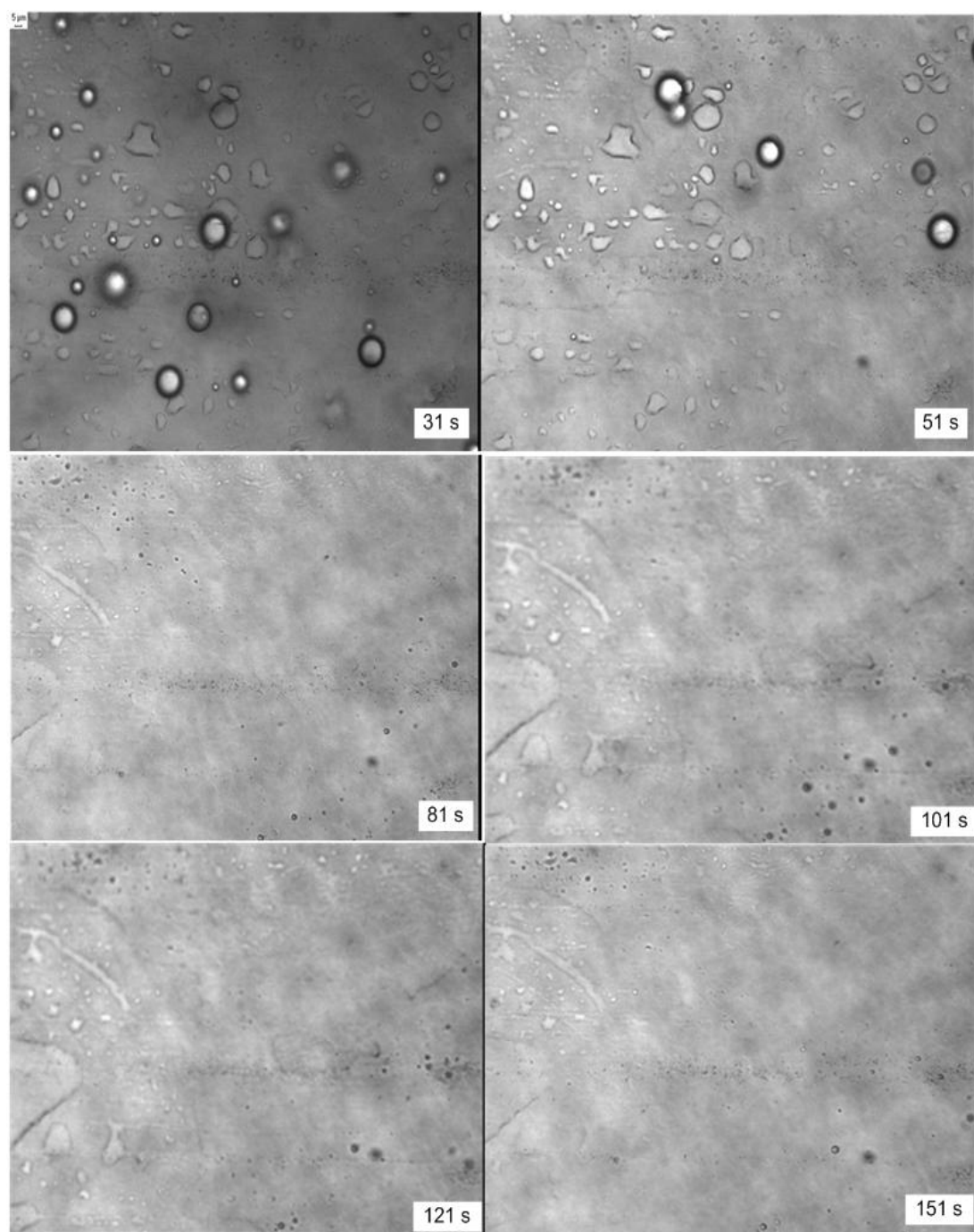


Figure 7.7: Emulsion without mucoadhesive polymer on the clean slide.

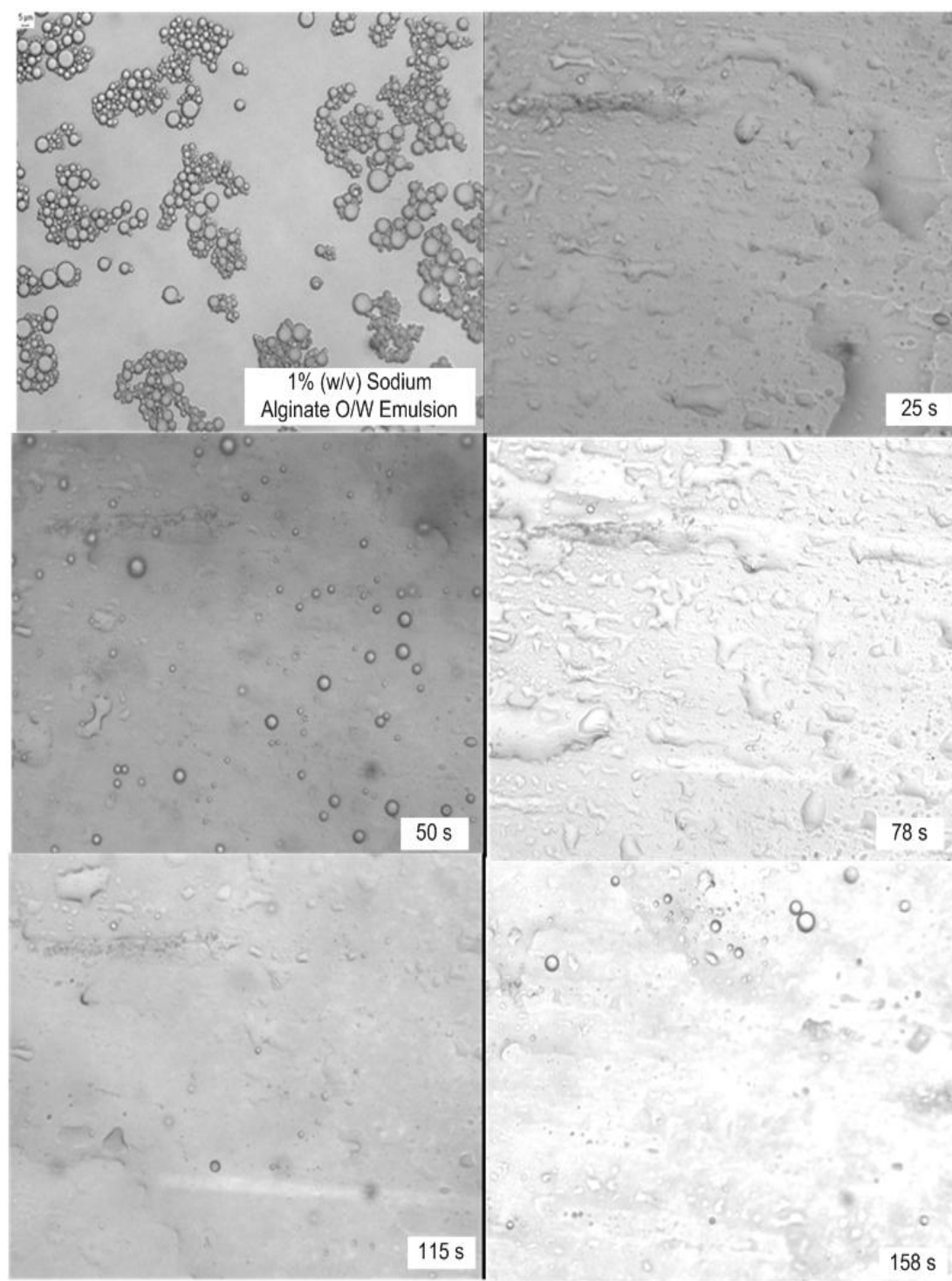


Figure 7.8: 1% (w/v) sodium alginate O/W emulsion on clean slide.

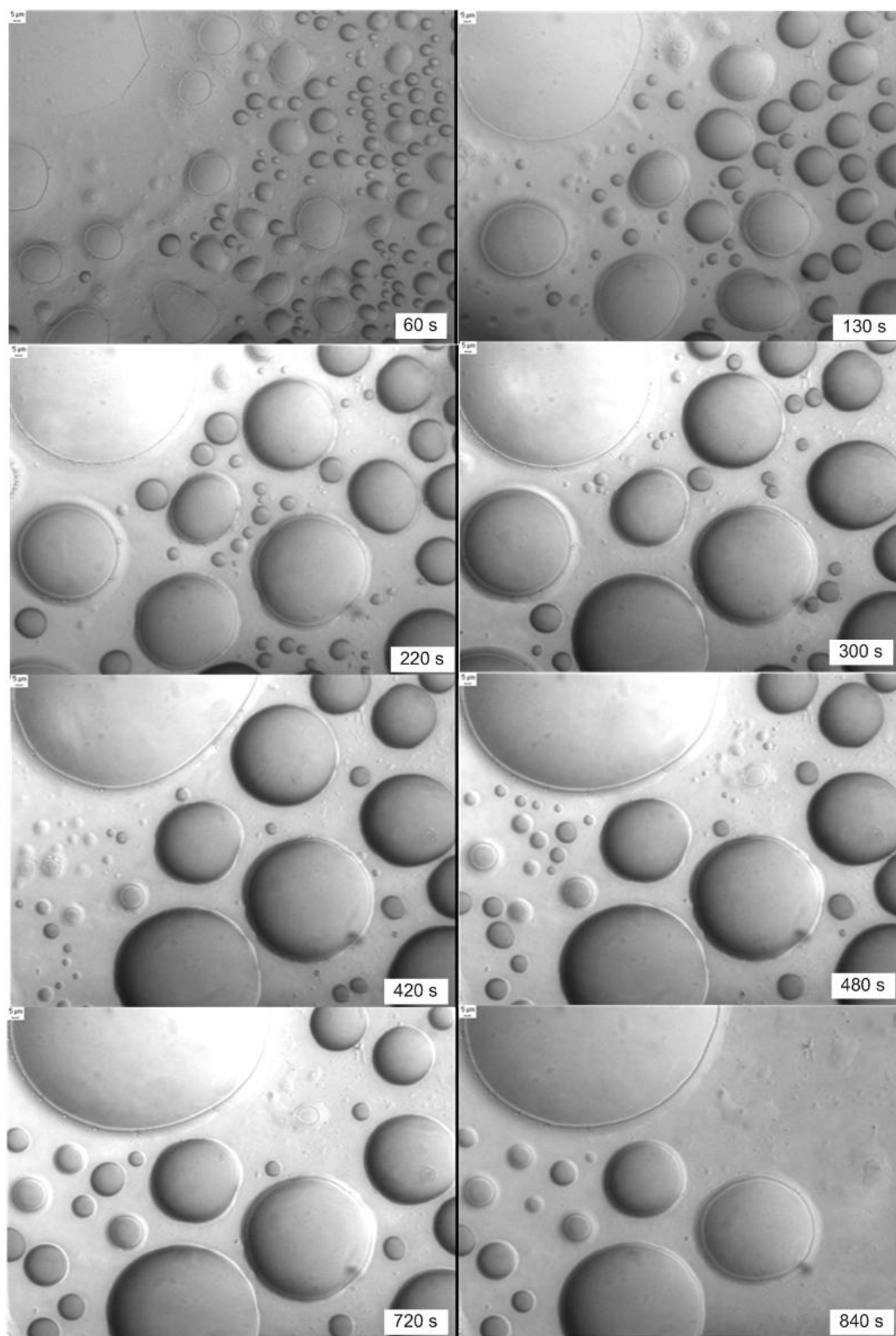


Figure 7.9: 1% (w/v) sodium alginate O/W emulsion on mucin coated slide.

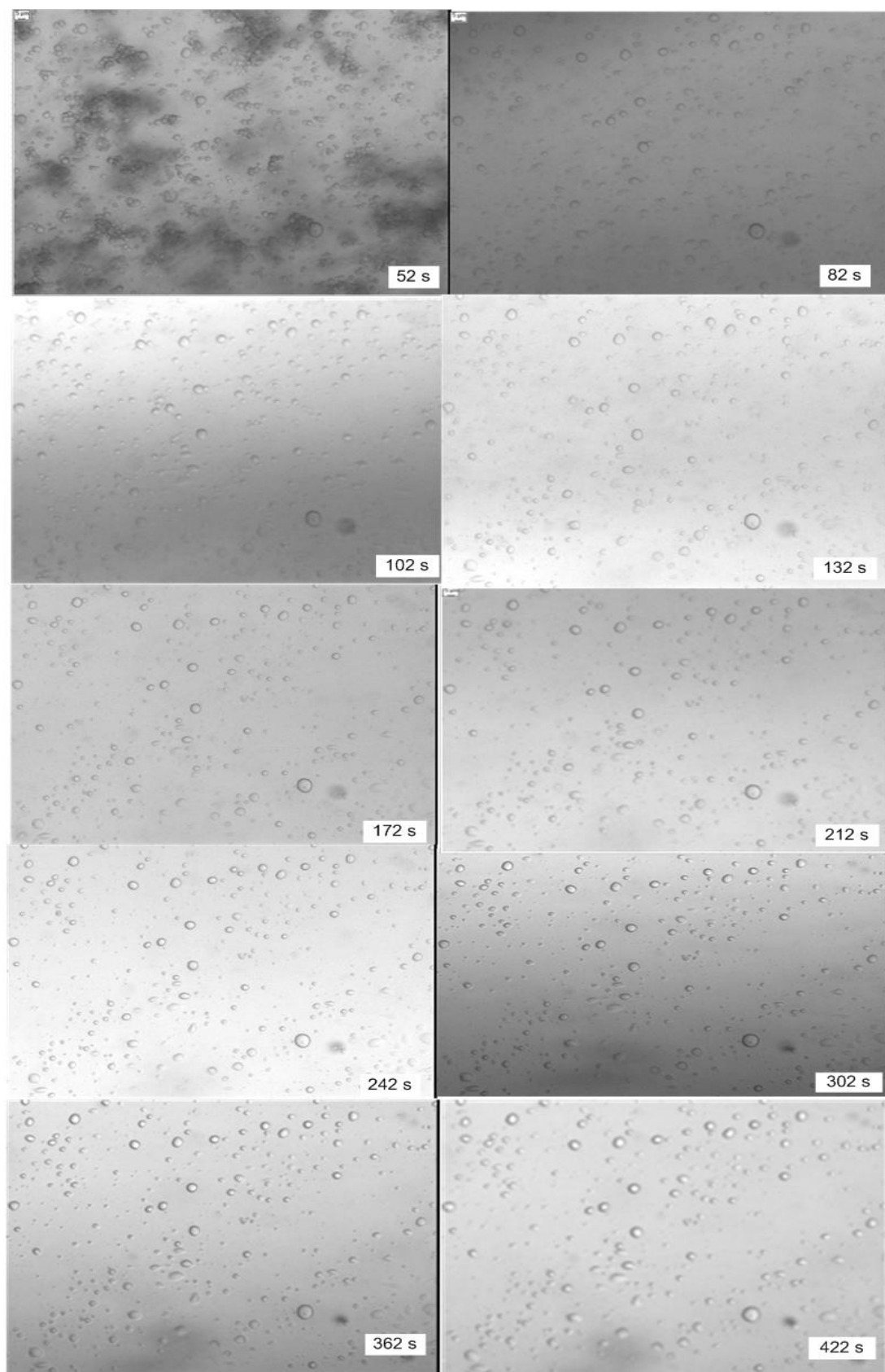


Figure 7.10: 2% (w/v) sodium alginate O/W emulsion on mucin coated slide.

7.3.4 Agar Gel Particles

The mucoadhesiveness of agar has not been studied in this research but agar has been studied extensively as a sustain release system in pharmaceutical use (Bera et al., 2013). They have reported that mucoadhesion of agar microspheres were affected by pH due to different degree of ionisation. Bhimavarapu et al. (2014) used sodium alginate with agar as co-polymer to form mucoadhesive beads with the content of mosapride citrate in order to evaluate the mucoadhesion properties and release efficiency. The nature of agar that exists in form of solid gel at room temperature with thermally reversible properties give an advantage to be used in a control and sustained release system in food and pharmaceutical application. However, the mucoadhesion properties of agar as compared to other mucoadhesive biopolymers have not yet been studied extensively.

Normally, agar microsphere beads are prepared using hot-cold congealing method as described by Bera et al., (2013) with adaptation of the method used by Sapia et al., (2002). Hot-cold congealing method was done by dispersing hot agar solution into light liquid paraffin while stirring in an ice-surrounded vessel. Another interesting form of mucoadhesive control release system using agar is in the form of fluid gel particles. Figure 7.11 shows the viscosity profile during gelation and formation of fluid gel particles by shearing at different shear rate with cooling rate of 1.5°C/min. The viscosity of agar solution increased gradually with decreasing temperature. At this stage, the agar structure slowly tightened together before the gelation point. Norton et al. (1999) observed the gelation point was at about 45°C and $T_{\max} = 35^{\circ}\text{C}$. Meanwhile Figure 7.11 shows that gelation occurred at 40°C and

T_{\max} is 32°C. The difference in gelation temperature obtained in this study could be affected by different sample of agar used and also a small difference in concentration of prepared sample as these points are specific biopolymer dependent. The viscosity of agar solution was rapidly increased from gelation temperature to T_{\max} . At this range, small gel nuclei were formed and then grow to form gel at T_{\max} . Norton et al. (1999) explained that the agar starts to form double helices structure and aggregation of each structure happened until gel is formed when the system reaches above the critical concentration. Further shearing causes the packed gel network to break up and form fluid gel system. The differences in viscosity measured during the formation of fluid gel with different shear rate caused the different degree of gel particles size to form. Furthermore, the smoother viscosity profile after T_{\max} shown by blue line (shear rate of 100 s⁻¹) indicates the fluid gel particles formed structurally 'smoother' than with shear rate of 40 s⁻¹. The size differences were observed by Norton et al. (1999) by using Confocal Scanning Light Microscopy as shown in Figure 7.12. The gel particle sizes were in range of 10-20 µm (shear rate of 40 s⁻¹) and 1-5 µm (shear rate of 750 s⁻¹).

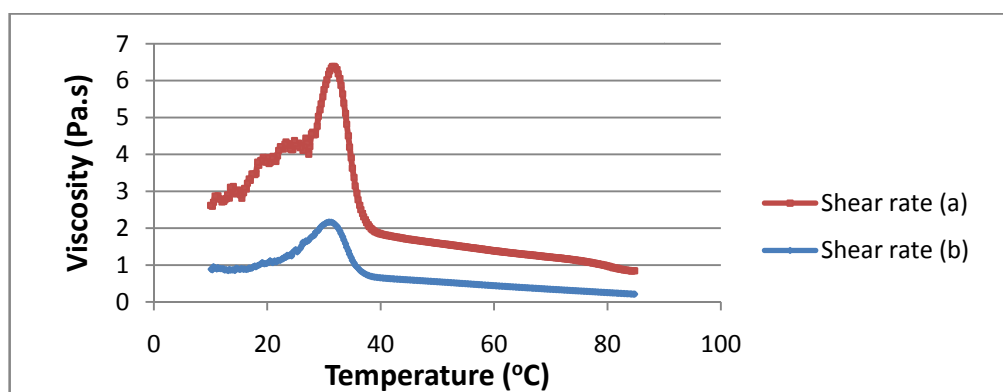


Figure 7.11: Temperature ramp of 3% (w/v) agar with different shear rate: (a) 40 s⁻¹ and (b) 100 s⁻¹. Cooling rate is 1.5°C/min.

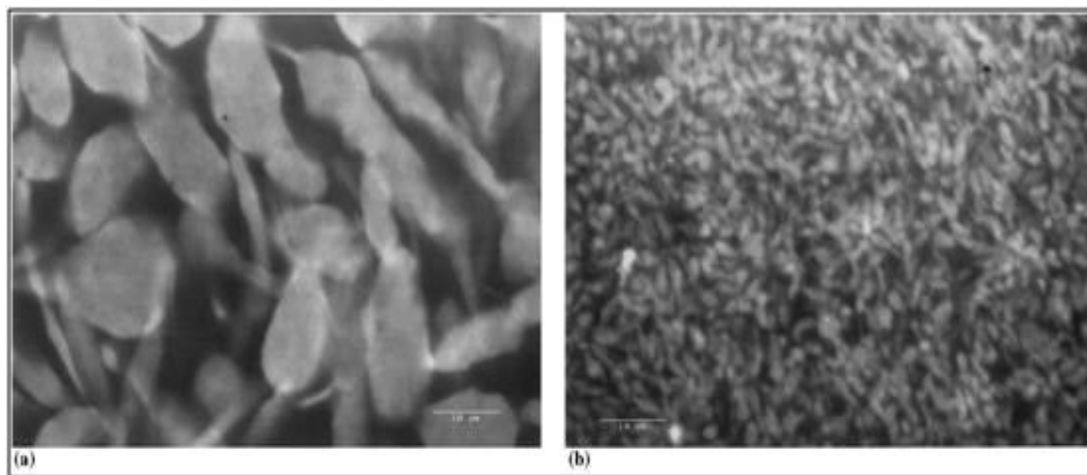


Figure 7.12: Images of fluid agar gel formed with different shear rate. (a) 40 s^{-1} and (b) 750 s^{-1} . (Source: Norton et al., 1999).

Figure 7.13 shows the G' (elastic modulus) and G'' (viscous modulus) profile of fluid gel particles measured by the frequency sweep step. The gel particle network formed by lower shear rate (40 s^{-1}) has stronger strength and more elastic compared to shear rate of 100 s^{-1} as shown by higher value of G' (elastic modulus). Both fluid gel particles show minimal effect on the change of applied frequency (0.1 to 20 Hz). The formation of gel was conformed by the dominance of G' over the G'' value and this modulus were independent over the applied frequency.

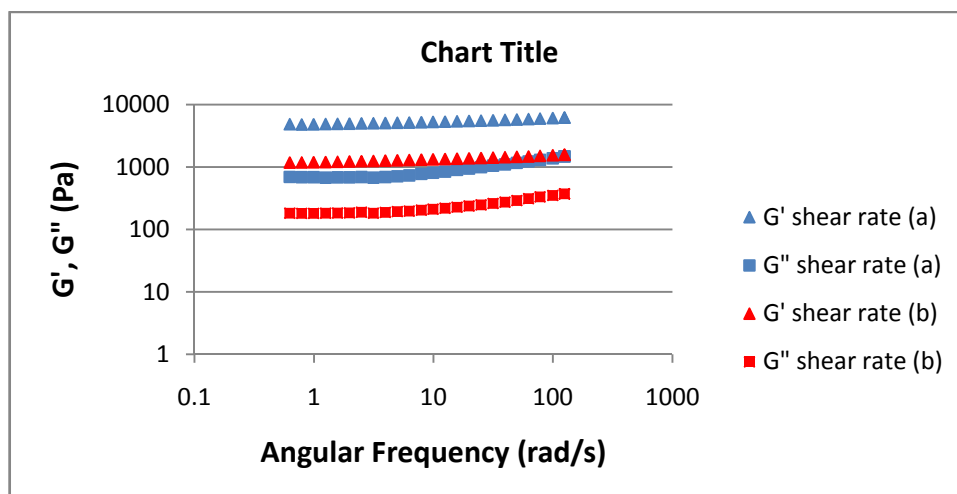


Figure 7.13: Frequency sweep of 3% (w/v) Agar gel particle at 0.5% strain. Shear rate: (a) 40 s^{-1} and (b) 100 s^{-1} .

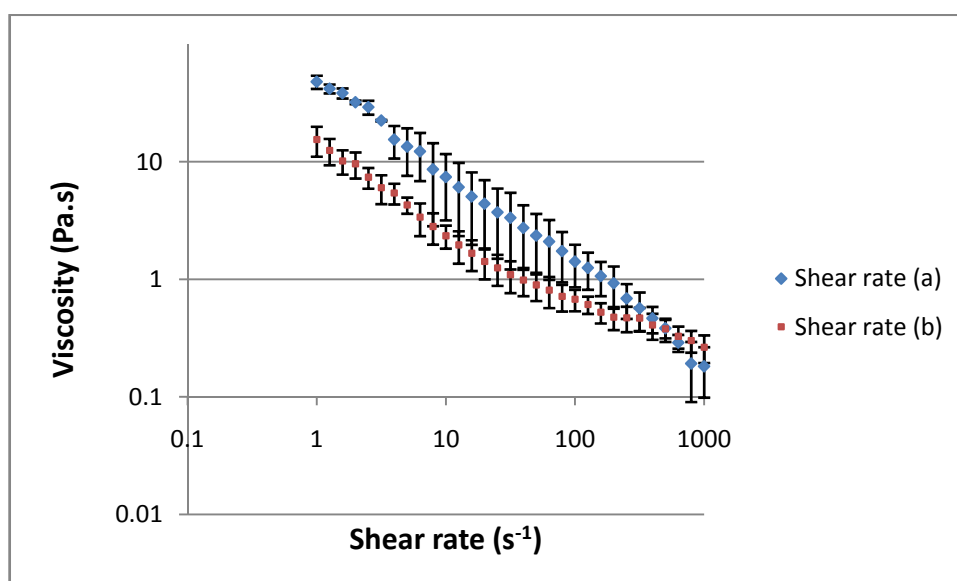


Figure 7.14: Flowcurve of 3% (w/v) agar gel particle produced by applying different shear rate: (a) 40 s^{-1} and (b) 100 s^{-1} .

The agar gel formed by physical disruption of shearing process is not the same as typical gel. The process results in the formation of gel at the scale μm rather than cm with fluid or paste like behaviour. In order to study the behaviour of fluid

agar gel, a viscosity measurement was done with the shear rate in the range of 1 s^{-1} to 1000 s^{-1} . From the experiment, both fluid agar gels proposed of shear thinning behaviour as shown in Figure 7.14 where viscosity decreased with increasing shear rate. Fluid gel formed with the shear rate 40 s^{-1} has higher viscosity than the fluid gel formed with the shear rate of 100 s^{-1} from the shear rate of 1 s^{-1} until 500 s^{-1} whilst further increased in shear rate results in lower viscosity. This behaviour could be explained by the different recovery ability of the gel structures at higher shear rate. Bigger structure of fluid gel had difficulty to reform the gel network after experiencing the disruption at very high shear rate. Meanwhile, smaller and smoother gel structures have more flexible network that can recover and rebuild the internal structure at a short time after the changes caused by a very high shear rate. This behaviour shows less viscosity changes as observed from the flow curve graph.

7.4 Conclusion

Emulsion formulation with sodium alginate in aqueous phase has been made and tested for its mucoadhesion capability with two different methods which are rheological characterisation (viscometry experiment) and newly designed in-vitro flow analysis called flow cell. The emulsion sizes were affected by the concentration of sodium alginate in aqueous phase where higher concentration produced smaller size of the droplets. Measurement of sodium alginate emulsion interaction with mucin by using viscometry experiment shows high difference synergism value as compared to sodium alginate solution. The oil contains in the emulsion system prevented or hindered mucoadhesion to take place between the sodium alginate structure with mucin network. Applied shear by the rheometer geometry during the

shearing process would break the emulsion droplets and released oil into the mixture. The newly designed rig or apparatus (flow cell) as an alternative of in-vitro analysis method was capable to give good information on the mucoadhesion properties of the mucoadhesive micro-formulation. The emulsion droplets were shown to have interaction with mucin when the harder removal of the droplets were observed with the mucin coated slide as compared to clean slide. Addition of sodium alginate in the emulsion system has increased the ability of the droplets to remain on the mucin layer at longer time during the flushing process. The agar fluid gel particles were not tested in the flow cell due to the inability of the microscope to observe the gel particles images.

Chapter 8:

Conclusion and Future Work

8.1 Introduction

In this study five different *in-vitro* methods; rheology, pull-off, tensile test, Atomic Force Microscopy (AFM) and Quartz Crystal Microscopy with Dissipation monitoring (QCMD) were employed to evaluate the mucoadhesion property of five biopolymers namely chitosan, sodium alginate, sodium carboxymethylcellulose (CMC), high DE (degree of esterification ~60%) pectin and low DE (degree of esterification ~35%) pectin. The influence of various factors on mucoadhesion of the biopolymers on mucin was also investigated. An alternative method with the use of flow cell was employed to study mucoadhesion of sodium alginate O/W emulsion with mucin. In this chapter, each method is reviewed and the comparison of the methods discussed. Results from the different analytical methods are collectively analysed and the findings are summarised. The possibilities of future works are also recommended for further improvement on the existing experimental techniques and theoretical concepts for the correct assessment of mucoadhesive properties.

8.2 Conclusions

8.2.1 Rheological Characterisation

Rheological technique that studies the flow and deformation of materials (fluid) under applied stress is useful in determining the mucoadhesion ability of biopolymers. This is the molecular mucin-based technique that uses mucin as the adherent substrate surface onto which the biopolymer would adhere. In this study mucin films (mimic the mucous membrane) were used instead of mucin solution (imitate the saliva) as employed by others in earlier studies because the purpose of the present study is to investigate the mucoadhesion of polymers with mucin as on

the mucous membrane. This rheological technique is an indirect method, which assess the interactions between the biopolymers and mucin through the measurements of viscosity and viscoelasticity. The viscometric method introduced the parameter η_{enh} (viscosity enhancement or viscosity synergism) which characterises the strength of interaction between the biopolymers with mucin. Other parameters used to quantify mucoadhesion include the relative viscosity enhancement, η_{rel} or known as normalised parameter and the force of mucoadhesion (F) which represents the intermolecular frictional force per unit area. The theoretical aspects of rheology is further emphasised by G' (elastic modulus) and G'' (viscous modulus) profiles obtained from oscillatory rheology. These values of G' and G'' are directly related to the nature or the structural strength (viscoelasticity) of the biopolymer-mucin networks. The extent of viscoelasticity in the biopolymer-mucin structure can also be quantified using the value of $\tan \delta$ (the tangent of the phase angle) which is the ratio of G'' to G' .

The rheological properties and flow behaviour of some biopolymers studied were measured using a rheometer (TA AR1000) with 60 mm acrylic plate geometry. When the viscosity of chitosan was measured on different days after storage in the refrigerator ($T = \sim 5^{\circ}\text{C}$), the values showed a decrease with increase of storage time due to partial degradation by acetic acid. This observation was supported by findings from previous studies, which showed that chitosan stability was affected by the duration and temperature of storage. Higher temperature increased the rate of degradation of the chitosan networks forming shorter chain as reflected by lower value of the apparent viscosity. Solution of 1% (w/v) chitosan in 1% (v/v) acetic acid

exhibited two different flow behaviours at different range of shear rate. At a range of 0.2 s^{-1} to 5 s^{-1} , the viscosity was independent of the shear rate which indicates the Newtonian behaviour. But, at higher range (5 s^{-1} to 1000 s^{-1}), the viscosity decreased with increasing of shear rate indicating that chitosan solution has shear thinning behaviour, an attribute of a non-Newtonian fluid. The different behaviours resulted from the different recovery response of chitosan structure after experiencing different shear rates. Initially, chitosan was chosen as one of the polymers to be used in the study because being a cationic polymer (positively charge), chitosan would have a good mucoadhesion with mucin (anionic) through electrostatic interaction. However, chitosan did not show viscosity synergism. Instead, the strong electrostatic interaction of chitosan with mucin resulted in the formation of white precipitate with the extrusion of water into the system rendering the mixture less viscous. Because of its instability and high degree of disintegration in acidic solution, chitosan was not used for further investigation in this research.

The rheological behaviour of the polymer-mucin mixture was determined using flow curve analysis (measuring the viscosity at different shear rate). Viscosity measurement of 2% (w/v) biopolymer solutions with mucin film at shear rate of 50 s^{-1} showed sodium alginate as having the highest mucoadhesion ability with viscosity synergism of $1.705 \pm 0.057 \text{ Pa.s}$ followed by CMC ($1.544 \pm 0.053 \text{ Pa.s}$) and high DE pectin ($1.321 \pm 0.067 \text{ Pa.s}$). But, for 1% (w/v) biopolymer solution, there was no significant difference in viscosity synergism between them probably because there was insufficient biopolymer in the mixture to form maximum interaction with mucin. In contrast, higher polymer concentration provides enough binding sites for

maximum interaction with mucin thus differentiating the mucoadhesive ability of the different biopolymers. When high DE pectin-mucin mixture was sheared under different shear rates, the mixture showed shear thinning behaviour at high shear rate, suggesting that the high DE pectin-mucin networks did not have ample time to reform after disentanglement caused by shearing effect. Presumably, during disentanglement, hydrogen bonds and entangled networks of high DE pectin structure and mucin chains were broken and untangled resulting in a reduction in the dimension of the mixture's networks hence a decrease in viscosity. In addition, the rheological characterisation technique was employed to study the influence of several factors on mucoadhesion of the tested biopolymers to mucin. These factors were classified as the polymer related factors (molecular weight and concentration) and environment related factors (shear rate, initial contact time, and presence of ionic strength).

The effect of molecular weight on the mucoadhesion interaction was investigated using two different types of pectin with a different degree of esterification (60% DE and 35% DE). Low DE pectin has lower molecular weight than high DE pectin due to the breaking down of the pectin's backbone polymer chain of D-galacturonic acid by hydrolysis process. From this study, it is observed that high DE pectin shows greater interaction based on the higher viscosity synergism value. High molecular weight polymer provides more active sites or components to interact with mucin network and longer chain structures can strengthen the interfacial interaction of polymer and mucin. However previous studies showed there is an optimum molecular weight for the polymer to have a good

interaction with mucin network. Polymer with low molecular weight favours interpenetration into mucin network while polymer with a very high molecular weight has higher degree of entanglement within the structures that will hinder intermolecular diffusion and interlocking between polymer and mucin networks. The effect of holding time between the high DE pectin and mucin before shearing or mixing was also studied based on the measurement of initial viscosity. The measured initial viscosity value increased linearly with increasing holding time with a good linear regression value (R^2) of 0.964. This result showed that longer holding time allowed more interactions between the polymer and mucin.

Sodium alginate was used to study the effect of different biopolymer:mucin ratio in the mixture and the influence of ionic strength on mucoadhesion. The viscosity of the sodium alginate-mucin mixture increased significantly with increasing amount of mucin in the system. The results also showed the optimum (limiting) amount of mucin (0.5 g) was at sodium alginate:mucin weight ratio of 1:17 (0.03 g of sodium alginate and 0.5 g of mucin in 1.5 ml mixture). This suggests that there is a maximum stoichiometry of interaction between sodium alginate and mucin at 0.5 g mucin and would expect the specific viscosity to come to a plateau after this point. However, the results showed a decrease in specific viscosity beyond the limiting amount of mucin. This suggests that an excessive of mucin binding sites caused high degree of entanglement in mucin networks which inhibits the interaction (interpenetration) between sodium alginate and mucin. The effect of ionic strength (NaCl and KCl) on the mucoadhesion of sodium alginate with mucin was investigated. The result showed that increasing the concentration of both salts led to

a decrease in mucoadhesion of sodium alginate with mucin. It is due to the compression of interfacial double layer and the subsequent decrease in zeta potential. The compression of the double layer would reduce the ability sodium alginate to interact with mucin networks. This phenomenon also reduced the apparent viscosity of sodium alginate solution itself. It is in contrast to the effect of ionic strength on pectin as reported by Thirawong et al. (2008) where high DE pectin was relatively insensitive (independent) to the increasing of ionic strength (up to 0.20 M NaCl) but low DE pectin showed large increment in apparent viscosity with increasing ionic strength. The difference in structural conformation of sodium alginate with different ions is caused by the different electrochemical properties of Na^+ and K^+ . K^+ is more electropositive than Na^+ which results in less interaction with negatively charge binding sites of sodium alginate due to its tendency to be in the ionic form.

Besides the viscosity parameters, mucoadhesion characteristic was also assessed by other rheology parameter (G' , G'' and $\tan \delta$). These parameters can be interpreted to describe the strength of internal network and bonding of the mucoadhesive biopolymer-mucin mixture. This study showed that all tested biopolymers formed a weak gel (physically entangled) network with mucin as characterised by the value of $\tan \delta$ of more than 1 within range of oscillation frequency (0.1 Hz to 20 Hz). Several control experiments were conducted as a check on the reliability of the method. Replacing mucin film with starch and plain flour was a failure because these two materials did not mix with sodium alginate solution. In other control experiments, sodium alginate solution was replaced with mucin solution and sugar as a model of polymer that had no mucoadhesive ability. Mucin-

mucin mixture showed no viscosity synergism when the mucin solution was mixed with the dried mucin film. Surprisingly, 30% (w/v) sugar reduced the dissolution of dried mucin layer with water.

The results obtained from this study suggest that this slightly modified rheological method is suitable for preliminary study of mucoadhesion properties. Valuable information provided by the viscosity profiles and other rheological parameters (viscoelastic) can be used to describe the structural properties of tested mucoadhesive biopolymer, mucin and also the mixtures of biopolymers and mucin. Hydrogen bonding was the main interaction contributed by hydroxyl (-OH) and carboxyl (-COOH) group of the tested mucoadhesive biopolymer with mucin sialic acid component in mucin network. Diffusion or interpenetration and physical entanglement was also believed to be important mechanisms in mucoadhesion by strengthening the interfacial interaction between the mucoadhesive biopolymer structures with mucin network.

8.2.1.1 Recommendation for Rheological Characterisation

Despite the assumption of no loss of solvent through evaporation of the sample during the rheological analysis, the use of solvent trap might not be able to fully prevent the evaporation of water component from the sample due to long duration of analysis time at a temperature of 37°C. The loss of even a small amount of water might affect the consistency and reproducibility of the result depending on the environmental conditions. Another way to prevent evaporation is by applying silicon oil (very low viscosity) around the edge of the rheometer geometry. However

this method would increase the contact time between the samples with dried mucin layer before the shearing process. Apart from that, the amount of sample (ratio of biopolymer solutions to mucin solution) must be accurately applied in the system in order to get a consistent result as there would be a large difference in the measured rheological parameters if the ratio differs from one experiment to another.

8.2.2 Pull-off and Tensile Test Using Texture Analyser

Unlike the rheological technique, pull-off (modified Wilhelmy plate method) and tensile test are direct methods, which measure the force or time required to detach the biopolymer from mucin using a texture analyser. In pull-off experiments, effect of biopolymer concentration and holding time were studied. In addition, the effect of different speed configuration during the dipping in and pulling out of the slide was also investigated. From the pull-off experiment, it was noted that the maximum pull-off force increased with increasing concentration as demonstrated by high DE pectin where 3% (w/v) solution showed the highest maximum pull-off force followed by 2% (w/v) and 1% (w/v) solution. Mucoadhesive interactions between biopolymer and mucin could also be quantified as the percentage of pull-off force of mucin coated slide to pull-off force of clean slide or the relative increment of pull-off force to clean slide. Even though 2% (w/v) sodium alginate had lower maximum pull-off force than pectin of the same concentration, it showed higher mucoadhesion interaction of 215% (115% relative increment to clean slide) as compared to pectin which is 171% (71% relative increment to clean slide). This result showed that mucoadhesion is also dependent on polymer types.

Besides concentration and polymer types, increasing the holding time after dipping also increased the maximum pull-off force as revealed by the 2% (w/v) high DE pectin solution. This is because the interaction between biopolymer and mucin is a function of time as discussed earlier. Another interesting aspect investigated was the rate of interaction during holding time. Slow dipping would allow the attachment of polymers to mucin before the start of holding time (initial contact effect), hence a higher mass of absorbed polymer would be measured. Initial contact effect during dipping was confirmed using sodium alginate as a biopolymer model which demonstrated that initial contact during the dipping process was affecting the total mass absorbed into mucin layer. In order to eliminate the initial contact effect before mass change analysis during holding time, the fast dipping mode was employed. The result obtained from the mass changed rate analysis during holding time (with fast dipping in) showed all three tested biopolymers (sodium alginate, high DE pectin and CMC) had almost the same rate of mass change. However, sodium alginate and CMC showed better interaction with mucin layer as indicated by the higher increase in rate of interaction as compared to high DE pectin after 200 s holding time. It was also noted that the rate of interaction was increasing at a constant rate even after 420 s holding time. In practice, a limiting (maximum) holding time should be considered so as to avoid mucin layer from softening and dissolving into polymer solution. Disintegration of mucin layer could be observed through a decrease in recorded mass change value during holding time. Despite the impressive results obtained from this method, the pull-off experiment is not actually measuring the exact mucoadhesion force between polymer and mucin. The measured pull-off force acquired from this method is also contributed by the cohesiveness of the polymer solution as well as the

cohesiveness of the ‘pulled’ polymers with the total (bulk) polymer attached to mucin layer rather than the exact separation between the interfaces of polymer and mucin layer. Thus it is concluded that pull-off experiment was not really suitable to measure the separation force between these polymers and mucin but can be used to screen for potential mucoadhesives.

Another experimental method using texture analyser is the tensile test which enables the estimation of the detachment force and the adhesion work from the force displacement curve recorded. The detachment force is represented by the peak force and the adhesion work, which is the total work to separate the polymer sample from mucin solution is represented by area under curve (AUC). This experiment was performed with the same mucoadhesive biopolymers (sodium alginate, CMC and high DE pectin) of the same concentrations (1% (w/v) and 2% (w/v)). From the tensile test, sodium alginate showed the highest rank of specific mucoadhesion interaction with mucin with the value of 256.05 ± 167.90 g (1% w/v) and 491.45 ± 27.43 g (2% w/v) net peak force (detachment force) followed by CMC and high DE pectin. This result is consistent with the results obtained from rheological characterisation and pull-off experiment where sodium alginate has higher mucoadhesion ability compared to CMC and high DE pectin. The ranking order of mucoadhesion for the tested biopolymers is further supported by the total work (AUC) which shows close correlation with peak force for the tested biopolymers. However, the calculated normalised parameter values for the biopolymers did not correlate with peak force and AUC.

8.2.2.1 Recommendations for Pull-Off and Tensile Test Experiments

Equipment with higher sensitivity could be used to investigate the dynamic absorption in pull-off experiment during the holding time. TA.XT. Plus texture analyser used in this research has 0.1 g sensitivity for load cell of 5 kg (manufacturer specification) is not sensitive enough to give an accurate measurement for dynamic absorption study because the mass change during the holding time is in microgram scale. However, the technique can be considered as a reliable and efficient method to screen potential mucoadhesive biopolymers. Moreover it is simple and easy to run. The tensile test could be utilised to study the mucoadhesion properties with different forms of samples such as tablet, gel and also film. The effect of temperature on the mucoadhesion properties can be investigated if there is a jacketed vessel for temperature controlled experiment.

8.2.3 Mucoadhesion Measurement Using Atomic Force Microscopy (AFM)

A highly sensitive and powerful tool offered by AFM was utilised to study the mucoadhesion response on different tested environment for sodium alginate, CMC and high DE pectin. Mucoadhesion strength was measured based on peak force and work similar to the parameters measured in tensile test. But the micro-scale measurement by AFM is more accurate and more importantly, the cohesive factor was eliminated due to the nature of the prepared samples. The mucoadhesive biopolymers and mucin were absorbed onto Au substrates and gold tip cantilever thus the adhesion force measured between the biopolymers with mucin was solely contributed by the interfacial interaction. In air environment, sodium alginate shows the highest peak force followed by high DE pectin and CMC. In contrast, CMC has the biggest work followed by sodium alginate and high DE pectin. The high

molecular weight of CMC compared to sodium alginate could be the factor that contributed to bigger work due to the presence of more binding sites to interact with mucin. However, sodium alginate may form less but stronger bonding with mucin structure as shown by the high peak force. Sodium alginate has the highest peak force and work when measurement was done in distilled water environment followed by high DE pectin and CMC. The forces increased after 60 s of contact time but decreased after 300 s due to over wetting that caused the formation of slippery mucilage at the interfacial region.

Ionic strength of substrate showed minimal effect on the peak force of sodium alginate with mucin when measurement was done in air environment except for 0.2 M NaCl whereby there was a sharp decrease. However, measurement in distilled water environment showed a significant decrease in both peak force and work of sodium alginate when the ionic strength was increased from 0 M to 0.05 M NaCl after 300 s contact time. Generally, mucoadhesion of sodium alginate decreases when there is ionic strength in the system due to the contraction of sodium alginate double layer and the subsequent decrease in zeta potential. Ionic strength might also impose a hydrophobic effect that prevents longer contact time between the cantilever tip with sodium alginate substrate. In addition, the cantilever was experiencing higher resistance in distilled water environment resulting in less deflection. But in this study, sodium alginate with 0.10 M, 0.15 M and 0.20 M NaCl were showing higher peak force with increasing contact time from 0 s, 60 s and 300 s.

The effect of ionic strength and pH of the environment on mucoadhesion were investigated using sodium alginate, CMC and high DE pectin. The results obtained showed that different environments also influenced mucoadhesion strength of the biopolymers. Mucoadhesion strength of sodium alginate was greatly affected by ionic strength in the environment followed by CMC and high DE pectin. Peak force and work for sodium alginate measured in different ionic strength environment after 60 s contact time showed erratic change. The peak force decreased when the ionic strength was increased from 0 M NaCl to 0.05 M NaCl but increased from 0.1 M NaCl to 0.15 M NaCl and decreased again at 0.20 M NaCl. CMC showed a slight increase in peak force with increasing ionic strength. There was no correlation between peak force and work as demonstrated by high DE pectin which showed a large decrease of work with increasing ionic strength but irregular change in peak force. The same effect was observed for sodium alginate where its work decreased at ionic strength of 0 M NaCl to 0.10 M NaCl in contrast to the erratic change in peak force as discussed earlier.

The mucoadhesion measurement in different pH environment was successful, with all the tested biopolymers showing a good correlation of result with the theories. Each biopolymer demonstrated maximum mucoadhesion at pH of 4-5, close to its pK_a value: high DE pectin (pK_a 3.50-4.50), sodium alginate (pK_a 5.40) and CMC (pK_a 4.30). In principle, if pH of environment is $> pK_a$, polymers are in ionised form and if pH is $< pK_a$ the polymers are highly unionised. At pH close to pK_a of polymers, the amount of ionised and the unionised forms are at the optimum level, where the repulsion between ionised polymers (not favourable for

mucoadhesion) is minimised and at the same time there is sufficient unionised form to interact with mucin through hydrogen bonding. At pH close to pK_a , the mucin and biopolymer were partly ionised causing the polymer chains and mucin networks to expand to a certain degree. This network expansion will promote better interlocking between the polymer chains and mucin network thus increasing the mucoadhesion ability. At the same time there is an optimum amount of the unionised polymer which favours interaction with mucin through hydrogen bonding. Hence mucoadhesion is maximum at pH close to pK_a . Further increased in pH (> 5) favours the formation of loosely pack polymer network and higher degree of free entanglement chains which result in ineffective interlocking. The electrostatic repulsion between the ionised polymers would also decrease the mucoadhesion interaction. These two effects lead to lower mucoadhesion between polymer and mucin.

Different ranking order was obtained from AFM measurement under different conditions. High DE pectin showed stronger peak force than CMC in air and distilled water environment but CMC had the highest work compared to high DE pectin and sodium alginate. There was no correlation between peak force and work. This could be contributed by the factor of high molecular weight. CMC with very high molecular weight would prevent the effectiveness of interpenetration due to high degree of network entanglement but offers more binding sites for the interaction with mucin to occur. However, lower work of CMC was recorded when the measurement was done in distilled water. Different peak force and work ranking were also observed when the measurements were done at different ionic strength and

pH. For example, CMC showed higher peak force than sodium alginate when the measurements were done in environment of pH 2 and pH 3. However, the opposite results were obtained when the measurement was done in other pH environments (pH 4, 5, 6, 7 and 8). Based on the AFM measurement, sodium alginate is ranked as the most mucoadhesive biopolymer among the three tested biopolymers because it demonstrates as having the highest peak force in most tested conditions.

8.2.3.1 Recommendations for Mucoadhesion Measurement using AFM

The surface morphology and structure of biopolymer substrates in different environment after different duration of immersion provide valuable information on the effect of the environment conditions on biopolymer structure. This can be used to explain and validate the force measurement obtained after certain duration of immersion. The images obtained from imaging technique after certain time of immersion in different liquid could be used to provide more information on the unstable trend or result obtained from this experiment. As the measurement was done at 15 different points with certain holding time, structure of the polymer substrate might have changed during the measurement process. This assumption was supported by the fact that biopolymer substrates were affected by the liquid environment and the force measurement was influenced by the holding time. The effect of temperature on the mucoadhesion could also be investigated by incorporating a temperature controlled system with AFM instrument in order to study mucoadhesion at human physiological temperature.

8.2.4 Mucoadhesion Kinetic Studies

A QCMD was used to study the absorption kinetic of three biopolymers namely sodium alginate, CMC and high DE pectin into mucin layer. The absorption process of biopolymer onto mucin layer was monitored through the changes of frequency and dissipation value. The advantage of QCMD over the old QCM is its ability to identify the properties of the absorbed layer, whether the layer is elastic and rigid or viscoelastic, through monitoring the dissipation value. Higher dissipation value indicates the absorbed layer is viscoelastic and vice versa.

There were unexpected results obtained from the mucoadhesion kinetic investigation using QCMD in this research. Theoretically, when there is an additional mass on the mucin layer, the frequency ($-\Delta f/n$) value will increase. However, the values of frequency ($-\Delta f/n$) for all tested biopolymers decreased after injecting sample into the controlled loop. This occurred because the absorbed mucin mass was removed from the QCMD gold chip upon introduction of biopolymer solution. Thus the analysis of interaction kinetic between biopolymers with mucin was done based on the removal rate of mucin instead of absorption of biopolymers into mucin layer. Higher rate of mucin removal and total mass of mucin layer removed indicates higher interaction of biopolymer with mucin. The Sauerbrey model was used instead of Voigt model to interpret this data because the nature of mucin layer was elastic and rigid as shown by the low dissipation value.

The percentage of mucin mass removed from the gold chip was 82.92% for CMC, 76.43% by sodium alginate and 51.08% by high DE pectin respectively.

Based on the results, the ranking order of mucoadhesion ability is CMC > sodium alginate > high DE pectin. This ranking of mucoadhesion strength does not correlate with the results obtained from the rheological characterisation, pull-off and tensile test experiments which indicate sodium alginate as having the highest mucoadhesion ability. However, this finding is supported by the ranking order proposed by Smart et al. (1984) which listed CMC as having higher mucoadhesion properties than sodium alginate and also complied with the finding by Chen and Cyr (1970). Nonetheless, the percentage removal of absorbed mucin mass by CMC and sodium alginate from this experiment varies very slightly, with a difference of only 6.49% thus the result obtained from this research could be concluded as comparable with the previous research done by others.

The data obtained from the rheological characterisation can be used to investigate the mucoadhesion kinetic between tested biopolymer with mucin besides the total intermolecular friction force or viscosity. The mucoadhesion kinetic is shown by the viscosity profile during the shearing process before the mixture becomes homogeneous (plateau line). There are two components of interaction during the shearing process which are dissolution of mucin layer into biopolymer solutions and mucoadhesion interaction between mucin with biopolymer. The following examples elucidate the mucoadhesion kinetic from the rheological characterisation experiment. The first example is the comparison of mucoadhesion kinetic between high DE pectin with low DE pectin. High DE pectin shows higher mucoadhesion. The second example is the control experiments by using sugar solution. The presence of sugar in water was slowing the dissolution rate of mucin

layer into the bulk solution as shown by increasing the sugar content in the water from 10% (w/v) to 30% (w/v) concentration.

8.2.4.1 Recommendations for Mucoadhesion Kinetic Study

There are a few recommendations in the methodology for better results from QCMD experiment. The size of particles in the sample solution is an important factor that contributes to the effectiveness of absorption process into QCMD gold chip. All the solutions (biopolymer and mucin) can be filtered with a suitable filter to remove large aggregates of mucin in the solution because mucin is not fully dissolved in distilled water and forms a heterogeneous suspension. This could explain why mucin was not absorbed into gold chip strongly resulting in the loosening of the mucin layer from the chip as mentioned earlier. It has been reported that mucin would not be absorbed effectively onto the QCMD gold chips when there were big aggregate particles present in the solution (Feldötö et al., 2008). The absorption kinetic study could also be done by injecting the biopolymer solution first followed by mucin solution. The biopolymer solutions might be better absorbed on the gold chip to provide a stable base layer. Apart from that, a range of different chip materials could be used in order to identify which material provides a better absorption of mucin before introducing the biopolymer solution. An example of this is the precoated gold chip with polystyrene surface used by Feiler et al. (2007) to study the absorption behaviour of protein into fractionated mucin from bovine submaxillary gland (BSM).

8.2.5 Mucoadhesion Testing on Mucoadhesive Biopolymer Formulation

Sodium alginate was used for the formulation of a type of delivery system, the O/W emulsion. The mucoadhesion of the sodium alginate emulsion was investigated using two methods, the rheological characterisation (viscosity measurement) and flow cell. Sodium alginate was chosen because it is a well known emulsifier and stabiliser in food and pharmaceutical formulation. The addition of biopolymer in emulsion system can increase emulsion droplets stability. Besides enhancing the stability of emulsion droplets, biopolymer also affects the size of emulsion droplets. Presence of 2% (w/v) biopolymer produced smaller emulsion droplets compared to the emulsion droplets in 1% (w/v) and without biopolymer in the system. Biopolymer helps to reduce the interfacial tension contributed by oil component hence reducing the droplet size.

Mucoadhesion study on sodium alginate emulsion by viscosity measurement during the mixing with mucin layer revealed a low viscosity synergism and small normalised parameter with the value of 1.46 for 1% (w/v) sodium alginate emulsion and 1.85 for 2% (w/v) sodium alginate emulsion. The low viscosity synergism and normalised parameter were due to hydrophobic effect of oil component in the system which reduced the interfacial mucoadhesion interaction. Moreover, the oil component in the emulsion separated out of the emulsion through the breakage of the emulsion droplets caused by shearing during the viscosity measurement. The presence of two different phases in the rheometer geometry would give erroneous viscosity measurements. This means that rheological characterisation

is not suitable to study mucoadhesion properties of mucoadhesive biopolymer emulsion due to the unstable nature of emulsion to shearing.

An alternative method using a specially designed flow cell was used to study mucoadhesion properties (mucoadhesiveness) of emulsion with different concentration of sodium alginate. The mucoadhesiveness was assessed by observing the ability of sodium alginate emulsion droplet to adhere onto the mucin layer based on the microscopic images recorded after certain time of flushing with distilled water. Some of the emulsion droplets without sodium alginate were removed as early as 70 s of flushing while emulsion with 1% (w/v) sodium alginate took almost 200 s before being removed. This observation proved that the presence of sodium alginate in emulsion formulation enhanced the ability of the droplet to remain attached to the mucin layer. The results obtained from this experiment suggest that this flow cell can be used to evaluate mucoadhesion of mucoadhesive micro formulation such as microspheres, gel particles and other kind of delivery system by monitoring the movement of microparticles in the flow cell after experiencing certain flow force. The flow cell with a simulated physiologic flow of fluid in the chamber can be used as a model representing *in vivo* condition of the buccal cavity and gastrointestinal (GI) tract where the carrier systems are experiencing various forces including those contributed by fluid movement.

The production of agar gel particles using shearing effect was studied by applying different shear rates during the cooling process of hot agar. The properties of agar gel particles were characterised by the viscosity profile and rheological

parameters. The size of agar gel particles decreased with the increasing of shear rate during the cooling process. Shear rates also influenced the viscoelastic properties of gel particles. Particles produced at higher shear rate (100 s^{-1}) were less viscoelastic than particles produced at lower shear rate (40 s^{-1}). The value of G' and G'' for gel particles at shear rate 40 s^{-1} were higher than the gel particles at shear rate 100 s^{-1} .

8.2.5.1 Recommendations for Mucoadhesion Testing on Mucoadhesive Polymer Formulation

Assessing mucoadhesion based on loss of droplets is not reliable since the loss of droplets after flushing could also be caused by the breakage of the droplet itself due to the unstable nature of emulsions used in this experiment. A more stable carrier such as gel particles could be used for this flow cell experiment. Besides determining the removal of droplets or particles, the evaluation could also be done by calculating the difference in the amount of particles before and after flushing. The use of advanced observing tool such as confocal light scanning microscope could give a clearer observation of the movement or the removal process of droplets in the flow cell.

8.3 Correlation of Mucoadhesion from Different Analytical Methods

The evaluation of mucoadhesion on three tested mucoadhesive biopolymers namely, sodium alginate, CMC and high DE pectin was performed using five analytical methods. The result in table 8.1 shows consistency in ranking order of the biopolymers for four analytical methods which is based on the specific assessment parameter for each method. The consistency indicates the reliability of this research and confirms the ranking order of the biopolymers based on mucoadhesive

properties. The evaluation of mucoadhesion from four analytical methods shows sodium alginate as the most mucoadhesive followed by CMC and high DE pectin. However, there was a conflicting result between CMC and high DE pectin from peak force measurement using AFM. High DE pectin has higher peak force than CMC when the measurement was done in air and distilled water but the opposite result was obtained when measurement was done in different ionic strength and pH environment. This result could be contributed by experimental error during the sample preparation. Due to high sensitiveness of AFM, small error in sample preparation could result in difference of measurements. The result from QCMD showed CMC as a stronger mucoadhesive polymer than sodium alginate. As for high DE pectin, it remains as the least mucoadhesive polymer based on four measurement techniques.

The factors such as environmental conditions (ionic strength and pH), temperature and the nature of the sample for specific analytical method could contribute to the different results obtained in the mucoadhesion investigation. The same conflicting result was reported by previous researchers. For example, Hagesaether and Sande (2007) reported low methoxy pectin has stronger mucoadhesive effect compared to high methoxy pectin from tensile test experiment whilst the opposite result was obtained by Sriamornsak and Wattanakorn (2008) from the rheological characterisation. Roy and Prabhakar (2010) reported a close value of mean adhesive force between sodium alginate (126.2 ± 12.0 %) and CMC (128.0 ± 2.4 %) which indicates sodium alginate and CMC have almost the same mucoadhesion ability. The result obtained from this research is more consistent, thus

confirming sodium alginate as having the highest mucoadhesive ability followed by CMC and high DE pectin.

Table 8.1: Ranking order of mucoadhesion for the tested mucoadhesive biopolymers by different analytical methods.

Mucoadhesion Ranking	Rheological Characterisation	Pull-Off	Tensile Test	AFM	QCMD
Assessment Parameter	Viscosity Synergism	Absorption rate	Peak force	Peak force	Total removal of mass of mucin
1	Sodium alginate	Sodium Alginate	Sodium Alginate	Sodium Alginate	CMC
2	CMC	CMC	CMC	CMC/High DE pectin	Sodium Alginate
3	High DE pectin	High DE pectin	High DE pectin	CMC/High DE pectin	High DE pectin

8.4 Review of the Analytical Methods used in This Study

The study of mucoadhesion by evaluating relevant characteristics could enhance the understanding on the mechanisms and the influence of factors on the biopolymer-mucin interaction. Each analytical method offers the advantage to be used effectively for a specific characterisation purpose. In general, the different analytical methods for evaluating mucoadhesion can be classified as direct and

indirect methods. Examples of the direct methods are pull-off experiment, tensile test and AFM which give direct measurement of strength of mucoadhesion of polymer on mucin. The strength is characterised by two parameters namely, the detachment force and the work. Detachment force is the force required to start separating the mucoadhesive polymer from mucin and the work is the total work or energy required to fully separate the polymer from mucin. In this study, detachment force analysis was done by pull-off and tensile test using texture analyser and AFM. The question that arises is whether the force measured in pull-off and tensile test is the exact measure of detachment force since the measurement was done at macroscopic level while the interaction in mucoadhesion occurred at microscopic level, and the interface was artificially created. Moreover, it was found that the detachment force obtained from the pull-off experiment was representing more of the cohesiveness of the polymer solution instead of the adhesiveness between the polymer and mucin. Besides, the recorded forces which were expressed as the percentage of mucin coated slide over the clean slide were not exactly representing mucoadhesion of polymer to mucin as the polymer mass attached to the mucin coated slide was more than it should be. The cohesiveness effect caused more biopolymer to be attached to the slide than it should be based on mucoadhesion alone. The proposed analytical method using pull-off experiment in this study which is analysing the mass changes during the holding time in the polymer solution can provide some insights on the mucoadhesion properties of mucoadhesive biopolymer. Different mucoadhesive biopolymer would have different interaction rate that can be analysed through the mass changes over the holding time. However, the use of texture analyser for this analysis was not suitable due to low sensitivity (0.1 g) and high noise production that

affect the data accuracy. The use of more sensitive microbalance equipment such as microbalance tensiometer (0.01 mg) is recommended for this analysis.

Tensile test is another direct method that characterises the mucoadhesion through the detachment force between biopolymer and mucin. The calculated specific force (interaction) which eliminates the unspecific interactions is representing the mucoadhesion. However, the detachment force measured using solution form as the sample (spread on the Benchkote paper) could also be contributed by the cohesive effect of solution due to formation of string. Thus this method is recommended to be used for evaluation of a more rigid form of mucoadhesive formulation such as film and tablet. The sensitivity of texture analyser for tensile test is suitable due to high force value recorded in the test compared to mass change analysis in pull-off experiment which is at microgram scale. Basically, both pull-off and tensile test can be used to screen potential mucoadhesive biopolymers since the reliability of the method is confirmed by the close correlation of results from these two methods with those obtained from rheology. Furthermore, tensile test has the advantage to be used as an *ex-vivo* method by replacing the mucin coated slide with specimen of mucous membrane taken from GI tract or buccal cavity of animals or human. The experiment can then be conducted in conditions very similar to the physiological conditions and the results obtained would be more reliable in interpreting the *in-vivo* mechanism of mucoadhesion.

In contrast to pull-off and tensile test, AFM can measure force at nano scale. The exact measure of detachment force can be acquired since the microscopic

measurement is done at the molecular interface of polymer and mucin where the interaction actually occurs. The cohesive effect of polymer solution is eliminated since both mucin and polymer are absorbed onto the Au substrate surface and the tip of the cantilever. Thus the recorded detachment force when cantilever separates from the substrate surface is the exact measure of the force to separate polymer substrates from mucin at the interface. Besides the force measurement, the ability of AFM to analyse the nature of mucin, polymer and polymer-mucin structures by producing the morphology images could provide additional information in studying mucoadhesion properties and mechanism. The correlation between the force measurements and morphology images can be used to explain the actual process that occurs when polymer is detached from mucin. AFM can also generate surface topography which can be analysed to give the details of the surface molecular alteration when tested polymer interacts with mucin. AFM can be used to study the mucoadhesion properties of formulated sample such as microspheres by attaching the particle to the cantilever tip. However, AFM needs to be handled by specially trained personnel due to the fragility of the sophisticated instrument. The preparation of samples is more complicated and difficult compared to other analytical methods in this research.

Besides the detachment force, mucoadhesion properties can be characterised by assessing the interaction between polymer and mucin without separating the two materials. This can be done using QCMD. This technique characterises the interaction of polymer with mucin based on the measurement of polymer absorption. QCMD can capture the kinetics of structural changes and mass changes

simultaneously providing a new understanding of the nature of polymer:mucin interface. Absorption kinetics data could be used to analyse on how favourable a mucoadhesive polymer is to interact with mucin layer under the influence of certain factors (pH, ionic strength, different molecular weight and others). Besides the mass changes, the properties of the absorbed layer could also be evaluated through the dissipation monitoring. Low dissipation value would mean the contraction or structural collapsing due to certain mechanism of interaction. The information on the nature of the polymer and mucin structure after interaction can provide further explanation on the mechanism of interaction. However, the information obtained from QCMD (absorption kinetics and the total mass absorbed) cannot represent the strength of mucoadhesive polymers adhered onto the mucin layer. This is because QCMD is not giving a force based measurement like the texture analyser and AFM. QCMD is also a direct method since it measures the actual kinetics of mucoadhesion.

Unlike the methods already discussed, rheology is an indirect method that measures viscosity and viscoelasticity of materials. Rheological characterisation using rheometer has the working principle based on the structural changes when a polymer has an interaction with mucin and this is reflected as the viscosity changes. A polymer is interpreted as being mucoadhesive if the viscosity of the system is more than the algebraic sum of polymer and mucin constituting the system. The enhancement is termed viscosity synergism and is the result of the interaction between polymer and mucin. It reflects the overall magnitude of interaction. The measurements of two dynamic moduli, G' and G'' obtained from oscillatory rheology reveals the strength and stability of the polymer-mucin internal network. The method

is simple to perform and if the right fixtures are used, the results obtained are reproducible. Rheological method is recommended for preliminary study in confirming mucoadhesion properties of materials. The result obtained from the modified method used in this study (mucin film) enable the analysis of interaction kinetics which cannot be done with the method (mucin solution) used in previous studies. However, rheological characterisation is not suitable to evaluate the mucoadhesion of mucoadhesive formulation (emulsion) because shearing can cause the formation of two phases in the rheometer geometry and results in erroneous viscosity measurements. There are other issues associated with rheological method that raise some questions on its validity in evaluating mucoadhesion. In this study for example, chitosan which is known to be highly mucoadhesive did not show viscosity synergism and can be interpreted as non mucoadhesive. There is a possibility for other cationic polymers to show the same rheological response and being misinterpreted as non mucoadhesive. Shearing can cause the disruption of the polymer-mucin network and would not show synergism as demonstrated by chitosan which has weak structure that is easily disrupted or disturbed when sheared. Again a wrong interpretation would lead to a wrong conclusion if the potential mucoadhesive has weak structure as chitosan. Hence rheological method is not suitable for screening potential mucoadhesives but can be used to reaffirm the mucoadhesion property of a polymer already evaluated by other methods.

Flow cell is a simple device for evaluating mucoadhesion processes using microscopy and image analysis. It can be used to analyse mucoadhesion of mucoadhesive formulation (at micro or nano size) onto mucin. The retention of the

formulated carrier system on the mucin layer under different flow forces is observed through a microscope. Flow cell offers an alternative to animal model testing and allows for more rapid evaluation under well-controlled experimental conditions. Thus the influence of various factors such as different pH, ionic strength and amount of mucin on the interaction of carrier system with mucin layer can be studied. However, flow cell cannot imitate the exact properties of physiological conditions. A similar flow through technique can be employed using biological samples of animal anatomy such as the GI tract to replace the flow cell in order to study the mucoadhesion of formulation under physiological conditions. But the results are not repeatable when using different samples of the same anatomy because the properties of the biological sample (GI tract) differ from one animal to another. Moreover, direct observation of the microparticles attachment to the mucous layer of the GI tract cannot be done as the system is not integrated with a microscope.

8.4.1 Conclusion of Review

There are many aspects of mucoadhesion that need to be evaluated before confirming a given polymer as being mucoadhesive. Hence, various methods of evaluation need to be employed and the finding is only conclusive if the results from the various methods correlate with each other. Correlation of results from various methods is not just for the purpose of ranking the polymers according to their mucoadhesive properties. More importantly, the results can give theoretical insights into the mucoadhesion phenomenon. The results obtained from rheology and tensile test in this study show a good correlation between the detachment force and viscosity in describing mucoadhesion. Thus, rheology corroborates the observation in force

measurement from tensile test that there is some interaction between mucin and the assayed biopolymers that results in mucoadhesion. Consequently, the degree of interaction is measured as viscosity synergism.

A comparison of mucoadhesiveness is definite if it is based on comparable measurements, for example comparing the strength of interaction using tensile test and AFM. Otherwise there will be conflicting mucoadhesion ranking orders for the polymers being evaluated. In this research for example, QCMD showed that CMC has the highest mucoadhesion ability but other analytical methods showed sodium alginate as having the highest mucoadhesion property. This conflicting result was caused by the different principle in measuring the mucoadhesion. Force measurement as in tensile test or AFM, is measuring how strong the mucoadhesive polymer adheres or interacts with mucin layer. This depends on the quality of interaction through physical entanglement and interlocking as well as through chemical bonding (electrostatic, van der Waals and hydrogen bonding). Whereas, absorption kinetics study by QCMD is based on the rate of interaction and quantity of the mucoadhesive molecules that interact with mucin layer. This measurement is dependent on the availability of binding sites for the interaction to occur. In this case, CMC with higher molecular weight (250000 Da) contains more binding sites as compared to sodium alginate (12000-180000 Da) and high DE pectin (25000-72000 Da) thus demonstrating a higher absorption kinetics and total mass interacting with mucin. However, the quality of the CMC-mucin interaction might be less than sodium alginate-mucin. Therefore, it is more meaningful if the QCMD results are compared

with Surface Plasmon Resonance (SPR), FTIR-ATR and turbidity analysis which have the same basis of measurement.

In conclusion, all the methods employed in this research are suitable for evaluating mucoadhesion. It is important that no one method should be used as a stand-alone method as the results may not be conclusive. Double checking with another method can reaffirm the finding. The choice of methods depends on the aspect to be evaluated. If it is for structural mechanical features, strength and stability of the internal network, rheology is a suitable method. It is simple and easy to conduct and highly recommended for preliminary study of mucoadhesion. For the measurement of force at macroscopic level, pull-off and tensile test would be a good choice. These two methods are suitable for comparing mucoadhesion properties of polymers but not for measuring the numerical values of the detachment force as the measurements are over-emphasized by the cohesive effect of the polymer solution itself. Pull-off and tensile test are easy to perform and can be conducted as an *ex-vivo* method. As for a more accurate detachment force measurement and a good understanding of the molecular interaction at the polymer-mucin interface in mucoadhesion, AFM is the ultimate choice. The study of absorption kinetics which gives valuable information on the affinity of polymer to mucin is possible by employing QCMD. Flow cell is an alternative method to study mucoadhesion of mucoadhesive polymers formulation which cannot be evaluated by other methods.

8.5 Future Work

The high consistency of the results obtained from the analytical methods used in this research indicates the reliability of the methods to evaluate mucoadhesion properties of materials. The conflicting result for CMC with different methods emphasizes the need for further improvement in the existing experimental techniques for the correct evaluation of mucoadhesive properties. There is a need to adopt a standard universal test method to facilitate sharing of valuable information on mucoadhesion among researches. It is also imperative to establish a standard parameter for mucoadhesion of materials so that these materials can be ranked accordingly for easy references.

Previously, most of the works in mucoadhesion investigation were focused on the detachment force between the mucoadhesive materials and mucin (mucous) to be used as the main assessment parameter. The scope of study should be expanded to include mucoadhesion kinetics, one aspect of mucoadhesion that has not been extensively studied. Mucoadhesion kinetics offers valuable information for the designing of new mucoadhesive formulations. More studies on mucoadhesion kinetics in relation to different factors could be done using other methods such as dynamic contact angle using goniometer, absorption kinetic using FTIR-ATR spectroscopy and turbidimetry. One of the factors that have been ignored is temperature. Chemical interaction is known to be temperature dependent and even a small difference in temperature would alter the rate of reaction. Thus the effect of temperature on mucoadhesion kinetics should be explored since it has some

significance to the physiological temperature of human and animals which changes with their health state.

There is a recent interest of using mucilage, gum and resin from plants such as okra, tamarind seed and aloe vera in formulation of controlled delivery system (Amelia et al., 2010). This natural source could also be used in food formulation. A comprehensive study on the mucoadhesion properties of these naturally occurring substances could be done via the same analytical methods or other methods. The study should include the factors that affect mucoadhesion and the mechanisms involved in the interaction. Evaluation of mucoadhesive performance could also be done for different formulations such as combination of these natural substances with well known mucoadhesive biopolymers (same charge) and also by formation of polyelectrolyte with other mucoadhesive polymers that contain different charges. The potential uses of these bioadhesive materials and others in drug delivery systems should be exploited not just for the formulation of GI tract and buccal cavity as the primary focus but should also explore the possibilities of drug targeting and site specific drug delivery system. The advancement in nanoscience should also be taken advantage of as this offers another alternative to the designing of formulations in the form of nanoparticles that suit the need of the latter delivery systems. Another possibility being explored recently is the use of mucoadhesion as anchoring mechanism for surgical application in order to minimise the invasiveness of surgery. In conclusion, more research is encouraged to utilise the tremendous qualities possessed by bioadhesives for pharmaceutical and food application.

References

- Ahuja, R.P. and Khar, J. A. (1997). Mucoadhesive Drug Delivery Systems. *Drug Development and Industrial Pharmacy*. Vol 23: 489– 515.
- Akhtar,M., Murray, R. and Dickinson, E. (2006). Perception of Creaminess of Modal Oil-Inwater Dairy Emulsions:Influence of the Shear-Thinning Nature of A Viscosity-Controlling Hydrocolloid. *Food hydrocolloids*. Vol 20: 839-847.
- Albrecht, K., Greindl, M., Kremser, C., Wolf, C., Debbage, P., Bernkop-Schnürch, A. (2006). Comparative *In Vivo* Mucoadhesion Studies of Thiomers Formulations Using Magnetic Resonance Imaging and Fluorescence Detection. *Journal of Controlled Release*. Vol 115: 78 - 84.
- Al-Homadh, E. S. (2000). The Effect of Shear Force on the Stability of A Solid Free Emulsion Mud. *Journal of Engineering and Applied Science*. Vol 47: 965-979.
- Allamneni, Y., Reddy, B. V. V. K., Chary, P. D., Rao, V. B. N., Kumar, S. C and Kalekar, A. K. (2012). Performance Evaluation of Mucoadhesive Potential of Sodium Alginate on Microspheres Containing an Anti-Diabetic Drug: Glipizide. *International Journal of Pharmaceutical Sciences and Drug Research*. Vol 4(2): 115-122
- Allen, A., Pain, R. H. and Robson, T. R. (1976). Model for the Structure of the Gastric Mucous Gel. *Nature*. Vol 264: 88-89.
- Amelia, M. A., Rakesh, R. D. and Shilpa, N. S. (2010) Recent Investigations of Plant Based Natural Gums, Mucilages and Resins in Novel Drug Delivery Systems. *Indian Journal of Pharmaceutical Education and Research*. Vol 45(1): 86-99.
- Andreas, B. S. (2005). Mucoadhesive Systems in Oral Drug Delivery. *Drug Discovery Today: Technologies*. Vol 2(1): 85 - 87.

- Andrews, G. P., Lavery, T. P. and Jones, D. S. (2009). Mucoadhesive Polymeric Platforms for Controlled Drug Delivery. *European Journal of Pharmaceutics and Biopharmaceutics*. Vol 71: 505-518.
- Angewandte Physik website (accessed on 26th November 2014).
<http://www3.physik.uni-greifswald.de/method/afm/eafm.htm>
- AR 500/1000 Rheometers Hardware Manual (2000). TA Instruments: Thermal Analysis and Rheology.
- Aspinall, G. O. (1980). Chemistry of Cell Wall Polysaccharides. The Biochemistry of Plants, New York: Academic Press.
- Asteriadou, K., Othman, A.M., Goode, K. and Fryer, P.J. (2009). Improving Cleaning of Industrial Heat Induced Food and Beverages Deposits: A Scientific Approach to Practice. IN International Conference on Heat Exchanger Fouling and Cleaning VIII. Edited by H. Muller-Steinhagen, M.R. Malayeri and A.P. Watkinson. Schladming, Austria. 159-164.
- Aulton, M. E., Twitchell, A. M. and Hogan, J. E. (1997) Physical Properties of HPMC Solutions and Their Role in the Film Coating Process and the Quality of the Coated Product. In J. W. McGinity (Ed.), Aqueous Polymeric Coatings for Pharmaceutical Dosage Forms. New York: Marcel Dekker.
- Benitez, E. I. and Lozano, J. E. (2006). Influence of Soluble Solids on the Zeta Potential of a Cloudy Apple Juice. *Latin American Applied Research*. Vol 36: 163-168.
- Bera, K., Sarwa, K. K. and Mazumder, B. (2013). Metformin HCl Loaded Mucoadhesive Agar Microspheres for Sustained Release. *Asia Journal of Pharmaceutics*. Vol 7: 75-82.

- Bhimavarapu, R., Nissankararao, S., Rani, M. S., Eswar, K. S. and Ahalya, G. (2014). Formulation and In-Vitro Evaluation of Mosapride Citrate Mucoadhesive Beads. *An International Journal of Advanced in Pharmaceutical Sciences*. Vol 5: 2081-2090.
- Blandino, A., Machias, M. and Cantero, D. (1999). Formation of Calcium Alginate Gel Capsules: Influence of Sodium Alginate and CaCl_2 Concentration on Gelation Kinetics. *Journal of Bioscience and Bioengineering*. Vol 88(6): 686-689.
- Bowen, J., Cheneler, D., Walliman, D., Arkless, S. G., Zhang, Z., Ward, M. C. L. and Adams, M. J. (2010). On the Calibration of Rectangular Atomic Force Microscope Cantilevers Modified by Particle Attachment and Lamination. *Measurement Science and Technology*. Vol 21 (11): 106-115
- Burey, P., Bhandari, B. R., Howes, T. and Gidley, M. J. (2008). Hydrocolloid Gel Particles: Formation, Characterisation and Application. *Critical Reviews in Food Science and Nutrition*. Vol 48(5): 361-377.
- Catron, N.D., Lee, H. and Messersmith, P.B. (2006). Enhancement of Poly(ethylene glycol) Mucoadsorption by Biomimetic End Group Functionalization. *Biointerphases*. Vol 1: 134–141.
- Cerquiera, M. A., Bournon, A. I., Pinheir, A. C., Silva, H. D., Quintas, M. A. C. and Vicente, A. A. (2013). Edible Nano Laminate Coatings for Food Applications. IN Silvestre, C. and Cimmino, S. (2013). Ecosustainable Polymer Nanomaterials for Food Packaging: Innovative Solutions, Characterization Needs, Safety and Environmental Issues. CRC press

- Chang, K. L. B. and Lin, J. (2000). Swelling Behaviour and the Release of Protein from Chitosan-Pectin Composite Particles. *Carbohydrate Polymers*. Vol 43: 163-169.
- Chayed, S. and Winnik, F. M. (2007). In Vitro Evaluation of the Mucoadhesive Properties of Polysaccharide-Based Nanoparticulate Oral Drug Delivery Systems. *European Journal of Pharmaceutics and Biopharmaceutics*. Vol 65: 363–370.
- Chen, J. L. and Cyr, G. N. (1970). Compositions Producing Adhesion through Hydration, IN Manly, R. S. (Ed), Adhesion in Biological Systems, Academix Press, New York, page 163-181.
- Christensen, P. E. (1954). Methods of Grading Pectin in Relation to the Molecular Weight (Intrinsic Viscosity) of Pectin. *Food Research*. Vol 19: 163-171.
- Cleary, J. Bromberg, L. and Magner, E. (2004). Adhesion of Polyether-Modified Poly(acrylic acid) to Mucin. *Langmuir*. Vol 20: 9755-9762.
- College of Engineering, University of Utah. Lecture 10: Basics of Atomic Force Microscopy.
- Collins-Gold, L. C., Lyons, R. T. and Bartholow, L. C. (1990). Parenteral Emulsions for Drug Delivery. *Advanced Drug Delivery Reviews*. Vol 5(3): 189-208.
- Cui, F., Qian, F. and Yin, C. (2006). Preparation and Characterisation of Mucoadhesive Polymer-coated Nanoparticles. *International Journal of Pharmaceutics*. Vol 316: 154-161.
- Curie, P. and Curie, J. (1880). Piezoelectric and Allied Phenomena in Rochelle Salt. *Comput Rend Acad Sci Paris*. Vol 91: 294-297.

- Deacon, M. P., McGurk, S., Roberts, C. J., Williams, P. M., Tendler, S. J. B., Davies, M. C., Davis, S. S. and Harding, S. E. (2000). Atomic Force Microscopy of Gastric Mucin and Chitosan Mucoadhesive Systems. *Biochemical Journal*. Vol 348: 557-563.
- Derjaguin, B. V., Toporov, Y. P., Muller, V. M. and Aleinikova, I. N. (1977). On The Relationship Between The Electrostatic and Molecular Component of The Adhesion of Elastic Particles to a Solid Surface. *Journal of Colloid and Interface Science*. Vol 58: 528-533.
- Deshmane, S. V., Channawar, M. A., Chandewar, A. V., Joshi, U. M. and Biyani, K. R. (2009). Chitosan Based Sustained Release Mucoadhesive Buccal Patches Containing Verapamil HCl. *International of Pharmacy and Pharmaceutical Sciences*. Vol 1: 216-229.
- Dhawan, S., Singla, A. K. and Sinha, V. R. (2004). Evaluation of Mucoadhesive Properties of Chitosan Microspheres Prepared by Different Methods. *AAPS Pharmaceutical Science Technology*. Article 67: 5 (4)
- Diftis, N. and Kiosseoglou, V. (2003). Improvement of Emulsifying Properties of Soybean Protein Isolate by Conjugation with Carboxymethyl Cellulose. *Food Chemistry*. Vol 81(1): 1-6.
- Dodou, D., Breedveld, P. and Wieringa, P. A. (2005). Mucoadhesives in the Gastrointestinal Tract: Revisiting the Literature for Novel Applications. *European Journal of Pharmaceutics and Biopharmaceutics*. Vol 60: 1-16.
- Drelich, J. and Mittal, K. L. (2005). Atomic Force Microscopy in Adhesion Studies .(Eds). VSP/Brill, Leiden.

Drugfuture website (accessed on 29th October 2014).

<http://www.drugfuture.com/chemdata/carboxymethylcellulose-sodium.html>

Ducker, W. A., Senden, T. J and Pashley, R. M. (1991). Direct Measurement of Colloidal Forces Using An Atomic Force Microscope. *Nature*. Vol 353: 239 – 241.

Durrer, C., Irache, J. M., Puisieux, F., Duchene, D. and Ponchel, G. (1994). Mucoadhesion of Latexes. I. Analytical Methods and Kinetic Studies. *Pharmaceutical Research*. Vol 11: 674-679.

Dutta, P. K., Dutta, J. and Tripathi, V. S. (2004). Chitin and Chitosan: Chemistry, Properties and Applications. *Journal of Scientific and Industrial Research*. Vol 63: 20-31.

Fefelova, N. A., Nurkeeva, Z. S., Mun, G. A. and Khutoryanskiy, V. V. (2007). Mucoadhesive Interactions of Amphiphilic Cationic Copolymers Based On [2-(Methacryloyloxy)Ethyl]Trimethylammonium Chloride. *International Journal of Pharmaceutics*. Vol 339: 25–32.

Feiler, A. A., Sahlholm, A., Sandberg, T. and Cladwell, K. D. (2007). Adsorption and Viscoelastic Properties of Fractionated Mucin (BSM) and Bovine Serum Albumin (BSA) Studied with Quartz Crystal Microbalance (QCM-D). *Journal of Colloid and Interface Science*. Vol 315: 475–481.

Feldötö Z., Pettersson, T. and Dédinaïté, A. (2008). Mucin-Electrolyte Interactions at the Solid-Liquid Interface Probed by QCM-D. *Langmuir*. Vol 24: 3348-3357.

Ferrari, F., Rossi, S., Martini, A., Muggetti, L., De Ponti, R. and Caramella, C. (1997). Technological Induction of Mucoadhesive Properties on Waxy Starches by Grinding. *European Journal of Pharmaceutical Sciences*.

- Ferry, J. D. (1980). *Viscoelastic Properties of Polymers*. New York: Wiley.
- Finch, C. A. and Bodmeier, R. (2005). *Microencapsulation*. Wiley-VCH Verlag GmbH & Co. KGaA, Weinheim. Page 1-16.
- Firstenberg Machinery website (accessed on 10th November 2014).
http://www.firstenbergequip.com/general/inventory/search_detail.lasso?id=16
- Fraeye, I., Colle, I., Vandevenne, E., Duvetter, T., van Buggenhout, S., Moldenaers, P., van Loey, A. and Hendrickx, M. (2010). Influence of Pectin Structure on Texture of Pectin-Calcium Gels. *Innovative Food Science and Emerging Technologies*. Vol 11: 401-409.
- Fröhlich, E. and Roblegg, E. (2014). Mucous as Physiological Barrier to Intracellular Delivery. IN Prokop, A., Iwasaki, Y. and Harada, A. (2014). Intracellular Delivery II: Fundamentals and Applications. *Fundamental Biomedical Technologies*. Springer Dordrecht Heidelberg New York London.
- Fuongfuchat, A., Jamieson, A. M., Blackwell, J. and Gerken, T. A. (1996). Rheological Studies of the Interaction of Mucins with Alginate and Polyacrylate. *Carbohydrate Research*. Vol 284: 85-99.
- Garti, N. (1997). Double Emulsions- Scope, Limitations and New Achievements. *Colloids Surfaces. A Physicochemical Engineering Aspects*. Vol 123-124: 233-246.
- Garti, N. and McClements, D. J. (2012). *Encapsulation Technologies and Delivery Systems for Food Ingredients and Nutraceuticals*. Woodhead Publishing Limited.

- Govender, S., Pillay, V., Chetty, D. J., Essack, S. Y., Dangor, C. M. and Govender, T. (2005). Optimisation and Characterisation of Bioadhesive Controlled Release Tetracycline Microspheres. *International Journal of Pharmaceutics*. Vol 306: 24-40.
- Grabovac, V., Gugli, D., Bernkop-Schnurch, A. (2005). Comparison of the Mucoadhesive Properties of Various Polymers. *Advanced Drug Delivery Reviews*. Vol 57: 1713-1723.
- Graessley, W.W. (1974) The Entanglement Concept in Polymer Rheology. *Advanced Polymer Science*. Vol 16: 1-179.
- Hägerström, H. and Edsman, K. (2001). Interpretation of Mucoadhesive Properties of Polymer Gel Preparations Using a Tensile Strength Method. *Journal of Pharmaceutical and Pharmacology*. Vol 53: 1589-1599.
- Hagesaether, E. and Sande, S. A. (2007). In Vitro Measurements of Mucoadhesive Properties of Six Types of Pectin. *Drug Development and Industrial Pharmacy*. Vol 33: 417-425.
- Hagesaether, E. and Sande, S. A. (2008). Effect of Pectin Type and Plasticizer on In Vitro Mucoadhesion of Free Films. *Pharmaceutical Development and Technology*. Vol. 13: 105-114.
- Hassan, E. E. and Gallo, J. M. (1990). A Simple Rheological Method for the in Vitro Assessment of Mucin-Polymer Bioadhesives Bond Strength. *Pharmaceutical Research*. Vol 7: 491-495.
- He, P., Davis, S. S. and Illum, L. (1998). In Vitro Evaluation of the Mucoadhesive Properties of Chitosan Microspheres. *International Journal of Pharmaceutics*. Vol 166: 75-68

- Heinzen, C. (2002). Microencapsulation Solve Time Dependent Problems for Foodmakers. *European Food and Drink Review*. Vol 3: 27–30.
- Henriksen, I., Green, K. L., Smart, J. D., Smista, G. and Karlsen, J. (1996). Bioadhesion of Hydrated Chitosans: An In Vitro and In Vivo Study. *International Journal of Pharmaceutics*. Vol 145: 231–240.
- Hunter, R. J. (1986). Foundations of Colloid Science. Vol. 1. New York, Oxford.
- Hwang, J.K., 1995, Rheological properties of citrus pectin solutions. *Korean Journal of food Science and Technology*. Vol 27: 799-806.
- Inoue, T., Chen, G. and Hoffman, A. S. (1998). A hydrophobically modified Bioadhesive Polymeric Carrier for Controlled Drug Delivery to Mucosal Surfaces. *Journal of Bioactive and Compatible Polymers*. Vol 13: 50-64.
- Joergensen, L., Klösgen, Simonsen, A. C., Borch, J., Hagesaether, E. (2011). New Insights into the Mucoadhesion of Pectins by AFM Roughness Parameters in Combination with SPR. *International Journal of Pharmaceutics*. Vol 411: 162–168
- Jun, H. K., Kim, J. S., No, H. K., & Meyers, S. P. (1994). Chitosan as A Coagulant for Recovery of Proteinaceous Solids from Tofu Wastewater. *Journal of Agricultural and Food Chemistry*. Vol 42: 1834–1838.
- Ko, J. A., Park, H. J., Hwang, S. J., Park, J. B. and Lee, J. S. (2002). Preparation and Characterization of Chitosan Microparticles Intended for Controlled Drug Delivery. *International Journal of Pharmaceutics*. Vol 249: 165-174.
- Ko, J. A., Park, H. J., Park, Y. S., Hwang, S. J. and Park, J. B. (2003). Chitosan Microparticle Preparation for Controlled Drug Release by response Surface Methodology. *Journal of Microencapsulation*. Vol 20(6): 791-797.

- Lee, B. B., Chan, E. S., Ravindra, P. and Khan, T. A. (2012). Surface Tension of Viscous Biopolymer Solutions Measured Using the Du Nouy Ring Method and The Drop Weight Methods. *Polymer Bulletin*. Vol 69: 471–489.
- Lehr, C. M. (2000). Lectin-mediated Drug Delivery: The Second Generation of Bioadhesives. *Journal of Controlled Release*. Vol 65: 19-29.
- Lehr, C. M., Bouwstra, J. A., Schacht, E. H. and Junginger, H. E. (1992). In Vitro Evaluation of Mucoadhesive Properties of Chitosan and Some Other Natural Polymers. *International Journal of Pharmaceutics*. Vol 78: 43-48.
- Lehr, C. M., Poelma, F. G. J., Junginger, H. E. and Tukker, J. J. (1991). An Estimate of Turnover Time of Intestinal Mucous Gel Layer in the Rate In Situ Loop. *International Journal of Pharmaceutics*. Vol 70: 235-240.
- Lenaerts, V. M. and Gurny, R. (1990). Bioadhesive Drug Delivery Systems. *CRC Press Inc*.
- Li, D., Yamamoto, H., Takeuchi, H. and Kawashima, Y. (2010). A Novel Method for Modifying AFM Probe to Investigate the Interaction between Biomaterial Polymers (Chitosan-coated PLGA) and Mucin Film. *European Journal of Pharmaceutics and Biopharmaceutics*. Vol 75: 277–283.
- MacClements, D. J. (2012). Nanoemulsions Versus Microemulsions: Terminology, Differences and Similarities. *Soft Matter*. Vol 8: 1719-1729.
- Madene, A., Jacquot, M., Scher, J. and Desobry, S. (2006). Flavour Encapsulation and Controlled Release- A Review. *International Journal of Food Science and Technology*. Vol 41: 1–21.

- Madsen, F., Eberth, K. and Smart, J. D. (1998). A Rheological Examination of the Mucoadhesive/Mucus Interaction: The Effect of Mucoadhesive type and Concentration. *Journal of Controlled Release*. Vol 50(1-3): 167-178.
- Maheshwari, R. and Dhathathreyan, A. (2006). Mucin at Solution/Air and Solid/Solution Interfaces. *Journal of Colloid and Interface Science*. Vol 293: 263–269.
- Malvern Note (2012). Part 1: Rotational Rheometry.
- Marx, K. A. (2003). Quartz Crystal Microbalance: A Useful Tool for Studying Thin Polymer Films and Complex Biomolecular Systems at the Solution-Surface Interface. *Biomacromolecules*. Vol 4(5): 1009-1120.
- Mason Technology website (accessed on 25th November 2014).
<http://www.masontechnology.ie/product/StableMicroSystems/TextureAnalysers/TAXTplusTextureAnalyser>
- Meyer, G. and Amer, N. M. (1988). Novel Optical Approach to Atomic Force Microscopy. *Applied Physics Letters*. Vol 53: 1045-1047.
- Mishra, S. K., Garud, N. and Singh, R. (2011). Development and Evaluation of Mucoadhesive Buccal Patches of Flurbiprofen. *Acta Poloniae Pharmaceutica – Drug Research*. Vol. 68 (6): 955-964.
- Mitra, T., Pattnaik, S., Panda, J., Sahu, P. K., Rout, B. K., Murthy, S. R. and Sahu, R. K. (2012). Formulation and Evaluation of Salbutamol Sulphate Mucoadhesive Sustained Release Tablets Using Natural Excipients. *Journal of Chemical and Pharmaceutical Sciences*. Vol 5 (2): 62-66.
- Mortazavi, S. A. (1995). An In Vitro Assessment of Mucus/Mucoadhesive Interactions. *International Journal of Pharmaceutics*. Vol 124: 173-182.

- Mortazavi, S. A. (2003). Extended Frequency Sweep: A More Realistic Rheological Approach to Investigate the Process of Mucoadhesive Polymer-mucus Gel Chain Interpenetration. *Iranian Polymer Journal*. Vol 12 (5): 413-420.
- Mortazavi, S. A. and Moghimi, H. R. (2003). Effect of Surfactant Type and Concentration on the Duration of Mucoadhesion of Carbopol 934 and HPMC Solid Compacts. *Iranian Journal of Pharmaceutical Research*. Vol 2: 191-199.
- Nielsen, L.E., 1977, *Polymer Rheology*, Marcell Dekker, Inc., p48.
- Nikhil, S. and Bhattacharya, A. (2009). A Basic and Therapeutic Potential of Oral Mucoadhesive Microparticulate Drug Delivery Systems. *International Journal of Pharmaceutical and Clinical Research*. Vol 1: 10-14.
- Nikovska, K. (2012). Study of Olive Oil-in-Water Emulsions with Protein Emulsifiers. *Emirates Journal of Food and Agriculture*. Vol 24(1): 17-24.
- No, H. K., Kim, S. H., Lee, S. H., Park, N. Y. and Prinyawiwatkul, W. (2006). Stability and Antibacterial Activity of Chitosan Solutions Affected by Storage Temperature and Time. *Carbohydrate Polymers*. Vol 65: 174–178
- Norton, I. T., Jarvis, D. A. and Foster, T. J. (1999). A Molecular Model for the Formation and Properties of Fluid Gels. *International Journal of Biological Macromolecules*. Vol 26: 255-261.
- Oberyukhtina, I.A., Bogolitsyn, K.G. & Popova, N.P. 2001. Physicochemical Properties of Solutions of Sodium Alginate Extracted from Brown Algae *Laminaria Digitata*. *Russian Journal of Applied Chemistry*. Vol74(10), 1645-1649
- Ouyang, Q., Ishida, K. and Okada, K. (2001). Investigation of Micro-Adhesion by Atomic Force Microscopy. *Applied Surface Science*. Vol 169-170: 644-648.

- Pallandre, S., Decker, E. A. and McClements, D. J. (2007). Improvement of Stability of Oil-in-Water Emulsions Containing Caseinate-Coated Droplets by Addition of Sodium Alginate. *Journal of Food Science*. Vol 72(9): 5185-524.
- Palmer Jr, R. J. (1999). Microscopy Flowcells: Perfusion Chambers for Real-Time Study of Biofilms. *Methods in Enzymology*. Vol 310: 160-166.
- Paradies, H. H., Wagner, D. and Fischer, W. R. (2010). Multicomponent Diffusion of Sodium Alginate Solutions with Added Salt. II. Charged vs. Uncharged System. *Berichte Bunsenges Physical Chemistry*. Vol 100(8): 1299–1307.
- Particle Science, Drug Development Service article (2011). *Technical Brief*. Vol 2.
- Patel, D., Smith, J. R., Smith, A. W., Grist, N., Barnett, P. and Smart, J. D. (2000). An Atomic Force Microscopy Investigation of Bioadhesive Polymer Adsorption onto Human Buccal Cells. *International Journal of Pharmaceutics*. Vol 200: 271–277.
- Patil, P., Kulkarni, S. V., Rao, S. B., Ammanage, A., Surpur, C. and Basavaraj. (2011). Formulation and In-Vitro Evaluation of Mucoadhesive Tablets of Ofloxacin Using Natural Gums. *International Journal of Current Pharmaceutical Research*. Vol 3(2): 93-98.
- Peppas, N. A. and Buri, P. A. (1985). Surface, Interfacial and Molecular Aspects of Polymers Bioadhesion on Soft Tissues. *Journal of Controlled Release*. Vol 2: 257-275.
- Peppas, N. A. and Huang, Y. (2004). Nanoscale Technology of Mucoadhesion Interactions. *Advanced Drug Delivery Reviews*. Vol 56: 1675-1687.
- Peppas, N. A. and Sahlin, J. J. (1996). Hydrogels as Mucoadhesive and Bioadhesive materials: A Review. *Biomaterials*. Vol 17: 1553-1561.

- Pinhas, M. D. and Peled, H. B. (2010). Mucoadhesion: A Review of Characterisation Techniques. *Expert Opinion on Drug Delivery*. Vol 7(2): 259-271.
- Pongsawarmanit, R., Harnsilawat, T. and McClements, D. J. (2006). Influence of Alginate, pH and Ultrasound Treatment on Palm Oil-in-Water Emulsions Stabilized by β -Lactoglobulin. *Colloids and Surfaces A: Physiochemical and Engineering Aspects*. Vol 287 (1-3): 59-67.
- Punitha, S. and Girish, Y. (2010). Polymers in Mucoadhesive Drug Delivery Systems. *International Journal of Research and Pharmaceutical Sciences*. Vol 1: 170-186.
- Ralet, M. C., Bonnin, E. and Thibault, J. F. (2002). Pectins. In: Steinbüchel A (ed) Biopolymers. Wiley-VCH, Weinheim. Page: 345-380.
- Ravi, B., Biswajit, B., Kevin, G., Bhavik, J. and Kuldeep, M. (2010). Buccoadhesive Drug Delivery Systems. *International Journal of Pharma and BioSciences*. Vol 1: 1-32.
- Riley, R. G., Smart, J. D., Tsibouklis, J., Dettmar, P. W., Hampson, F., Davis, J. A., Kelly, G. and Wilber, W. R. (2001). An Investigation of Mucus:Polymer Rheological Synergism Using Synthesised and Characterised Poly(Acrylic acid)s. *International Journal of Pharmaceutics*. Vol 217: 87–100.
- Rodahl, M. and Kasemo, B. (1996). A Simple Setup to Simultaneously Measure the Resonant Frequency and the Absolute Dissipation Factor of a Quartz Crystal Microbalance. *Review of Scientific Instruments*. Vol 67: 3238-3241.
- Ron, E. S. and Bromberg, L. E. (1998) Temperature-Responsive Gels and Thermogelling Polymer Matrices for Protein and Peptide Delivery. *Advanced Drug Delivery Review*. Vol 31 (3): 197-221

- Rossi, S., Bonferoni, M. C., Ferrari, F., Bertoni, M. and Caramella, C. (1996). Characterisation of Mucin Interaction with Three Viscosity Grades of Sodium Carboxymethylcellulose. Comparison Between Rheological and Tensile Testing. *European Journal of Pharmaceutical Science*. Vol 4: 189-196.
- Rossi, S., Ferrari, F., Bonferoni, M. C. and Caramella, C. (2000). Characterisation of Chitosan Hydrochloride-Mucin Interaction by Means of Viscometric and Turbidimetric Measurements. *European Journal of Pharmaceutical Sciences*. Vol 10: 251-257.
- Rossi, S., Ferrari, F., Bonferoni, M. C. and Caramella, C. (2001). Characterization of Chitosan Hydrochloride-Mucin Rheological Interaction: Influence of Polymer Concentration and Polymer:Mucin Weight Ratio. *European Journal of Pharmaceutical Sciences*. Vol 12: 479-485.
- Roy, S. K. and Prabhakar, B. (2010). Bioadhesive Polymeric Platforms for Transmucosal Drug Delivery Systems- A Review. *Tropical Journal of Pharmaceutical Research*. Vol 9 (1): 91-104.
- Säkkinen, M., Marvola, J., Kanerva, H., Lindevall, K., Ahonen, A. and Marvola, M. (2006). Are Chitosan Formulations Mucoadhesive in the Human Small Intestine? An Evaluation Based on Gamma Scintigraphy. *International Journal of Pharmaceutics*. Vol 307: 28-291.
- Sam, A. P., van den Heuij, J. T. M. and Tukker, J. J. (1992). Mucoadhesion of Both Film-Forming and Non-Film-Forming Polymeric Materials As Evaluated with the Wilhelmy Plate Method. *International Journal of Pharmaceutics*. Vol 79: 97-105.

- Saparia, B., Murthy, R. S. R. and Solanki, A. (2002). Preparation and Evaluation of Chloroquine Phosphate Microspheres Using Cross-Linked Gelatin for Long-Term Drug Delivery. *Indian Journal of Pharmaceutical Sciences*. Vol 64: 48-52.
- Sauerbrey, G. (1959). Use of A Quartz Crystal Vibrator for Weighing Thin Films on A Microbalance. *Zeitschrift Fur Physik*. Vol 155: 206-222.
- Seixas, F. L., Turbiani, F. R. B., Salomão, P. G., Souza, R. P. and Gimenes, M. L. (2013). Biofilms Composed of Alginate and Pectin: Effect of Concentration of Crosslinker and Plasticizer Agents. *Chemical Engineering Transactions*. Vol 32: 1693-1698.
- Senthil, A., Hardik, T. R., Sivakumar, T. and Jain, D. A. (2011). Formulation and Evaluation of Mucoadhesive Glipiside Microspheres Using Carboxy Methyl Cellulose. *International Journal of Preclinical and Pharmaceutical Research*. Vol 2(1): 45-51.
- Shaheen, S. M., Hossen, M. N., Islam, K. M., Ahmed, M., Amran, M. S. and Rashid, M. (2006). Effect of Bio-Adhesive Polymers Like HPMC, Gelatin, Na-CMC and Xanthan Gum on Theophylline Release from Respective Tablets. *International Journal of Pharmacology*. Vol 2 (5): 504-508.
- Shahidi, F. and Han, X.Q. (1993). Encapsulation of Food Ingredients. *Critical Reviews in Food Science and Nutrition*. Vol 33: 501–547.
- Sharad, S., Amit, A., Ajazuddin, Junaid, K. M. and Swarna. (2011). Theories and Factors Affecting mucoadhesion Drug Delivery Systems: A Review. *International Journal of Research in Ayurveda and Pharmacy*. Vol 2: 1155-1161.

- Shojaei, A. H., Paulson, J. And Honary, S. (2000). Evaluation of Poly(Acrylic Acid-Co-Ethylhexyl Acrylate) Films For Mucoadhesive Transbuccal Drug Delivery: Factors Affecting the Force of Mucoadhesion. *Journal of Control. Release*. Vol 67: 223–232.
- Singh, A., Singh, D. and Irchhaiya, R. (2013). Mucoadhesive Microsphere: A Review. *Journal of Pharmaceutical and Biomedical Analysis Letters*. Vol 1(1): 47-54.
- Singh, I. and Rana, V. (2012). Techniques for the Assessment of Mucoadhesion in Drug Delivery Systems: An Overview. *Journal of Adhesion Science and Technology*. Vol 26(18-19): 2251-2267
- Singh, S., Govind, M. and Bothara, S. B. (2013). A Review on In Vitro-In Vivo Mucoadhesive Strength Assessment. *Pharma Tech Medica*. Vol 2 (1): 221-229.
- Smart, J. D. (2005). The Basics and Underlying Mechanisms of Mucoadhesion. *Advanced Drug Delivery Reviews*. Vol 57: 1556-1568.
- Smart, J. D., Kellaway, I. W. and Worthington, H. E. C. (1984). An In-vitro Investigation of Mucosa-adhesive Materials for Use in Controlled Drug Delivery. *Journal of Pharmacy and Pharmacology*. Vol 36: 295-299.
- Sogias, I. A., Williams, A. C. and Khutoryanskiy, V. V. (2008). Why is Chitosan Mucoadhesive?. *Biomacromolecules*. Vol 9: 1837-1842.
- Somwangthanaroj, A. (2010). Rheology and Polymer Characterisation. <http://pioneer.netserv.chula.ac.th/~sanongn1/course.html>

- Sophanodora, P. and Hutadilok, N. (1995). Feasibility Study of a Shrimp-Based Chitin/Chitosan Industry in Southern Thailand. In Zakaria, M. B., Muda, W. M. W. and Abdullah, M. P. (Eds.), *Chitin and Chitosan: The Versatile Environmentally Friendly Modern Materials* (pp. 35–42). Bangi: Penerbit Universiti, Kebangsaan, Malaysia.
- Sriamornsak, P. (2003). Chemistry of Pectin and Its Pharmaceutical Uses: A Review. *Silpakorn University International Journal*. Vol 3: 206-228.
- Sriamornsak, P. and Puttipipatkachorn, S. (2004). Chitosan-Pectin Composite Gel Spheres: Effect of Some Formulation Variable on Drug Release. *Macromolecular Symposia*. Vol 216: 17-21.
- Sriamornsak, P. and Wattanakorn, N. (2008). Rheological Synergy in Aqueous Mixtures of Pectin and Mucin. *Carbohydrate Polymers*. Vol 74: 474-481.
- Sriamornsak, P., Wattanakorn, N. and Takeuchi, H. (2010). Study on the Mucoadhesion Mechanism of Pectin by Atomic Force Microscopy and Mucin-Particle Method. *Carbohydrate Polymers*. Vol 79: 54–59.
- Stable Micro Systems website (accessed on 25th November 2014).
<http://www.stablemicrosystems.com/frameset.htm?http://www.stablemicrosystems.com/TAXTplus.htm>
- Stanford Research Systems. QCM100-Quartz Crystal Microbalance Theory and Calibration. www.thinkSRS.com (accessed on 25th November 2014).
- Sternberg, C. and Tolker-Nielsen, T. (2006). Growing and Analyzing Biofilms in Flow Cells. *Current Protocols in Microbiology*. Chapter 1. Unit 1B.2.

- Sudhakar, Y., Kuotsu, K. and Bandyopadhyay, A. K. (2006) Buccal Bioadhesive Drug Delivery– A Promising Option for Orally Less Efficient Drugs. *Journal of Controlled Release*. Vol 114: 15–40.
- Svensson, O. (2008). Interactions of Mucins with Biopolymers and Drug Delivery Particles. PhD Thesis.
- Tabak, L. A. (1990). Structure and Function of Human Salivary Mucins. *Critical Reviews in Oral Biology and Medicine*. Vol 1(4): 229-234.
- Thirawong, N., Kennedy, R. A. and Srimornsak, P. (2008). Viscometric Study of Pectin-Mucin Interaction and Its Mucoadhesive Bond Strength. *Carbohydrate Polymers*. Vol 71: 170-179.
- Thirawong, N., Nunthanid, J., Puttipipatkachorn, S. and Srimornsak, P. (2007). Mucoadesive Properties of Various Pectins on Gastrointestinal Mucosa: An In Vitro Evaluation Using Texture Analyzer. *European Journal of Pharmaceutics and Biopharmaceutics*. Vol 67 (1): 132-140.
- Tur, K. M. and Ch'ng, H. S. (1998). Evaluation of Possible Mechanism(s) of Bioadhesion. *International Journal of Pharmaceutics*. Vol 160: 61-74
- Vaclavik, V. A. and Christian, E. W. (2014). Essentials of Food Science. 4th Edition. *Springer Dordrecht Heidelberg New York London*.
- Valasek, J. (1921). Piezo-Electric and Allied Phenomena in Rochelle Salt. *Physical Review*. Vol 17(4): 475-481.
- van Aken, G. A., Vingerhoeds, M. H. and de Hoog, E. H. A. (2007). Food Colloids Under Oral Conditions.

- Vaz Junior, M., de Souza Neto, E. A. and Munoz-Rojaz, P. A. (2011). Advanced Computational Materials Modelling: From Classical to Multi-Scale Techniques. *John Wiley and Sons*.
- Voinova, M. V., Rodahl, M., Jonson, M. and Kasemo, B. (1999). Viscoelastic Acoustic Response of Layered Polymer Films at Fluid-Solid Interfaces: Continuum Mechanics Approach. *Physica Scripta*. Vol 59: 391-396.
- Wang, X., Ruengruglikit, C., Wang, Y. W. and Huang, Q. (2007). Interfacial Interactions of Pectin with Bovine Serum Albumin Studied by Quartz Crystal Microbalance with Dissipation Monitoring: Effect of Ionic Strength. *Journal of Agricultural and Food Chemistry*. Vol 55: 10425–10431
- Weiss, J. and Muscholik, G. (2007). Factors Affecting the Droplet Size of Water-in-Oil Emulsions (W/O) and the Oil Globule Size in Water-in-Oil-in-Water Emulsions (W/O/W). *Journal of Dispersion Science and Technology*. Vol 28(5): 703-716.
- Weitz, D. A., Wyss, H. M. and Larsen, R. J. (2007). Oscillatory Rheology: Measuring the Viscoelastic Behavior of Soft Materials. *G. I. T. Laboratory Journal Europe*. Vol 11(3-4): 68-70.
- Wikipedia website (accessed on 25th November 2014).
<http://en.wikipedia.org/wiki/Viscosity>
- Wilson, R. A. and Bullen, H. A. (2007). Introduction to Scanning Probe Microscopy (SPM): Basic Theory of Atomic Force Microscopy. Department of Chemistry, Northern Kentucky University.

- Wittaya-areekul, S., Kruenate, J. and Prahsarn, C. (2006). Preparation and In Vitro Evaluation of Mucoadhesive Properties of Alginate/Chitosan Microparticles Containing Prednisolone. *International Journal of Pharmaceutics*. Vol. 312: 113–118.
- Wolff, M. and Kleinberg, I. (1998). Oral Mucosal Wetness in hypo- and Normopsalivators. *Archives of Oral Biology*. Vol 43: 455-462.
- Wu, S. (1982). Formation of Adhesive Bond, Polymer Interface and Adhesion. *Marcel Dekker Inc, New York*. Page 359-447.
- Xiao, X. and Qian, L. (2000). Investigation of Humidity-Dependent Capillary Force. *Langmuir*. Vol 16: 8153-8158.
- Yadav, V. K., Gupta, A. B., Yadav, J. S. and Kumar, B. (2010). Mucoadhesive Polymers: Means of Improving the Mucoadhesive Properties of Drug Delivery System. *Journal of Chemical and Pharmaceutical Research*. Vol 2(5): 418-432.
- Yang, J., Chen, S. H. and Fang, Y. (2009). Viscosity Study of Interactions Between Sodium Alginate and CTAB in Dilute Solutions at Different pH Value. *Carbohydrate Polymers*. Vol 75: 333-337.
- Yang, X. H. and Zhu, W. L. (2007). Viscosity Properties of Sodium Carboxymethylcellulose Solutions. *Cellulose*. Vol 14: 409-417.
- Yu, T., Andrews, G. P. and Jones, D. S. (2014). Chapter 2: Mucoadhesion and Characterization of Mucoadhesive Properties IN das Neves, J. and Sarmento, B. (eds). *Mucosal Delivery of Biopharmaceuticals: Biology, Challenges and Strategies*. Springer Science and Business Media.

- Zalewska, A., Zwierz, K., Zolkowski, K. And Gindzienski, A. (2000). Structure and Biosynthesis of Human Salivary Mucins: Review. *Acta Biochimica Polonica*. Vol 47(4): 1067-1079.
- Zangi, R., Hagen, M. and Berne, B. J. (2007). Effect of Ions on the Hydrophobic Interaction between Two Plates. *Journal Of The American Chemical Society*. Vol 129: 4678-4686.
- Zhang, H., Wang, H., Wang, J., Guo, R. and Zhang, Q. (2001). The Effect of Ionic Strength on the Viscosity of Sodium Alginate Solution. *Polymers for Advanced Technologies*. Vol 12: 740-745.